



The University of  
**Nottingham**

**Effect of Dietary Fat on Lipid  
Accumulation and Macrophage  
Activation *in vivo*.**

**Fatiha Benslimane, BS.C, MS.C**

Thesis submitted to the University of Nottingham for the  
degree of Doctor of Philosophy

July 2016

## Abstract

---

The rat was used as a model for the assessment of a high fat diet (HFD) and HFD/streptozotocin (STZ) induced Type II diabetes upon lipid deposition and development of inflammation in metabolically active tissues.

HFD feeding for a period of 10 weeks did not induce significant weight gain in animals compared to those fed on normal chow (NC). There was also no significant effect of HFD feeding upon blood glucose and insulin levels. Adipose and skeletal muscle tissues showed minimal effects of HFD feeding at both the histological and molecular level. Histological assessment of liver tissue revealed marked steatosis in HFD fed animals. Molecular studies showed that genes involved in lipid and glucose metabolism and insulin signalling were decreased while genes involved in endoplasmic reticulum (ER) stress were elevated. Liver triglyceride fatty acid profiles resembled those of the diet with no significant differences in lipoprotein triglyceride levels observed between experimental groups. STZ injection induced hypoinsulinemia and hyperglycaemia. The changes observed at the molecular level were related to insulin depletion. Pioglitazone intervention did not cause any major changes in the STZ treated animals.

The main conclusion was that HFD induces liver steatosis due to increase lipid flux from the diet despite the absence of weight gain or increased adipose tissue or skeletal muscle lipid content. This suggests that consumption of a high fat diet may cause the development of fatty Liver disease in the absence of weight gain or overt obesity.

## Research Presentation:

Benslimane F, Bennett A. **High Fat Diet–Induced Liver Steatosis in the Absence of Obesity.** 5<sup>th</sup> European Lipidomic Meeting, Swansea, United Kingdom. September 2015

Benslimane F. Chapman V. Bennett A. **The Role of Macrophage Infiltration in Insulin Resistance and Diabetes.** School of Life Sciences Postgraduate Symposium, University of Nottingham, United Kingdom. July 2012.

# Acknowledgement

---

Many thanks to the Almighty Allah, who blessed me with health, courage, enthusiasm and the determination which enabled me to carry out and conclude this thesis.

I would like to take this opportunity to thank everyone for their unconditional support and solidarity throughout the time of this research. I am deeply grateful to my supervisor Dr. Andrew Bennet, his stimulating suggestions and encouragement helped me in all the time of research. His wide knowledge and understanding, encouraging and personal guidance have provided a good basis for the present thesis.

I wish to extend my warmest thanks to all those who have helped me in the FRAME, AMU and ARUK Pain labs. I would particularly like to extend my thanks to my second supervisor Professor Victoria Chapman for her assistance and help with providing the animal models. I would like to thank Prof Andrew Salter and his technician Calum in SB campus for their assistance with the GC work.

I would like to thank all my friends for their motivation and moral support that encouraged me to complete this thesis.

For most I am deeply grateful to my family for their love, support and encouragement in helping me to complete this work as it should be.

My gratefulness to my parents, Messaoud Benslimane and Khadra Bendjillali, who made me believe that this was possible. Their belief in me never wavered, even when mine did. I continue to realize and appreciate how fortunate I am to have them for parents. I could never adequately express thanks for all that they have given to me, or all that they have meant to me. They have always been, and continue to be, my inspiration. I want to thank my father for believing in me and for supporting my stay in the UK, and I want to thank my mother for dealing with me being worlds away, only sporadically calling home and even then mainly to complain about the thesis.

Many thanks to my brothers: Jamal, Youcef and Habib for their encouragement. Habib, whom I am truly blessed to have as a brother, no words could describe how I am grateful for your care, kindness, extensive support, help and patience. A big thank you for being there when I needed you the most and I do hope I wasn't a horrible housemate!

Special thanks to my adorable little sisters, Zahra and Rodaina, whom I consider like my own daughters, for understanding why I was away all this time, for not being there for their birthdays and triumphs.

This thesis is dedicated to my parents and the memory of my grandmother, Frayha Hashani. I miss her every day, but I am glad that I had the opportunity to hear her encouraging prayers upon the start of my PhD.

# Table of Content

---

<b>ABSTRACT .....</b>	<b>II</b>
<b>ACKNOWLEDGEMENT .....</b>	<b>IV</b>
<b>LIST OF FIGURES .....</b>	<b>X</b>
<b>LIST OF TABLES .....</b>	<b>XII</b>
<b>LIST OF ABBREVIATIONS .....</b>	<b>XIII</b>
<b>CHAPTER I: GENERAL INTRODUCTION .....</b>	<b>1</b>
<b>1.1 INTRODUCTION .....</b>	<b>2</b>
<b>1.2 LIPOPROTEINS .....</b>	<b>3</b>
1.2.1 CHYLOMICRON METABOLISM: THE EXOGENOUS PATHWAY.....	4
1.2.2 VLDL METABOLISM: THE ENDOGENOUS PATHWAY.....	6
1.2.3 HDL METABOLISM AND REVERSE CHOLESTEROL TRANSPORT .....	6
1.2.4 REGULATION OF LIPOPROTEIN METABOLISM .....	7
<b>1.3 ADIPOSE TISSUE AND INFLAMMATION.....</b>	<b>9</b>
1.3.1 MACROPHAGE INFILTRATION INTO ADIPOSE TISSUE IN OBESITY .....	10
<b>1.4 OVERVIEW OF HEPATIC FATTY ACID METABOLISM .....</b>	<b>14</b>
1.4.1 HEPATIC TRIGLYCERIDE METABOLISM .....	15
1.4.2 HEPATIC FATTY ACID METABOLISM .....	16
1.4.3 HEPATIC GLUCOSE METABOLISM.....	17
1.4.4 INSULIN ACTION .....	19
1.4.5 INTERACTIONS OF GLUCOSE AND LIPID METABOLISM .....	20
<b>1.5 NON-ALCOHOLIC FATTY LIVER DISEASE (NAFLD) .....</b>	<b>22</b>
1.5.1 METABOLIC PATHWAYS LEADING TO LIPID ACCUMULATION .....	23
1.5.2 NAFLD AND THE DEVELOPMENT OF NASH .....	24
<b>1.6 INTERACTIONS BETWEEN DIET AND NAFLD.....</b>	<b>25</b>
1.6.1 DIETARY HISTORY ASSESSMENTS IN NAFLD.....	25
1.6.2 DIETARY ASSESSMENT IN NAFLD IN LIVER BIOPSY LIPID ANALYSES .....	28
<b>1.7 POLYUNSATURATED FATTY ACIDS.....</b>	<b>30</b>
<b>1.8 ANIMAL MODELS OF NAFLD AND PUFA SUPPLEMENTATION .....</b>	<b>31</b>
1.8.1 HIGH FAT DIET IN COMBINATION WITH DIABETIC-INDUCED ANIMAL MODELS.....	33
<b>1.9 AIMS OF THE THESIS .....</b>	<b>35</b>
<b>CHAPTER II: ANIMAL MODEL OF DIET-INDUCED DIABETES .....</b>	<b>36</b>
<b>2.1 INTRODUCTION .....</b>	<b>37</b>
2.1.1 ANIMAL MODEL OF DIABETES.....	37
2.1.2 STREPTOZOTOCIN (STZ) MODEL OF DIABETES .....	37
2.1.3 PIOGLITAZONE: EFFECT ON DIABETES.....	39
<b>2.2 AIM OF THE STUDY.....</b>	<b>39</b>
<b>2.3 MATERIAL AND METHODS .....</b>	<b>40</b>
2.3.1 ANIMAL MODEL.....	40

2.3.2	HFD/STZ MODEL OF DIABETES .....	41
2.3.3	HFD/STZ + PIOGLITAZONE MODEL OF DIABETES .....	41
2.3.4	BLOOD SAMPLING.....	41
2.3.5	TISSUE COLLECTION.....	42
2.3.6	STATISTICS .....	42
<b>2.4</b>	<b>RESULTS.....</b>	<b>43</b>
2.4.1	EFFECTS OF HFD ON BODY WEIGHT AND FOOD AND WATER INTAKE .....	43
2.4.2	THE EFFECT OF HFD ON METABOLIC PARAMETERS .....	43
2.4.3	EFFECTS OF STREPTOZOTOCIN AND PIOGLITAZONE INTERVENTION ON BODY WEIGHT, FOOD AND WATER INTAKE .....	44
2.4.4	EFFECTS OF STREPTOZOTOCIN AND PIOGLITAZONE INTERVENTION ON METABOLIC PARAMETERS .....	46
<b>2.5</b>	<b>DISCUSSION .....</b>	<b>48</b>
2.5.1	EFFECTS OF HFD FEEDING.....	48
2.5.2	IS HFD/STZ A GOOD MODEL OF DIABETES? .....	49
2.5.3	EFFECTS OF PIOGLITAZONE IN THE HFD/STZ MODEL.....	51
2.5.4	CONCLUSION .....	52
 <b>CHAPTER III: EFFECT OF HFD ON MACROPHAGE INFILTRATION AND ACTIVATION..</b>		<b>53</b>
<b>3.1</b>	<b>INTRODUCTION .....</b>	<b>54</b>
3.1.1	ADIPOSE TISSUE MACROPHAGES IN OBESITY .....	54
3.1.2	MACROPHAGES AND INFLAMMATION IN LIVER AND MUSCLES .....	55
3.1.3	AIM .....	56
<b>3.2</b>	<b>MATERIALS AND METHODS .....</b>	<b>57</b>
3.2.1	HISTOLOGICAL AND IMMUNOFLUORESCENT ANALYSIS .....	57
3.2.1.1	Cryostat sectioning .....	57
3.2.1.2	Fixed Paraffin-embedded tissue sectioning .....	57
3.2.1.3	Hematoxylin and Eosin (H&E) Staining.....	58
3.2.1.4	Fluorescent Immunohistochemistry .....	59
3.2.1.5	Antigen retrieval .....	60
3.2.1.6	Sudan Black staining .....	60
3.2.1.7	Volocity software analysis.....	60
3.2.2	RNA EXTRACTION AND QUANTIFICATION .....	61
3.2.2.1	RNA extraction .....	61
3.2.2.2	Complementary DNA (cDNA) synthesis .....	62
3.2.2.3	TaqMan real-time quantitative PCR .....	62
3.2.3	ANALYSIS OF PROTEIN EXPRESSION.....	64
3.2.3.1	Protein extraction and quantification .....	64
3.2.3.2	Western blotting .....	66
3.2.3.3	Immunodetection and densitometry analysis.....	68
<b>3.3</b>	<b>RESULTS.....</b>	<b>69</b>
3.3.1	ADIPOSE TISSUE HISTOLOGY.....	69
3.3.2	IMMUNOHISTOCHEMISTRY: CONTROL OF TISSUE AUTOFLUORESCENCE AND VALIDATION OF ANTIBODIES .....	71

3.3.3	ADIPOSE TISSUE MACROPHAGE PHENOTYPE .....	72
3.3.4	VISCERAL ADIPOSE TISSUE INFLAMMATORY GENE EXPRESSION .....	74
3.3.5	SKELETAL MUSCLE TISSUE HISTOLOGY, MACROPHAGES AND TISSUE INFLAMMATORY GENE EXPRESSION .....	75
3.3.6	LIVER TISSUE HISTOLOGY .....	76
3.3.7	LIVER TISSUE MACROPHAGE PHENOTYPE .....	78
<b>3.4</b>	<b>DISCUSSION .....</b>	<b>80</b>
3.4.1	ADIPOSE TISSUE: A STATE OF CHRONIC, LOW-GRADE INFLAMMATION? .....	80
3.4.2	EFFECT OF HFD ON MUSCLE TISSUES.....	82
3.4.3	LIVER TISSUE STEATOSIS AND MACROPHAGE MARKERS.....	82
3.4.4	CONCLUSION .....	83
 <b>CHAPTER IV: EFFECT OF HFD ON PERIPHERAL TISSUE DEPOSITION .....</b>		<b>84</b>
<b>4.1</b>	<b>INTRODUCTION .....</b>	<b>85</b>
<b>4.2</b>	<b>AIMS.....</b>	<b>86</b>
<b>4.3</b>	<b>MATERIAL AND METHODS .....</b>	<b>87</b>
4.3.1	TAQMAN GENE EXPRESSION ANALYSIS.....	87
4.3.2	TAQMAN LOW DENSITY ARRAY .....	87
4.3.3	TRIGLYCERIDE ANALYSIS BY GAS CHROMATOGRAPHY .....	93
4.3.3.1	Tissue lipid extraction .....	93
4.3.3.2	Separation of lipids by thin layer chromatography (TLC) .....	93
4.3.3.3	Extraction of Triacylglycerol from TLC plates .....	94
4.3.3.4	Direct Fatty Acid Methyl Ester (FAME) Synthesis .....	94
4.3.3.5	Gas Chromatography .....	95
4.3.4	TRIGLYCERIDE ASSAY .....	96
4.3.5	WESTERN BLOTTING .....	97
4.3.6	IMMUNOHISTOCHEMISTRY .....	97
4.3.6.1	Secondary antibody incubation .....	98
4.3.6.2	Detection .....	98
4.3.6.3	DAB reaction (3, 3`Diaminobenzidine tetrahydrochloride).....	98
4.3.6.4	Counterstaining, dehydration and mounting.....	98
4.3.7	PICRO-SIRIUS RED (PSR) STAIN .....	99
<b>4.4</b>	<b>RESULTS.....</b>	<b>100</b>
4.4.1	SREBP-1C MRNA RELATIVE EXPRESSION .....	100
4.4.2	LIVER SCORING.....	100
4.4.3	LIVER TAQMAN LOW DENSITY ARRAY .....	102
4.4.4	TAQMAN GENE ARRAY VALIDATION .....	105
4.4.5	LIVER C/EBP HOMOLOGOUS PROTEIN (CHOP) EXPRESSION AND LOCALIZATION .....	106
4.4.1	LIVER TRIGLYCERIDES CONTENT AND COMPOSITION.....	108
4.4.2	MUSCLE TAQMAN GENE ARRAY .....	111
4.4.3	SKELETAL MUSCLE TOTAL TRIGLYCERIDE CONTENT .....	113
<b>4.5</b>	<b>DISCUSSION .....</b>	<b>114</b>
4.5.1	MEASUREMENT STEROL RESPONSIVE ELEMENT BINDING PROTEIN-1C MRNA.....	114
4.5.2	HFD AND NON-ALCOHOLIC FATTY LIVER DISEASE (NAFLD) .....	115

4.5.3	MOLECULAR INVESTIGATION OF LIVER METABOLIC PATHWAYS .....	116
4.5.4	HFD AND LIVER ENDOPLASMIC RETICULUM STRESS .....	119
4.5.5	DIET FAT COMPOSITION: DOES IT REFLECT LIVER FATS? .....	120
4.5.6	MOLECULAR INVESTIGATION OF SKELETAL MUSCLE GENE EXPRESSION AND TOTAL TRIGLYCERIDE CONTENT .....	121
4.5.7	CONCLUSION .....	121
<b>CHAPTER V: EFFECT OF HFD ON PLASMA LIPOPROTEINS .....</b>		<b>122</b>
<b>5.1</b>	<b>INTRODUCTION .....</b>	<b>123</b>
<b>5.2</b>	<b>AIM .....</b>	<b>124</b>
<b>5.3</b>	<b>MATERIALS AND METHODS .....</b>	<b>125</b>
5.3.1	ANIMAL MODEL.....	125
5.3.2	BLOOD SAMPLING AND TISSUE COLLECTION .....	126
5.3.3	LIVER TISSUE ANALYSIS .....	126
5.3.4	ULTRACENTRIFUGATION OF PLASMA LIPIDS.....	126
5.3.4.1	Separation of chylomicrons .....	126
5.3.4.2	Separation of VLDL.....	127
5.3.5	LIPID EXTRACTION FROM PLASMA LIPOPROTEIN SAMPLES.....	127
5.3.6	ANALYSIS OF TRIGLYCERIDE CONTENT OF CHYLOMICRON AND VLDL FRACTIONS .....	128
5.3.7	STATISTICS .....	128
<b>5.4</b>	<b>RESULTS.....</b>	<b>129</b>
5.4.1	EFFECTS OF HFD ON BODY WEIGHT AND PLASMA GLUCOSE LEVELS .....	129
5.4.2	LIVER TISSUE HISTOLOGY AND TRIGLYCERIDE CONTENT.....	130
5.4.3	PLASMA LIPID TRIGLYCERIDES ASSESSMENT.....	132
<b>5.5</b>	<b>DISCUSSION .....</b>	<b>137</b>
<b>CHAPTER VI: GENERAL DISCUSSION.....</b>		<b>139</b>
<b>REFERENCES .....</b>		<b>143</b>
<b>APPENDIX.....</b>		<b>A-1</b>

# List of Figures

---

## CHAPTER I:

FIGURE 1.1   MEDIA PERCEIVING THE EFFECT OF FAT .....	2
FIGURE 1.2   LIPOPROTEIN COMPOSITION.....	4
FIGURE 1.3   MECHANISM OF ADIPOSE TISSUE MACROPHAGE POLARIZATION. ....	13
FIGURE 1.4   INFLAMMATION AND INSULIN RESISTANCE.....	14
FIGURE 1.5   HEPATIC LIPID METABOLISM IN HEALTH.....	16
FIGURE 1.6   REGULATION OF HEPATIC GLUCOSE METABOLISM. ....	18
FIGURE 1.7   DEVELOPMENT OF NAFLD AND NASH.....	26
FIGURE 1.8   FREE FATTY ACID STRUCTURE .....	31

## CHAPTER II:

FIGURE 2.1   TIME LINE OF THE STUDY. ....	42
FIGURE 2.2   EFFECT OF DIETS, STREPTOZOTOCIN AND PIOGLITAZONE ON ANIMALS' BODY WEIGHT.....	44
FIGURE 2.3   EFFECT OF DIET, STREPTOZOTOCIN AND PIOGLITAZONE ON ANIMAL FOOD INTAKE. ....	45
FIGURE 2.4   EFFECT OF DIETS, STREPTOZOTOCIN AND PIOGLITAZONE ON WATER INTAKE .....	46
FIGURE 2.5   EFFECT OF DIETS, STREPTOZOTOCIN AND PIOGLITAZONE ON FASTING PLASMA GLUCOSE AND INSULIN. .....	47

## CHAPTER III:

FIGURE 3.1   TAQMAN REAL-TIME PCR STANDARD CURVE.....	64
FIGURE 3.2   EXAMPLE OF PROTEIN STANDARD CURVE FOR THERMO SCIENTIFIC PIERCE BCA PROTEIN KIT. ....	66
FIGURE 3.3   VISCERAL ADIPOSE TISSUE H&E STAINING AND ADIPOCYTE SIZING. ....	70
FIGURE 3.4   VISCERAL ADIPOSE TISSUE IMMUNOHISTOCHEMISTRY OF NON-IMMUNE-LABELLED SECTIONS. ....	71
FIGURE 3.5   RAT PAW SKIN TISSUE IMMUNOHISTOCHEMISTRY .....	72
FIGURE 3.6   VISCERAL ADIPOSE TISSUE IMMUNOHISTOCHEMISTRY.....	73
FIGURE 3.7   MACROPHAGE CLS FORMATION IN VISCERAL ADIPOSE TISSUE. ....	74
FIGURE 3.8   VISCERAL ADIPOSE TISSUE INFLAMMATORY GENE EXPRESSION.....	75
FIGURE 3.9   SKELETAL MUSCLE TISSUE INFLAMMATORY GENE EXPRESSION. ....	76
FIGURE 3.10   LIVER HISTOLOGY.....	77
FIGURE 3.11   LIVER TISSUE IMMUNOFLUORESCENCE. ....	78
FIGURE 3.12   RABBIT ANTI-CD86 LIVER TISSUE IMMUNOHISTOCHEMISTRY.....	78
FIGURE 3.13   WESTERN BLOT ANALYSIS OF KUPFFER CELL MARKERS IN LIVER TISSUE. ....	79

## CHAPTER IV:

FIGURE 4.1   GAS CHROMATOGRAMS. ....	96
FIGURE 4.2   TOTAL TRIGLYCERIDES ASSAY STANDARD CURVE .....	97
FIGURE 4.3   HFD EFFECT ON ADIPOSE, LIVER AND SKELETAL MUSCLE SREBP-1C MRNA EXPRESSION LEVEL. ....	100
FIGURE 4.4   LIVER PICO-SIRIUS RED STAIN. ....	102
FIGURE 4.5   LIVER TISSUE TAQMAN GENE ARRAY SIGNIFICANT CHANGES. ....	104
FIGURE 4.6   LIVER GENE ARRAY VALIDATION USING TAQMAN.....	105
FIGURE 4.7   LIVER TISSUE CHOP PROTEIN EXPRESSION.....	106
FIGURE 4.8   CHOP PROTEIN LOCALIZATION IN LIVER TISSUE .....	107

FIGURE 4.9   LIVER TISSUE TOTAL TRIGLYCERIDE CONTENT. ....	108
FIGURE 4.10   THIN LAYER CHROMATOGRAPHY OF LIVER TISSUE. ....	109
FIGURE 4.11   DIET TRIGLYCERIDES FATTY ACID COMPOSITION .....	110
FIGURE 4.12   LIVER TISSUE TRIGLYCERIDES FATTY ACID COMPOSITION .....	110
FIGURE 4.13   SKELETAL MUSCLE TISSUE TAQMAN GENE ARRAY SIGNIFICANT CHANGES. ....	112
FIGURE 4.14   SKELETAL MUSCLE TOTAL TRIGLYCERIDES .....	113

**CHAPTER V:**

FIGURE 5.1   HFD EFFECT ON BODY WEIGHT. ....	129
FIGURE 5.2   HFD EFFECT ON PLASMA GLUCOSE.....	130
FIGURE 5.3   LIVER HISTOLOGY.....	131
FIGURE 5.4   LIVER TISSUE TOTAL TRIGLYCERIDE CONTENT. ....	132
FIGURE 5.5   PLASMA LIPOPROTEIN TOTAL TRIGLYCERIDE CONTENT.....	133
FIGURE 5.6   VLDL/CHYLOMICRON TRIGLYCERIDE RATIO. ....	133
FIGURE 5.7   THIN LAYER CHROMATOGRAPHY OF PLASMA FRACTIONS' TOTAL LIPID EXTRACT. ....	134
FIGURE 5.8   DIET FATTY ACID COMPOSITION .....	134
FIGURE 5.9   PLASMA FRACTIONS TRIGLYCERIDES COMPOSITION .....	135

# List of Tables

---

## CHAPTER I:

TABLE 2-1   DIET COMPOSITION IN KCAL % .....	40
--	----

## CHAPTER III:

TABLE 3-1   DEHYDRATION/PARAFFIN EMBEDDING PROGRAM .....	58
TABLE 3-2   IMMUNOHISTOCHEMISTRY ANTIBODIES. ....	60
TABLE 3-3   CDNA REACTION MIXTURE. ....	62
TABLE 3-4   TAQMAN REACTION MIXTURE.....	63
TABLE 3-5   PRIMERS AND PROBES USED FOR TAQMAN GENE EXPRESSION ANALYSIS.....	64
TABLE 3-6   SDS PAGE ASSAY BUFFERS .....	66
TABLE 3-7   SDS PAGE GEL COMPONENT.....	67
TABLE 3-8   ANTIBODIES USED TO DETECT PROTEIN EXPRESSION USING WESTERN BLOTTING .....	68
TABLE 3-9   MACROPHAGE SUBTYPES MARKERS.....	71

## CHAPTER IV:

TABLE 4-1   SREBP-1C, PCK AND G6PC TAQMAN PRIMERS AND PROBES .....	87
TABLE 4-2   TAQMAN LOW DENSITY ARRAY GENE LIST. ....	87
TABLE 4-3   MOUSE ANTI-CHOP ANTIBODY .....	97
TABLE 4-4   LIVER TISSUE SCORING. ....	101
TABLE 4-5   LIVE TAQMAN GENE ARRAY SIGNIFICANT CHANGES. ....	103
TABLE 4-6   SKELETAL MUSCLE TAQMAN GENE ARRAY SIGNIFICANT CHANGES. ....	111

## CHAPTER V:

TABLE 5-1   DIET COMPOSITION IN KCAL % .....	125
--	-----

# List of Abbreviations

---

<b>Acetyl CoA</b>	ACETYL COENZYME A
<b>AFLD</b>	ALCOHOLIC FATTY LIVER DISEASE
<b>APS</b>	AMINOSILANE COATED SLIDES
<b>ATM</b>	ADIPOSE TISSUE MACROPHAGE
<b>BMI</b>	BODY MASS INDEX
<b>CHOP</b>	C/EBP HOMOLOGOUS PROTEIN
<b>ChREBP</b>	CARBOHYDRATE RESPONSIVE ELEMENT BINDING PROTEIN
<b>CLS</b>	CROWN-LIKE STRUCTURES
<b>CVD</b>	CARDIOVASCULAR DISEASE
<b>ER</b>	ENDOPLASMIC RETICULUM
<b>FAME</b>	FATTY ACID METHYL ESTER
<b>FAS</b>	FATTY ACID SYNTHASE
<b>G6P</b>	GLUCOSE 6 PHOSPHATE
<b>G6PC</b>	G6P CATALYTIC SUBUNIT
<b>GC</b>	GAS CHROMATOGRAPHY
<b>H&amp;E</b>	HAEMATOXYLIN AND EOSIN
<b>H2O2</b>	HYDROGEN PEROXIDE
<b>HDL</b>	HIGH DENSITY LIPOPROTEIN
<b>HFD</b>	HIGH FAT DIET
<b>IDL</b>	INTERMEDIATE DENSITY LIPOPROTEINS
<b>IL</b>	INTERLEUKIN
<b>iNOS</b>	INDUCIBLE NITRIC OXIDE SYNTHASE
<b>IRS1</b>	INSULIN RECEPTOR SUBSTRATE 1
<b>KBr</b>	POTASSIUM BROMIDE SOLUTION
<b>LDL</b>	LOW DENSITY LIPOPROTEINS
<b>LPL</b>	LIPOPROTEIN LIPASE
<b>MCP-1</b>	MONOCYTE CHEMOTACTIC PROTEIN-1
<b>NAFLD</b>	NON-ALCOHOLIC FATTY LIVER DISEASE
<b>NASH</b>	NON-ALCOHOLIC STEATOHEPATITIS
<b>NC</b>	NORMAL CHOW
<b>NEFA</b>	NON-ESTERIFIED FATTY ACIDS
<b>PAGE</b>	POLYACRYLAMIDE GEL ELECTROPHORESIS

<b>PBS</b>	PHOSPHATE BUFFERED SALINE
<b>PEPCK</b>	PHOSPHOENOLPYRUVATE CARBOXYKINASE
<b>PFA</b>	PARAFORMALDEHYDE
<b>PPAR</b>	PROLIFERATOR-ACTIVATED RECEPTORS
<b>PSR</b>	PICRO-SIRIUS RED
<b>PUFAs</b>	POLYUNSATURATED FATTY ACIDS
<b>RT</b>	REVERSE TRANSCRIPTASE
<b>SDS</b>	SODIUM DODECYL SULPHATE
<b>SOCS3</b>	CYTOKINE SIGNALLING SUPPRESSOR 3
<b>SREBP</b>	STEROL RESPONSIVE ELEMENT BINDING PROTEIN
<b>TBS</b>	TRIS BUFFER SALINE
<b>TLC</b>	THIN LAYER CHROMATOGRAPHY
<b>TLR4</b>	TOLL-LIKE RECEPTOR 4
<b>TNF<math>\alpha</math></b>	TUMOUR NECROSIS FACTOR A
<b>VLDL</b>	VERY LOW DENSITY LIPOPROTEINS

# **CHAPTER I:**

## **General Introduction**

## 1.1 Introduction

The World Health Organization reported that since 1980 worldwide obesity has more than doubled. In 2008, 1.5 billion adults aged 20 or older were overweight and almost 43 million children under the age of 5 were overweight in 2010. This raised concerns and pushed more resources to be spent on spreading awareness regarding the matter. A number of researchers conducted studies to understand complications caused by obesity, particularly insulin resistance, non-alcoholic fatty liver and metabolic syndrome (Shoelson *et al.*, 2007, Hotamisligil *et al.*, 1994, Bechmann *et al.*, 2012). This in turn raised some fascinating debates regarding dietary intake particularly surrounding sugar and fat. In the past few years, and while fat was marginalized, focus has turned toward sugar as being the major contributor to the burden of the biggest diseases in the modern world (Malhotra, 2013), Figure 1-1.



**Figure 1.1 | Media perceiving the effect of fat.**

Time Magazine covers from 1961, 1984 to 2014, showing how the media's perceived effect of fat changed over time. The concept changed from cholesterol and saturated fat being the key causative of cardiovascular diseases and metabolic syndrome to "fat is not the enemy" and it is not what cause all of those problems after all.

Sugar has been linked to weight gain (Maslova *et al.*, 2015), tooth decay and poor nutrition. Recently a 'low-carb diet' has been introduced as a way to

jump start weight loss, this came from the fact that once the body uses the stored glucose, in the form of glycogen, it starts burning the stored fat instead (Mobley *et al.*, 2009). Since most of our understanding regarding the metabolic syndrome has been linked to obesity, particularly in the case of sugar, the effect of both sugar and fat in the absence of weight gain was neglected. This made the study of early dietary effects of various macronutrients, especially fat, of interest. Therefore the introduction of this thesis will concentrate on the metabolic pathways of lipids and the complications associated with their excessive consumption.

## **1.2 Lipoproteins**

Lipids are naturally occurring compounds that are essential for various aspects of cellular biology including energy homeostasis, organ development and reproductive physiology. They are either hydrophobic or amphiphilic molecules and in order to be in an aqueous environment they are structured in vesicles or membranes. In plasma, these structures are known as lipoprotein complexes (Lee *et al.*, 2003). Their composition varies according to the classes of lipids (i.e. phospholipids, cholesterol or triglycerides) and are bound to specific proteins known as apo-lipoprotein. The lipoprotein molecule core is mainly formed by triglycerides and cholesterol esters with the surrounding surface as phospholipids and apo-lipoproteins (Roheim, 1986). The major lipids are classified as either triglyceride-rich lipoproteins including chylomicrons and very low density lipoproteins (VLDL) or cholesterol-rich lipoprotein which includes low density lipoproteins (LDL) and high density lipoprotein (HDL)

(Figure 1-2) (Lee *et al.*, 2003). The main function of these lipoproteins is the transportation of triglycerides and cholesterol in the circulation between dietary and liver lipids and peripheral tissue (Frayn, 2003). Circulating lipids are highly affected by diet and to better understand the consequence of diet-induced lipid changes it is important to recognise the pathways involved in its homeostasis.

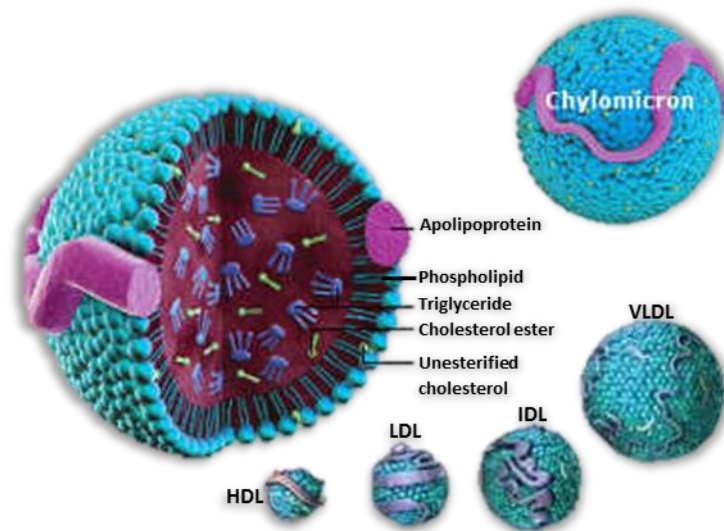


**Figure 1.2 | Lipoprotein composition.**

Lipoproteins are made up of a lipid core with cholesterol esters and triglycerides and an outer cover of phospholipids, cholesterol and Apo lipoprotein which is different according to the type of lipoprotein. Chylomicron are the largest of the lipoproteins followed by very low-density lipoproteins (VLDL), intermediate density lipoproteins (IDL), low-density lipoproteins (LDL) then high-density lipoproteins (HDL), modified from (Aizawa *et al.*, 2015, Sips *et al.*, 2014).

### 1.2.1 Chylomicron Metabolism: The Exogenous Pathway

Ingestion of fats stimulates secretion of cholecystokinin causing the gall bladder to contract and release bile into the duodenum (Glatzle *et al.*, 2003). The bile emulsifies and breakdown the fats allowing the intestinal epithelial cells to absorb triglycerides and esterified cholesterol, where they get processed by incorporation into the core of nascent chylomicrons (Ginsberg *et al.*, 2005). Triglycerides form approximately 90% of the chylomicrons' core and

the remaining 10% is comprised of phospholipids, cholesterol esters, free cholesterol and protein (Green and Glickman, 1981). Apo B-48 lipoprotein is the key protein for chylomicrons assembly (van Greevenbroek and de Bruin, 1998), once assembled the chylomicrons complexes are liberated into the circulation via basolateral site of enterocytes to lacteals and travel to the lymphatic system, into the thoracic duct then to the blood stream. In addition to the apo B-48 lipoprotein, chylomicrons also carry various apo A lipoproteins (Frayn, 2003) and as they circulate they further acquire apo C and apo E lipoproteins (Ginsberg *et al.*, 2005). While in the blood stream, the chylomicron triglycerides are hydrolysed by the enzyme lipoprotein lipase (LPL). Once hydrolysed, free fatty acids are then translocated to functional sites at the endothelial cells' luminal surface (Wang and Eckel, 2009).

Triglyceride hydrolysis releases glycerol and non-esterified fatty acids (NEFA). NEFA can either be re-esterified upon entry to adipocytes with glycerol-3-phosphatase for triglyceride storage or liberated into the NEFA systemic pool for peripheral tissue uptake (Frayn, 2003, Green and Glickman, 1981). The outcome of the hydrolysis process is smaller chylomicron remnants that have altered surface phospholipid composition, apo C lipoprotein is reduced to 20%, and enriched in dietary-derived cholesterol ester and apo E (Cooper, 1997, Ginsberg *et al.*, 2005). The residual particles are conveyed to the liver where they are either directly cleared by the lipoprotein receptor-related protein (LRP) receptor or further hydrolysed by hepatic lipase (Crawford and Borensztajn, 1999). Evidence indicates that the LDL receptor in the liver

recognizes the chylomicron remnants through apo E that they acquire in the circulation (Cooper, 1997).

### **1.2.2 VLDL Metabolism: The Endogenous Pathway**

The liver produces VLDL, it forms the surface of the VLDLs by assembling apo B-100 lipoprotein, phospholipids and free cholesterol while the triglycerides and esterified cholesterol are assembled in the core of the molecule (Davis *et al.* 1982). Other apo-lipoproteins, including apo C and apo E, that are of hepatocyte origin are present on the nascent VLDL particles, however after their entry to the circulation the majority is transferred to HDL (Ginsberg *et al.*, 2005, Frayn, 2003). Plasma VLDL and chylomicron share a common catabolic pathway as they are both substrates for LPL (Frayn, 2003). Upon hydrolysis, VLDL releases NEFA and glycerol which form a smaller and denser VLDL, with 50% less apo C lipoprotein, and, successively, intermediate density lipoproteins (IDL) (Qin *et al.*, 2011, Kwiterovich, 2000). Similar to the chylomicrons, the liver LDL receptor and LDL receptor related protein interact with apo E and apo B-100 to clear the IDL particles (Mahley and Ji, 1999). Hepatic lipase can alternatively further hydrolyse IDL triglycerides to produce LDL which is rich in cholesterol. LDL receptor also removes IDL by uptake into tissues (Frayn, 2003).

### **1.2.3 HDL Metabolism and Reverse Cholesterol Transport**

Reverse cholesterol transport is a multi-step metabolic process that results in the net movement of cholesterol from peripheral tissues to the liver, and as such it plays a major role in controlling body cholesterol homeostasis. HDL

particles are the main players in this mechanism which is inversely related to atherosclerotic events (Hersberger and von Eckardstein, 2003, Franceschini *et al.*, 1991). However, this mechanism is beyond the scope of this thesis hence it will not be further discussed

#### **1.2.4 Regulation of Lipoprotein Metabolism**

Lipoprotein metabolism is tightly controlled by insulin particularly the post-absorptive and postprandial states (Sparks and Sparks, 1994). During the post absorptive state, the drop in insulin levels upregulates adipocytes lipolytic activity liberating NEFA and triglycerides into the circulation (Frayn, 2003) where the key player in the mechanism is HSL (Holm, 2003, Haemmerle *et al.*, 2002). Another class of important lipolysis stimulators are catecholamines that are released within the adipose tissue by sympathetic innervations with HSL as a major target of this regulation (Holm, 2003). Triacylglycerol hydrolase and adipose triglyceride lipase are also adipose tissue lipases involved in the lipolysis process (Soni *et al.*, 2004, Schweiger *et al.*, 2006). Skeletal muscles predominately uptake the NEFA released in the circulation as an oxidative fuel substrate and the liver uses NEFA either for beta oxidation or the production of VLDL-triglycerides. There is evidence indicating that VLDL and chylomicrons compete for LPL hydrolysis (Karpe *et al.*, 1993, Bjorkegren *et al.*, 1996). Even though chylomicrons, due to their larger size, appear to be the favoured LPL substrate (Karpe *et al.*, 1993), chylomicron removal is said to be a saturation prone process due to the limited LPL activity (Goldberg, 1996). Lipolysis that is mediated by LPL causes NEFA release which are then up taken by FAT/CD36

receptors that are located on the surface of adipocytes and myocytes (Goldberg *et al.*, 2009). Fatty acids are converted to Acyl CoA and undergo mitochondrial beta oxidation to provide direct energy or are used for storage (Dallinga-Thie *et al.*, 2010, Preiss-Landl *et al.*, 2002). Meanwhile, adipocyte lipolysis is inhibited by insulin through its inhibitory mechanism on adipose tissue HSL which in turn suppresses NEFA release from the adipocytes. Furthermore, insulin stimulates the re-esterification of NEFA that is produced within the adipose tissue (Frayn, 2003). There are in vitro (Taniguchi *et al.*, 2000) and in vivo (Malmström *et al.*, 1998) studies that have uncovered evidence showing that hepatic apo B-100 is acutely suppressed by insulin. This suggests that VLDL-triglyceride secretion is mostly likely inhibited in the postprandial period. This is partially due to the lack of NEFA as a substrate to produce hepatic VLDL-triglycerides since their flux to the liver is interrupted (Frayn, 2003). This is supported by findings in which intralipid/heparin-induced NEFA have been shown to stimulate hepatic and intestinally derived triglyceride-rich lipoprotein particle production in healthy humans in the fed state (Pavlic *et al.*, 2010). All of the above metabolic events emphasise insulin's important role during the postprandial state in the regulation of substrate metabolism. Hence any dysregulation in insulin secretion or development of insulin resistance leads to postprandial lipid metabolism perturbations (DeFronzo and Ferrannini, 1991).

### 1.3 Adipose tissue and inflammation

Adipose tissue is considered as an endocrine organ that has the ability to secrete adipocyte-derived cytokines. It is the storage unit for any excess fatty acids. Adipose tissue expansion leads to several complications including Type 2 Diabetes, cardiovascular disease (CVD), stroke, hypertension, hypercholesterolemia, and non-alcoholic fatty liver disease (NAFLD) (Shoelson *et al.*, 2007). Even though our understanding of the underlying mechanism is incomplete, growing evidence around the low-grade inflammation that presents with obesity delivers a molecular link to some of these comorbidities.

Epidemiologic evidence linking obesity and inflammation has existed for many decades. For instance, fibrinogen levels in obese patients and other acute phase reactants were found to be increased (Grace and Goldrick, 1968, Bennett *et al.*, 1966). Recent epidemiologic studies have supported and extended these findings as they provided evidence for an increase in pro-inflammatory cytokines and chemokines such as Tumour necrosis factor  $\alpha$  (TNF $\alpha$ ), monocyte chemoattractant protein-1 (MCP-1) and Interleukin-6 (IL-6) (Yang *et al.*, 2006, Christiansen *et al.*, 2005). Interestingly, the development of obesity-induced comorbidities can be predicted by the circulating levels of some inflammatory factors, suggesting a fundamental link between obesity-associated pathologies and inflammation (Pradhan *et al.*, 2001). That being said, the primary source of inflammatory molecules released in obesity appears to be macrophages resident in the adipose tissue (Weisberg *et al.*, 2003). During obesity, increased body mass index (BMI) is directly related to adipose tissue macrophage

accumulation (Weisberg *et al.*, 2003, Xu *et al.*, 2003). In fact, where there is an increased proportion of adipose tissue macrophages there is a linear increase in the expression of pro-inflammatory cytokines (Lumeng *et al.*, 2007b).

### **1.3.1 Macrophage Infiltration into Adipose Tissue in Obesity**

Macrophage infiltration into adipose tissue during obesity has been firmly established yet the mechanisms behind recruitment remain unclear. Some hypotheses include: lipid oversupply, hypoxia and adipocyte cell death, and increased expression of cytokines that initiate recruitment (Figure 1-2).

In many cases, the development of obesity is associated with over-nutrition, including lipid oversupply. Saturated fatty acids, in particular, have been linked with instigating inflammation via the activation of macrophage toll-like receptor 4 (TLR4) (Nguyen *et al.*, 2007, Lee *et al.*, 2001). Upon stimulation, TLR4 activates the I $\kappa$ B kinase  $\beta$ /nuclear factor  $\kappa$ B (IKK $\beta$ /NF- $\kappa$ B) signalling cascade, ultimately resulting in translocation of NF $\kappa$ B into the nucleus to upregulate the transcription of inflammatory cytokines (Tsukumo *et al.*, 2007, Ghanim *et al.*, 2004). As the adipose tissue expands in obesity, sufficient vascularization often fails to occur (Pang *et al.*, 2008), creating a hypoxic environment (Hosogai *et al.*, 2007). Not only does hypoxia directly increase the expression of inflammatory genes in both adipocytes and adipose tissue macrophages, but it also results in adipocyte death (Ye *et al.*, 2007). Consequently, macrophages infiltrate the adipose tissue to phagocytose the dead or dying cells, Figure 1-2. Adipose tissue expansion heightens the expression of signalling molecules that promote macrophage infiltration,

including MCP-1, adhesion molecules, and leptin. The expression of MCP-1, a chemo-attractant for macrophages, increases with adipose tissue hypertrophy, effectively recruiting circulating bone-marrow derived monocytes into the adipose tissue (Tsou *et al.*, 2007). Endothelial cell adhesion molecules are necessary for immune cells to migrate from the circulation into the adipose tissue. During obesity the expression of intercellular adhesion molecule increases, which facilitates the transport of macrophages into the adipose tissue (Brake *et al.*, 2006). Finally, leptin, a hormone associated with metabolism and appetite, may also attract macrophages to the adipose tissue, either by directly recruiting immune cells (Gruen *et al.*, 2007) or by increasing the expression of endothelial cell adhesion molecules (Curat *et al.*, 2004).

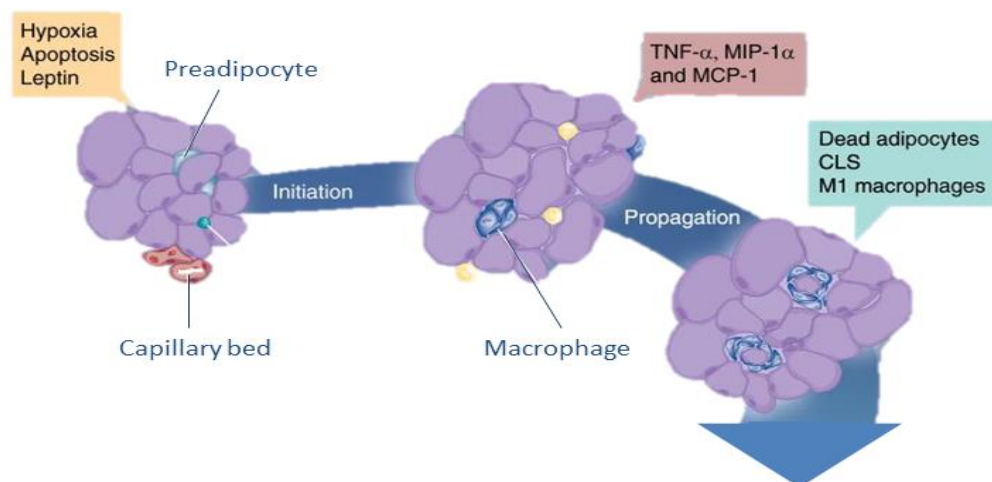


**Figure 1-2| macrophage infiltration Stages into adipose tissue obesity**

Macrophages are recruited during weight gain to the expanding adipose tissue (AT). Factors released by adipocytes initiate this process leading to the migration immune cells including macrophages to the tissue. AT macrophages (ATM) secretes inflammatory cytokines which contributes to the recruitment of additional macrophages causing a propagation of inflammation. This contributes to the remodelling of AT. Moreover there is an increase in the turnover of M2 to M1 macrophages. CLS: Crown-like structures; MCP-1: Monocyte chemoattractant protein-1; MIP-1α: Macrophage inflammatory protein 1α. *Adapted from: (Surmi and Hasty, 2008).*

While many different subpopulations of macrophages likely exist at any given time, macrophages are largely grouped as either classically or

alternatively activated. Classically activated, or M1, macrophages typically express pro-inflammatory cytokines, while alternatively activated, or M2, macrophages express anti-inflammatory cytokines. Inflammatory markers that characterize M1 macrophages include TNF $\alpha$ , IL6, IL1 $\beta$ , and the induction of inducible nitric oxide synthase (iNOS). M2 macrophages are associated with increased production of the anti-inflammatory cytokine IL10 and arginase (Lumeng *et al.*, 2008). In the adipose tissue of lean mice, macrophages are typically alternatively activated, i.e. fall under M2 phenotype. However, during obesity the polarization of adipose tissue macrophages changes from M2 to M1 (Lumeng *et al.*, 2007b). Interestingly, the change in polarization of adipose tissue macrophages may not be caused by a “switch” of resident M2 macrophages to the M1 polarization, but appears to be due to increased recruitment of inflammatory M1 macrophages from the circulation (Lumeng *et al.*, 2008).

Regardless, the shift from M2 to M1 adipose tissue macrophages has significant implications for insulin resistance. M2 macrophages have the potential to protect the adipose tissue from inflammation, while M1 macrophages have been shown to contribute to insulin resistance (Lumeng *et al.*, 2007b), Figure 1-3. An important characteristic of inflammatory macrophages found in the adipose tissue is the formation of crown-like structures (CLS). Large, multi-nucleate aggregations form around dead adipocytes as the macrophages scavenge free fatty acids (Cinti *et al.*, 2005). In obese mice, these macrophages show unique dendritic-cell specific markers

which are not found on macrophages of lean mice and is likely involved in the formation of the CLS (Lumeng *et al.*, 2008).

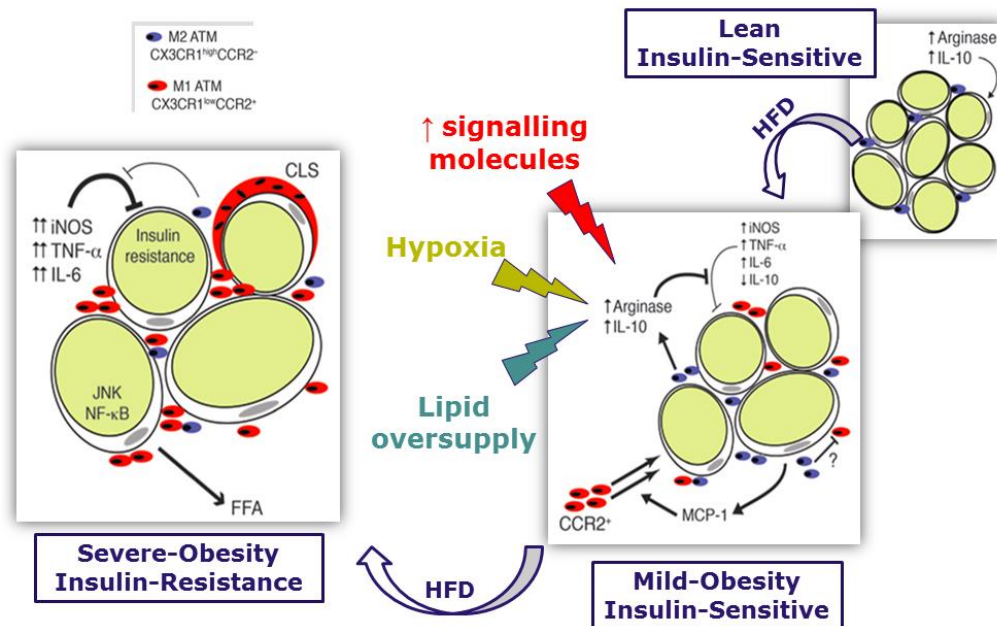


**Figure 1.3 | Mechanism of adipose tissue macrophage Polarization.**

In insulin-sensitive lean state, ATMs are polarized toward an M2 state with anti-inflammatory properties; expressing IL-10 and arginase. Adipocytes undergo hypertrophy during HFD treatment this cause the release of M1 attracting chemokines increasing iNOS and TNF- $\alpha$  production. With increased adiposity, M1 macrophages form crown like structures alongside heightened levels of TNF- $\alpha$  and iNOS which in turn leads to insulin resistance in adipocytes. ATM: Adipose tissue macrophages, HFD: High Fat Diet. *Modified from: (Lumeng et al., 2007b).*

As one of the most widely studied inflammatory cytokines, TNF $\alpha$  provides a valuable example of how pro-inflammatory cytokines directly affect insulin signalling and glucose uptake (Pedersen, 2006). In healthy individuals, insulin stimulates the insulin receptor to phosphorylate tyrosine residues of insulin receptor substrate 1 (IRS1), which is required for the normal biological action of insulin on a cell. However, TNF $\alpha$  interferes with the insulin receptor and decreases insulin-stimulated tyrosine phosphorylation, causing a blunted, or resistant, response to insulin (Hotamisligil *et al.*, 1994). Other inflammatory markers that affect insulin sensitivity are summarized in Figure 1-4.

Overall the excess flux of fatty acids to the adipose tissue leads to its

expansion which in turn leads to chronic inflammation and an insulin resistant state in the adipose tissue. Furthermore, increased adipocyte size and insulin resistance lead to increased release of fatty acids. This increases the total fatty acids in circulation, in turn influencing other organs, mainly the liver and skeletal muscle. This effect will be discussed later in this literature review.

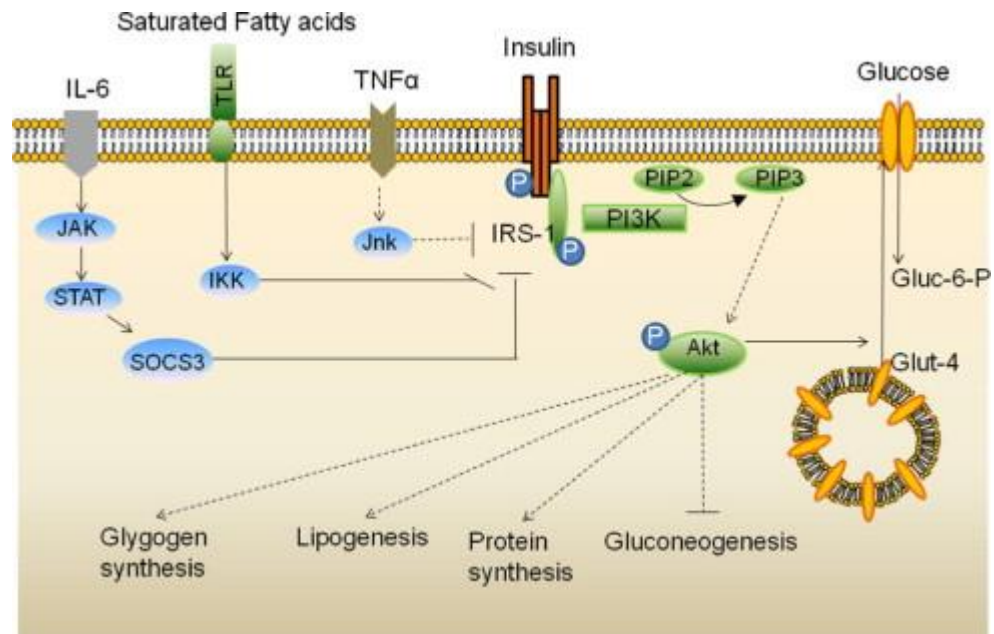


**Figure 1.4 | Inflammation and Insulin Resistance**

C-Jun kinase (JNK), is activated by pro-inflammatory cytokines or free fatty acids (FFA) increasing inflammatory cytokine production and also phosphorylates and inhibits IRS1 at Ser307 disrupting insulin signalling. The suppressor of cytokine signalling 3 (SOCS3) expression increases in response to the activation of the Janus kinase (JAK)/Signal Transducer and Activator of Transcription (STAT) pathway by inflammatory cytokines then it interferes with the insulin receptor and inhibits tyrosine phosphorylation of IRS1. In adipose tissue, SOCS3 also promotes the degradation of IRS1. Toll like receptor (TLR4) activation promotes intracellular inflammatory pathways associated with insulin resistance, including the IKK  $\beta$  signalling cascade. *Obtained from (Kalupahana et al., 2012)2.*

## 1.4 Overview of hepatic fatty acid metabolism

The liver is the key player in lipoprotein and free fatty acid metabolism. Lipoproteins are circulated through the liver and free fatty acid uptake from plasma, beta oxidation, *de novo* synthesis and secretion are largely controlled by the liver. Free fatty acids have a major effect on the expression level of many

key genes and since they serve as ligands for a number of transcription factors that are crucial in the regulation of fat and glucose metabolism.

#### **1.4.1 Hepatic Triglyceride Metabolism**

The production of hepatic VLDL-triglyceride is determined by the individual nutritional and hormonal states however it is mostly substrate driven. As described previously the assembly and secretion of VLDL is a twostep process (Alexander *et al.*, 1976). Initially, core lipids are associated with apo B where microsomal triglyceride transfer protein plays an important part as it catalyses the transfer of lipids to apo B. This immature particle then fuses with lipid droplets to produce a mature VLDL particle. This step is mainly influenced by the flux of fatty acids to the liver and its triglyceride content. That being said, this association is not always straightforward. Total triglycerides that accumulate within the liver do not directly determine the level of VLDL production. In vivo experiments on rats has demonstrated that the acute stimulation of *de novo* lipogenesis leads to steatosis with no effect on the production of VLDL (Bandsma *et al.*, 2001). Similarly, increased liver free fatty acid flux is not always a cause for increased VLDL production, Figure 1-5 (Goudriaan *et al.*, 2005).

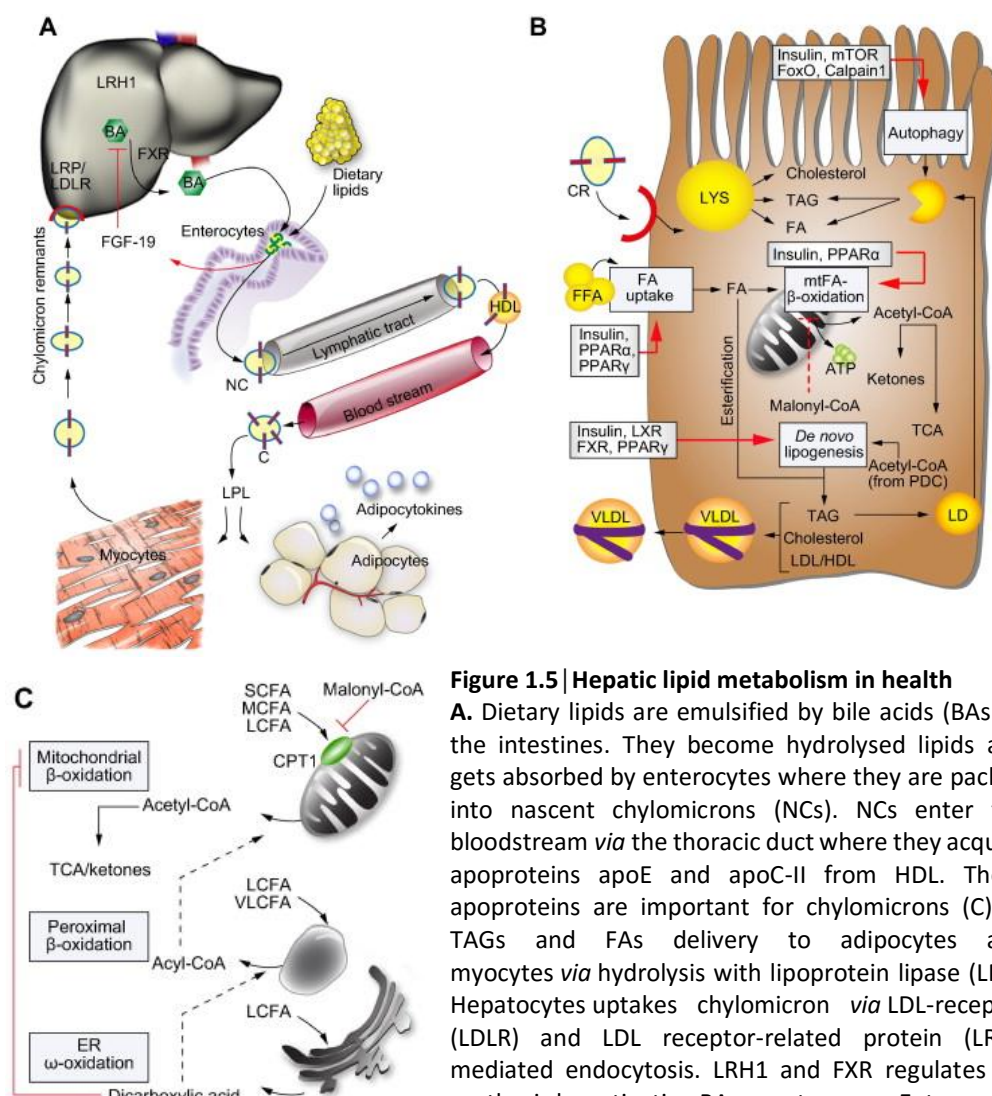


**Figure 1.5 | Hepatic lipid metabolism in health**

**A.** Dietary lipids are emulsified by bile acids (BAs) in the intestines. They become hydrolysed lipids and gets absorbed by enterocytes where they are packed into nascent chylomicrons (NCs). NCs enter the bloodstream *via* the thoracic duct where they acquire apoproteins apoE and apoC-II from HDL. These apoproteins are important for chylomicrons (C) to TAGs and FAs delivery to adipocytes and myocytes *via* hydrolysis with lipoprotein lipase (LPL). Hepatocytes uptake chylomicron *via* LDL-receptor (LDLR) and LDL receptor-related protein (LRP)-mediated endocytosis. LRH1 and FXR regulates BA synthesis by activating BA export pumps. Enterocytes re-uptakes BA stimulates the release of FGF-19 into the portal blood, this inhibits BA synthesis

**B.** insulin (Ins) and nuclear receptor signalling regulates the uptake of adipose tissue derived free fatty acids (FFA) by various FA transporters. Under physiological conditions, the bulk of FAs is oxidized intra-mitochondrially and providing ATP and acetyl-CoA for the tricarboxylic acid cycle (TCA). Lipogenesis triglycerides (TAGs) are either stored in lipid droplets (LD) or packed into VLDL and exported into the blood stream. Acetyl-CoA for lipogenesis is provided by the pyruvate dehydrogenase complex (PDC), which catalyzes oxidation of pyruvate, the end product of glycolysis.

**C.** Under physiological conditions,  $\beta$ -oxidation of short-, medium- and long-chain FAs (SCFA, MCFA, LCFA) are degraded in mitochondria. Therefore, FAs are activated to acyl-CoA and shuttled across the mitochondrial membrane by carnitine palmitoyltransferase-1 (CPT1). Malonyl-CoA, an intermediate of lipogenesis, inhibits CPT1 and thus FA oxidation in the mitochondria. *Obtained from (Bechmann et al., 2012).*

#### 1.4.2 Hepatic Fatty Acid Metabolism

The majority of long and medium chain fatty acids entering the liver are subjected to mitochondrial  $\beta$ -oxidation while the very long fatty acids chain are predominantly oxidized in the peroxisome. While fasting, fatty acids entering

the liver are metabolized to acetyl coenzyme A (acetyl CoA) which is then used to form ketone bodies that are then used as fuel by other tissues. Once the liver fatty acid flux exceeds  $\beta$ -oxidation capacity this can lead to triglyceride accumulation within the liver.

Fatty acids are constantly being esterified to triglycerides to be used for hepatic VLDL synthesis and secretion. For instance plasma VLDL-triglycerides are derived from plasma fatty acids that were re-esterified by the liver and secreted to the plasma, Figure 1-5 (Frayn, 2003, Eaton *et al.*, 1996).

### **1.4.3 Hepatic glucose metabolism**

The most important energy source in the mammalian body is glucose particularly for the brain as it depends on glucose being readily available. That being said, disturbance in plasma glucose concentrations leads to complications including diabetes, neuropathy, kidney failure and many others, hence glucose levels need to be controlled tightly. Blood glucose levels are determined by the balance between dietary uptake in the intestines, glucose uptake by peripheral tissues and the production of glucose by the liver. The liver is a key player when it comes to glucose homeostasis, it does this by controlling the balance of release and uptake of glucose (Bechmann *et al.*, 2012). The molecular mechanism behind the regulation of hepatic glucose metabolism is illustrated in Figure 1-6.

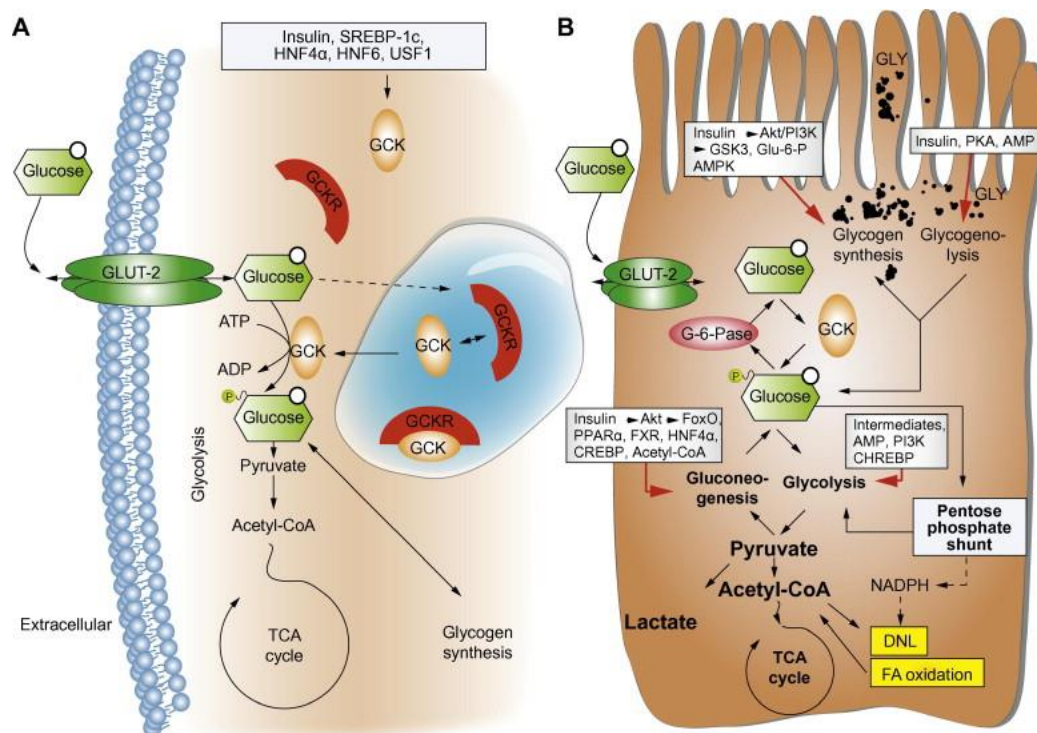


**Figure 1.6 | Regulation of hepatic glucose metabolism.**

**A.** Glucose (Glu) is absorbed by the intestine and then delivered to the hepatocyte *via* the portal vein. The glucose transporter 2 (GLUT2), which is insulin-independent, shuttles Glu across the membrane. Abundance of glucose induces conformational changes of the glucokinase regulatory protein (GSKR), which binds to glucokinase (GSK) and keeps it in the nucleus in the fasting state. GSK is then released into the cytosol and phosphorylates Glu to glucose-6-phosphate (Glu-6-P); depending on the nutritional state, it serves as a substrate for glycolysis or glycogen synthesis, respectively. GSK is transcriptionally regulated by insulin and nuclear receptor signaling. **B.** Glu-6-P is a central intermediate in the hepatic glucose metabolism. It is degraded during glycolysis, which provides energy in the form of two ATP and two NADH molecules per glucose molecule. The product pyruvate is further decarboxylated to acetyl-CoA, which enters the intramitochondrial tricarboxylic acid cycle (TCA). Alternatively, Glu-6-P is degraded in the pentose-phosphate shunt, which provides NADPH, a co-substrate for DNL. Acetyl-CoA is an important product of the TCA, linking glucose and lipid metabolism. Gluconeogenesis and glycogenolysis provide Glu-6-P as a substrate for glucose synthesis in the fasting state. Glycogenolysis is catalyzed by glycogen phosphorylase, activated by AMP, and repressed by insulin. The key enzyme in gluconeogenesis is PECK, which is repressed by insulin signaling *via* Akt-mediated FoxO phosphorylation and activated by PPAR $\alpha$ . *Obtained from (Bechmann et al., 2012).*

Excess glucose is stored in the form of glycogen. Since the liver's storage capacity is limited, not all glucose can be stored as glycogen. The excess is broken down to acetyl CoA to be used in *de novo* lipogenesis.

In the fasting state the human body is dependent upon the liver to produce glucose and to a lesser extent the kidneys as well (Ekberg *et al.*, 1999). During

the early phase of fasting, the liver produces glucose by hydrolysing glycogen. It is a three step process that starts with glycogen phosphatase mediated-cleavage of a single glucose-1-phosphate then a debranching enzyme converts glucose-1-phosphate to G6P. Finally, and under the control of glucose-6 phosphatase (G6Pase), G6P is dephosphorylated to glucose (Nordlie *et al.*, 1993). Other substrates including amino acids, glycerol, pyruvate and lactate could be used for liver gluconeogenesis as an alternative way to maintain blood glucose levels (Exton and Park, 1967). The latter mechanism is controlled by phosphoenolpyruvate carboxykinase (PEPCK). During prolonged periods of fasting the liver progressively increases gluconeogenesis to protect against complete breakdown of the glycogen stores (Tirone and Brunicardi, 2001).

#### **1.4.4 Insulin action**

Insulin is a hormone produced by pancreatic  $\beta$ -cells. It is secreted in response to increased levels of blood glucose in a biphasic manner. The initial burst is secreted as preformed insulin secretory granules are exocytosed and lasts around 5 to 15 minutes. That stimulates the biosynthesis of new insulin molecules and results in a more sustained secretion. Once in circulation, insulin binds to insulin receptors which in turn leads to a phosphorylation cascade and activation of downstream target genes. Insulin plays a crucial role in hepatic VLDL and glucose outputs (Saltiel and Kahn, 2001). Liver, skeletal muscle and adipose tissue are the main organs targeted by insulin and the overall net result of its action is fuel storage of both glucose and lipids. Insulin exerts a direct effect on VLDL production although the mechanism behind this effect remains

unclear (Lewis and Steiner, 1996), it is thought that because insulin accelerates apo B degradation (Fisher *et al.*, 2001) it decreases VLDL secretion. Moreover it has an indirect inhibitory effect on hormone sensitive lipase again decreasing VLDL secretion indirectly. This decrease in triglyceride hydrolysis by hormone sensitive lipase leads to decreased flux of fatty acids of the liver and consequently decreased substrate availability for hepatic VLDL synthesis.

The rate of hepatic glycogen breakdown is regulated by G6P, which is regulated by PEPCK, and is determined by hepatic glucose output (Foster *et al.*, 1997). In the fed state insulin inhibits hepatic glucose output via inhibition of the two mentioned regulatory enzymes. The action of insulin on stimulating glucose uptake in peripheral tissue including skeletal muscle and adipose tissue is similar to that of the liver. It stimulates the translocation of the glucose transporter-4 (Glut-4) mediating uptake of glucose (Fukumoto *et al.*, 1989).

#### **1.4.5 Interactions of glucose and lipid metabolism**

In the liver, glucose and lipid metabolism are closely related. When glucose availability is decreased, glucose oxidation also drops and the need for fatty acid oxidation increases.

In 1963, Randle postulated glucose-fatty acid cycle. Based on experimental evidence, this cycle states that the availability of fatty acid determines the rate of fatty acid oxidation and that fatty acid oxidation directly inhibits glucose oxidation (Randle *et al.*, 1963). Several mechanisms have been proposed to explain this link between fatty acids and glucose oxidation including the accumulation of intermediates of fatty acid and glucose metabolism (Randle *et*

*al.*, 1994). Some studies investigated the effects of increasing plasma fatty acids by infusion but observed no effects on the intermediates such as citrate or glucose 6 phosphate (G6P) levels (Boden *et al.*, 1994, Goodman *et al.*, 1974). On the other hand the infusion of lipids or fatty acids can induce insulin resistance leading to decreased uptake of glucose. However, this does not automatically include decreased glucose oxidation. When plasma fatty acid levels were increased during hyperinsulinemic hyperglycemic clamp conditions, no effects on glucose oxidation were observed. Therefore, it was proposed that glucose availability may be the most important determinant for substrate utilisation (Wolfe, 1998).

Transcription factors in the liver can be significantly affected by fatty acids (Jump *et al.*, 2005). For instance fatty acids directly activate peroxisome proliferator-activated receptors (PPAR)  $\alpha$  leading to the induction of hepatic fatty acid oxidation (Xu *et al.*, 1999). Furthermore fatty acids inhibit hepatic fatty acid production via suppressing sterol responsive element binding protein-1c (SREBP-1c). On the other hand, glucose can activate carbohydrate responsive element binding protein (ChREBP) (Towle, 2001). Most lipogenic enzyme gene promoters have response elements for binding ChREBP and SREBP1c. These two factors work synergistically to induce transcription of the lipogenic enzyme genes in the presence of glucose and insulin. The activation of both ChREBP and SREBP1c can be inhibited by glucagon and fatty acids. In this way the control of expression of lipogenic enzyme genes is regulated in an integrated manner by multiple nutrient and hormonal signals. Taken together, fatty acids and glucose control hepatic lipid content and the type and quantity

of lipids available for hepatic VLDL-triglyceride production. Ultimately, increased plasma levels of fatty acids and glucose contribute to the onset and progression of chronic diseases such as atherosclerosis, diabetes and obesity (Jump *et al.*, 2005). It may well be that the interactions between glucose and fatty acid metabolism may be dependent on the circumstances and on tissue specific mechanisms. Nevertheless, all evidence points towards important interactions between glucose and fatty acid metabolism.

### **1.5 Non-Alcoholic Fatty Liver Disease (NAFLD)**

Humans are generally comprised of 10-30% adipose tissue by body weight. This composition provides the human body with the ability to store large amounts of triglycerides, reflected by the ability of humans to develop obesity. Liver and skeletal muscle cells can also store triglycerides to a much lesser degree. Fatty liver, or hepatic steatosis, is the histopathological condition indicated by an increase in the storage of lipids in hepatocytes. Depending on the condition and progression of the disease several distinct forms of Hepatic Steatosis can be discerned. While the most well known cause of hepatic steatosis is excessive, repeated alcohol consumption, this thesis concentrates on non-alcoholic fatty liver disease.

In the post-absorptive state non-oxidised fatty acids are taken up by organs, with liver and adipose tissue being central to this process. Hepatic steatosis occurs when the input of fatty acids into the liver exceeds fatty acid oxidation and output of VLDL. Even though hepatic steatosis occurs mostly in obese and overweight persons it can be observed in humans with a normal BMI.

The prevalence of fatty liver disease in the general public is estimated at between 3% to 24%, with most estimates in the range of 6% to 14% (Clark, 2006), though levels are much higher for obese and diabetic populations. Patients who are considered eligible for bariatric surgery have a BMI of  $\geq 40$  kg/m<sup>2</sup> or, if there are other extenuating factors like type 2 diabetes,  $\geq 35$  kg/m<sup>2</sup>. In this fraction of the population the prevalence of Fatty Liver Disease is estimated to range from 84% to 96% (Clark, 2006). In about half of subjects with Hepatic Steatosis the condition progresses to fibrosis, 15% progressed to cirrhosis and 3% eventually experienced liver failure or required a liver transplant (Sheth *et al.*, 1997). Hepatic Steatosis also affects the metabolism of glucose and lipids in the liver and can potentially extend these effects to the rest of the body.

### **1.5.1 Metabolic pathways leading to lipid accumulation**

The main concern about NAFLD, aside from insulin resistance and affecting whole body lipid metabolism, is that it could lead to steatohepatitis. While the exact biochemical pathway of Non-Alcoholic steatohepatitis (NASH) is not fully understood there exist strong links between the accumulation of triglycerides and inflammation in the liver. Potential reasons for dietary fat accumulation in NAFLD could be i) high amount of fat intake into the liver through chylomicrons, ii) a suppression of mitochondrial beta-oxidation in the liver, iii) a high influx of non-esterified fatty acids from adipose tissue to the liver (lipolysis), iv) fatty acids formed within the liver via *de novo* lipogenesis or v) a low secretion rate of VLDL by the liver (Dallinga-Thie *et al.*, 2010). However the relative

contribution of each of these pathways, and the effect of genetic predisposition and diet/environmental factors in the development of NAFLD remains unclear.

There appear to be more factors beyond increased NEFA delivery that connect visceral obesity and steatosis. Adipocyte derived proinflammatory cytokine TNF $\alpha$  and adipokine adiponectin are the main regulators of hepatic metabolic homeostasis (Tilg and Hotamisligil, 2006). Increased TNF $\alpha$  and reduced adiponectin production are independent characteristics of visceral adiposity and NAFLD. Notably, this causes a pro-inflammatory and insulin resistant state (Schäffler *et al.*, 2005). This suggests that the effects of both adiposity and insulin resistance on metabolic processes in the liver are directly linked.

### **1.5.2 NAFLD and the development of NASH**

NASH is the term used to describe the accumulation of fat in the liver which has progressed to include fibrosis and inflammation (Neuschwander-Tetri and Caldwell, 2003, Harmon *et al.*, 2011). Although fatty liver may be a benign state it can under some circumstances progress to NASH and then cirrhosis which is characterised by inflammation, oxidative stress and scarring (Angulo, 2002). The multiple factors that lead to this progression are uncertain, but involve the production of pro-inflammatory cytokines, activation of stellate cells, dysregulation of lipolysis and lipogenesis (Postic and Girard, 2008) and oxidative changes possibly influenced by the type of fat (Stanton *et al.*, 2011). Figure 1-6 illustrates the 2-hit hypothesis explaining the progression of NAFLD

then to NASH. This hypothesis states that insulin resistance and reduced hepatic fatty acid oxidation causes NAFLD and the progression from steatosis in the presence of inflammation leads to fibrogenesis (Day and James, 1998).

## **1.6 Interactions between diet and NAFLD**

Studies regarding nutritional effects in the liver raised speculations that dietary macronutrient intakes have a specific role in NAFLD aetiology rather than just excessive caloric intake (Sullivan, 2010). The source of most hepatic lipids is from dietary intake, either from ingested carbohydrates or fat. The composition of a diet has been shown to be a potent inducer and suppressor of major pathways in hepatic fatty acid metabolism.

### **1.6.1 Dietary history assessments in NAFLD**

Assessments of dietary intake taken prior to bariatric surgery do not accurately represent long term dietary patterns. It is common for patients undergoing bariatric surgery to over-report actions and dietary patterns that contribute to weight loss, such as calorie restriction. Several studies compared the diets of patients with NAFLD that haven't undergone bariatric surgery with those of healthy controls (Musso *et al.*, 2003, Cortez-Pinto *et al.*, 2006, Allard *et al.*, 2008, Oya *et al.*, 2010). However only a couple studies have matched their controls BMI to their investigated group. Together with possible underreporting of dietary intake, the reliability of this data comes in to question.

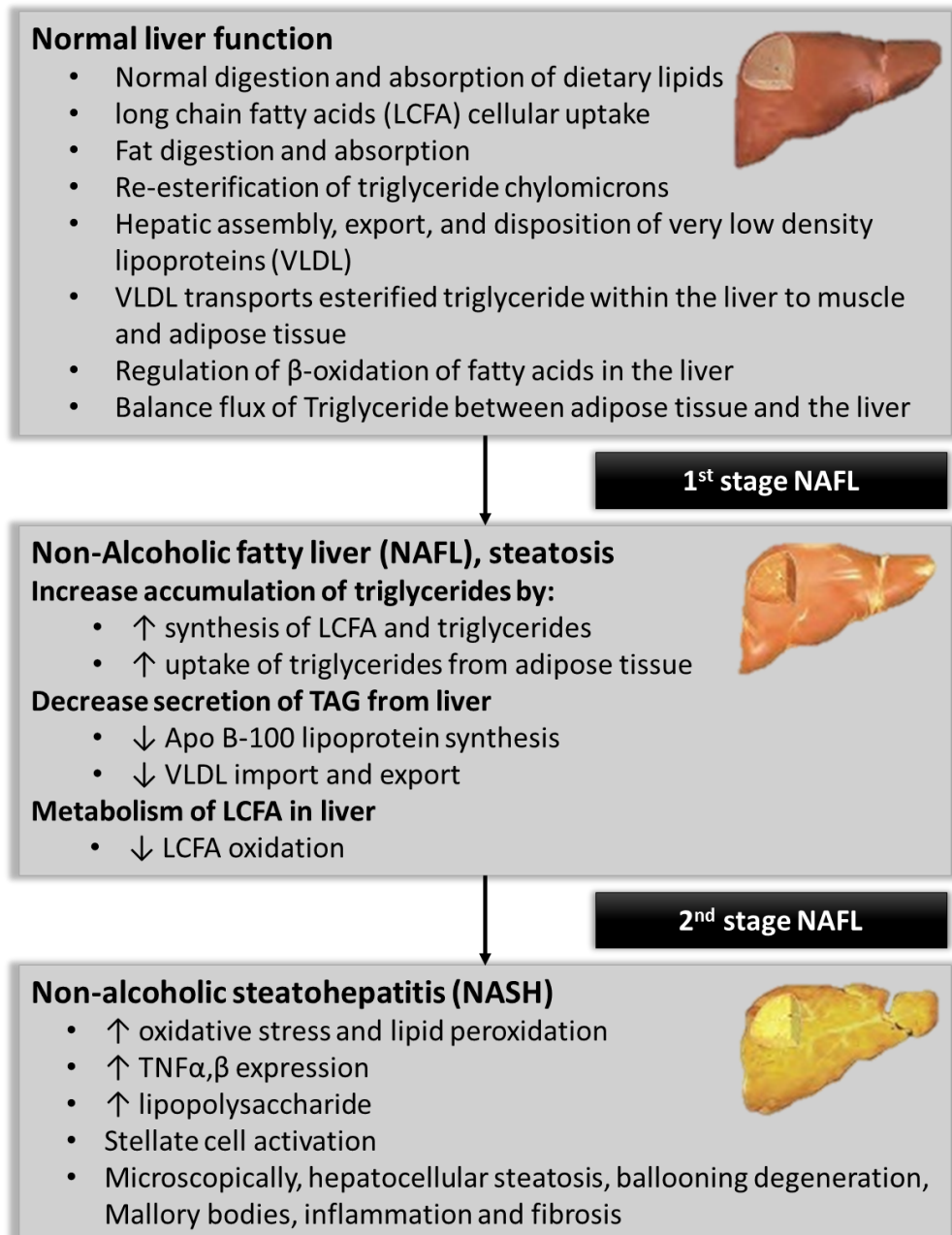


**Figure 1.7 | Development of NAFLD and NASH.**

A flow chart representing the two step hit of lipid metabolism leading to non-alcoholic fatty liver (NAFL) disease and non-alcoholic steatohepatitis (NASH). Adapted from (Day and James, 1998) and (Bradbury and Berk, 2004).

A study analysed the food records for a period of seven days of 25 NAFLD patients and compared them to 25 controls. The subjects were matched for age, sex and BMI. Their results showed that both groups had similar overall energy, total fat and carbohydrate intakes over the studying period. However, the patients with NAFLD reported significantly higher intakes of daily saturated

fatty acids and reduced intakes of polyunsaturated fatty acids and fibre (Musso *et al.*, 2003).

Another study used a semi-quantitative food frequency questionnaire for the analysis of food intake. A total of 45 NAFLD patients and 856 controls were recruited. Even though the control were sex and age balanced, they were not BMI-matched nor checked for NAFLD absence. Similar to the previously mentioned study there was no difference in the energy intakes nevertheless NAFLD patients consumed less carbohydrates, a similar amount of fibre, and had a tendency to consume a greater amount of simple sugars and a greater amount of total fat. They further analysed the fatty acid profile and identified a larger intake of n-6 polyunsaturated fatty acids (PUFAs) by the NAFLD patients (Cortez-Pinto *et al.*, 2006).

A more invasive study examined fatty acid profiles in liver biopsies from subjects with a seven day record on their food diary. A total of 73 patients with records of elevated liver enzymes as an indication of NAFLD were analysed. Results showed that 17 had a normal liver biopsy, 18 presented simple steatosis and 38 had NASH. Biopsies with NASH were to patients that had a significant high BMI. The macronutrient analysis showed no difference between the three groups (Allard *et al.*, 2008).

Another large scale study compared the intake pattern of adults who are alcohol abstinent and show a healthy appearance. The subjects were divided in to groups based on gender and ultra sound scans screening for NAFLD. They reported that the dietary contribution of PUFA was lower in men

who presented with steatosis however that observation was not the same in women. The data were adjusted for age, waist and physical activity levels and even so, the previous observed results were not changed. Even though the male patients with steatosis had a higher BMI they had similar energy intake and physical activity levels (Oya *et al.*, 2010).

Using an entirely different approach, Kechagias *et al.* analysed the effect of short-term fast-food overfeeding on the liver. The intake was double that of the controls with exercise restricted to less than 5,000 steps a day. A total of 18 volunteers were recruited. Over a period of 4 weeks they had a mean weight gain of 9.5%, the increased liver enzymes indicating liver injury and increased hepatic lipid stores. Three day food diaries prior to and during the period of the intervention were used to analyse the nutrient intakes. This showed that liver enzyme only correlated with monosaccharide intake concluding a direct fat-food attribution to hepatic changes (Kechagias *et al.*, 2008).

It has not yet been proven that a single or set of dietary intake patterns unequivocally cause the development of NAFLD. There exist flaws in the studies cited with regards to data collection and nutrient analysis; the only macronutrients that were associated with NAFLD in some of the studies were PUFAs and simple sugars.

### **1.6.2 Dietary assessment in NAFLD in liver biopsy lipid analyses**

Quantifying the liver biopsy's fatty acid profile is one way to assess the liver's exposure to ingested fat. The procedure presupposes that the liver fatty acid profile has a direct correlation to ingested fats, and that all fatty acid

subtypes are processed in the same way during a healthy state and a state of disease. Inflammation, along with oxidative stresses, possibly could change the way fatty acids are synthesized as well as alter the metabolism and peroxidation of complex lipids. As such it cannot be determined whether any observations are a product of the symptoms of the disease. This assumption made lipidomic analyses an interesting nutritional assessment technique to understand the interaction between hepatic fatty acid metabolism and nutrients.

In a study, liver fatty acids profiling using gas liquid chromatography in 19 patients with NAFLD and 11 matched, non-BMI, controls showed that both saturated and monounsaturated fatty acids had an equal contribution to the liver fatty acids. However the NAFLD patients had significantly lower PUFAs. The marked reduction was mainly in the n-3 PUFAs (Araya *et al.*, 2004). A similar study was performed in NAFLD patients matched with controls for age, sex and BMI and generated the same observation in terms of fatty acid profile (Puri *et al.*, 2007). The study described previously by Allard *et al.* analysing fatty acid profiles of liver biopsy in 73 patients with elevated liver enzymes reported that patients with simple steatosis had higher n-6 PUFA content than those with normal biopsies. On the other hand NASH liver biopsies had a mild increase in monounsaturated fatty acid composition and a marked reduction in long-chain n-3 PUFA (Allard *et al.*, 2008).

As per the findings of the above studies, patients with NAFLD seem to have increased intake of simple sugars and reduced intake of PUFAs, especially

of n-3 PUFAs. While these observations have not been widely reproduced, though are supported by other observations. Hence, the exact effect of nutrition on liver metabolic pathways remains to be well understood.

## **1.7 Polyunsaturated fatty acids**

In the UK, 35% of the total energy intake on an adult diet is originated from fatty acids (Pot *et al.*, 2012, Swan, 2004). The number of double bonds in a fatty acid classifies it as saturated fatty acid which has none, a monounsaturated fatty acid having only one, or a polyunsaturated fatty acid (PUFAs) which has two or more cis double bonds. They are further classified by the location of the initial double bond toward the methyl end on the chain. If the double bond is at the third carbon-carbon bond its it a n-3 PUFA while if the double bond falls at the six carbon-carbon bond it is an n-6 PUFA, Figure 1-8. Dietary PUFAs are usually of the 18-carbon form, namely linoleic acid (n-6) and the  $\alpha$ -linolenic acid (n-3) (Mann and Truswell, 2007).

The physiological effects of PUFAs are the modification of the function of cellular walls, gene transcription rates and eicosanoid production and balance. While the cellular protein expression is determined genetically, the cellular membrane is largely dependent on diet (Benatti *et al.*, 2004). Their effect on transcription rates is through PPARs. PPAR are transcription factors that control whole-body lipid and glucose metabolism (Forman *et al.*, 1997). They recognise n-6 PUFAs, but not saturated fatty acids, as very weak ligands (Price *et al.*, 2000). Another transcriptional regulator that is effected by PUFAs is SREBPs. There are three subtypes with SREBP-1C as the most important in

lipid metabolism and *de novo* lipogenesis. Its expression is related the development of dyslipidaemia, type 2 diabetes and hepatic steatosis (Ferré and Foufelle, 2007). SREBPs maturation is controlled by a negative feedback mechanism. Factors that are central to this control include insulin, glucose, long chain PUFAs and intra-cellular levels of cholesterol (Loewen and Levine, 2002).

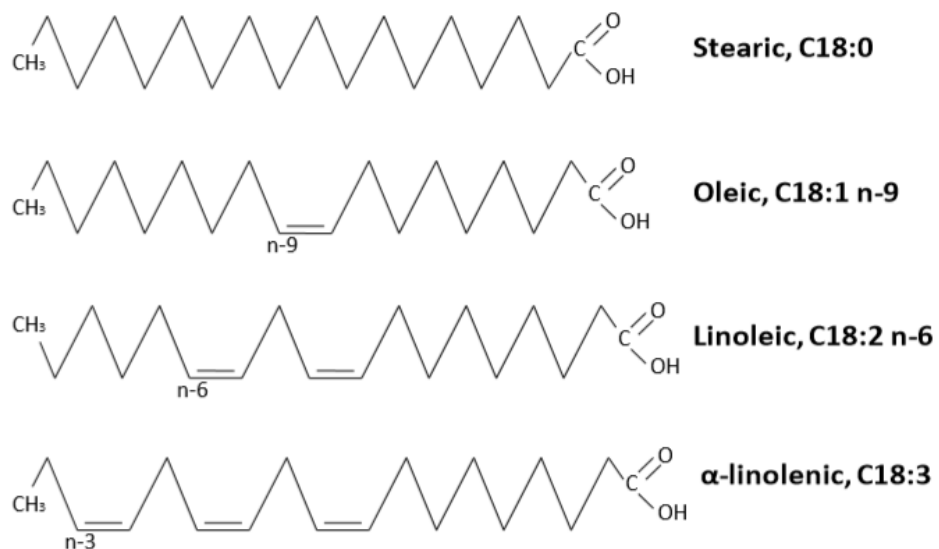


**Figure 1.8 | Free Fatty Acid structure**

Names and structures of common 18-carbon chained saturated (stearic), monounsaturated (oleic), n-6 polyunsaturated (linoleic) and n-3 polyunsaturated ( $\alpha$ -linolenic) fatty acids. Adapted from (Mann and Truswell, 2007).

## 1.8 Animal models of NAFLD and PUFA supplementation

There are several NAFLD rodent models and the different PUFAs that gave the opportunity to better understand the areas of steatosis, metabolic profile, gene expression, inflammatory stature and fatty acid profile. One of the major used animal model is the leptin-deficient *ob/ob* mice. They are well validated model of obesity, insulin resistance, and hepatic steatosis. Gonzalez-Periz *et al.* (2009) used this model where he randomised the mice to either receive standard chow or chow supplemented with PUFAs for a period of 5

weeks. The animals did not show any difference in terms on weight gain. In the group fed with PUFA supplemented chow PPAR $\alpha$  and PPAR $\gamma$  were up-regulated and the hepatic expression of Fatty acid synthase (FAS), an enzyme that catalysis fatty acids, was reduced. Furthermore, adiponectin expression was up regulated with no changes in TNF $\alpha$ . These changes resulted in of the improvement of hepatic steatosis and insulin sensitivity (Gonzalez-Periz *et al.*, 2009).

On the other hand, Pachikian *et al.* fed a 2<sup>nd</sup> generation PUFA depleted mice a standard chow for 34 weeks with either 2% or 9% of fatty acids as PUFA. The group fed the 2% PUFA diet had reduced weight gain with the same amounts of visceral adipose tissue as the 9% fed group. Nevertheless they developed an obvious systemic insulin resistance and had a 1.5 fold higher hepatic triglyceride content. The hepatic steatosis correlated strongly with the n-6 PUFA however the mechanism behind this was not identified (Pachikian *et al.*, 2008). When rats are on a standard high fat and high energy diet their visceral obesity increased along with NEFAs and TNF $\alpha$  while adiponectin is suppressed and hepatic insulin resistance is induces. These changes resulted in a NAFLD model with hepatic steatosis, oxidative stress, necroinflammation (necrosis and inflammation), apoptosis and ultimately fibrosis. When this model was used with and in the absence of n-3 PUFA supplementation, the supplementation resulted in the induction of PPAR $\alpha$  expression and the restoration of adiponectin and TNF $\alpha$  expression level. This concluded that n-3 PUFA supplementation decreased the amount of hepatic steatosis to half. This

indicated that n-6 PUFA contributes more to hepatic steatosis (Svegliati-Baroni *et al.*, 2006).

### **1.8.1 High fat diet in combination with diabetic-induced animal models**

Diabetes mellitus is a metabolic disorder characterised by elevated blood glucose. Diabetes is divided into either type 1, which is an autoimmune disease effecting individuals with a genetic predisposition that targets beta cells consequently decreasing the levels of insulin production, and type 2 diabetes, which accounts for approximately 90% of diabetic cases. Type 2 is a case of insulin resistance where the peripheral tissue lose their response to insulin stimulation. The main risk factor for developing diabetes is obesity and over nutrition (Rydén *et al.*, 2007). In research there are various animal models that are used to study both types of diabetes. These are produced either in response to chemical interference or genetic manipulations with streptozotocin being the most used model. Streptozotocin selectively destroys pancreatic  $\beta$ -cells reducing the amounts of blood insulin. A HFD/STZ model is set up in a way that feeding with HFD induces a state of insulin resistance which then followed by a low doses of streptozotocin enough to lower insulin concentration to levels mimicking that of an end stage type 2 diabetic (Zhang *et al.*, 2008).

In conclusion, dietary intake has a major effect on lipid metabolism. Overfeeding with macromolecules leads to liver steatosis, insulin resistance and diabetes. However the mechanism behind this effect remains to be fully elucidated. Studies on human are tricky to control and are limited to clinical observations, hence, animal models resembling disease state gained

importance to aid in better understanding the molecular mechanisms behind dietary fat changes.

## 1.9 Aims of the thesis

The hypothesis was that consumption of a high fat diet will lead to weight gain and the development of low grade inflammation particularly in adipose tissue. The use of a low dose STZ model in conjunction with high fat feeding was intended to mimic late stage Type II diabetes in which individuals are hypoinsuliemic and insulin resistant. The study was conducted to examine the potential effects of pioglitazone treatment upon diabetic neuropathy. The collection and analysis of tissue samples from these animals allowed a second study to be conducted without the use of additional animals in the spirit of the 3R's (Refinement, Replacement and Reduction) in animal research. The aim of the study was to determine the extent of fat deposition in the main metabolic tissues – adipose, skeletal muscle and liver – and to determine the extent of immune cell infiltration and activation in individual tissues. Using gene and protein expression analysis, immunocytochemistry and analysis of tissue and circulating lipids, the relative effects of a high fat diet in healthy and diabetic animals upon metabolism and inflammatory status in liver, adipose and skeletal muscle would be determined.

**CHAPTER II:**

**Animal Model of Diet-  
Induced Diabetes**

## **2.1 Introduction**

### **2.1.1 Animal model of diabetes**

Sprague-Dawley rats have been used as a model of obesity that presumably shares several characteristics with the common form of obesity in human. When rats are fed with a varied and palatable diet that mimics the Western diet of humans they become obese. The high fat, energy dense nature of the diet and the ensuing higher intake of total energy contributes to the reduction of insulin and leptin sensitivity. This effect is rapid and occurs only after a few day of high fat diet consumption. The composition of the fatty acids in the diet seems to have a major role in this effect since saturated fat is far more deleterious than unsaturated fat (Lutz and Woods, 2012).

### **2.1.2 Streptozotocin (STZ) model of diabetes**

Of the wide range of diabetic animal models, the STZ model is the most frequently used as it is easy to set up, quick and cheap. Streptozotocin (2-deoxy-2-(3-(methyl-3-nitrosoureido)-D-glucopyranose) is a selective toxin that destroys pancreatic  $\beta$ -cells upon entry through the glucose transporter, GLUT2. Administration of STZ leads to alkylation of DNA and the formation of superoxide radicals. This causes the release of nitric oxide at toxic concentrations, eventually leading to  $\beta$ -cell necrosis and inhibition of insulin synthesis and secretion (Szkudelski, 2001, Lenzen, 2008). GLUT2 receptors are predominantly found in the pancreas and liver (Farrell *et al.*, 2013) however its effect is not as profound in the liver, this could be attributed to the detoxification mechanism of the liver. Its systemic effects are observed a few

hours after administration, indicated by hyperglycaemia and hypoinsulinaemia. Stunted growth, hyperphagia and polyuria are also typical symptoms associated with STZ administration (Chatzigeorgiou *et al.*, 2009).

A wide range of STZ doses are used to induce diabetes in animal models. However, STZ injection alone at higher doses, leads to symptoms that resemble type 1 diabetes. Luo *et al.* reported that combining high fat or high carbohydrate diet with a lower dose of STZ in mice induced diabetes with disease progression which resembles that of type 2 diabetes in humans. The diet initiated a pre-diabetic state where there was a compensatory increase in the production of insulin due to insulin resistance. It was not until a portion of  $\beta$ -cells were destroyed by STZ injection, which resulted in decreased insulin production, that mice developed hyperglycaemia (Luo *et al.*, 1998). This model was replicated by Srinivasan *et al.* in rats. They were put on a high fat diet (58% energy as fat) which lead to an increase in body weight, plasma insulin, glucose, total cholesterol and triglyceride in addition to a decreased glucose uptake during insulin-glucose tolerance tests; all of which are indicative of insulin resistance (Srinivasan *et al.*, 2005). A low dose (35mg/kg) of STZ in high fat diet (HFD) rats caused overt hyperglycaemia and decreased plasma insulin to levels deemed close to be normal. Hence they proposed the use of this model as it was more clinically relevant to type 2 diabetes. Later studies investigated the effect of various STZ doses in combination with HFD. A single dose of 45mg/kg produced diabetes more consistently compared to a single dose of 25-35mg/kg STZ. This dose was the only one to produce blood glucose levels profoundly higher than normal ( $24.5\pm 3.75\text{mM}$ ) (Zhang *et al.*, 2008). *In vitro*, lower doses

of STZ induced beta cells apoptosis but cell, depending on the exposure time to STZ, were able to recover (Saini *et al.*, 1996).

### **2.1.3 Pioglitazone: effect on diabetes**

Pioglitazone is a thiazolidinedione (TZD); a class of drugs used to treat type 2 diabetes. It is an anti-hyperglycaemic agent that activates peroxisome-proliferator activated receptor- $\gamma$  (PPAR $\gamma$ ) to increase insulin sensitivity. It increases peripheral insulin sensitivity, consequently increasing splanchnic and peripheral glucose uptake and inhibiting hepatic gluconeogenesis. Pioglitazone also increases whole body adiposity by promoting lipid storage, and differentiation of adipocytes (Waugh *et al.*, 2006).

In clinical trials, patients that are type 2 diabetic and on pioglitazone, as monotherapy or in combination with other drugs, had improved glycaemic control and serum lipid profiles. Pioglitazone has been demonstrated to also reduce some arteriosclerosis and cardiovascular risk measures. With that in mind, pioglitazone treatment offers an option in managing type 2 diabetic patients.

## **2.2 Aim of the study**

The aim of this study is to investigate the effect of HFD and HFD in combination with STZ (HFD/STZ) on rat metabolism and assess the metabolic changes that are related to insulin resistance and diabetes and furthermore, to also examine whether pioglitazone treatment alters any of the effects of HFD/STZ.

## 2.3 Material and Methods

### 2.3.1 Animal Model

Animals used in this study were handled by Frederika Byrne, Ph.D. under the supervision of Professor Victoria Chapman, School of life Sciences, QMC, University of Nottingham.

All experiments were carried out under Personal Home Office Licence 40/9559 and Project Home Office Licence 40/3124, in accordance with the UK Home Office Animals (Scientific Procedures) Act 1986 and IASP guidelines. Twenty-two young Sprague-Dawley rats (200-250g) were obtained from Charles River (Kent, U.K.) and individually housed for 10 weeks on a normal light cycle (12/12hrs light-dark cycles).

Animals were randomly allocated into two groups; normal chow (NC) fed (n=6) or high fat diet (HFD) fed (n=18). The HFD (D12492 from Research Diets, Inc. UK) contained 60% calories as fat compared to 18% in the normal chow diet (2018 from Harlan Laboratories, UK), Table 2-1. Animals had free access to food and water at all times. Food and water intake, and body weight were monitored at least twice weekly.

**Table 2-1 | Diet composition in Kcal %**

<b>Ingredient</b>	<b>High Fat diet</b>	<b>Normal Chow</b>
Protein	20	24
Carbohydrate	20	58
Fat	60	18

### **2.3.2 HFD/STZ model of diabetes**

After three weeks of HFD consumption, rats were further divided into two groups. They received an IP injection of STZ (45mg/kg, n=12) or citric acid buffer (n=6). STZ was prepared by dissolving in 0.05M citric acid, pH 4.5. Very strict criteria was set to monitor the state of the rats to assure changes were due to the state of diabetes and not poor health. Blood samples were drawn from the tail vein for plasma glucose determination. Diabetes was defined by a hyperglycaemic state with fasting plasma glucose levels higher than 15mM.

### **2.3.3 HFD/STZ + pioglitazone model of diabetes**

The HFD/STZ rats were sub-divided into two groups; dosed with either 10mg/kg pioglitazone (n=6) or 1% methylcellulose vehicle (n=6). Pioglitazone doses of 10mg/kg was showed to decrease carrageenan induced-inflammation and rat paw oedema (Cuzzocrea *et al.*, 2004). They were orally dosed from day 21 to 49 of the study on a daily basis. Pioglitazone was purchased from Tocris Cookson (Bristol, UK) and dissolved in 1% methylcellulose vehicle. The study time line is illustrated in figure 2-1.

### **2.3.4 Blood sampling**

Blood samples were taken at day 18 and 46 after a 4hr fast. Plasma was separated from 100µl of blood collected in lithium heparinised tubes for glucose (Thermoelectron infinity glucose reagent; Microgenics, UK) and insulin (Mercodia rat insulin ELISA; Diagenics, Milton Keynes, UK) assays.

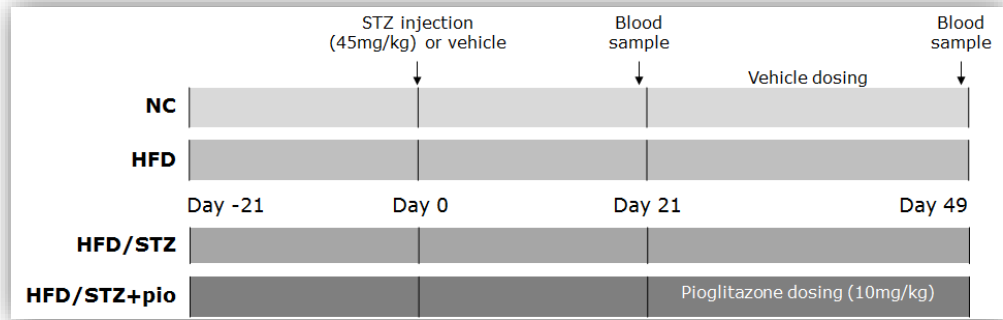


**Figure 2.1 | Time line of the study.**

Sprague-Dawley rats were divided into 4 groups with 6 animals in each group. They were put on either normal chow (NC) or High fat diet (HFD) for a period of 10 weeks. Three weeks into the study rats were injected with either 45mg/kg streptozotocin (STZ) or 0.05M citric acid vehicle (PH 4.5). After a further 3 weeks rats were dosed with either 10mg/kg pioglitazone (pio) or 1% methylcellulose vehicle. Blood was collected in to a lithium heparinised tube from the lateral tail vein at day 21 and 49 for glucose and insulin assays.

### 2.3.5 Tissue collection

At the end of the study animals were anesthetized for electrophysiological studies. Once these studies were carried out, the rats were decapitated and fresh tissue including visceral adipose, liver and skeletal muscle tissue was removed and flash frozen in liquid nitrogen. Tissues were stored in  $-80^{\circ}\text{C}$  until further required.

### 2.3.6 Statistics

GraphPad prism 6 statistical software was used to analyse the data. Analysis of body weight, food and water intake was by two-way analysis of variance (2-way-ANOVA) with bonferroni post-hoc test comparing pairs; NC vs HFD, HFD vs HFD/STZ and HFD/STZ vs HFD/STZ+Pio. Analysis of plasma glucose and plasma insulin was by one way analysis of variance (one-way-ANOVA) with bonferroni post-hoc test comparing pairs; NC vs HFD, HFD vs HFD/STZ and HFD/STZ vs HFD/STZ+Pio. In all analyses a p value of less than 0.05 was considered statistically significant. Raw data is given in the appendix.

## **2.4 Results**

### **2.4.1 Effects of HFD on body weight and food and water intake**

The HFD did not have any significant effect on the animal weights when compared to NC fed rats, figure 2-2-A. Rats in both groups exhibited a steady weight gain averaged at  $59.8 \pm 12.12$  g/week and  $66.4 \pm 17.8$  g/week, respectively, for the first 3 weeks. The rate of weight gain reduced in both groups towards the end of study, Figure 2-2-B. The NC group consumed a significant amount of diet by weight compared to the HFD group, Figure 2-3-A, however, when total caloric intake was calculated there was no significant difference in consumption. The NC group also had a higher water intake during the study with significant increases at various time points during the study, Figure 2-3.

### **2.4.2 The effect of HFD on metabolic parameters**

Plasma glucose and insulin levels were measured as metabolic parameters that are indicative of insulin resistance and diabetes. Mean fasting glucose concentration for the HFD group was  $7.42 \pm 0.47$  mM compared to  $6.05 \pm 0.37$  mM for NC group. HFD group insulin levels was  $\sim 1.5$  fold higher than NC group ( $1.94 \pm 1.24$  vs  $2.76 \pm 1.11$ , respectively). Although the HFD group exhibited an increased trend in both parameters, it was not statistically significant, Figure 2-5.

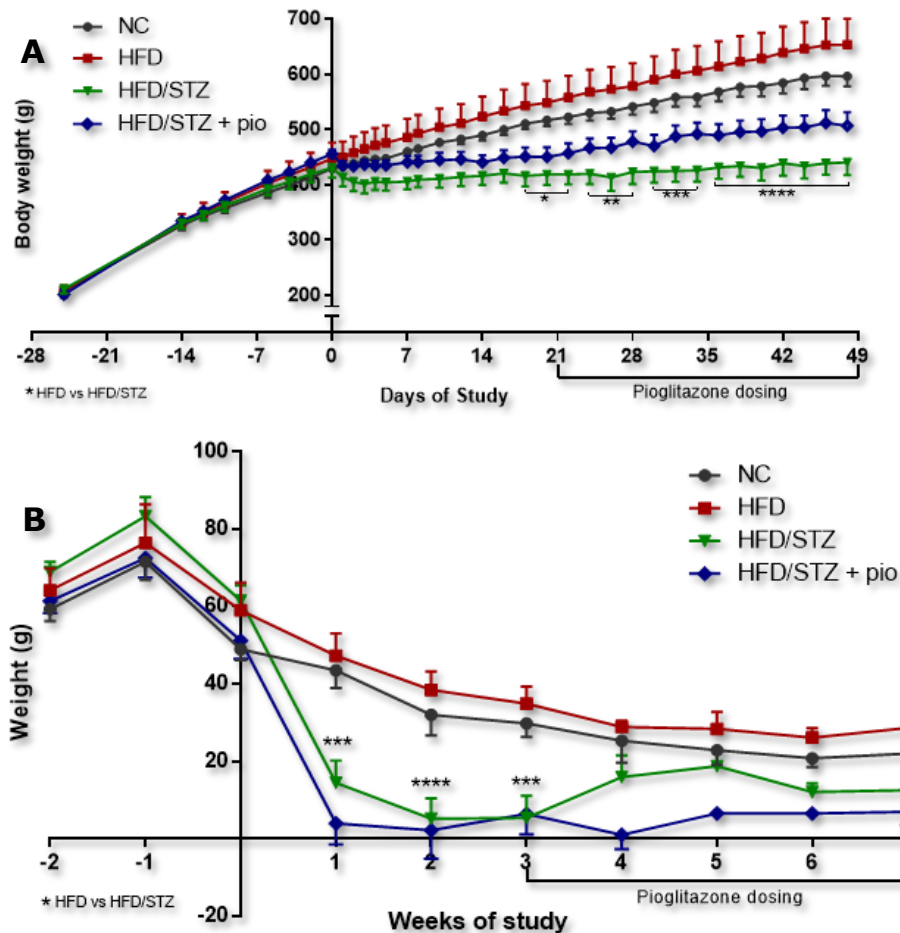


**Figure 2.2 | Effect of diets, streptozotocin and pioglitazone on animals' body weight.**

**A.** The animal weights were monitored and recorded through the course of the study and **B.** average weekly weight gain was calculated. Day 0 represents streptozotocin (STZ)/vehicle injection and between day 21/week 4 and day 49/ week 7, rats were dosed with pioglitazone (pio). High fat diet (HFD) group gained the most weight yet it was not significant when compared to the normal chow diet (NC) fed group. Both STZ injected groups exhibited a significantly reduced weight gain compared to the HFD group. Pio treatment did not have any significant effect on animal weights. All data are represented as mean  $\pm$  SEM, analysis was by Two-way-ANOVA with bonferroni post-hoc test comparing pairs; NC and HFD, HFD and HFD/STZ, HFD/STZ and HFD/STZ+Pio: \* $p < 0.01$ , \*\* $p < 0.001$ , \*\*\* $p < 0.0001$  ( $n = 5$  for NC and HFD,  $n = 6$  for HFD/STZ and HFD/STZ+pio).

### 2.4.3 Effects of streptozotocin and pioglitazone intervention on body weight, food and water intake

All groups exhibited a steady weight gain of  $\sim 66.5 \pm 13.5$ g per week prior to STZ injection, Figure 2-2-B. Post injection, rats in both STZ groups had a reduction in body weight. Thereafter, and even though their food consumption was comparable to the HFD group, Figure 2-3, they failed to gain weight and

exhibited a significant lower weight in comparison to the HFD group ( $\sim 150 \pm 44.7\text{g}$  difference at the end of the study,  $p > 0.0001$ ).

Water consumption for the HFD/STZ group was 4 fold higher ( $25.2 \pm 5.5\text{g}$  vs.  $104.6 \pm 10.8\text{g}$  at day 49 post STZ), compared to the HFD group ( $P < 0.0001$ ). This was evident immediately after injection with STZ, Figure 2-3. Pioglitazone intervention did not have a major effect on the rats' weight, food or water intake.

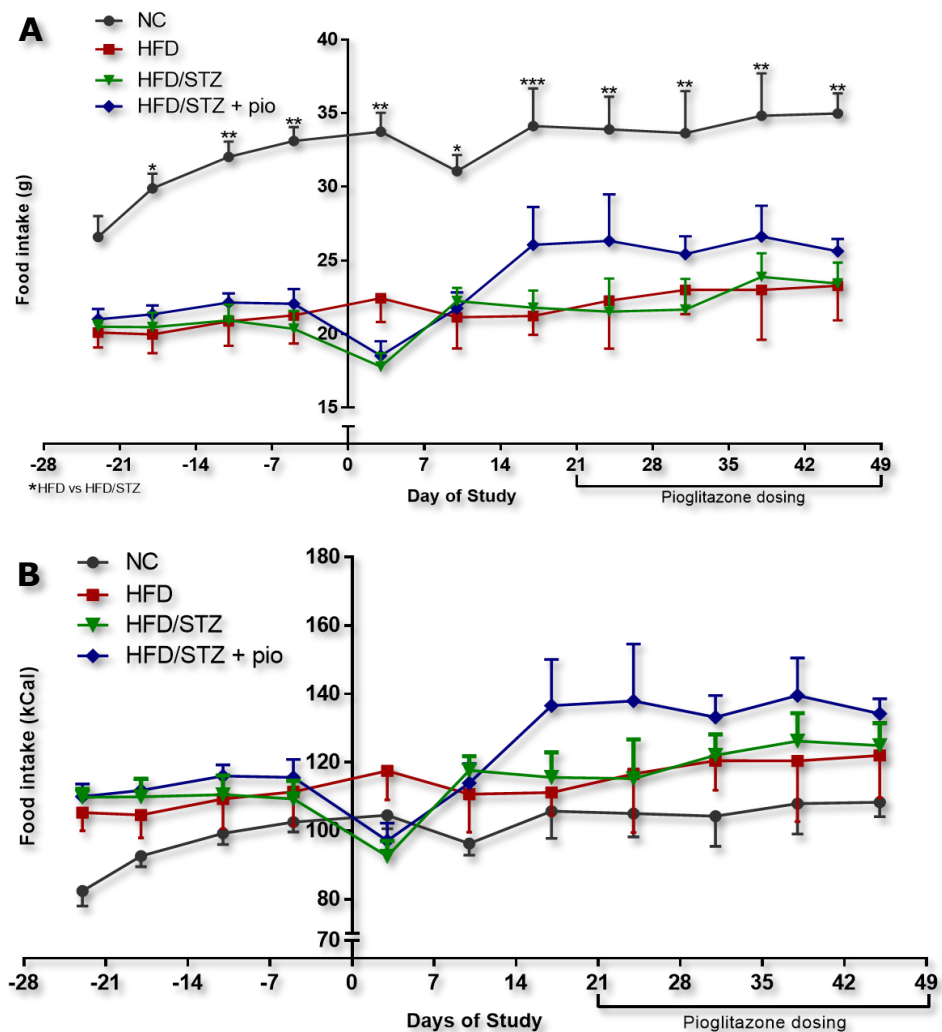


**Figure 2.3 | Effect of diet, streptozotocin and pioglitazone on animal food intake.**

**A.** The rats' food was weighed twice weekly and recorded. Normal chow (NC) group consumed most amounts of food **B.** however when the caloric intake was calculated there was no significant difference in the average food intake. All data are represented as mean  $\pm$  SEM, analysis was by Two-way-ANOVA with bonferroni post-hoc test comparing pairs; NC and HFD, HFD and HFD/STZ, HFD/STZ and HFD/STZ+Pio: \* $p < 0.01$ , \*\* $p < 0.001$ , \*\*\* $p < 0.0001$  ( $n = 5$  for NC and HFD,  $n = 6$  for HFD/STZ and HFD/STZ+pio). HFD; High Fat Diet, STZ; streptozotocin, Pio; pioglitazone.

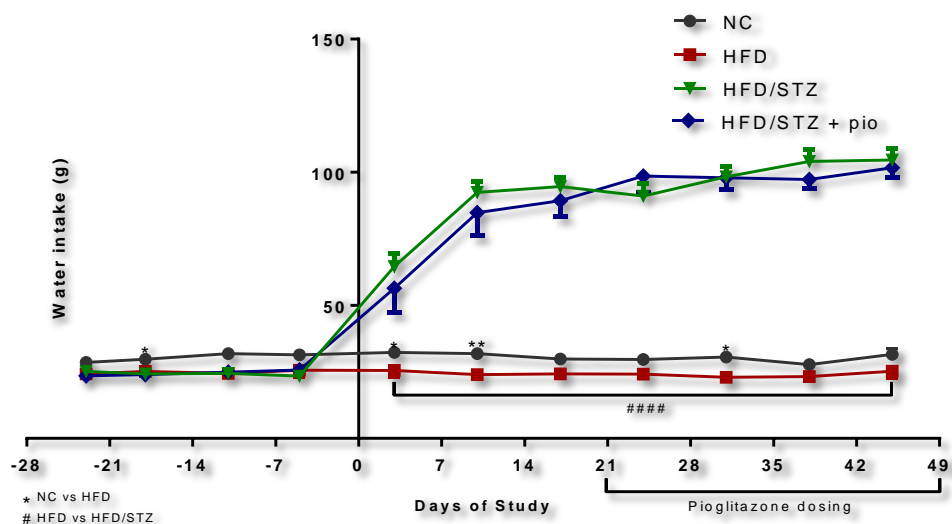


**Figure 2.4 | Effect of diets, streptozotocin and pioglitazone on water intake**

The rats' water intake was weighed twice weekly and recorded. Both streptozotocin (STZ) groups consumed most amounts of water. All data are represented as mean  $\pm$  SEM. Error bar for both NC and HFD group are too small to be visible. Analysis was by Two-way-ANOVA with bonferroni post-hoc test comparing pairs; NC and HFD, HFD and HFD/STZ, HFD/STZ and HFD/STZ+Pio: \* $p < 0.01$ , \*\* $p < 0.001$ , ### $p < 0.0001$  ( $n = 5$  for NC and HFD,  $n = 6$  for HFD/STZ and HFD/STZ+pio). NC; Normal Chow, HFD; High Fat Diet, Pio; pioglitazone.

#### 2.4.4 Effects of streptozotocin and pioglitazone intervention on metabolic parameters

STZ injection had major effects on metabolic parameters; following the injection fasting plasma glucose concentration was  $\sim 3$  fold higher ( $20.41 \pm 1.33$  mM in HFD/STZ group compared to  $7.47 \pm 0.34$  mM in HFD group,  $p < 0.0001$ ). This remained stable throughout the course of the study, Figure 2-5-A. STZ/HFD plasma insulin concentration decreased significantly ( $p < 0.001$ ) with a 6 fold drop post STZ injection compared to the HFD group ( $0.27 \pm 0.17$  ng/ml compared to  $2.76 \pm 1.11$ ). This increased to a 10 fold difference by the end of the study with a  $p$  values of 0.0002, Figure 2-5-B. Pioglitazone administration slightly decreased both levels of plasma glucose ( $21.92 \pm 2.7$  mM pre-treatment vs  $20.80 \pm 1.4$  post-treatment) and plasma insulin ( $0.57 \pm 0.35$  pre-treatment vs  $0.45 \pm 0.23$  post-treatment) but that drop was not statistically significant.

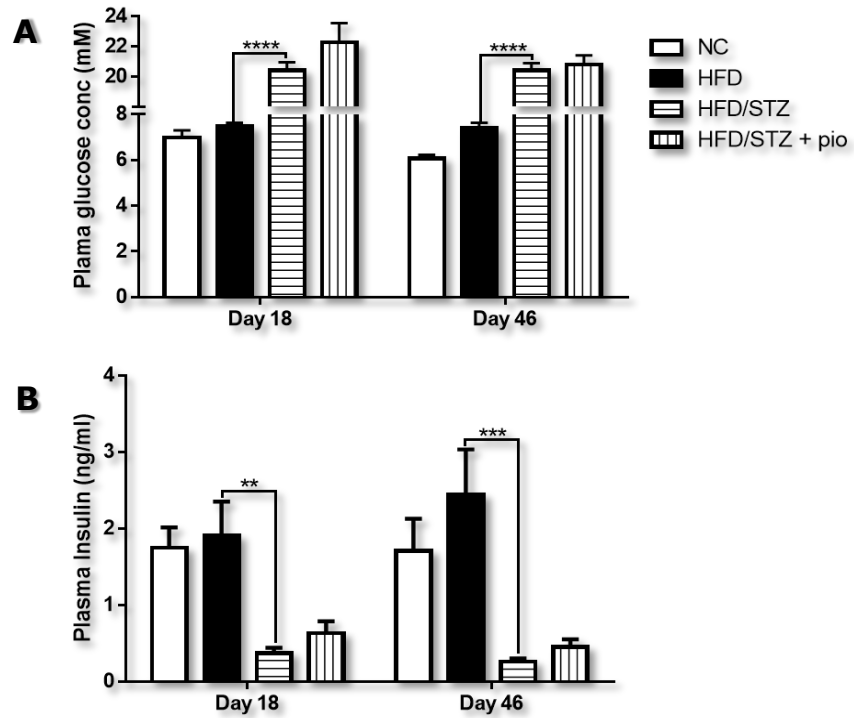


**Figure 2.5 | Effect of diets, streptozotocin and pioglitazone on fasting plasma glucose and insulin.**

Blood was collected after a four hour fast in lithium heparinised tube from the lateral tail vein at day 21 and 49 of the study. Plasma was separated for the measurement of **A.** glucose and **B.** insulin levels. All data are represented as mean  $\pm$  SEM, analysis was by one-way-ANOVA with bonferroni post-hoc test comparing pairs of columns; NC and HFD, HFD and HFD/STZ, HFD/STZ and HFD/STZ+Pio: \*\* $p < 0.01$ , \*\*\* $p < 0.001$ , \*\*\*\* $p < 0.0001$  ( $n = 5$  for NC and HFD,  $n = 6$  for HFD/STZ and HFD/STZ+pio). NC; Normal Chow, HFD; High Fat Diet, Pio; pioglitazone.

## 2.5 Discussion

### 2.5.1 Effects of HFD feeding

Dietary fat intake has often been posited as a major dietary factor for increasing adiposity. Human studies have illustrated that HFD, with >30% of energy as fat, can lead to obesity. This observation was also the same in the case of animals, including rats and mice, and they are deemed to gain weight faster than those on diets with a high carbohydrate (Hariri and Thibault, 2010). In this study, a diet that provides 60% energy as fat did not have a major effect on the body weight of rats when compared to the NC fed group. It is known that Sprague-Dawley rats become obese when given a HFD, however some rats have a diet resistant state where their body weight trajectory parallels that of rats on a low-energy diet. Like humans, this was attributed to an underlying genetic predisposition to either be obesity prone or resistant (Lutz and Woods, 2012, Hariri and Thibault, 2010). Some researchers linked this obesogenic effect to the higher energy intake, while others, where there was comparable intake, suggested that obesity-prone animals displayed greater efficiency in storing energy (Lutz and Woods, 2012). However animals of this study had comparable energy intake. It is possible that the amount consumed was sufficient or that simply that the diet was not palatable.

Until recently, HFD was thought to be the major player in developing not only obesity but also deteriorating insulin sensitivity and diabetes. Currently sugar is in the spot light as causative of obesity induced insulin resistance and cardiovascular complications. An article by Malhotra. A. in 2013

had a major impact in deflecting the attitude towards fats in diets particularly saturated fats. His observations were mainly based on epidemiological studies and an original article by Kekwick and Pawan (1956). The argument was that lowering fat energy content in the diet to <30% of total calories and replacing it with other dietary components increases CVD risk. This increase in risk was attributed to either increased sugar content, preservatives or that the decrease in fat lowers the uptake of certain vitamins that are known to influence CVD risk (Kekwick and Pawan, 1956, Malhotra, 2013). Literature has focused on monitoring metabolic parameters, including insulin and glucose as an assessment of whole body insulin resistance and the effect of HFD on those parameters (Matsuo *et al.*, 1999) but there are fewer reports when it comes to histological or molecular assessments on tissue. Therefore, it became of particular interest to assess the effect of a HFD on metabolically active tissues in the absence of weight gain.

### **2.5.2 Is HFD/STZ a good model of diabetes?**

The STZ-model has been well characterized and widely used as a robust model of type 1 diabetes (King, 2012). However, the combination of HFD and STZ (HFD/STZ) in a model has emerged as an interesting alternative since the vast majority of diabetic patients are type 2 diabetics. Therefore the need of an animal model that is relevant to the clinical situation of type 2 diabetes was of importance.

The HFD/STZ model is often considered as representative of end stage type 2 diabetes where animals are hyperglycemic and hypoinsulinemic (Kaiser

*et al.*, 2005), for this reason it was used in this study. As discussed in section 2.1.1, exposure to HFD causes insulin insensitivity within a few days so the model was based on feeding a HFD for a period of 3 weeks prior to STZ injection. HFD fed rats showed a trend for increasing plasma insulin and glucose, however, with the absence of a glucose tolerance test it was not enough to conclude an insulin resistant state. STZ injection resulted in a hyperglycaemic (all rats developed plasma glucose levels higher than 15mM) and hypoinsulinemic state that is reflective of diabetes. The effect of STZ was rapid and observed from the day after the injection. In reality this does not mimic the pre-diabetic state observed in humans which is known to last years before developing overt diabetes (Meigs *et al.*, 2003).  $\beta$ -cell dysfunction develops slowly in response to long term compensation for insulin resistance (Meigs *et al.*, 2003). In this phase plasma insulin levels are fairly similar to those observed in non-diabetic individuals and as the disease progresses they develop hyperinsulinemia (Reaven *et al.*, 1993). To further refine the model so that it more closely reflects clinical situations, a lower dose of STZ could have been used. This would have caused only a small portion of  $\beta$ -cells to be destroyed and therefore maintain a relatively normal level of insulin. However, as this animal model was in collaboration with the ARUK pain lab, the use of a lower dose of STZ did not fit into their aim of studying symptoms of allodynia. Both the pilot study carried out and previous literature (Ferhatovic *et al.*, 2013) reported that doses lower than 45mg/kg did not cause any change in the mechanical withdrawal thresholds. In this instance it is feasible to argue that longer HFD exposure prior to STZ injection, with a lower dose or multiple

treatments, would possibly, with constant monitoring for fluctuations in insulin levels, result in significant gradual changes that closely resemble the development of type 2 diabetes.

### **2.5.3 Effects of pioglitazone in the HFD/STZ model**

The absence of a pioglitazone effect on glucose and insulin levels is in agreement with similar previous studies on STZ treated rats (Majithiya *et al.*, 2005). Pioglitazone, in type 2 diabetes, has an insulin sensitizing effect on peripheral tissue in addition to improving  $\beta$ -cell function (Kawasaki *et al.*, 2005). However, in the model used, STZ destroyed a large proportion of  $\beta$ -cells and that it is evident by the 6 fold drop in plasma insulin levels. This level of insulin insufficiency renders the insulin sensitizing effects of pioglitazone virtually irrelevant, as a result pioglitazone is ineffective in improving the peripheral insulin sensitivity.

The effect of Pioglitazone on preserving  $\beta$ -cell function by increasing islet mass, maintaining insulin content and improving its secretion (Baggio and Drucker, 2006) is not observed in this model. Pioglitazone works by decreasing beta cell lipotoxicity which in turn inhibits apoptosis (Berger *et al.*, 2005), in this context  $\beta$ -cells are destroyed by an external toxin (STZ) and prior to the administration of pioglitazone.

Previously, Srinivasan *et al.* studied the effect of 7 days of pioglitazone (10mg/kg) treatment on HFD/STZ rats, with STZ concentrations ranging from 35 to 55 mg/kg. Pioglitazone was able to significantly reduce plasma glucose in rats that received the lowest dose of STZ. Those rats had plasma insulin levels

reduced to levels seen in the normal diet fed rats. In rats that were injected with higher doses (45 or 55mg/kg), there was a considerably greater reduction in plasma insulin and, similar to this study, pioglitazone was ineffective at decreasing plasma glucose levels. This indicates that pioglitazone is mostly effective in the case of improving whole body insulin sensitivity by enhancing glucose disposal in skeletal muscle that is mediated by insulin and by decreasing adipose tissue lipolysis (Kahn *et al.*, 2000).

#### **2.5.4 Conclusion**

In conclusion, it is important to select an appropriate animal model that fits the goal of a study. The HFD fed rats in this study could be a good model in assessing the effect of different levels of fat intake on peripheral tissue in the absence of weight gain. In this study, the aim was to investigate symptoms of allodynia produced by peripheral diabetic neuropathy (by the ARUK pain lab) and the effect of HFD combined with hypoinsulinemia that is comparable to that found in type 2 diabetics, so using the STZ model of diabetes was suitable. Using different time lines and STZ concentrations to that used in this study, would have created a more physiologically relevant model of diabetes. However, this model created reliable pain behaviour and also mimicked certain aspects of diabetes which made it suitable to use for both studies. Pioglitazone is dependent upon insulin in order to exert its beneficial effect. Therefore it was not unusual that no major effect was observed in the pioglitazone treated hypoinsulinemic rats. Regardless, this group of animals were still considered for further experiments.

**CHAPTER III:**

**Effect of HFD on  
Macrophage Infiltration  
and Activation**

## 3.1 Introduction

### 3.1.1 Adipose Tissue Macrophages in Obesity

An intriguing observation about obesity is the appearance of chronic, low-grade inflammation, especially in the adipose tissue. This inflammation is associated with the accumulation of tissue macrophages that display specific characteristics that are not observed in lean individuals, including a shift in polarization towards a pro-inflammatory phenotype and the formation of crown-like structures, which is observed as macrophages surrounding dying or dead adipocytes. It has also been suggested that newly recruited macrophages have a more inflammatory phenotype compared to resident macrophages (Lumeng *et al.*, 2007b).

While many different subpopulations of macrophages exist at any given time, macrophages are largely grouped as either classically, M1, or alternatively, M2, activated. Inflammatory markers that characterize M1 macrophages include  $\text{TNF}\alpha$ , IL-6 and IL-1 $\beta$ . M2 macrophages are associated with increased production of the anti-inflammatory cytokine IL-10 and arginase. In the adipose tissue of lean mice, macrophages are typically alternatively activated, i.e. have an anti-inflammatory phenotype. However, during obesity the polarization of adipose tissue macrophages changes from M2 to M1. The shift from M2 to M1 adipose tissue macrophages has significant implications for insulin resistance. M2 macrophages have the potential to protect the adipose tissue from inflammation, while M1 macrophages have

been shown to contribute to insulin resistance (Lumeng *et al.*, 2007a, Lumeng *et al.*, 2008).

Adipose tissue is an endocrine organ that secretes adipocyte-derived cytokines; however, the primary source of inflammatory molecules released in obesity appears to be macrophages resident in the adipose tissue (Weisberg *et al.*, 2003). During obesity, the increase in body mass index (BMI) is directly related to the accumulation of macrophages in the adipose tissue (Weisberg *et al.*, 2003, Xu *et al.*, 2003). In fact, as the proportion of macrophages within the adipose tissue increases so does the expression of pro-inflammatory cytokines (Lumeng *et al.*, 2007b).

### **3.1.2 Macrophages and inflammation in liver and muscles**

In the setting of obesity, hepatic insulin resistance is associated with steatosis, and a heightened expression of inflammatory mediators. In the liver, Kupffer cells residing in the liver sinusoids are the major macrophage population in the liver. While there is much literature regarding adipose tissue macrophages, Kupffer cells have been less extensively studied in the context of insulin resistance. However they have been implicated in the development of insulin resistance via their production of inflammatory mediators. Macrophage specific murine Knockouts showed a reduction in hepatic insulin resistance when put on a high-fat diet (HFD) regardless of the development of hepatic steatosis indicating that both fat accumulation and inflammatory cell activation are required for the development of insulin resistance (Schenk *et al.*, 2008, Arkan *et al.*, 2005).

There is also evidence showing an increase in macrophage accumulation in skeletal muscles in HFD induced obesity. Similar to adipose tissue, these skeletal muscle macrophages exhibit a proinflammatory M1 like phenotype (Patsouris *et al.*, 2008, Nguyen *et al.*, 2007), however, histological studies showed that in obesity there are intermuscular adipose depots in skeletal muscles and they are the primary location for macrophages. This finding suggests that these macrophages possibly play a role in a paracrine mechanism via increasing the secretion of inflammatory cytokines including TNF $\alpha$  and IL6 that contributes to insulin resistance. Nevertheless, this is only a hypothesis and has not been directly demonstrated (Olefsky and Glass, 2010).

### **3.1.3 Aim**

The aim of this chapter is to study the macrophage infiltration within adipose, skeletal muscle and liver tissue in response to dietary intervention and determine activation state of tissue resident immune cells. Furthermore, to assess the inflammatory state of the tissues by analyzing the gene expression levels of interleukins and cytokines.

## **3.2 Materials and methods**

### **3.2.1 Histological and immunofluorescent analysis**

#### **3.2.1.1 Cryostat sectioning**

Fresh frozen or tissue fixed overnight in 4% paraformaldehyde (PFA) was embedded in Tissue Tek (VWR, UK) and allowed to solidify in a -15°C cryostat microtome (Leica CM-1900). Ten- $\mu\text{m}$  or 5  $\mu\text{m}$  thick cryostat sections were then cut and thawed on amino silane coated slides (APS). The slides were stored at -80°C until required.

#### **3.2.1.2 Fixed Paraffin-embedded tissue sectioning**

The protocol was altered several times, particularly in the case of adipose tissue, to enable the production of morphologically intact sections. Fresh frozen tissues were briefly thawed on ice then fixed in freshly prepared 4% paraformaldehyde (PFA) for 24hr. Sections were processed to dehydration and embedded in paraffin using a Leica TP1020 automated tissue processor, as illustrated in Table 3-1. Tissues were collected and instantly embedded in wax then left for 2hrs on a cold plate. Four 10 $\mu\text{m}$  sections of adipose tissue and four 5 $\mu\text{m}$  sections of liver and muscle tissue were cut at 50 $\mu\text{m}$  intervals using a SLEE Cut Microtome (model 4060) and subsequently mounted on APS treated slides. They were then left to dry overnight.

**Table 3-1 | Dehydration/paraffin embedding program**

Chemicals	Incubation Time
70% Alcohol	1hr 30min
80% Alcohol	1hr 30min
90% Alcohol	1hr 30min
100 % Alcohol	1hr
100 % Alcohol	1hr
100 % Alcohol	1hr
Xylene	1hr 30min
Xylene	1hr 30min
Paraffin	6hr

### 3.2.1.3 Hematoxylin and Eosin (H&E) Staining

The integrity of the tissue was assessed by H&E staining. Sections were deparaffinized in two changes of xylene, 5 min each. They were then rehydrated in 3 changes of absolute alcohol, 1 min each followed by a incubating in gradient of ethanol concentration; 95%, 75%, and 50% for 1 min. This was followed by briefly washing in distilled water and staining in Harris hematoxylin solution for 5 min. After that, sections were washed in running tap water for 5 min until the color cleared and then differentiated in 1% acid alcohol for 10 sec. Sections were again washed in running tap water for 1 min then dipped for 15 sec in Scott's Tap water bluing solution. Another wash in running tap water was followed by counterstaining in eosin solution for 5 min and followed by a final wash with tap water. Finally, the sections were dehydrated through ascending series of alcohol concentrations; 50%, 75%, 90%, and 3 changes of absolute alcohol, 1 min each, then cleared in two changes of xylene for 2 min each. Slides were mounted using DPX mounting media. Sections were viewed using Leica DM4000B light microscope attached to Q-imaging MircroPublisher 3.3 RTV digital camera and supported with open lab software.

#### **3.2.1.4 Fluorescent Immunohistochemistry**

Sections were cleared in xylene for 5 min twice then rehydrated through a series of descending ethanol gradients 100% x3, 90%, 75%, 50% each for 1 min, then finishing in water. They were then washed in 1x PBS for 5 min. The endogenous peroxidases were blocked by incubating the slides in 0.3% hydrogen peroxide (H<sub>2</sub>O<sub>2</sub>) prepared in 50% methanol and diluted in 1x PBS. After a 5 min wash in 1x PBS the tissue was blocked with 1% goat serum diluted in 1X Tris buffer saline with 0.05% or 0.1% tween 20 (TBST).

The blocking buffer was decanted and primary antibody diluted in the blocking buffer was incubated with the section overnight at 4°C in a humid chamber. The slides were washed for 10 min three times in 1x TBST. Secondary antibody diluted to 1:1000 in blocking buffer was incubated at 4°C overnight, in the dark and in a humid chamber. Table 3-2 summarizes the primary antibodies origin dilution, their corresponding secondary antibody and any special conditions required. They were then washed for 10 min three times in 1x TBST then counter stained with DAPI staining. A final concentration of 2ng/ml DAPI solution diluted in water was added on the slides and incubated for 10 min followed by washing in two 5 min long changes of water. Finally the slides were mounted using VectaShield (Vector Laboratories, Inc. USA) mounting medium. A negative control stained with only the secondary antibody was performed in each run.

**Table 3-2 | Immunohistochemistry antibodies.**

Primary Antibody	Catalogue	Dilution	Secondary antibody <sup>#</sup>	AR <sup>+</sup>
Rabbit anti-CD86	Ab53004	1:100	Goat anti-mouse Alexa Fluor 488	✓
Mouse anti-CD163	MCA342GA*	1:100	Goat anti-mouse Alexa Fluor 568	NA
Rabbit anti-CD206	Ab64693	1:200	Goat anti-Rabbit Alexa Fluor 488	✓

Secondary antibody dilution = 1:1000

\*AbD Serotec, #Invitrogen

+Antigen retrieval

Using the appropriate filter (DAPI 350nm, FITC 480nm or TRITC 545nm), fluorescent signals from four random fields in each section were analysed using Leica LETZ DMRB upright fluorescence microscope attached to Hamamatsu digital camera and supported with Open-Lab software.

### 3.2.1.5 Antigen retrieval

After rehydration and before blocking endogenous peroxidase, slides were microwaved in 10mM sodium citrate buffer 0.01% Tween20 in deionized distilled water (D.D.H<sub>2</sub>O, pH 6), for 30 min. They were then left to cool down at RT for 20 min followed by washing in two changes of PBS each for 5 min.

### 3.2.1.6 Sudan Black staining

A 0.3% Sudan Black (w/v) in 70% ethanol (v/v) solution was prepared by stirring in the dark for 2 hours. The solution was left to stand overnight. Before usage, it was filtered to get rid of undissolved particles. Sections were stained by incubating slides in the stain solution for 10mins followed by 3 washes in water each for 10 min. Slides were finally mounted in a homemade mounting media made up by diluting glycerol to 80% with Tris buffer pH 7.3.

### 3.2.1.7 Volocity software analysis

Positive signals were analysed using PerkinElmer Volocity 3D Image Analysis Software. An embedded automated function designed to count the

number of DAPI positive cells was used to calculate the total number of nucleus. Positive cells for a specific antibody were counted based on the fluoresce signal. Cells that exhibited fluoresces around a nucleus were considered as positive and the program was set to eliminate the count of all other signals. The same program was used to analyse all the samples.

### **3.2.2 RNA extraction and quantification**

#### **3.2.2.1 RNA extraction**

Total RNA was extracted from tissues using Tri-reagent® according to the manufacturer's instructions. Tissue was weighed (250mg for adipose and 50mg for muscles) and homogenized (Ultra-turrax, T25, IKA®-Labortechnik) in 1.5ml of ice cold Tri-reagent for 15-30 seconds at room temperature. The homogenate was then processed according to the manufacturer's instructions. When dealing with adipose tissue the samples were centrifuged at 12000g for 10 min at 4°C to remove the insoluble fat that separates to the top of the aqueous phase. The lower interphase and organic phase were stored at -80°C for later protein extraction.

A Nanodrop-1000 Spectrophotometer (Thermo Scientific, USA) was used to measure total RNA concentration at the absorbance of 260nm. Purity was assessed using 260/280nm and 260/230nm ratio of ~2.0 and 2.0-2.2 respectively were accepted as indication of pure total RNA. To further assess the RNA purity and integrity, samples analysed using a Agilent 2100 Bioanalyzer (Agilent Technologies, USA) as per manufacturer's protocol, appendix figure 2.

### 3.2.2.2 Complementary DNA (cDNA) synthesis

According to the manufacturer's instructions, AffinityScript Reverse Transcriptase (RT) was used to reverse transcribe 500ng of total RNA to cDNA. The reaction mixture is described in table 3-3.

**Table 3-3 | cDNA reaction mixture.**

Solution	Conc.	Volume	Company
HPLC H <sub>2</sub> O	-	12.5 µl	-
Random Primer	100ng	1µl	Promega
dNTP mix	10Mm	1µl	Promega
First-Strand Buffer	10X	3µl	AffinityScript
DTT	0.1M	1µl	AffinityScript
RNaseOUT™	40u/µL	1µl	Invitrogen
<b>Recombinant RNase Inhibitor</b>			
AffinityScript RT	200u/µL	1µl	AffinityScript
RNA Sample	100ng	5 µl	-
	TOTAL	25.5 µl	

The reaction mixture was then incubated at 25°C for 10 minutes, 50°C for 60 minutes and 70°C for 15 minutes in a Thermocycler (MWG-Biotech Primus 69 Plus). Once the reaction was complete, cDNA was stored at -20°C until required.

### 3.2.2.3 TaqMan real-time quantitative PCR

Taqman was performed using the automated Step-One Plus™ Real Time PCR system (Applied Biosystems). Data was analysed using the relative standard curve method; 5 point 1:2 serial dilutions were prepared. The starting pooled cDNA, prepared from synthesised cDNA of all studied samples were then diluted 1:4 and mixed with gene specific primers and probes (Table 4-4, Eurofins, Germany) and TaqMan Fast Universal PCR Master Mix (Applied Biosystems) as shown in table 3-4.

**Table 3-4 | TaqMan reaction mixture.**

Reagents	Volume ( $\mu$ l)
TaqMan® Universal Fast PCR Master Mix I	6.5
Forward primer (10 $\mu$ M)	0.4
Reverse primer (10 $\mu$ M)	0.4
Probe (10 $\mu$ M)	0.25
HPLC H <sub>2</sub> O	2.45
cDNA	3
Total Volume	13

All samples and standard curve points were run in triplicates with a negative control (no cDNA) and a negative reverse transcriptase (no RT enzyme). The thermo-cycling parameters were performed as follows:

- Stage 1: 50°C for 2 min and 95°C for 10 min.
- Stage 2: 95°C for 15 sec (40 cycles) and 68°C for 1 min

The standard curve was generated by plotting the Ct values against the log of the dilution factor. The assay data were deemed acceptable when the sensitivity (y intercept) and the amplification efficiency ( $=10^{(-1/\text{slope})}-1$ ) are both within the effective range. The efficiency of the PCR product and the slope should range between 90-100% and 3.1-3.6, respectively, Figure 3.1 with no more than 0.5 Ct value difference between triplicates and no detectable amplification in the negative controls. Each sample was expressed relative to a reference gene that was found to be stable across the studied groups.

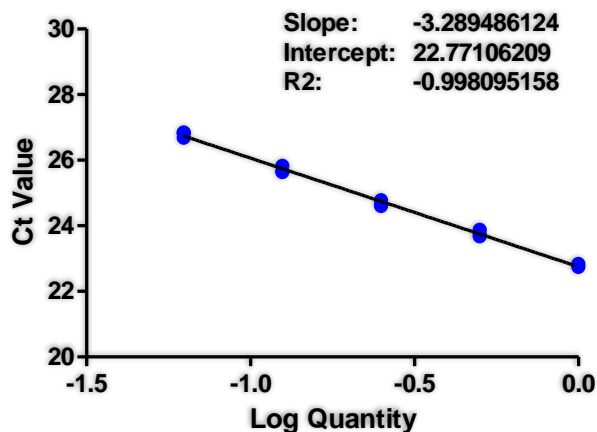


**Figure 3.1 | TaqMan Real-time PCR standard curve**

A representation of an accepted standard curve with linear regression showing a slope value of -3.2 and correlation co-efficient ( $r^2$ ) value of 0.99.

**Table 3-5 | Primers and probes used for Taqman gene expression analysis**

Gene	Sequence 5' → 3'	Origin
ACTB NM_031144.3	Fwd: AGCCATGTACGTAGCCATCCA Rev: TCTCCGGAGTCCATCACAATG Probe: TGCCCTGTATGCCTCTGGTCGTACCAC	FRAME database
GAPDH NM_017008	Fwd: TCTGCTCCTCCCTGTTCTAGAGA Rev: CGACCTTCACCATCTTGTCTATGA Probe: ATCTTCTTGTGCAGTGCCAGCCTCGT	FRAME database
POLR2A XM_001079162.4	Fwd: TGTGTTTCATGTGGGCTTCCT Rev: CCTTAATCTTCGGGTTGTTAGAATCT Probe: CGCTGTGTCTGCTTCTTTTGCTCCAAAC	FRAME database
IL-6 NM_012589.2	Fwd: TCAGGAACAGCTATGAAGTTTCTCTCCG Rev: CGAAACTGGCTGGAAGTCTCT Probe: GGCAACTGGCTGGAAGTCTCT	FRAME database
TNF- $\alpha$ XM_008772775.1	Fwd: GCAGGAGAAAGTCAGCCTCCT Rev: TACTACCAGGGCTTGAGCTCA Probe: AGAGCCCTTGCCCTAAGGACACCCCT	FRAME database
IL-10 XM_006249712.2	Fwd: CCCTGGGAGAGAAGCTGAAGA Rev: CACTGCCTTGCTTTTATTCTCACA Probe: CAGCTGCGACGCTGTCATCGATTTC	FRAME database
IL-1 $\beta$ NM_031512.2	Fwd: CACCTCTCAAGCAGAGCACAG Rev: GGGTCCATGGTGAAGTCAAC Probe: TGCCCGACCATTGCTGTTTCCTAGG	FRAME database

### 3.2.3 Analysis of protein expression

#### 3.2.3.1 Protein extraction and quantification

Protein was extracted after precipitating DNA organic phase after RNA Tri-reagent extraction with ethanol according to the manufacturer's protocol with minor alterations. Briefly, 0.3 volume per ml of Tri-reagent of 100%

ethanol was added, mixed and incubated for 2 min at room temperature then followed by centrifugation at 2000g for 5min at 4°C to precipitate the DNA. An aliquot of the supernatant was separated for protein precipitation. Three volumes of acetone were mixed with the aliquot for few seconds until a homogeneous solution was obtained. The solution was incubated at room temperature for 10 min followed by centrifugation at full speed (17000g) for 10 min to obtain a protein pellet. The supernatant was discarded then the pellet washed by dispensing in 0.5 volume of 0.3 M guanidine hydrochloride in 95% ethanol and 2.5 % glycerol (v:v). The solution was incubated at room temperature for 10 min then sedimented at 8000g for 5 min, this wash procedure was repeated 3 times. A final wash with ethanol containing 2.5% glycerol (v:v) was performed. The pellet was left to dry then appropriate volumes of 1% SDS was added according to pellet size and heated at 65°C for 10 min.

Protein quantification was carried out using a Pierce™ BCA Protein Assay Kit (Thermo scientific) according to manufacturer's protocol. A serial dilution (2 to 0.0125 mg/ml) of bovine serum albumin was prepared in 1% SDS and used as standards to generate a standard curve, Figure 3-2. Samples and standards were run in duplicates and the absorbance was measured using POLARstar Omega microplate reader. Sample protein concentration was calculated from the standard curve.

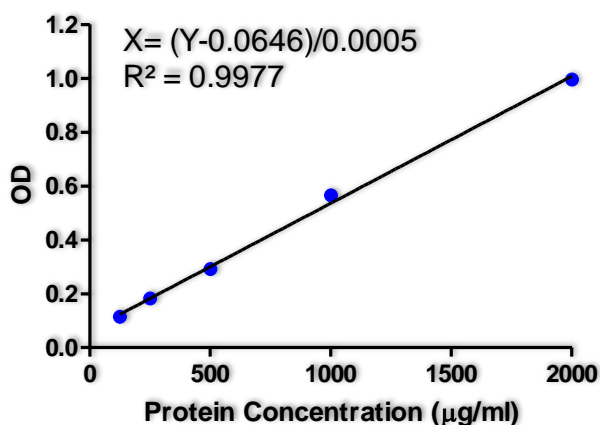


**Figure 3.2 | Example of protein standard curve for Thermo Scientific Pierce BCA protein kit.** Five concentrations of serum albumin prepared by 1:2 serial dilution, starting at 2000µg/ml were prepared in 1% SDS then analysed. The absorbance (response values) were plotted and a linear regression line drawn through the points to determine the line equation for unknown protein quantification. The coefficient of determination ( $R^2$ ) is to assess standards accuracy.

### 3.2.3.2 Western blotting

Solutions used for this experiment are summarized in table 3-6.

**Table 3-6 | SDS PAGE assay buffers**

6x laemmli loading buffer	Running Buffer	Transfer Buffer	Tris Buffer saline (TBS)
0.375M Tris (pH6.8)	25mM Tris-HCL	25mM Tris HCL	25 mM Tris
6% SDS (w/v)	0.192M glycine	0.192M glycine	150 mM NaCl
60% Glycerol	0.1% SDS (w/v)	0.1% SDS (w/v)	2 mM KCl
0.6M DTT	pH 8.8	20% methanol	pH 7.4
0.06% Bromophenol Blue			

Protein (65µg) was mixed with 6x loading buffer prior to loading onto sodium dodecyl sulphate-polyacrylamide gels. Either 10% or 8% gels were used to detect proteins that are smaller or larger than 100kDa, respectively (Table 3-7). Samples were then boiled for 5 min at 95°C. A protein molecular weight marker (Precision Plus Protein™ Standards, Kaleidoscope, Bio-Rad) was loaded with each run for size determination of target proteins. The proteins were separated by gel electrophoresis in Bio-Rad's Mini-PROTEAN cell under a constant voltage of 80V for 15 min then the voltage was increased to 150V for a further 45 min. Gels were stained with coomassie blue (1% coomassie brilliant blue, 50% methanol, 10% glacial acetic acid, 40% water, w/v) for an hour then

de-stained (water, methanol and acetic acid in a ratio of 50/40/10, v/v/v) overnight to visualize the proteins, appendix figure 1.

**Table 3-7 | SDS PAGE gel component**

Ingredients	Separating gel		Staking gel
	10%	8%	4%
Deionized Water	5	4.6	3.4
30% Acrylamide mix (29.3% Acrylamide + 0.8%N.N'-methylene bis-acrylamid)	2.3	2.7	0.83
1.5M Tris (pH 8.8)	2.5	2.5	-
1M Tris (PH 6.8)	-	-	0.63
10% Sodium dodecyl sulphate, SDS (w/v)	0.1	0.1	0.05
10% Ammonium persulphate, APS (w/v)	0.1	0.1	0.05
N,N,N',N'- Tetramethylethylenediamine,TEMED	0.007	0.006	0.005
<b>Total Volume</b>	10	10	5

Values are presented as ml of volume.

After the run, the gel containing the separated proteins, nitrocellulose membrane (GE Healthcare Life Sciences), whatman filter paper and sponge were soaked in transfer buffer. The gel and the membrane were sandwiched between the filter papers and sponges then locked within blotting cassettes. To transfer the proteins to the membrane, the cassette was placed in a Bio-Rad Mini Trans-Blot Cell Tank filled with chilled transfer buffer and run at 25 milliamps overnight at 4°C. Efficiency of the transfer was confirmed using Ponceau Red staining of the membrane. Before proceeding the stain was washed off using TBS. The membrane was incubated with 5% skimmed milk (w/v) in TBS with 0.1% Tween 20 for an hour under gentle agitation to block all nonspecific binding sites. The membranes were then incubated with primary antibodies diluted in the blocking solution at 4°C overnight. After the incubation, membranes were washed 3 times using TBS, 0.1% tween for 10 min each. The membranes were next incubated with the secondary antibodies diluted in the blocking buffer for an hour. Finally the membranes were washed

again as before. The antibody supplier and dilutions are summarized in table 3-8.

**Table 3-8|Antibodies used to detect protein expression using Western blotting**

Primary Antibody	Catalogue	Mwt	Dilution	Secondary antibody <sup>#</sup>
Rabbit anti-CD86	Ab53004	70	1:2000	IRDye <sup>®</sup> 800 CW Conjugated Goat Anti-Rabbit IgG, (926-32211)
Mouse anti-CD163	MCA342GA*	175	1:500	IRDY <sup>®</sup> 680LT Conjugated Goat-Anti- Mouse IgG (926-68020)
Rabbit anti-CD206	Ab64693	190	1:1000	IRDye <sup>®</sup> 800 CW Conjugated Goat Anti-Rabbit IgG, (926-32211)
Mouse anti- $\beta$ -actin	A5441 <sup>+</sup>	42	1:5000	IRDY <sup>®</sup> 680LT Conjugated Goat-Anti- Mouse IgG (926-68020)

Secondary antibodies dilution=1:5000

\*AbD Serotec. #Licor Bioscience, USA. +Sigma-Aldrich USA

### 3.2.3.3 Immunodetection and densitometry analysis

The membrane was immersed in distilled water then secondary antibody signal was visualised using the Odyssey<sup>®</sup> Infrared Image system (LICOR Biosystems, USA) at 700nm or 800nm. Densitometry analysis was performed using Odyssey<sup>®</sup> Imaging System Software (LICOR Biosystems, USA). The calculated targeted protein signal was then normalized to  $\beta$ -actin for each sample.

### **3.3 Results**

#### **3.3.1 Adipose tissue histology**

Adipose tissue was embedded in paraffin wax to maintain tissue integrity. Various fixative and paraffin wax incubation times were tried until the desired results were achieved, Figure 3-3-A-D. H&E stain was used to assess the integrity of the tissue; adipocyte area size was measured and presented as a percentage to the total field area, Figure 3-3.E. The HFD/STZ group had a significant decrease in adipocyte size compared to HFD. This effect was reversed with pioglitazone treatment. Adipocyte size and animal weights were significantly correlated when analysed with the Pearson test ( $p=0.0002$ , Figure 3-3-F). Adipocyte size difference between NC and HFD showed a significant increase with  $p$  value of 0.0201.

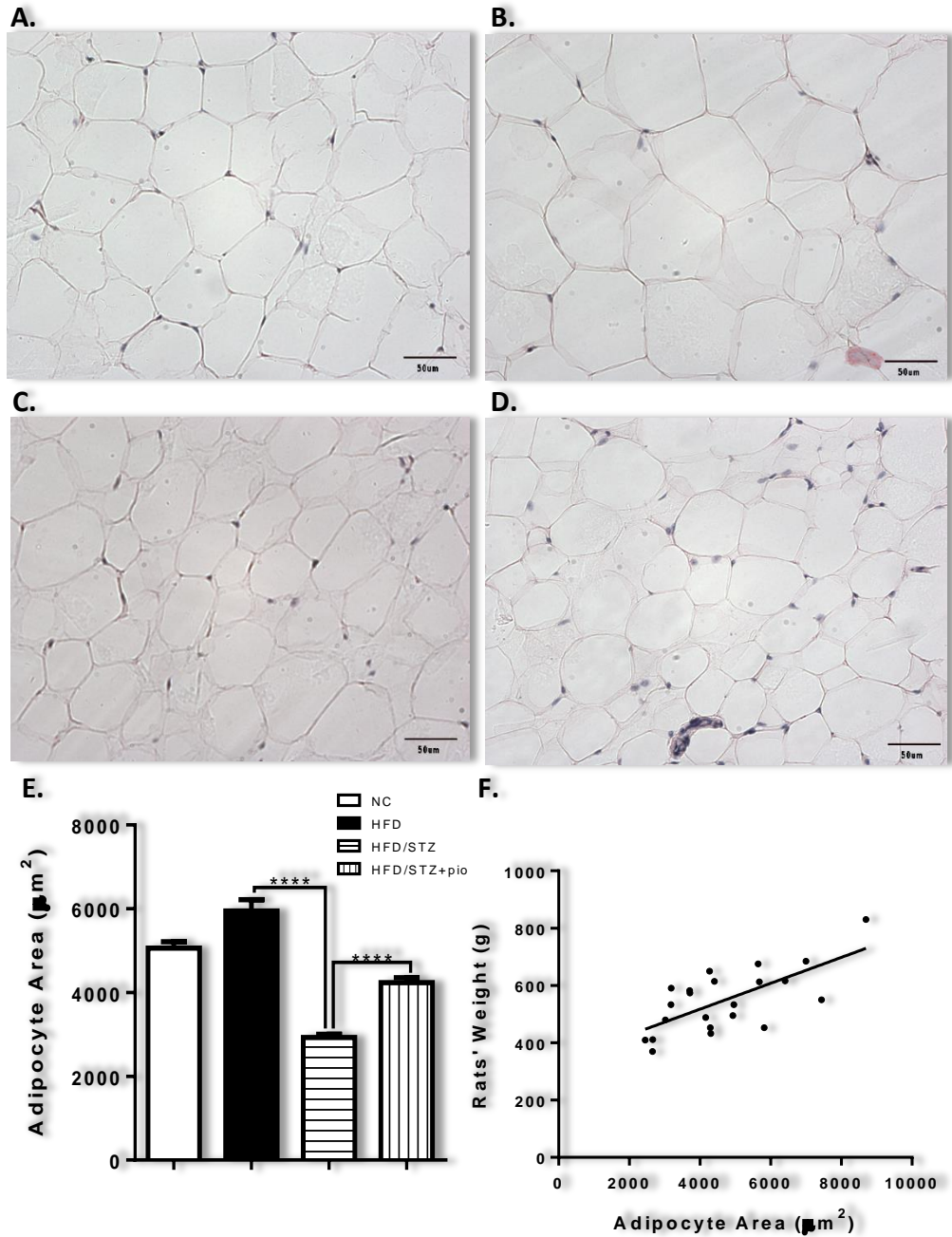


**Figure 3.3 | Visceral adipose tissue H&E staining and adipocyte sizing.**

Visceral adipose tissue from **A.**NC, **B.**HFD, **C.**HFD/STZ and **D.**HFD/STZ+pio groups were fixed in 4% paraformaldehyde, dehydrated then embedded in paraffin wax. Ten-µm thick sections were cut and stained with H&E to assess their histological structure, Magnification x200. Scale bar: 50µm. **E.** Two x200 fields were analysed using Image J software; adipocytes were outlined and their area was recorded. Size was calculated as a percentage to the total field area. HFD/STZ adipocytes were significantly smaller in size than HFD adipocytes, however, treatment with pioglitazone reversed that and increased their size. Data are presented as mean ± SEM from a Kruskal-Wallis test with Dunn's multiple comparisons test between pairs of columns (NC and HFD, HFD and HFD/STZ, HFD/STZ and HFD/STZ+Pio), \*\*\*p<0.0001 (n=5 for NC and HFD, n=6 for HFD/STZ and HFD/STZ+pio). # represent a significance (p=0.02) between NC and HFD analysed by student t-test **F.** Linear regression with Pearson test showed a significant correlation (p=0.0002) between adipocyte size and rats' weights. NC; Normal Chow, HFD; High Fat Diet, STZ; streptozotocin and Pio; pioglitazone.

### 3.3.2 Immunohistochemistry: control of tissue autofluorescence and validation of antibodies

Antibodies detecting different tissue macrophage phenotypic markers were used to identify their activation state. Table 3-9 illustrates those markers and their corresponding subtype.

**Table 3-9| Macrophage subtypes markers**

Primary Antibody	M1	M2a	M2b	M2c
Anti-CD86	+++		+	
Anti-CD163		+	+	+
Anti-CD206		+		+

Autofluorescence was observed in adipose tissue sections using DAPI, FITC and TRITC filters, Figure 3-4 top panel. Autofluorescence can be quenched with Sudan Black (Schnell *et al.*, 1999, Romijn *et al.*, 1999). Hence, tissues were stained with Sudan black solution which significantly reduced background fluorescence, Figure 3-4 bottom panel.

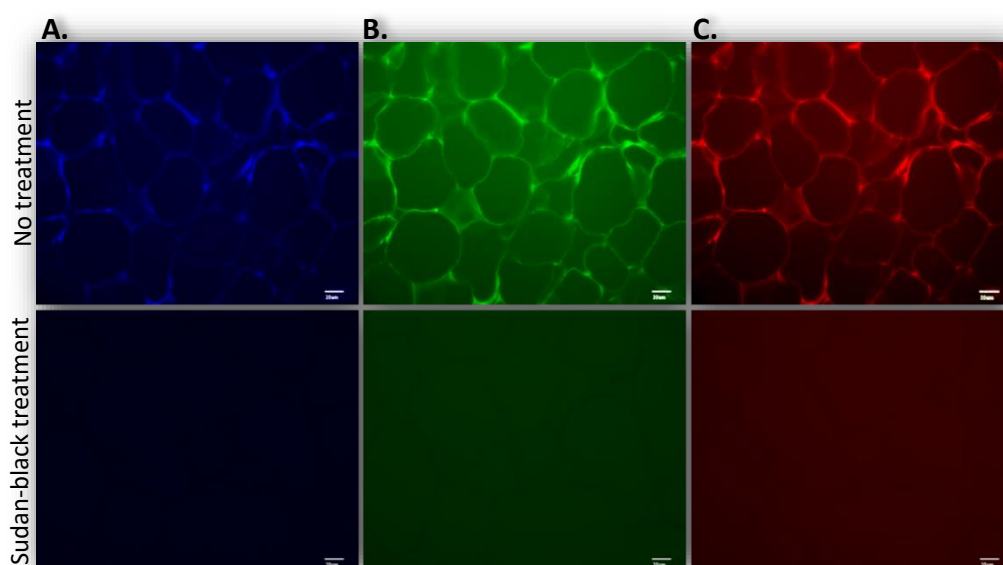


**Figure 3.4| Visceral adipose tissue immunohistochemistry of non-immune-labelled sections.** Fixed and paraffin embedded visceral adipose tissue cut at 10 $\mu$ m. Top panel; very high background signals is observed in all fluorescent channels; **A.** DAPI, **B.** FITC and **C.** TRITC, in non-immune-labelled sections. Bottom panel; signals were greatly reduced when sections were treated with 0.3% Sudan black solution for 10min. Magnification x400. Scale bar: 20 $\mu$ m

To determine antibody efficacy and specificity, sections from rat paw skin injected with Carrageenan, a widely used polysaccharide to produce localized inflammatory pain models (Fehrenbacher *et al.*, 2012), which has been generated during a different study were used, Figure 3-5.

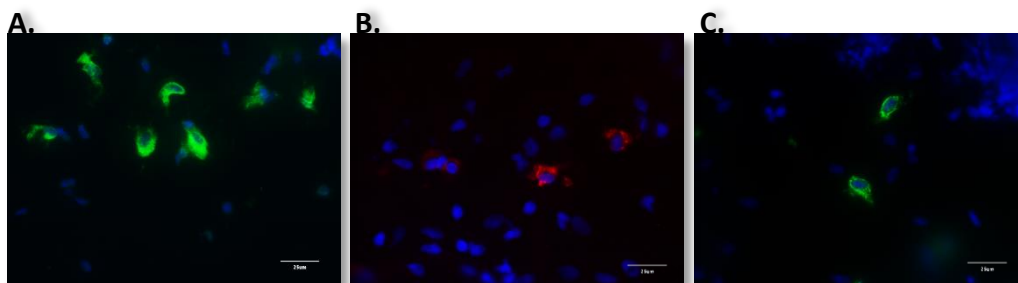


**Figure 3.5 | Rat paw skin tissue immunohistochemistry**

Carrageenan injected rat paw skin tissues were used as a positive control for macrophage markers. Tissue was fixed and 60µm thick sections were cut then stained with **A.** Rabbit anti-CD86 (green), **B.** Mouse anti-CD163 (red) and **C.** Rabbit anti-CD206 (green) as described in the methodology. Sections were treated with Sudan black and then the nuclei were stained blue with DAPI. Magnification x630. Scale bar: 25µm

### 3.3.3 Adipose tissue macrophage phenotype

The HFD group had elevated adipose tissue macrophage (ATM) numbers when compared to the NC group with significant increase in both CD86+ and CD206+ cells, with CD206+ correlating with the adipocyte size ( $p=0.017$ ). Treatment with STZ lead to a decrease in the number of CD206+ cells when compared to the HFD group, Figure 3-6. Pioglitazone treatment did not have any major effects on the number of macrophages within adipose tissue. Generally, the predominant macrophage phenotype in all groups was CD86+ cells and the least frequently observed were CD163/86+. Interestingly, most of the CD163/86+ cells were found in crown-like structures between adipocytes, Figure 3-7.

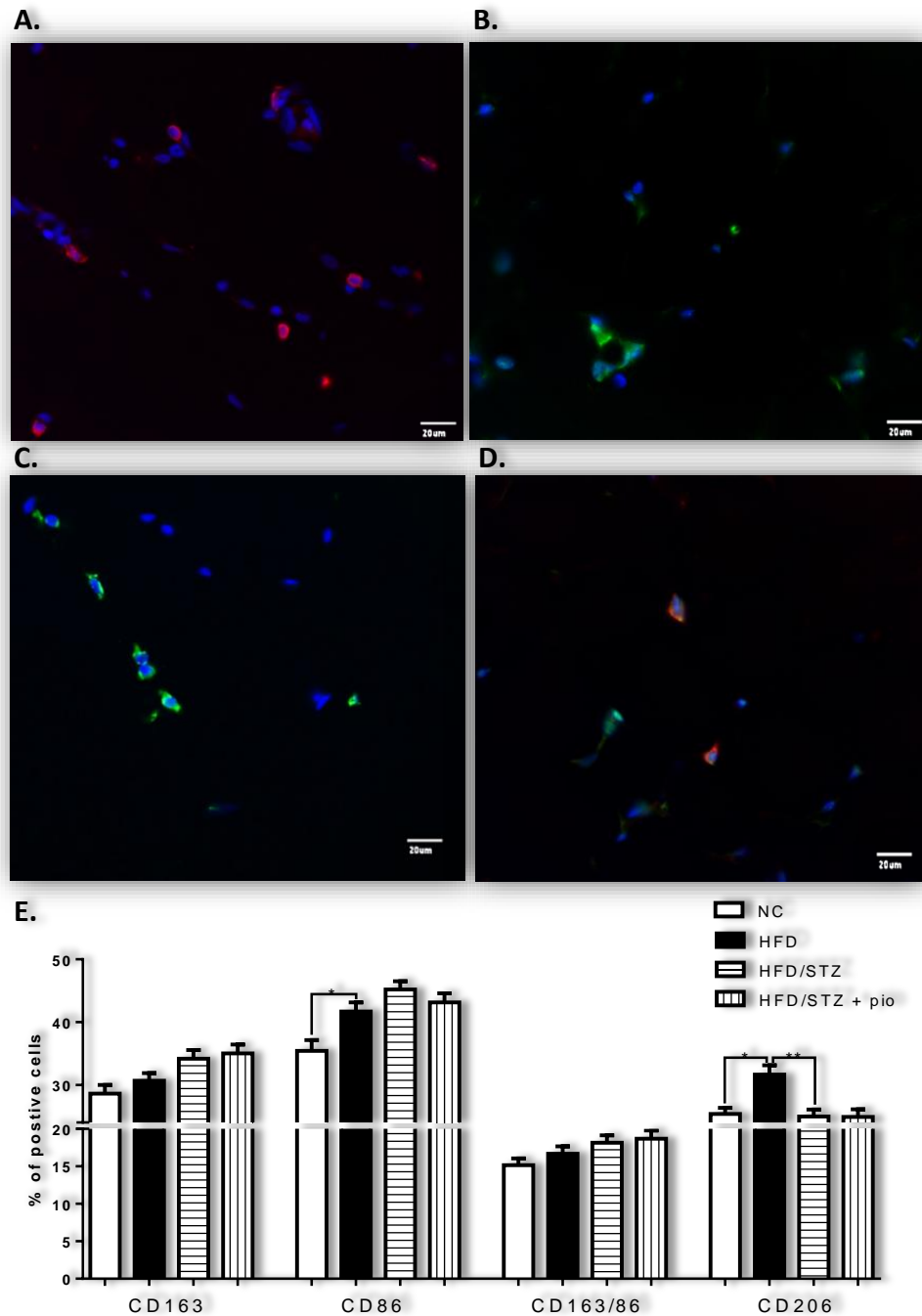


**Figure 3.6 | Visceral adipose Tissue Immunohistochemistry.**

A representation of **A.** mouse anti-CD163, **B.** rabbit anti-CD86, **C.** rabbit anti-CD206 and **D.** double staining of anti-CD86/163 immunohistochemistry staining on fixed and paraffin embedded adipose tissue; magnification x400, scale bar: 20 $\mu$ m. Four 10 $\mu$ m thick sections on 50 $\mu$ m intervals were processed as described in the methodology; positive cells are shown in green (B and C), red (A) or orange (D, a combination of green for CD86 and red for CD163), blue represents DAPI as a nucleus counter stain. **E.** Velocity software was used to count positive cells in 4 random fields from each section and present them as a percentage to the total number of nuclei. Kruskal-Wallis test with Dunn's multiple comparisons test between pairs of columns (NC and HFD, HFD and HFD/STZ, HFD/STZ and HFD/STZ+Pio) revealed a significant increase in HFD CD86+ cells compared to NC, HFD CD206+ cells compared to NC and STZ groups. Data are presented as mean $\pm$ SEM, \* $p$ <0.01 and \*\* $p$ <0.001 (n=5 for NC and HFD, n=6 for HFD/STZ and HFD/STZ+pio). NC; Normal Chow, HFD; High Fat Diet, STZ; streptozotocin and Pio; pioglitazone

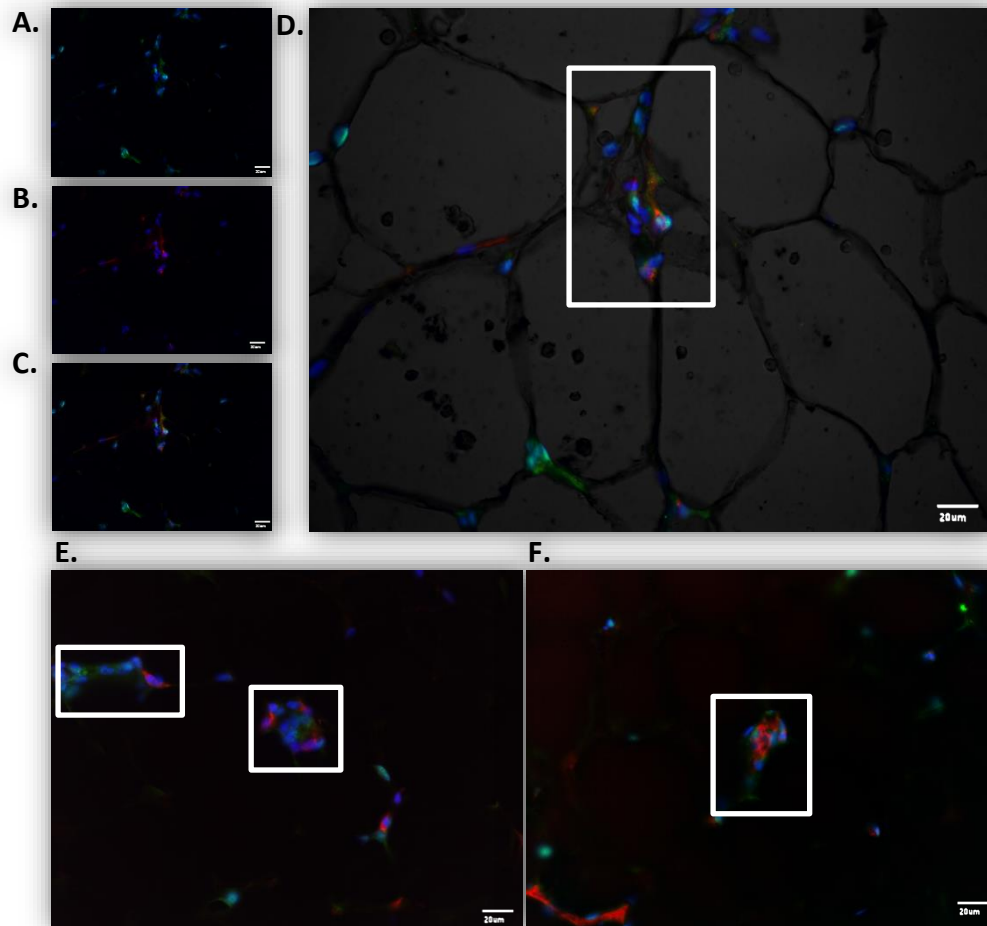


**Figure 3.7 | Macrophage CLS formation in visceral adipose tissue.**

A representation of immunohistochemistry staining on 10µm, fixed and paraffin embedded visceral adipose tissue sections stained with **A.** rabbit anti-CD86 (green), **B.** mouse anti-CD163 (red), **C.** merged A and B, **D.** merged A, B and bright field stained with Sudan black. **E** and **F** crown like structure (CLS) formation by CD163/86+ cells. Blue represents DAPI as a nucleus counter stain. Magnification x400, scale bar: 20µm.

### 3.3.4 Visceral adipose tissue inflammatory gene expression

Out of the several reference genes that were subjected to Taqman analysis, GAPDH was the most stable, therefore it was used to normalize the expression of the genes of interest. Pro and anti- Inflammatory cytokines and interleukins including TNF- $\alpha$ , IL-6, IL-1 $\beta$  and IL-10, that are secreted by macrophages and contribute to the chronic inflammation leading to

interruption of insulin signalling were analysed. There were no significant changes observed across the groups, Figure 3-8.

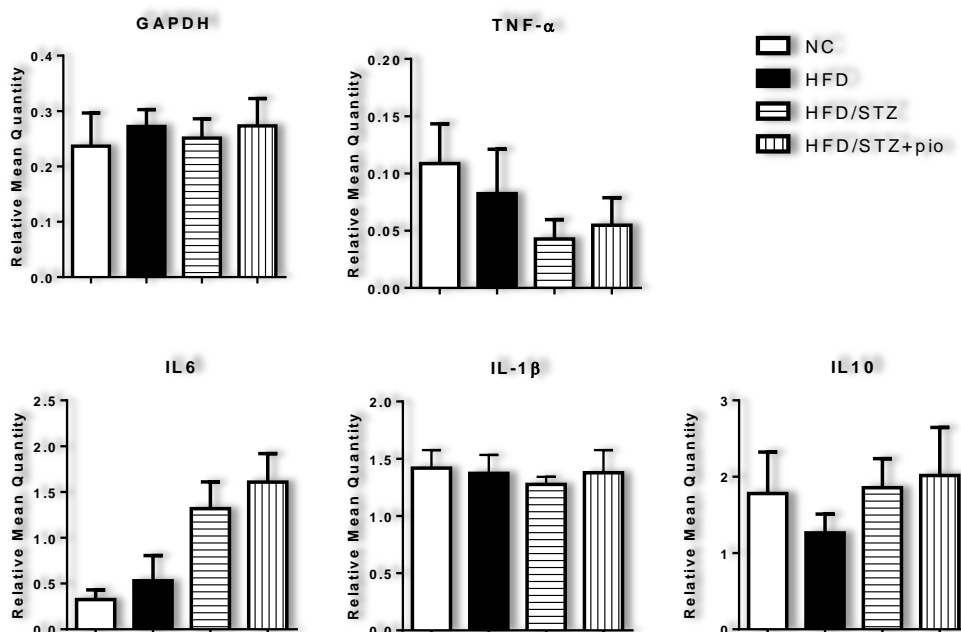


**Figure 3.8 | Visceral adipose tissue inflammatory gene expression.**

Liver mRNA was extracted using TRI-reagent then reversed transcribed to cDNA as described in the methodology. Expression level of GAPDH, TNF- $\alpha$ , IL6, IL-1 $\beta$  and IL10 was analysed using Taq-man RT-PCR where quantity was measured relative to a standard curve. GAPDH was stable across the groups therefore it was used to normalize the expression of targeted genes. No significant changes were observed when analysed with either one-way-ANOVA or Kruskal-Wallis test with bonferroni or Dunn's, respectively, post-hoc test comparing pairs; NC and HFD, HFD and HFD/STZ, HFD/STZ and HFD/STZ+Pio: (n=5 for NC and HFD, n=6 for HFD/STZ and HFD/STZ+pio). All data are presented as mean  $\pm$  SEM. NC; Normal Chow, HFD; High Fat Diet, STZ; streptozotocin, Pio; pioglitazone.

### 3.3.5 Skeletal muscle tissue histology, macrophages and tissue

#### inflammatory gene expression

H&E staining showed no difference in the histology of the muscle tissue (data not shown) between groups. Like adipose tissue, muscle was also subjected to immunohistochemistry however very few/no immune cells were observed in each tissue section, appendix figure 5. Therefore no further analysis was performed on macrophages in muscle tissue. However, inflammatory gene

level expression was still analysed. IL-10 and IL-1 $\beta$  expression was not detected, TNF- $\alpha$  and IL-6 expression level was not statistically altered across groups.

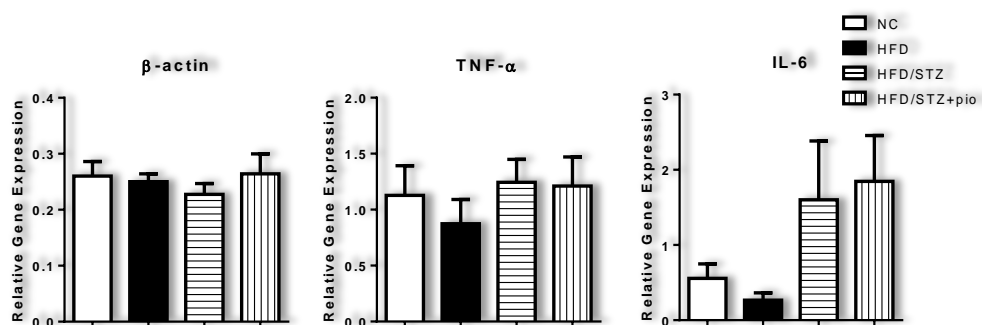


**Figure 3.9 | Skeletal muscle tissue inflammatory gene expression.**

Liver mRNA was extracted using TRI-reagent then reversed transcribed to cDNA as described in the methodology. Expression level of  $\beta$ -actin, TNF- $\alpha$  and IL6 was analysed using Taqman RT-PCR where quantity was measured relative to a standard curve.  $\beta$ -actin was stable across the groups therefore it was used to normalize the expression of targeted genes. No significant changes were observed when analysed with either one-way-ANOVA with bonferroni post-hoc test, respectively, post-hoc test comparing pairs; NC and HFD, HFD and HFD/STZ, HFD/STZ and HFD/STZ+Pio: (n=5 for NC and HFD, n=6 for HFD/STZ and HFD/STZ+pio). All data are presented as mean  $\pm$  SEM. NC; Normal Chow, HFD; High Fat Diet, STZ; streptozotocin, Pio; pioglitazone.

### 3.3.6 Liver tissue histology

Figure 4-10 shows liver sections stained with haematoxylin and eosin; interestingly the HFD group showed very high levels of fat deposition compared to the NC group, Figure 4-10-A & B,. This was represented by macrovesicular lipid vacuoles that displaced the nucleus to the periphery of the hepatocyte. Few samples of the HFD/STZ, and HFD/STZ+Pio groups showed microvesicular lipid vacuoles that did not displace the nucleus, Figure 3-10.

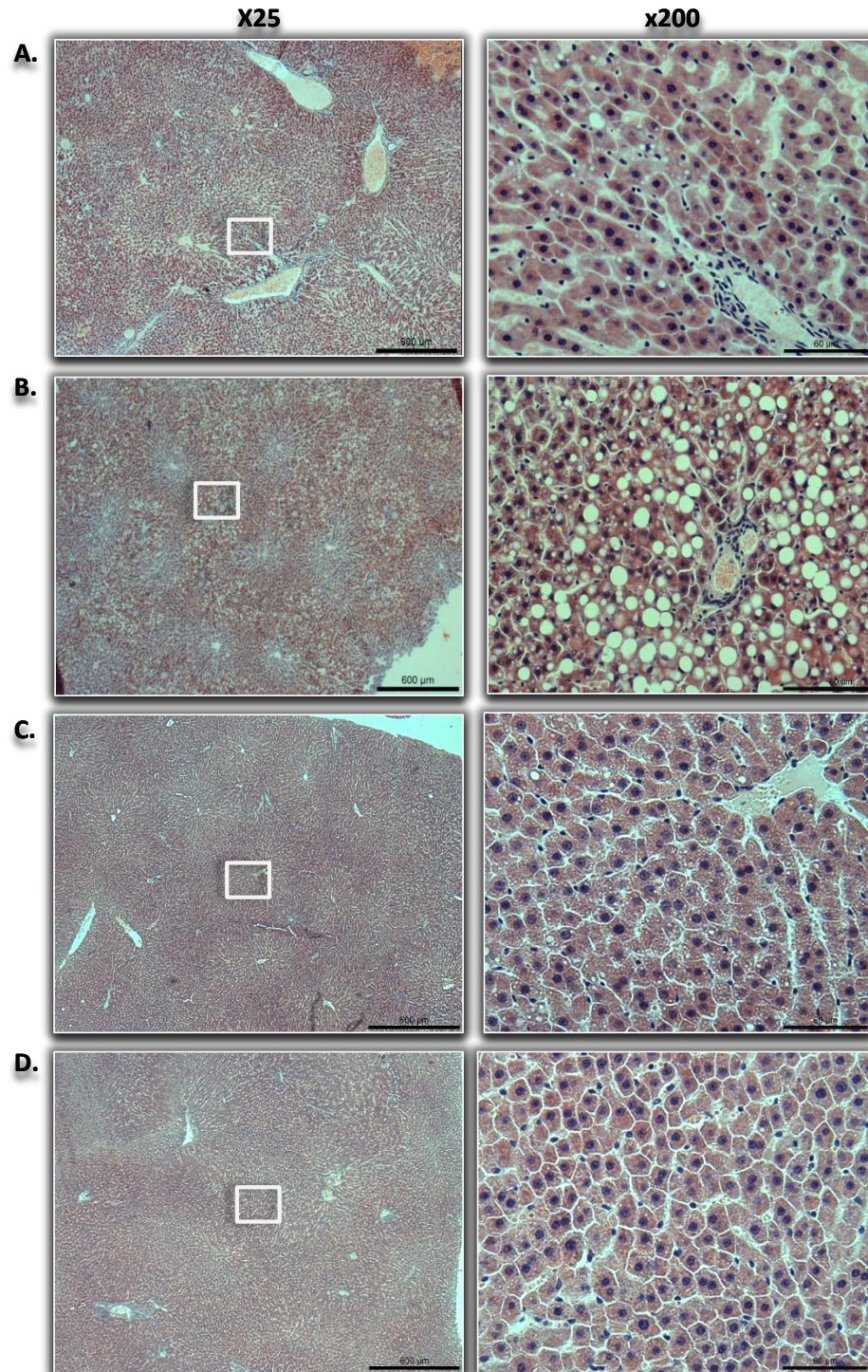


**Figure 3.10 | Liver histology.**

A representation of **A.** NC, **B.** HFD, **C.** HFD/STZ and **D.** HFD/STZ+pio histological sections at x25 and x200 magnification. Five- $\mu\text{m}$  paraformaldehyde fixed and paraffin embedded sections were stained with haematoxylin and eosin as describe in the methodology. Sections revealed steatosis represented by macrovesicular lipid droplets (B, A) or microvesicular lipid droplets (C). Scale Bar: at 25x 600 $\mu\text{m}$  and 200x 60 $\mu\text{m}$

### 3.3.7 Liver tissue macrophage phenotype

Liver tissue also exhibited an autofluorescent nature that was successfully reduced with Sudan black. However, the staining observed with macrophage marker antibodies appeared non-specific in that hepatocytes stained positive and the staining did not appear to be sinusoidal as could be expected, Figure 3-11.

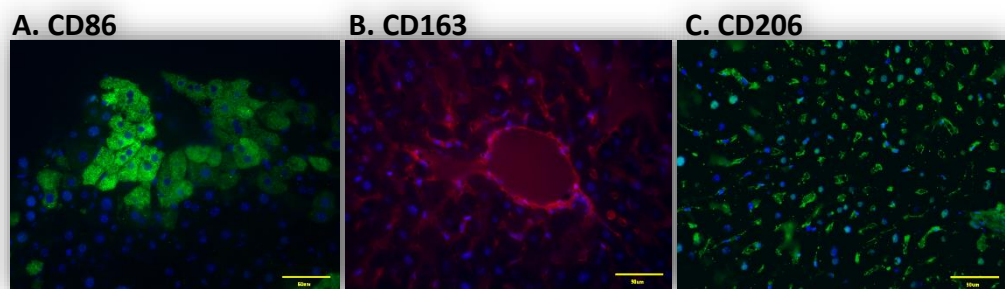


**Figure 3.11 | Liver tissue immunofluorescence.**

A representation of immunohistochemistry staining on 5µm, fixed and paraffin embedded liver tissue sections stained with **A.** rabbit anti-CD86 (green), **B.** mouse anti-CD163 (red), **C.** rabbit anti-CD206 as described in the methodology. Blue represents DAPI as a nucleus counterstain. Magnification x400, scale bar: 50µm.

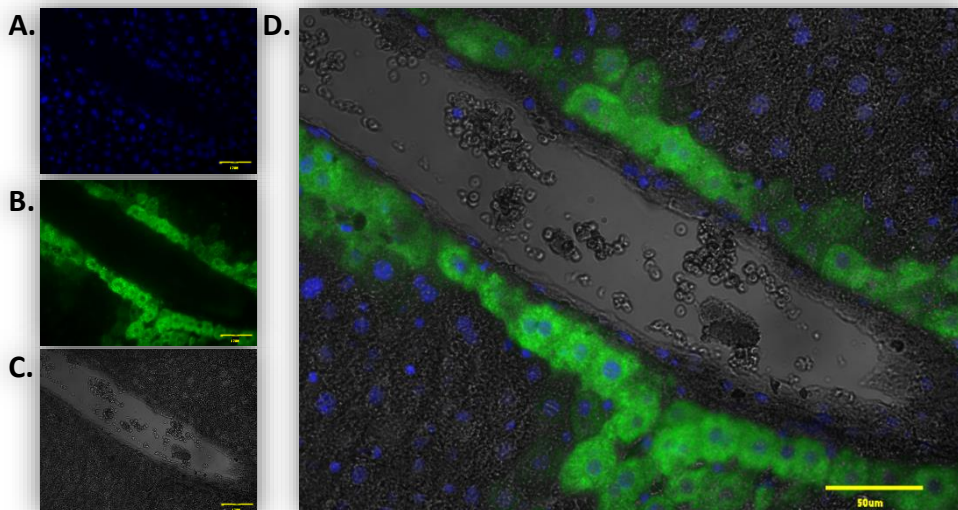


**Figure 3.12 | Rabbit anti-CD86 liver tissue immunohistochemistry.**

A representation of immunohistochemistry staining on 5µm, fixed and paraffin embedded liver tissue sections stained with **A.** DAPI as a counterstain, **B.** rabbit anti-CD86, **C.** Sudan black and **D.** merged of A, B and C as described in the methodology. Magnification x400, scale bar: 50µm.

Western blotting was used instead to determine the expression of macrophage markers. Western blotting analysis was only performed on the NC and HFD groups with CD206+ cells significantly increased in number in the HFD group (1.55 fold change).

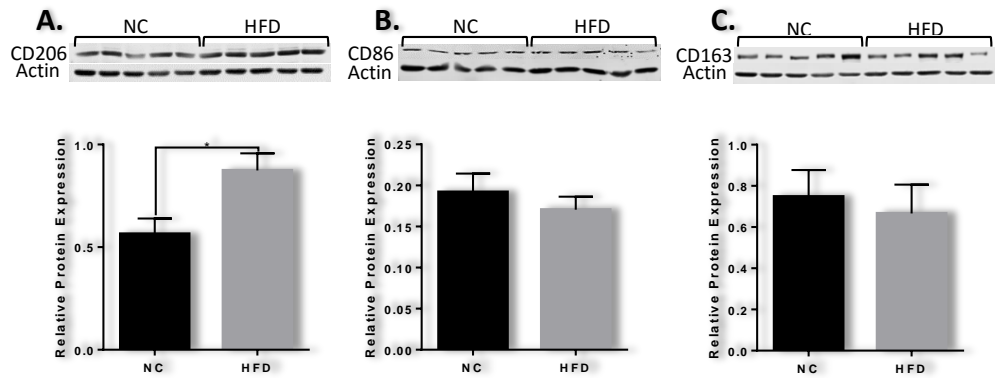


**Figure 3.13 | Western blot analysis of Kupffer cell markers in liver tissue.**

As described in the methodology, 65 $\mu$ g protein lysate extracted from liver tissue homogenized in Tri-reagent was separated by 8% (w/v) SDS-polyacrylamide electrophoresis gel and blotted onto nitrocellulose membrane. Immune-detection was performed using **A.** rabbit anti-CD206, **B.** rabbit anti-CD86 and **C.** mouse anti-CD163. Membrane was visualized using Odyssey<sup>®</sup> Infrared Image system followed by Image studio densitometric analysis and the detected signal was normalized to  $\beta$ -actin. High fat diet (HFD) group had a higher (\*  $P > 0.01$ ) CD206 protein expression compared to Normal chow (NC). Histograms were analyzed using student unpaired t-test, values are presented as mean  $\pm$  SEM.

### 3.4 Discussion

#### 3.4.1 Adipose tissue: A State of Chronic, Low-Grade Inflammation?

When adipose tissue mass increases, the pattern of adipokine secretion is altered. Adipose tissue production of pro-inflammatory cytokines such as IL-6 and TNF- $\alpha$  increases (Trayhurn and Wood, 2004), while the production of anti-inflammatory adiponectin decreases (Hu *et al.*, 1996). However, adipocytes are not the only cells responsible for the release of adipokines from adipose tissue (Fain *et al.*, 2004). The increase in inflammatory cytokines could in part be due to increased macrophage infiltration of adipose tissue (Xu *et al.*, 2003, Weisberg *et al.*, 2003). Recently obesity has been acknowledged to induce an immune system response characterized by myeloid cell activation and recruitment to key metabolic organs. In mice and humans increase in weight and adipose tissue mass are accompanied by inflammation that is characterized by macrophage infiltration and an increase in the expression of macrophage markers (Curat *et al.*, 2004, Weisberg *et al.*, 2003, Xu *et al.*, 2003, Cinti *et al.*, 2005) with positive correlations between BMI, adipocyte size and the number of macrophages (Arvidsson *et al.*, 2004). As described in chapter 3, HFD fed animals used in this study did not gain a significant amount of weight, however, HFD group adipocyte size was significantly larger and the difference in size correlated with the weight of the rats. This finding made the study of immune cells infiltration particularly interesting. The increase in CD206+ and CD86+ macrophage number correlated with the increase in adipocyte size.

An important characteristic of inflammatory macrophages found in adipose tissue is the formation of CLS. Large, multinucleate aggregations form around dead adipocytes as the macrophages scavenge free fatty acids (Cinti *et al.*, 2005). This CLS formation was observed in the adipose tissue of HFD fed animals, where CD86/163 also formed aggregations in the tissue. This double staining was meant to detect M2b type macrophages that are thought to have both pro and anti-inflammatory action.

Early studies by Hotamisligil and colleagues identified adipose tissue as an important source of obesity-induced inflammation (Hotamisligil *et al.*, 1993). They showed that inflammatory cytokine TNF- $\alpha$  is expressed in murine adipose tissue and that its expression was higher in obese rodents' adipocytes compared to lean rodents. They also found the same observations in obese human adipose tissue (Hotamisligil *et al.*, 1993). Since Hotamisligil's original study, scientists have found additional links between adiposity and the expression of a variety of inflammatory cytokines, including interleukin-1 $\beta$  (IL-1 $\beta$ ) and interleukin-6 (IL-6) (Strandberg *et al.*, 2006, Bruun *et al.*, 2003, Esposito *et al.*, 2003, Chida *et al.*, 2006). However this was not the case in the adipose tissue of animals in this study despite an increase in macrophage number in the HFD animals. This model could reflect the start of an inflammatory state prior to the development of obesity and it is possible that the number of macrophages was not yet high enough to cause inflammation.

### **3.4.2 Effect of HFD on muscle tissues**

Macrophages infiltrating liver and skeletal muscle tissues are poorly studied. In obesity, the number of skeletal muscle macrophages is much lower in relation to adipose tissue ATM content or the number of Kupffer cells in the liver. Almost no macrophage infiltration was seen in skeletal muscle in this study, which agreed with previous studies (Tam *et al.*, 2012, Bruun *et al.*, 2006, Di Gregorio *et al.*, 2005). However others reported an increase in muscle macrophage number when comparing lean to obese subjects (Kim *et al.*, 2011, Varma *et al.*, 2009, Bilan *et al.*, 2009, Weisberg *et al.*, 2003). As described in the introduction, some referred this finding to the increase in the fat depots with in the muscle. The lack of weight gain and absence of histological observation of lipid depots in muscle probably accounts for the failure to detect immune cells in skeletal muscle in this study.

### **3.4.3 Liver tissue steatosis and macrophage markers**

The effect of HFD feeding was most pronounced in liver tissue where steatosis was clearly evident and the histology was similar to that seen in NAFLD in humans. Liver lipid accumulation in NAFLD is the consequence of an imbalance in hepatic lipid turnover. There are various possible sites where alterations in the lipid metabolism can result in the appearance of hepatic steatosis: increased free fatty acid delivery to the liver; increased de novo lipogenesis; reduced  $\beta$ -oxidation rate within the liver and decreased triglyceride export through VLDL production and secretion. This finding indicated that the HFD group, even in the absence of weight gain showed

significant effects in their liver but not adipose or skeletal muscle which required further analysis to understand the underlying cellular mechanisms behind this pathology.

#### **3.4.4 Conclusion**

In conclusion, the lack of effect of the HFD on both adipose and muscle tissues in this study could be directly related to the lack of weight gain. Although HFD feeding lead to a slight increase in adipose tissue macrophage number, it seems that chronic inflammation occurs as a consequence of obesity. While the animal models of this study did not produce a typical obese model, they did provide insight on what could be key to the initial development of insulin resistance. The steatosis presented by the liver meant the investigation and further analysis of the liver became the focus of the rest of this study.

**CHAPTER IV:**

**Effect of HFD on  
Peripheral Tissue Lipid  
Deposition**

## 4.1 Introduction

Liver fat content in humans is normally below 5% (Neuschwander-Tetri and Caldwell, 2003). Under certain circumstances, excess fat may accumulate in the liver. Both high alcohol consumption and insulin resistance are associated with the development of fatty liver disease. Despite differences in etiology and different mechanisms leading to fat accumulation in the liver (Berk *et al.*, 2005), alcoholic fatty liver disease (AFLD) and non-alcoholic fatty liver disease (NAFLD) are histologically indistinguishable (Kneeman *et al.*, 2012). Hepatic steatosis is reversible, but if it persists, it can lead to inflammation in the liver known as steatohepatitis and further to cirrhosis and end-stage liver disease. NAFLD is becoming the most common chronic liver disease in the Western world (Adams *et al.*, 2005). The prevalence of NAFLD is estimated to be approximately one third of the adult population in western countries (Ryan *et al.*, 2002, Szczepaniak *et al.*, 2005), while 2-3% suffer from non-alcoholic steatohepatitis (NASH) (Reddy and Rao, 2006). The prevalence of NAFLD increases as a function of obesity (Kotronen and Yki-Järvinen, 2008) and is found in three quarters of type 2 diabetes patients (Del Gaudio *et al.*, 2002). The exact mechanisms underlying the development of NAFLD are under investigation. High fat diet is associated with NAFLD in both humans and in animal models (Westerbacka *et al.*, 2005). Hepatic insulin resistance is characterized by an impaired ability of insulin to suppress hepatic glucose production. Fat accumulation in the liver is associated with hepatic insulin resistance (Kotronen and Yki-Järvinen, 2008). In rats on a high fat diet, the activation of IRS1 and IRS2 in the liver is impaired,

leading to decreased glycogen synthase activity and increased gluconeogenesis (Samuel *et al.*, 2004).

## **4.2 Aims**

In the previous chapter data demonstrated the development of HFD mediated steatosis in liver tissue. Hence, the work of this chapter was directed to investigate the metabolic pathways that are associated with developing liver steatosis, understanding the composition of the deposited TG and determine its source. Furthermore, investigating the effect of the HFD on skeletal muscle tissue on genes expression related to lipid metabolism.

## 4.3 Material and methods

### 4.3.1 TaqMan gene expression analysis

Taqman was carried out as previously described and was used to measure the expression of SREBP-1C, Phosphoenolpyruvate carboxykinase 1 (PCK) and G6P catalytic subunit (G6PC). Primers and probes are listed in table 4-1.

**Table 4-1 | SREBP-1C, PCK and G6PC TaqMan primers and probes**

Gene	Sequence 5' → 3'	Origin
<b>PCK-1</b> NM_198780.3	<b>Fwd:</b> CCCAGGAGTCACCATCACTTC <b>Rev:</b> GGTGCAGAATCGCGAGTTG <b>Probe:</b> CACG GTTCCTCATCTGTGGTCTCCA	FRAME database
<b>G6PC</b> NM_13098.2	<b>Fwd:</b> GACCTCAGGAACGCCTTCTATG <b>Rev:</b> AGGAGATTGATGCCACAGTCT <b>Probe:</b> CCTCTTCCCATCTGGTTCCACATTCA	FRAME database
<b>SREB-1C</b> XM_006721570.2	<b>Fwd:</b> GGAGGGGTAGGGCCAAC <b>Rev:</b> GTCAAATAGGCCAGGGAAGTC <b>Probe:</b> CGCGGAGCCATGGATTGC	FRAME database

### 4.3.2 TaqMan low density array

TaqMan Low density array is a relative quantitation method that analyses 96 genes simultaneously. Genes that are thought to be involved in the mechanism and pathogenies of NAFLD were selected. Gene symbols, abbreviation and function are listed in table 4-2.

**Table 4-2 | TaqMan Low density array gene list.**

Symbol	Gene and Function
<b>Reference genes</b>	
<b>ABL1</b>	<b>C-abl Oncogene 1, Receptor Tyrosine Kinase:</b> Cell differentiation, cell division, cell adhesion, and stress response.
<b>HPRT1</b>	<b>Hypoxanthine phosphoribosyltransferase1:</b> Catalyses conversion of hypoxanthine to inosine monophosphate and guanine to guanosine monophosphate for energy production
<b>MRPL19</b>	<b>Mitochondrial ribosomal protein L19:</b> Protein synthesis within the mitochondrion
<b>RPLP0</b>	<b>Ribosomal protein of the L10P:</b> 60S ribosomal protein (Westerbacka <i>et al.</i> , 2007, Beaven <i>et al.</i> , 2013, Inoue <i>et al.</i> , 2005)
<b>TBP</b>	<b>TATA-binding protein:</b> A general transcription factor that binds specifically to TATA box (Westerbacka <i>et al.</i> , 2007)

<b>18sRNA</b>	<b>Endogenous control</b>
<b>Glycolysis genes</b>	
<b>LDHA</b>	<b>Lactate Dehydrogenase A:</b> Catalyzes lactate & NAD to pyruvate and NADH in the final step of glycolysis (Hedeskov <i>et al.</i> , 1992)
<b>Pklr</b>	<b>Liver Type pyruvate (LPK):</b> ChREBP can stimulate LPK gene transcription in response to high glucose conc without any apparent requirement of insulin
<b>Gluconeogenesis genes</b>	
<b>G6PC</b>	<b>Glucose 6-phosphatase, catalytic subunit:</b> Catalyzes the hydrolysis of glc 6-phosphate to glucose and orthophosphate, downstream of FOXO (Dufour and Clavien, 2009)
<b>PCK1</b>	<b>Phosphoenolpyruvate Carboxykinase (PEPCK):</b> Converts oxaloacetate into phosphoenolpyruvate and carbon dioxide. downstream of FOXO (Beaven <i>et al.</i> , 2013)
<b>FGF21</b>	<b>Fibroblast Growth Factor 21:</b> A cytokine that is considered as a new metabolic regulator of non-insulin dependent glucose transport in cells Stimulates glucose uptake in adipocytes (Novotny <i>et al.</i> , 2014, Fisher <i>et al.</i> , 2010, Kim <i>et al.</i> , 2014).
<b>FOXO1</b>	<b>Forkhead Box Protein O 1:</b> In the nucleus it binds to the insulin response sequence located in the promoter for glucose 6-phosphatase and increases its rate of transcription (Beaven <i>et al.</i> , 2013, Ueki and Kadowaki, 2011, Farrell <i>et al.</i> , 2013)
<b>IRS1</b>	<b>Insulin Receptor Substrate 1:</b> maintain metabolic homeostasis through their complementary roles in regulating insulin signalling and gene expression (Taniguchi <i>et al.</i> , 2005)
<b>Pentose phosphate pathway genes</b>	
<b>G6PD</b>	<b>Glucose 6-phosphate dehydrogenase:</b> Produce NADPH, a key electron donor in the defence against oxidizing agents and in reductive biosynthetic reactions (Farrell <i>et al.</i> , 2013)
<b>Glycogen metabolism genes</b>	
<b>GSK3<math>\beta</math></b>	<b>Glycogen Synthase Kinase 3 beta:</b> Phosphorylating and inactivating glycogen synthase. GSK3B is involved in energy metabolism, neuronal cell development, and body pattern formation (Farrell <i>et al.</i> , 2013, Song <i>et al.</i> , 2013)
<b>Kreb cycle genes</b>	
<b>PK2</b>	<b>Pyruvate Dehydrogenase Kinase 2:</b> Phosphorylate PDC inhibiting glycolysis (Farrell <i>et al.</i> , 2013)
<b>UCP2</b>	<b>Uncoupling protein 2:</b> Reduce the mitochondrial membrane potential in mammalian cells. (fatty acid oxidation) (Inoue <i>et al.</i> , 2005)
<b>Glucose transporter gene</b>	
<b>Slc2a2</b>	<b>Glucose Transporter 2 (GLUT2):</b> mediates facilitated bidirectional glucose transport (Farrell <i>et al.</i> , 2013)
<b>Fatty acid synthesis genes</b>	
<b>ACACB</b>	<b>Acetyl-Coenzyme A Carboxylase Beta (ACAC-<math>\beta</math> or ACC2):</b> Catalyzes the carboxylation of acetyl-CoA to malonyl- CoA, the rate-limiting step in fatty acid synthesis (Beaven <i>et al.</i> , 2013)
<b>ACACA</b>	<b>Acetyl-Coenzyme A Carboxylase Alpha (ACAC-<math>\alpha</math> or ACC1):</b> Catalyses the carboxylation of acetyl-CoA to malonyl-CoA, the rate-limiting step in fatty acid synthesis (Westerbacka <i>et al.</i> , 2007, Beaven <i>et al.</i> , 2013)
<b>FASN</b>	<b>Fatty Acid Synthase:</b> Catalyze the synthesis of palmitate from acetyl-CoA and malonyl-CoA, in the presence of NADPH, into long-chain saturated fatty acids (Beaven <i>et al.</i> , 2013, Gonzalez-Periz <i>et al.</i> , 2009, Buque <i>et al.</i> , 2010)
<b>Mlxipl</b>	<b>Carbohydrate response element binding protein (ChREBP-<math>\alpha</math>):</b> Promotes fatty acid synthesis genes (Beaven <i>et al.</i> , 2013, Anderson and Borlak, 2008)

<b>ME1</b>	<b>Malic enzyme 1:</b> Catalyzes the oxidative decarboxylation of malate to pyruvate (Buque <i>et al.</i> , 2010)
<b>SCD-1</b>	<b>Stearoyl CoA Desaturase:</b> Catalyzes a rate-limiting step in the synthesis of unsaturated fatty acids (Beaven <i>et al.</i> , 2013, Dufour and Clavien, 2009, Guillen <i>et al.</i> , 2009, Buque <i>et al.</i> , 2010)
<b>SCD-4</b>	<b>Stearoyl CoA Desaturase 4:</b> found to be affected by leptin receptor however its expression is not yet characterized in liver tissue ( <b>Dufour and Clavien, 2009</b> )
<b>SREBF</b>	<b>Sterol regulatory element binding transcription factor 1:</b> Promotes genes involved in sterol biosynthesis (Beaven <i>et al.</i> , 2013, Cable <i>et al.</i> , 2009, Dufour and Clavien, 2009, Anderson and Borlak, 2008)
<b>SREBF2</b>	<b>Sterol regulatory element binding transcription factor 2:</b> controls cholesterol homeostasis by stimulating transcription of sterol-regulated genes (Anderson and Borlak, 2008)
<b>GCK</b>	<b>Glucokinase:</b> An enzyme that Facilitates phosphorylation of glucose to glucose-6-phosphate (Beaven <i>et al.</i> , 2013, Farrell <i>et al.</i> , 2013)
<b>Elovl6</b>	<b>Fatty Acid Elongase 6:</b> During biosynthesis of essential fatty acids, an FA elongase alternates with different desaturases repeatedly inserting an ethyl group, then forming a double bond (Beaven <i>et al.</i> , 2013, Matsuzaka and Shimano, 2009)
<b>Triacylglycerol biosynthesis genes</b>	
<b>DGAT2</b>	<b>Diacylglycerol O-acyltransferase 2:</b> Utilizes diacylglycerol and fatty acyl CoA as substrates in order to catalyze the final stage of triacylglycerol synthesis
<b>GPD1</b>	<b>Glycerol-3-phosphate dehydrogenase 1:</b> Catalyzes the unidirectional conversion of glycerol-3-phosphate to dihydroxyacetone phosphate with concomitant reduction of the enzyme-bound FAD
<b>Lipid Metabolism genes</b>	
<b>ACADL</b>	<b>Acyl-Coenzyme A dehydrogenase, Long chain:</b> Catalyze the initial step of mitochondrial. beta-oxidation of straight-chain fatty acid (Zhang <i>et al.</i> , 2007, Nakamura <i>et al.</i> , 2014)
<b>ACADVL</b>	<b>Acyl-Coenzyme A dehydrogenase, very long chain:</b> Catalyzes the first step of the mitochondrial fatty acid beta-oxidation pathway. This acyl-Coenzyme A dehydrogenase is specific to long-chain and very-long-chain fatty acids (Zhang <i>et al.</i> , 2010)
<b>ACSL4</b>	<b>Acyl-CoA synthetase long-chain family member 4:</b> Controls the level of free arachidonic acid (AA) regulating eicosanoid production (Westerbacka <i>et al.</i> , 2007)
<b>Prkce</b>	<b>Protein Kinase C epsilon (PKCε):</b> A serine- and threonine-specific protein kinases that can be activated by calcium and the second messenger diacylglycerol. It inhibits lipid synthesis via disruption of the mitochondrial acyl-CoA:glycerol- <i>sn</i> -3-phosphate acyltransferase (Farrell <i>et al.</i> , 2013, Samuel <i>et al.</i> , 2007)
<b>ADIPOR1</b>	<b>Adiponectin receptor 1:</b> Mediate increased AMPK expression (Sun <i>et al.</i> , 2006)
<b>ADIPOR2</b>	<b>Adiponectin receptor 2:</b> Mediate increase PPARα expression (Sun <i>et al.</i> , 2006)
<b>CD36</b>	<b>CD36:</b> Promotes fatty acid uptake, transport (Inoue <i>et al.</i> , 2005, Farrell <i>et al.</i> , 2013, Guillen <i>et al.</i> , 2009, Buque <i>et al.</i> , 2010)
<b>Slc27a2</b>	<b>Fatty acid transport protein 2 and 5:</b> facilitates the transfer of fatty acids by binding to long-chain fatty acids and some other hydrophobic ligands. They are also thought to be involved in their uptake, transport and metabolism ( <b>Nassir and Ibdah, 2014, Doege <i>et al.</i>, 2008</b> )
<b>Slc27a5</b>	
<b>LPL</b>	<b>Lipoprotein Lipase:</b> Dual functions of triglyceride hydrolase and ligand/bridging factor for receptor-mediated lipoprotein uptake (Westerbacka <i>et al.</i> , 2007)
<b>CAT</b>	<b>Catalase:</b> Antioxidant gene shown to be upregulated in the liver in response to CYP2E1-dependent oxidative stress (Younossi <i>et al.</i> , 2005)

<b>HMGCS2</b>	<b>3-hydroxy-3-methylglutaryl-Coenzyme A synthase 2:</b> Rate limiting enzyme of the HMG-CoA pathway of fatty acid metabolism (ketogenesis)(Younossi <i>et al.</i> , 2005)
<b>PLIN</b>	<b>Perilipin 1 and 2 :</b> Coats lipid storage droplets in adipocytes, thereby protecting them until they can be broken down by hormone-sensitive lipase (Sun <i>et al.</i> , 2013)
<b>PLIN2</b>	
<b>Cidec</b>	<b>Fat-specific protein 27 (FSP27):</b> An adipocyte-specific lipid droplet-associated protein, promotes lipiddroplet growth by initiating lipid exchange and transfer (Guillen <i>et al.</i> , 2009, Sun <i>et al.</i> , 2013)
<b>FOXa2</b>	<b>Forkhead box protein A2:</b> It is a hepatocyte nuclear factors that functions as a transcriptional activators for liver-specific genes such as albumin and transthyretin (Anderson and Borlak, 2008, Wolfrum <i>et al.</i> , 2004).
<b>mTOR</b>	<b>The mechanistic target of rapamycin:</b> in obese individuals it was shown to activate SREBP-1c, promotes ER stress and inhibits autophagy (Bechmann <i>et al.</i> , 2012, Ricoult and Manning, 2013)
<b>HK2</b>	<b>Hexokinase II:</b> activates genes that encodes enzyme that are involved in the biosynthesis of fatty acids (Sebastian <i>et al.</i> , 2000)
<b>Sirt-3</b>	<b>Sirtuin 3:</b> it is a mitochondrial regulator is known to regulate many lipid metabolic genes. Its expression is said to be elevated in NASH (Nassir and Ibdah, 2014)
<b>Sirt-6</b>	<b>Sirtuin 6:</b> it is located in the nucleus, it had an indirect negative regulatory mechanism to glycolysis, triglyceride synthesis, and fat metabolism (Kim <i>et al.</i> , 2010)
<b>Cholesterol metabolism genes</b>	
<b>APOC3</b>	<b>Apolipoprotein C-III:</b> Inhibits lipoprotein lipase and hepatic lipase & delay the catabolism of triglyceride-rich particles (Cable <i>et al.</i> , 2009)
<b>Nuclear receptors genes</b>	
<b>PPAR<math>\alpha</math></b>	<b>Peroxisome Proliferator-activated Receptor alpha:</b> regulates the expression of genes involved in fatty acid beta-oxidation and is a major regulator of energy homeostasis (Westerbacka <i>et al.</i> , 2007, Inoue <i>et al.</i> , 2005, Kim <i>et al.</i> , 2014, Anderson and Borlak, 2008)
<b>Ppard</b>	<b>Peroxisome proliferator-activated receptor beta (delta):</b> Regulates lipid metabolism, and epidermal cell proliferation (Lee <i>et al.</i> , 2003)
<b>PGC1<math>\alpha</math></b>	<b>Peroxisome proliferator-activated receptor gamma, coactivator 1 alpha (PPARGC1<math>\alpha</math>) and beta (PPARGC1<math>\beta</math>):</b> Enhances metabolically relevant pathways, such as gluconeogenesis, fatty acid oxidation, thermogenesis, oxidative phosphorylation and mitochondrial biogenesis (Westerbacka <i>et al.</i> , 2007, Cable <i>et al.</i> , 2009)
<b>PGC1<math>\beta</math></b>	
<b>RXR<math>\alpha</math></b>	<b>Retinoid X receptor, alpha (RXR<math>\alpha</math>):</b> mediate the biological effects of retinoids by their involvement in retinoic acid-mediated gene activation (Anderson and Borlak, 2008)
<b>Nr1h4</b>	<b>Farnesoid X Receptor (FXR):</b> Suppressed cholesterol 7 alpha-hydroxylase (CYP7A1), the rate-limiting enzyme in bile acid synthesis from cholesterol.
<b>CREB-1</b>	<b>cAMP response element-binding protein 1 and 3:</b> activator of gluconeogenic gene transcription (Kim <i>et al.</i> , 2014)
<b>CREB-3</b>	
<b>EGR1</b>	<b>Early Grown Response Protein 1:</b> its activation is required for differentiation and mitogenesis. It controls tissue repair, wound healing, liver regeneration and in its downstream of FGF21 (Fisher <i>et al.</i> , 2010)
<b>Adipogenic genes</b>	
<b>CEBPA</b>	<b>CCAAT/enhancer binding protein (C/EBP), alpha:</b> Modulate leptin gene that help regulate body weight homeostasis
<b>CEBPB</b>	<b>CCAAT/enhancer binding protein (C/EBP), beta:</b> regulation of genes involved in immune and inflammatory responses

<b>Nr1h3</b>	<b>Liver-X-receptor alpha and beta (LXR-<math>\alpha</math>, LXR-<math>\beta</math>):</b> Regulating the expression of genes involved in hepatic bile and fatty acid synthesis, glucose metabolism as well as sterol efflux (Beaven <i>et al.</i> , 2013, Anderson and Borlak, 2008)
<b>NR1H2</b>	
<b>PPAR<math>\gamma</math></b>	<b>Peroxisome Proliferator-activated Receptor gamma:</b> Regulates of adipocyte differentiation (Westerbacka <i>et al.</i> , 2007, Inoue <i>et al.</i> , 2005, Anderson and Borlak, 2008)
<b>FABP4</b>	<b>Fatty acid binding protein 4:</b> Promotes in fatty acid uptake, transport, and metabolism (Westerbacka <i>et al.</i> , 2007)
<b>FABP5</b>	<b>Fatty acid binding protein 5:</b> Promotes in fatty acid uptake, transport, and metabolism (Westerbacka <i>et al.</i> , 2007)
<b>Inflammatory genes</b>	
<b>CASP3</b>	<b>Caspase 3:</b> Plays a central role in the execution-phase of cell apoptosis
<b>CCL2</b>	<b>Chemokine (C-C motif) Ligand 2 (MCP-1):</b> Regulates immunoregulatory and inflammatory processes (Monocyte chemoattractant protein-1) (Westerbacka <i>et al.</i> , 2007)
<b>CCL3</b>	<b>Chemokine (C-C motif) ligand 3 (MIP-1<math>\alpha</math>):</b> Macrophage Inflammatory Proteins. involved in acute inflammatory state to recruit and activate of leukocytes (Westerbacka <i>et al.</i> , 2007)
<b>IL6</b>	<b>Interleukin 6:</b> Induces a transcriptional inflammatory response through interleukin 6 receptor, alpha (Dowman <i>et al.</i> , 2010, Kim <i>et al.</i> , 2014, Farrell <i>et al.</i> , 2013)
<b>TNF<math>\alpha</math></b>	<b>Tumour necrosis factor alpha (TNF superfamily, member 2):</b> Regulates cell proliferation, differentiation, apoptosis, lipid metabolism, and coagulation. (Dowman <i>et al.</i> , 2010, Hotamisligil, 2005, Kim <i>et al.</i> , 2014)
<b>IL10</b>	<b>Interleukin 10:</b> It is an anti-inflammatory cytokine (Olefsky and Glass, 2010)
<b>IL1B</b>	<b>Interleukin 1<math>\beta</math>:</b> Produced by activated macrophages as a proprotein, which is proteolytically processed to its active form by caspase 1 (Dowman <i>et al.</i> , 2010, Kim <i>et al.</i> , 2014)
<b>Serpine1</b>	<b>Serpin Peptidase Inhibitor (Plasminogen activator inhibitor-1, PAI-1):</b> Is a serine protease inhibitor that functions as the principal inhibitor of tissue plasminogen activator (Westerbacka <i>et al.</i> , 2007).
<b>CPT1b</b>	<b>Carnitine Palmitoyltransferase I:</b> Is a mitochondrial enzyme responsible for the formation of acyl carnitines by catalyzing the transfer of the acyl group of a long-chain fatty acyl-CoA from coenzyme A to l-carnitine. (Fatty acid oxidation) (Westerbacka <i>et al.</i> , 2007, Inoue <i>et al.</i> , 2005, Cable <i>et al.</i> , 2009).
<b>Socs3</b>	<b>Suppressor of cytokine signalling 3:</b> regulation of cytokine and insulin signalling. It was shown to be increased in insulin-resistant obese mice (Sachithanandan <i>et al.</i> , 2010)
<b>Kuffer cells</b>	
<b>MRC1</b>	<b>Mannose receptor (CD206):</b> found on the surface of M2 activated macrophages (Wentworth <i>et al.</i> , 2010)
<b>CD86</b>	<b>CD86:</b> found on the surface of M1 activated macrophages (Orme and Mohan, 2012, David and Kroner, 2011)
<b>CD163</b>	<b>ED2:</b> found on the surface of both M2 and M1 (Orme and Mohan, 2012, David and Kroner, 2011)
<b>CD68</b>	<b>ED1:</b> found of the surface of monocytes and most of macrophages in tissue (Beaven <i>et al.</i> , 2013)
<b>Endoplasmic reticulum stress genes</b>	
<b>ERN1</b>	<b>Endoplasmic reticulum to nucleus signalling 1:</b> Possesses intrinsic kinase activity and an endo-ribonuclease activity and it is important in altering gene expression as a response to endoplasmic reticulum-based stress signals (Ning <i>et al.</i> , 2011).

<b>XBP1</b>	<b>X-box Binding Protein 1:</b> Regulates the expression of genes important to the proper functioning of the immune system and in the cellular stress response (Ueki and Kadowaki, 2011, Hotamisligil, 2006, Dufour and Clavien, 2009)
<b>ATF3</b>	<b>Activating Transcription Factor 3:</b> Transcriptional repressor induced by many stress signals. ATF3 represses gluconeogenic enzymes in liver. ATF3 increases in liver regeneration (Ning <i>et al.</i> , 2011)
<b>ATF4</b>	<b>Activating Transcription Factor:</b> (Dufour and Clavien, 2009)
<b>DDIT3</b>	<b>DNA-Damage-Inducible Transcript 3 (C/EBP homologous protein, CHOP):</b> Regulator induced by ER stress, down regulation of the anti-apoptotic mitochondrial protein Bcl-2 (Dufour and Clavien, 2009)
<b>HSPA5</b>	<b>Heat Shock Protein 5 (78 kDa glucose-regulated protein, GRP78):</b> folding and assembly of proteins in the endoplasmic reticulum (Dufour and Clavien, 2009)
<b>ERO1 L</b>	<b>ER Oxidoreductin:</b> Enzyme that catalyses the formation and isomerization of protein disulfide bonds in the endoplasmic reticulum (Dufour and Clavien, 2009).
<b>Edem2</b>	<b>ER degradation enhancer, mannosidase alpha-like 2:</b> misfolded proteins are retrotranslocated to the cytosol and degraded by the proteasome in a process known as ER-associated degradation (ERAD). EDEM2 belongs to a family of proteins involved in ERAD of glycoproteins (Mast ., 2005)
<b>New genes</b>	
<b>AHSG</b>	<b>Fetuin-A:</b> Secreted by liver, increased expression is related to insulin resistance (Heinrichsdorff and Olefsky, 2012, Ochi <i>et al.</i> , 2014)
<b>Klf11</b>	<b>Krüppel-like factor 11:</b> it leads diabetes development by impairing insulin secretion from the pancreas and it has also been shown to effect liver lipid metabolism (Zhang <i>et al.</i> , 2013, Neve <i>et al.</i> , 2005)
<b>ATG5</b>	<b>Autophagy-related protein 5 and 7:</b> both are activated in response to disturbance in cell homeostasis. Changes in their expression have been linked to hyperinsulinemia and insulin resistance in HFD-fed mice (Amir and Czaja, 2011)
<b>ATG7</b>	
<b>Rrad</b>	<b>Ras-related associated with diabetes:</b> blocking the RAS reduces fibrosis in experimental models of hepatic fibrosis.(Dyson <i>et al.</i> , 2015, Dufour and Clavien, 2009)
<b>Bace1</b>	<b>Beta-site APP cleaving enzyme 1:</b> it is activated by LXR and its activity is related to membrane cholesterol (Cui <i>et al.</i> , 2011)

A total of 500ng of RNA was reverse transcribed into cDNA as described in section 3.2.2.2. According to the manufacturers protocol 50µl of cDNA was mixed with 60µl HPLC water and 110µl of Taqman® Universal PCR master mix, No AmpErase® UNG (Applied Biosystem, USA) then loaded onto the cards. The mRNA expression was then quantified using an ABI PRISM® 7900HT sequence detection system instrument (Applied Biosystems, USA) and the CT values were exported from the SDS RQ Manager Software, Applied Biosystem (USA) for analysis.

Gene expression was analysed in GraphPad prism 6.0 using one-way ANOVA with a Bonferroni Post Hoc test. Gene expression patterns were further analysed using Ingenuity Pathway Analysis.

### **4.3.3 Triglyceride analysis by gas chromatography**

#### **4.3.3.1 Tissue lipid extraction**

A Polytron™ tissue homogeniser was used to homogenise 300 mg of liver tissue in 1.6 ml sodium sulphate (1g/15ml H<sub>2</sub>O). The homogenate was then mixed with 5.4 ml hexane:isopropanol (3:2 v/v) and a further 2 ml sodium sulphate. This was followed by vortexing for 30 sec then centrifugation at 1200g for 15 min at room temperature. The top solvent layer was transferred to a fresh tube then dried down under nitrogen gas. The dried extract was dissolved in 1 ml of hexane by mixing thoroughly and stored at -20°C until used.

#### **4.3.3.2 Separation of lipids by thin layer chromatography (TLC)**

A single solvent system for the separation of lipid fractions was prepared by mixing hexane:diethyl ether:glacial acetic acid (90:30:1 v/v) then added to a TLC tank that was lined with Whatman chromatography paper. The glass lid was affixed and the tank was left for at least 30 min so that the atmosphere is saturated with the solvent. A 100 µl of lipid extract was loaded onto a TLC plate - Silica gel 60 (20X20 cm) and left to dry thoroughly. To separate the lipid fractions, the plate was left to run for around 45 min until the solvent front reached 1-1.5 cm from the top of the plate. After that the plates were removed from the tank and left to dry completely. The separated lipids

were then visualized in iodine vapour. The bands of interest were marked with a pencil then the plate was left to destain overnight at room temperature.

#### **4.3.3.3 Extraction of Triacylglycerol from TLC plates**

The TG band area was cut from the TLC plate and placed in to a tube. A mixture of 2ml hexane:propan-2-ol (3:2) was added and placed in mixing rack for 30 min to elute lipid from Silica. A further 1 ml of the extraction solvent was added to the walls on the tube to assure all lipids are in solution. After that samples were centrifuge at 3000 rpm, 25°C for 10 min to pellet any silica fragments. The solution was then transferred to a fresh weighed tube and dried down under nitrogen. Tubes were re-weighed for an estimation of total amounts of lipid extracted.

#### **4.3.3.4 Direct Fatty Acid Methyl Ester (FAME) Synthesis**

This method was based on that of O'Fallon (2007). A volume of 0.7 ml of 10M potassium hydroxide was added and then 5.2 ml of methanol. The samples were incubated in a 55°C water bath for 1.5 hours with vigorous shaking for 5 sec every 20 min. After the incubation, they were cooled down below room temperature in a cold tap water bath for 10 min. A volume of 0.58ml of 12M sulphuric acid was added and mixed by inversion. The samples were returned to the 55°C water bath for a further 1.5 hours with vigorous shaking for 5 sec every 20 min. They were then cooled down below room temperature as previous. A 3 ml volume of hexane was added then vortex mixed for 30 sec. Finally the tubes were centrifuged at 500 g for 5 min at room temperature. The top hexane layer containing lipids was transferred in a new tube, dried down

under nitrogen gas then re-suspended in 150 µl of hexane. The total amount was then loaded in to 2ml gas chromatography (GC) vile with a low volume insert and stored at -20°C ready for GC processing (O'Fallon *et al.*, 2007).

#### 4.3.3.5 Gas Chromatography

Perkin Elmer Clarus 500 GC was used for lipid sample analysis. It was fitted with an auto sampler and a flame ionization detector equipped with Varian CP-Sil 88 column (100m x 0.25mm, film 0.2µM) and supported with TotalChrom Workstation.

Sample fatty acids were identified in reference to Supelco<sup>TM</sup>37-component FAME mix standard that was added with each run along with a solvent blank. A flame ionisation detector was used with an oven initial temperature of 45°C. A programme run time of 86 minutes was started with an initial oven temp of 45°C, held for 4 min, followed by 130°C/min ramp to 175, held for 27 min, followed by a final ramp of 4°C/min to 215 held for 35 min. The inlet temperature was set to 250°C, the split ratio was 100:1 and the injection volume was 1 µl. The detector temperature was 250°C, initial carrier gas split flow rate was 155.6ml/min, inlet pressure was 37.5psi, airflow was 450ml/min and the flow of hydrogen makeup gas was 45ml/min. Chromatograms were obtained and compared to that off the standard, Figure 4-1. Then the percentage area of the detected peaks were used for analysis.

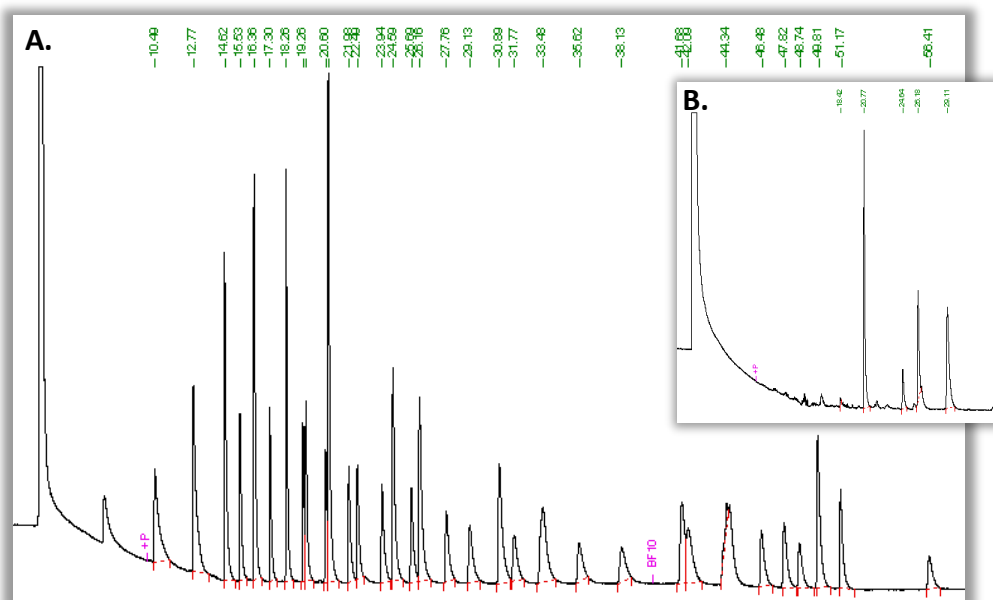


**Figure 4.1 | Gas Chromatograms.**

A representation of **A.** Supelco™ 37-component FAME mix standard and **B.** a liver tissue triglycerides chromatograms. The first peak represents hexane solvent and the green coloured numbers represents the time at when the peak was detected.

#### 4.3.4 Triglyceride assay

Triglyceride content was measured using Nile red fluorescence quantification assay. A 500 $\mu$ g/ml Nile red Stock was prepared by dissolving 5mg of Nile red powder in 10ml of acetone, this was stored in  $-20^{\circ}\text{C}$  in a dark glass tube until needed. A 5 point 1:2 serial dilution was prepared by diluting olive oil in isopropanol with a starting concentration of 0.4%; 4 $\mu$ l of olive oil in 1ml of Isopropanol (4 $\mu$ g/ml).

For the assay; a working solution was prepared by diluting the Nile red stock solution 1:90 and samples 1:5. In a 96 well plate, 10 $\mu$ l of each of the negative control, standards and samples was added. After that 90 $\mu$ l of the working solution was added with light shaking, at room temperature for 5 min in the dark. The plate was then measured using 485nm excitation and 590nm

emission. Standards were used to create a fitted linear curve and the linear equation was determined to assist in calculating total TG content, Figure 4-2.

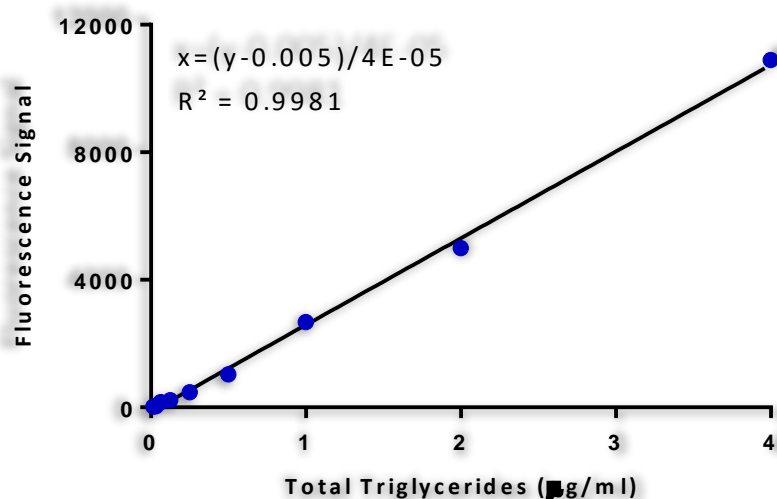


**Figure 4.2 | Total Triglycerides assay standard curve**

A representation of an accepted standard curve with linear regression with a correlation coefficient ( $r^2$ ) value of 0.99.

#### 4.3.5 Western blotting

Mouse anti-CHOP, table 4-3, was used for assessment of ER stress using western blotting as previously described in section 3.2.3.2. The transfer, however, was performed at 90V for an hour. The secondary antibody used was IRDY®680LT Conjugated Goat-Anti- Mouse IgG at 1:1000 dilution.

**Table 4-3 | Mouse anti-Chop antibody**

Primary Antibody	Catalogue	Mwt	Dilution	Company
Mouse anti-CHOP	2895*	27	IHC: 1:500 WB: 1:1000	Cell Signaling

#### 4.3.6 Immunohistochemistry

Liver tissue sectioned at 5µm was processed as previously described in section 3.2.1.4 with the primary antibody that is listed in table 4-3. However, instead of the fluorescent secondary antibody a biotinylated secondary antibody was used.

#### **4.3.6.1 Secondary antibody incubation**

The blocking solution was used to dilute the biotinylated secondary antibody according to the protocol provided with the Vector® M.O.M.™ Immunodetection Kit for mouse primary antibodies and the VECTASTAIN® ABC system for rabbit antibodies. The sections were incubated with the diluted secondary antibody in a humidified chamber for 1 hr and at room temperature. This was followed by three 10 min washes in PBS.

#### **4.3.6.2 Detection**

ABC reagent was premixed by adding 2 drops of reagent A to 5ml of buffer then 2 drops of reagent B and was left to stand for 30 min before use. The reagent mixture was applied to the slides and left to incubate for 30 min in a humidified dark chamber. After that, slides were washed with PBS three times for 10 min each.

#### **4.3.6.3 DAB reaction (3, 3`Diaminobenzidine tetrahydrochloride)**

Following the ABC detection steps, sections were incubated in 10% DAB solution prepared in 50% 100mM Tris (pH 7.5) and 50% H<sub>2</sub>O<sub>2</sub> (v/v). The slides were monitored closely and when the appropriate colour was achieved (4 min incubation), the reaction was stopped by washing gently in running tap water for 10 min.

#### **4.3.6.4 Counterstaining, dehydration and mounting**

The sections were counterstained using Harris Hematoxylin by immersing slides in solution for 5 min. The slides were then washed and dipped in 1% acid alcohol for 10 seconds followed by gentle washing in running tap water for 5

min. The slides were dehydrated in ascending alcohol concentrations; 50%, 70%, 95%, and 100% x2 for 20 sec each. The sections were then washed in two changes of xylene then mounted using DPX.

#### **4.3.7 Picro-Sirius Red (PSR) Stain**

A 0.1% concentration of Direct Red 80 was prepared in saturated aqueous solution of picric acid. Sections that are 5µm thick paraffin were de-wax in two change of xylene and hydrate in ascending alcohol concentrations. The nuclei was stained for 8 min in Weigert's haematoxylin then washed in tap water. Picro-sirius red was incubated with the section for an hour then followed with two washes in acidified water (0.5% acetic acid). Excess water was removed by vigorously shaking the slides. Finally slides were dehydrated in three changes of 100% ethanol, cleared in xylene and mounted in DPX medium.

## 4.4 Results

### 4.4.1 SREBP-1C mRNA relative expression

Quantitative real time PCR was designed to investigate changes in the mRNA levels of the transcription factor SREBP-1C in adipose, liver and skeletal muscle as it is downstream of insulin signalling and is a master regulator of lipogenesis. The HFD induced a 2 fold decrease in SREBP-1C expression relative to NC in liver tissue ( $P=0.011$ ) whereas in skeletal muscle it had the opposite effect ( $p=0.025$ , Figure 4-3). STZ and pioglitazone treated animals did not exhibit changes in SREBP-1C relative to NC, appendix figure 5.

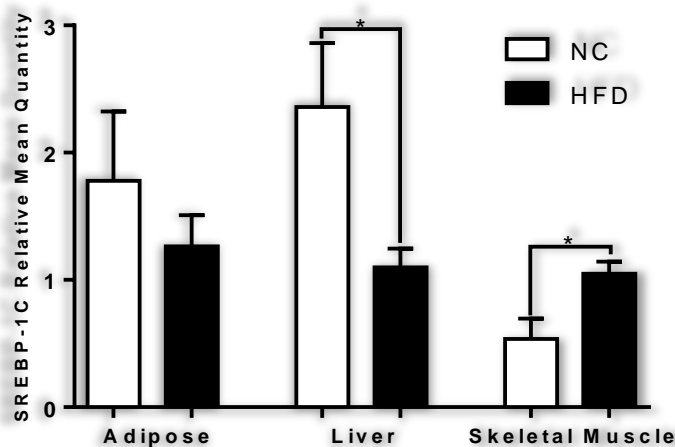


**Figure 4.3 | HFD effect on adipose, liver and skeletal muscle SREBP-1C mRNA expression level.**

Liver mRNA was extracted using TRI-reagent then reversed transcribed to cDNA as described in the methods. Expression level was analysed using Taqman RT-PCR where quantity was measured relative to a standard curve. GAPDH was used as a reference control for normalization. HFD significantly decreased liver SREBP-1C while it increased it in skeletal muscles. All data are presented as mean  $\pm$  SEM with a one-way-ANOVA test with bonferroni post-hoc test comparing pairs; NC and HFD, HFD and HFD/STZ, HFD/STZ and HFD/STZ+Pio: ( $n=5$  for NC and HFD,  $n=6$  for HFD/STZ and HFD/STZ+pio). \* $P<0.05$ , NC; Normal Chow, HFD; High Fat Diet, STZ; streptozotocin, Pio; pioglitazone.

### 4.4.2 Liver scoring

Liver tissues stained with H&E, Figure 3.10, and PSR, Figure 4-4, were sent to Queen's Medical Centre histopathology department for assessment. Prof.

Philip Kaye scored the tissue according to the Histological Scoring System for non-alcoholic Fatty Liver Disease Clinical Research Network (NASH CRN). The system assesses the severity, type and location of steatosis ballooning, mallories bodiess, glycogenesis, fibrosis and portal and lobular inflammation.

**Table 4-4 | Liver tissue scoring.**

	Sample	steatosis	%	zone	type	L.I
NC	5	0	0	-	-	0
	9	1	20	1,2	macro	0
	13	0	0	-	-	0
	18	0	0	-	-	0
	22	1	10	1	macro	0
HFD	8	1	25	1,2	macro	0
	10	1	15	1	macro	0
	16	2	60	1,2	macro	1
	20	2	40	1,2	macro	1
	26	3	70	1,2	macro	1
HFD/STZ	6	0	2	-	micro	0
	4	2	25	1,2	Mixed	0
	12	2	40	1,2	micro	0
	17	0	2	-	-	0
	19	2	60	1,2	micro	0
HFD/STZ+PIO	23	3	70	1,2	micro	0
	3	1	10	1,2,3	mixed	0
	11	1	10	1,2,3	micro	0
	15	1	30	1,2	mixed	0
	21	2	40	1,2	mixed	0
	24	1	5	1	micro	0
25	1	5	1	micro	0	

L.I: Lobular inflammation.

Two of the NC samples had low grade macro steatosis while HFD samples had an average of 42% macro steatosis that was localized in the periportal lobule and midzonal region. In addition, some samples had lobular inflammation. Streptozotocin and pioglitazone treated animals exhibited mixed steatosis at an average of 33% and 16.7% of the tissue, respectively mostly at the periportal lobule and midzonal region.

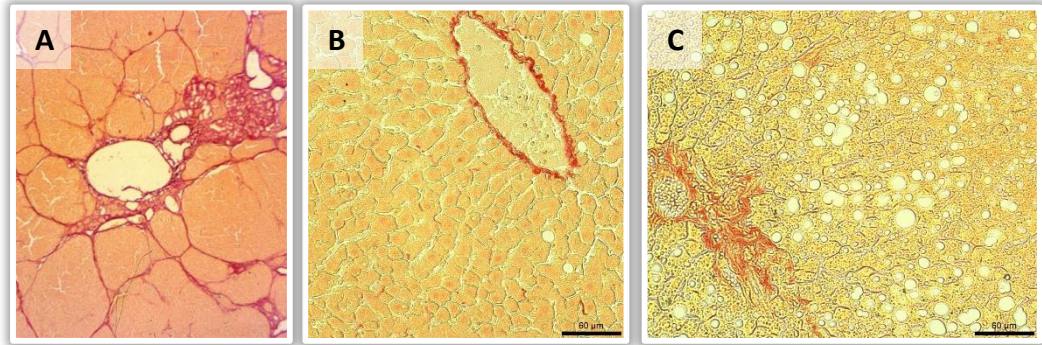


**Figure 4.4 | Liver Picro-Sirius red stain.**

A representation of **B.** NC, **C.** HFD liver sections stained with picro-sirius res (PSR). Five- $\mu\text{m}$  paraformaldehyde fixed and paraffin embedded sections stained with PSR describe in the methodology. **A.** A positive PSR stain showing fibroses stained in red, obtained from the histology lab in QMC. Magnification: x400 and Scale Bar: 60 $\mu\text{m}$

#### 4.4.3 Liver TaqMan low density array

In Chapter three, histological studies revealed sever steatosis as a sign of NAFLD therefore genes involved in an array of pathways that have a possible direct or indirect contribution to this disturbance in liver homeostasis were chosen to be analysed. Out of 96 genes, 5 reference genes were added for normalization. CEBPB, Plin1 and Scd4, IL6 and Rrad did not amplify reproducibly and were excluded from any further analysis.

Gene expression was quantified using the  $\Delta\Delta C_T$  method described by Hughes & Mood (Hughes *et al.*, 2007). Correlation statistics and Norm finder software (Andersen *et al.*, 2004) was used to determine reference genes stability values; the Geometric mean of all 5 reference genes was most stable and hence was used for normalization. However, since this is an animal study there was no basis for choosing a single animal to be set as a reference control. An alternative method described by Schmittgen and Livak, 2008 where the relative quantity is calculated by normalizing the average  $C_T$  value of a target gene for a particular sample to the average  $C_T$  value of its corresponding control

genes (Schmittgen and Livak, 2008) was also used. Even though both analyses produced comparable results, the second approach is presented here.

Changes in gene expression are illustrated in table 4-5 and figure 4-5. A full table of all gene expression values is given in appendix table 8.

**Table 4-5 | Live Taqman gene array significant changes.**

<b>HFD vs NC</b>			<b>HFD/STZ vs HFD</b>		
<b>Genes</b>	<b>P-value</b>	<b>Fold Change</b>	<b>Genes</b>	<b>P-value</b>	<b>Fold Change</b>
<b>Gluconeogenesis genes</b>			<b>Fatty Acid Synthesis</b>		
Pck1	0.00008	-2.25	Fasn	0.0062	-9.41
Atf4	0.0282	1.4	Gck	0.0034	-49.37
Fgf21	0.0450	4	<b>Glycolysis genes</b>		
Egr1	0.0114	2.03	Pklr	0.04	-5.07
<b>Fatty acid synthesis &amp; transport</b>			Ldha	0.0077	-1.94
Acaca	0.0483	-1.55	<b>Acyl CoA Synthesis</b>		
Scd1	0.0001	-3.2	Acsl4	0.0431	1.74
Srebf2	0.0430	-1.68	<b>Cholesterol Metabolism</b>		
Slc27a5	0.0111	-1.99	Apoc3	0.0293	-1.7
<b>ER stress</b>			<b>Lipid Metabolism</b>		
Ddit3	0.0078	1.64	Adipor1	0.0009	-1.75
Atf3	0.0063	3.56	<b>Inflammatory markers</b>		
<b>Inflammatory &amp; macrophage marker</b>			Ccl2	0.00006	-6.1
Cd68	0.0346	-1.4	<b>ER stress</b>		
Ccl2	0.0006	2.76	Edem2	0.006	-2.42
Socs3	0.0322	-1.27	Hspa5	0.0127	-1.85
<b>Insulin signalling</b>			<b>HFD/STZ+Pio vs HFD/STZ</b>		
Irs1	0.0190	-1.56	<b>Macrophage Marker</b>		
			Cd163	0.0304	-1.67

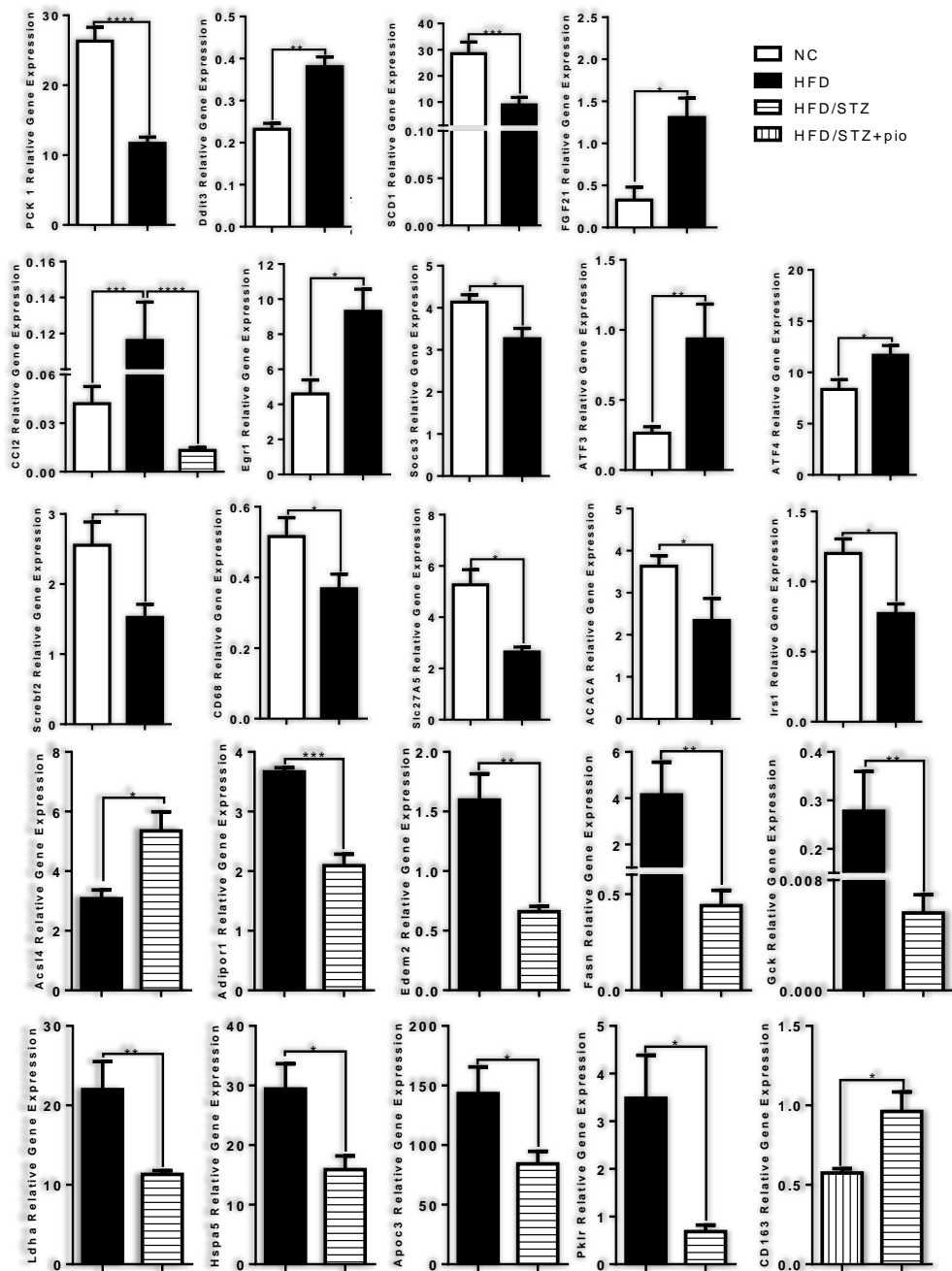


**Figure 4.5 | liver tissue Taqman gene array significant changes.**

A total of 500 ng of liver tissue RNA transcribed into cDNA was prepared according to Taqman® Universal PCR master mix, No AmpErase® UNG manufacturer protocol then loaded to a custom made Taqman gene array. Quantity was measured using  $2^{-\Delta Ct}$  method. Histograms present significant changes calculated by a one-way-ANOVA test with bonferroni post-hoc test comparing pairs. Data is presented as mean±SEM where \*p<0.05, \*\*p<0.001, \*\*\*p<0.0001 and \*\*\*\*p<0.00001, \*\*p<0.001 NC and HFD, HFD and HFD/STZ, HFD/STZ and HFD/STZ+Pio: (n=5 for NC and HFD, n=6 for HFD/STZ and HFD/STZ+pio). NC; Normal Chow, HFD; High Fat Diet, STZ; streptozotocin, Pio; pioglitazone.

#### 4.4.4 TaqMan gene array validation

To confirm and validate the data produced from the TaqMan gene array, the same cDNA samples were subjected to TaqMan qPCR. G6PC and PCK primers and probes from the FRAME data base were used to quantify their gene expression.

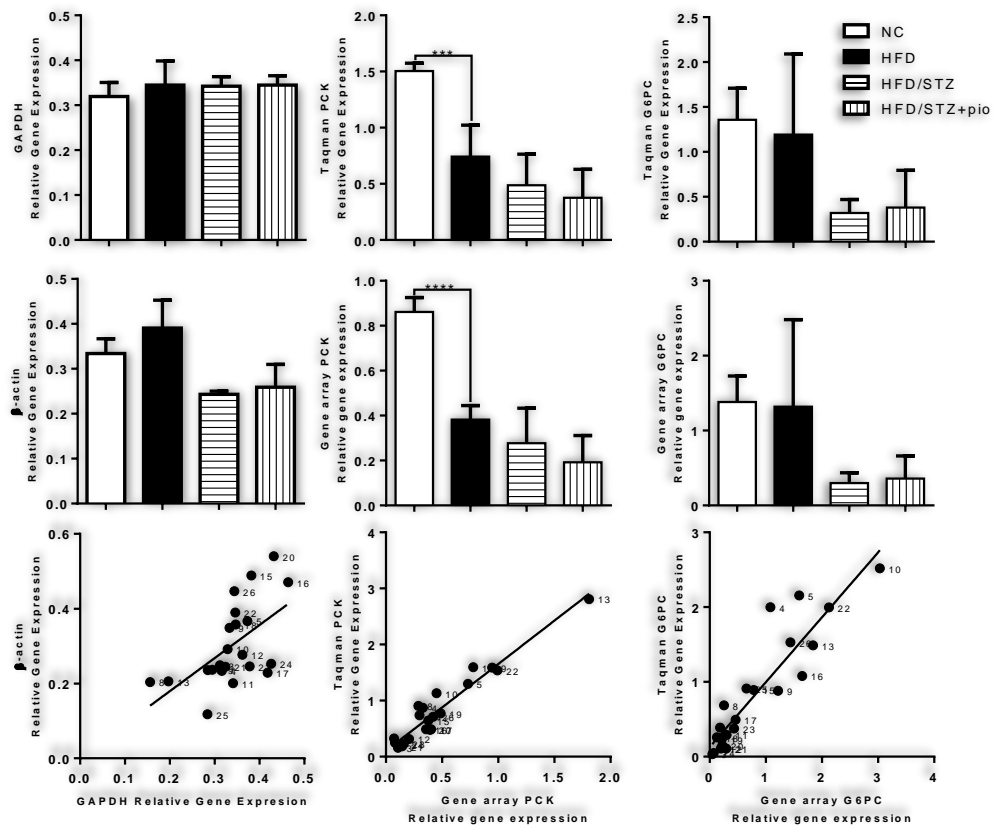


**Figure 4.6 | Liver Gene array validation using Taqman.**

Liver mRNA was extracted using TRI-reagent then reversed transcribed to cDNA as described in the methodology. Expression level was analysed using Taq-man RT-PCR where quantity was measured relative to a standard curve. Geometric mean of GAPDH and  $\beta$ -actin (Spearman p-value = 0.0007) was used as a reference for normalization. Taqman data correlated with the genearray data and showed similar pattern of expression (Person p value for PCK and G6PC <0.0001). All data are presented as mean  $\pm$  SEM with a one-way-ANOVA test with bonferroni post-hoc test comparing pairs; NC and HFD, HFD and HFD/STZ, HFD/STZ and HFD/STZ+Pio; (n=5 for NC and HFD, n=6 for HFD/STZ and HFD/STZ+pio). NC; Normal Chow, HFD; High Fat Diet, STZ; streptozotocin, Pio; pioglitazone.

Geometric mean of Glycerol-3-phosphate dehydrogenase (GPDH) and  $\beta$ -actin was used as reference genes for normalization after the spearman r test showed a high correlation between them with p value of 0.0007. Results of

TaqMan gene array and the qPCR were comparable, they produced similar patterns of expression and significance with a positive correlation and high correlation coefficient (p value < 0.0001 for both PCK and G6PC, Figure 4-6).

#### 4.4.5 Liver C/EBP homologous protein (CHOP) expression and localization

CHOP (Ddit3) is an ER stress marker whose mRNA expression level was elevated in HFD samples, hence Western blotting was used to assess the protein level. There was a significant increase in CHOP observed between NC and HFD groups with a p value of 0.04, Figure 4-7.

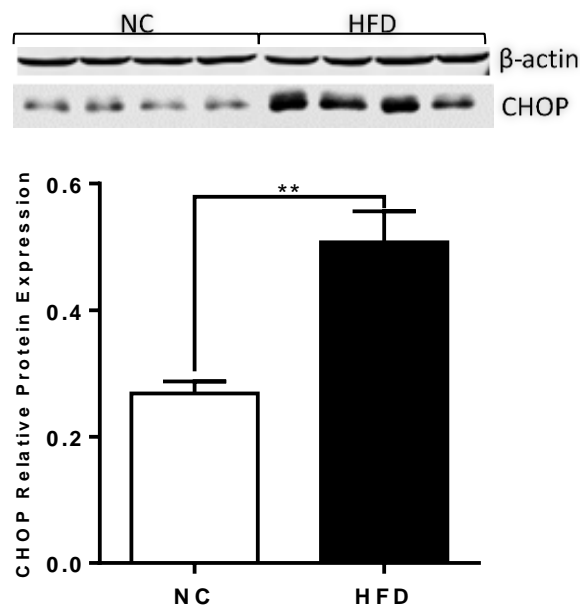


**Figure 4.7 | Liver tissue CHOP Protein expression.**

As described in the methodology, 65µg protein lysate extracted from liver tissue homogenized in Tri-reagent was separated by 12% (w/v) SDS-polyacrylamide electrophoresis gel and blotted onto nitrocellulose membrane. Immune-detection was performed using rabbit anti-CHOP at 1:1000 dilution. Membrane was visualized using Odyssey® Infrared Image system followed by Image studio densitometric analysis and the detected signal was normalized to actin. High fat diet (HFD) significantly increased the expression of CHOP compared to the normal chow (NC). Histograms were analyzed using Student's unpaired t-test, values are presented as mean ± SEM. \*\* P.value < 0.005.

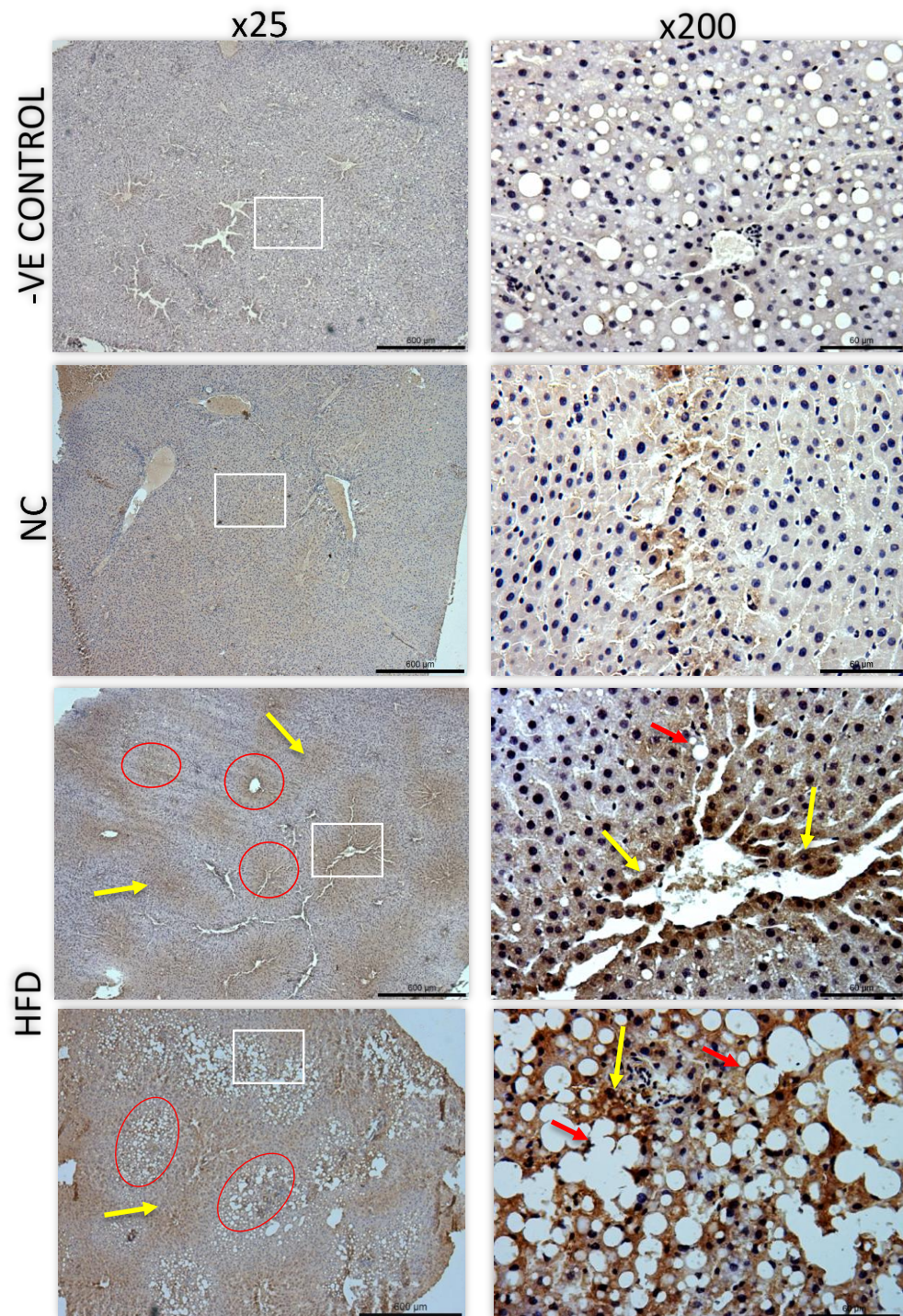


**Figure 4.8 | CHOP protein localization in liver tissue**

A representation of NC and HFD CHOP DAB staining at x25 and x200 magnification. Five- $\mu\text{m}$  paraformaldehyde fixed and paraffin embedded sections were stained with primary anti-CHOP (1:200) as described in the methodology. A negative control was performed without primary antibody. Positive staining is represented by a deep brown colour (yellow arrows). NC showed very faint stain while HFD had a deep brown colour localized around periportal lobule, where ischemia was suspected (red circles) and lipid droplets accumulations (red arrows). Magnification and Scale bar: x25 and x200, 600 and 60  $\mu\text{m}$  respectively.

As describe in chapter three, when liver tissue was stained with H&E some areas were lightly stained which was suggestive of ischemia, this was confirmed by the pathologist. Therefore it was though that those areas may exhibit higher expression of ER stress markers. Immunocytochemistry was used to determine if ER stress proteins co-localised with areas of ischemia, Figure 4-8.

#### 4.4.1 Liver triglycerides content and composition

Total triglyceride was measured after isolating lipids from the liver tissue and prior processing for TLC and GC analysis. The HFD induced a 3.5 fold increase in triglyceride content with a p value of 0.0014 when compared to the NC group, Figure 4-9.

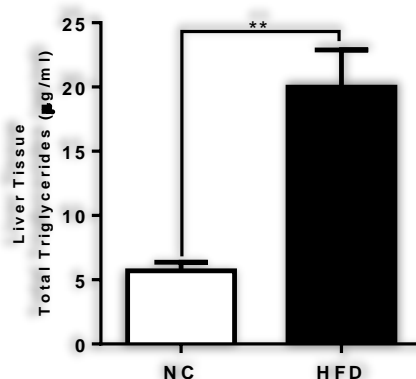


**Figure 4.9 | Liver tissue Total Triglyceride content.**

A 300mg of liver tissue was homogenized in sodium sulphate:hexane:isopropanol then total triglycerides was measured using Nile red triglycerides assay. Data were analysed using Student's unpaired t-test and is presented as mean  $\pm$  SEM. \*\* $P < 0.002$ , NC: Normal Chow, HFD: High Fat Diet.

The liver lipid extracts, along with lipids extracted from samples of the animal diets, were loaded to TLC plates, Figure 4-10 and appendix figure 6.

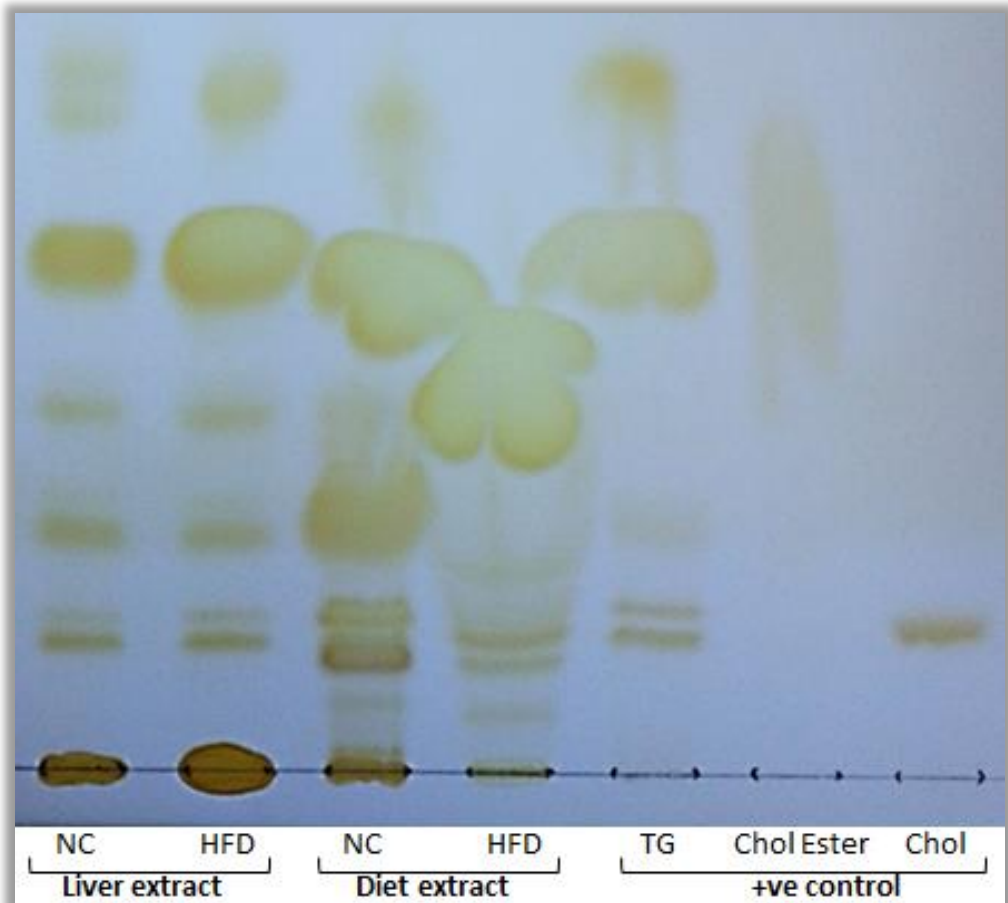


**Figure 4.10 | Thin layer chromatography of liver tissue.**

A representation of total lipids extracted from NC and HFD liver tissue and diet extracts. The extracts were loaded on a TLC plate then ran using hexane:diethyl ether:glacial acetic acid single solvent system. The TLC plate was dried after the running front has reach about 1inch of the top of the plate then stained using iodine fumes. The largest fragment was identified as TG the furthest was cholesterol ester. NC: Normal Chow, HFD: High Fat Diet, Chol: cholesterol, TG: Triglycerides.

GC analysis showed that the NC and HFD diets had similar free fatty acid composition. Linoleic acid was the predominant free fatty acid followed by oleic, palmitic then stearic acid, however the relative amounts of fatty acids were different. The NC had 46.21:25.5% ration of linoleic to oleic acid in comparison to 33.97:32.7% in the HFD, Figure 4-12.

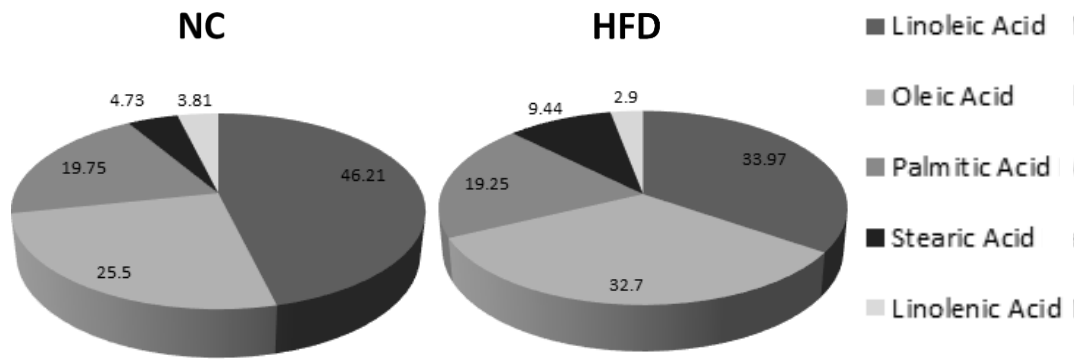


**Figure 4.11 | Diet triglycerides fatty acid composition**

A total of 500mg of each of the normal chow (NC) and the high fat diet (HFD) was homogenized in sodium sulphate:hexane:isopropanol solvent mixed, after running in a TLC plate TG fragment was cut out isolated, processed through FAME and subjected to gas chromatography (GC) analysis as described in the methodology.

Any peaks that were detected and had a percentage of lower than one were eliminated from analysis. The fatty acid composition of the two diets was broadly similar with palmitic oleic and linoleic acid making up the majority of fatty acid present in triglyceride. The major difference between the diets, therefore, was confirmed as fat content rather than differences in individual lipid species. The liver triglyceride content was similar in both groups with palmitic and oleic making up the majority of the fatty acids in the NC and HFD, respectively.

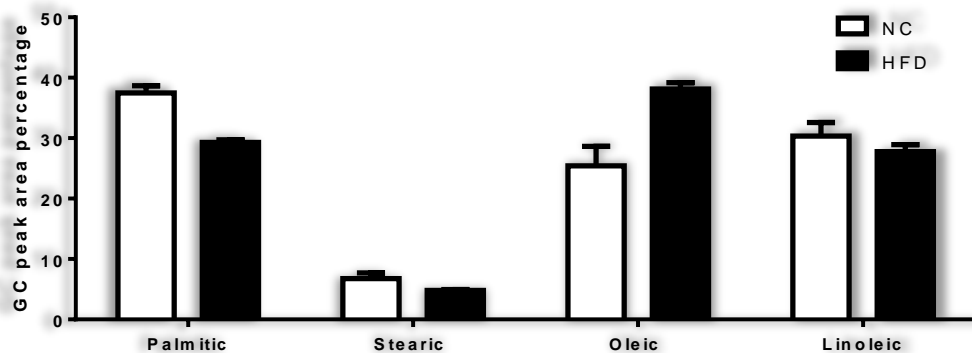


**Figure 4.12 | Liver tissue triglycerides fatty acid composition**

FAME processed TG isolated from TLC of liver tissue total lipid extract was subject to gas chromatography. Fatty acids were identified in reference to a commercialized standard. Data presented is by one-way-ANOVA test with bonferroni post-hoc test comparing pairs; NC and HFD for each TG, and TGs with in each group (n=5 for both NC and HFD).

#### 4.4.2 Muscle TaqMan gene array

Muscle tissue cDNA was also subjected to TaqMan gene array analysis. A total of 5 samples of NC and HFD and 4 of HFD/STZ and HFD/STZ+Pio groups were processed. Out of the 96 genes, 18 genes did not show any amplification, these include Ahsg, Apoc3, Ccl3, cd86, CEBPB, Foxa2, Fgf21, G6pc, Gck, Il10, Il1b, Nr1h4, Pck1, Pklr, SCD4, Slc27a2, Slc27a5, Slc2a and Tnf-a. As previously described, the geometric mean of the 5 reference genes were used to analyse the expression using the Schmittgen and Livak, 2008 method. HFD did not alter the expression of any genes relative to NC while streptozotocin and pioglitazone significantly affected the expression of 5 and 9 genes, respectively. These changes are summarized in table 4-6 and figure 4.13. A full table of all gene expression values is given in appendix table 13.

**Table 4-6 | Skeletal muscle Taqman gene array significant changes.**

HFD vs HFD/STZ			HFD/STZ vs HFD/STZ+pio		
Genes	P-value	Fold Change	Genes	P-value	Fold Change
<b>Autophagy genes</b>			<b>Adipogenic genes</b>		
Atg7	0.0024	-2.05	Fabp5	0.0003	2.28
<b>Fatty acid synthesis</b>			<b>Lipid Metabolism genes</b>		
Srebf1	0.0071	2.01	Hmgcs2	0.0013	5.88
Srebf2	0.0127	1.6	Cd36	0.0015	4.87
Mlxipl	0.0082	-2.04	<b>Fatty acid synthesis genes</b>		
<b>ER stress</b>			Elovl6	0.0343	6.28
Klf11	0.0357	1.66	Acaca	0.0262	1.66
			Srebf1	0.0155	-1.9
			<b>Insulin signalling</b>		
			Irs1	0.0433	-3.47
			<b>Nuclear receptors genes</b>		
			Rxra	0.0341	-1.38

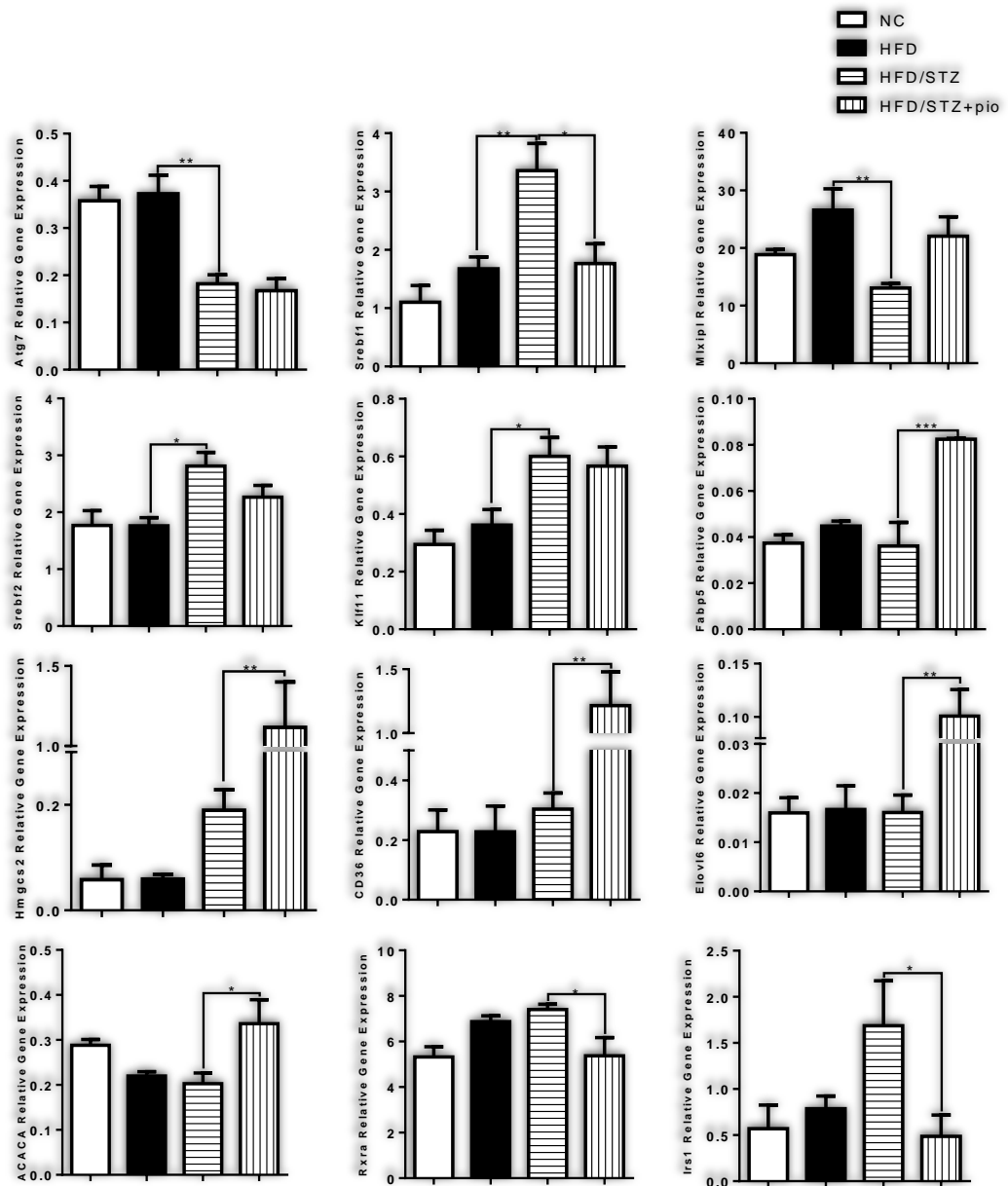


**Figure 4.13 | Skeletal muscle tissue Taqman gene array significant changes.**

A total of 500 ng of skeletal muscle cDNA was loaded onto a custom made Taqman gene array. mRNA was quantified using  $2^{-\Delta Ct}$  method. Histograms present significant changes calculated by a one-way-ANOVA with bonferroni post-hoc test. Data is presented as mean  $\pm$  SEM where \* $p < 0.05$ , \*\* $p < 0.001$  and \*\*\* $p < 0.0001$ . NC and HFD, HFD and HFD/STZ, HFD/STZ and HFD/STZ+Pio: (n=5 for NC and HFD, n=4 for HFD/STZ and HFD/STZ+pio). NC; Normal Chow, HFD; High Fat Diet, STZ; streptozotocin, Pio; pioglitazone

#### 4.4.3 Skeletal Muscle Total Triglyceride Content

Skeletal muscle total lipid extract was used to measure the content of total TG. The assay showed the HFD group had highest TG content however it was not statistically significant, Figure 4-14.

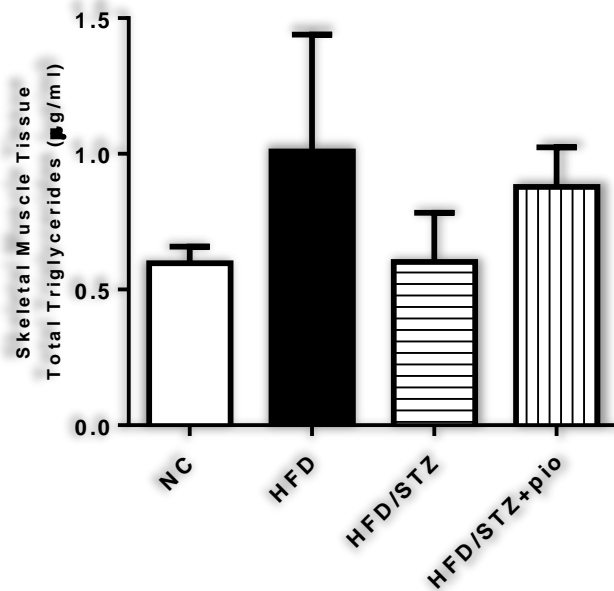


**Figure 4.14 | Skeletal Muscle Total Triglycerides**

A 150mg of skeletal muscle tissue was homogenized in sodium sulphate:hexane:isopropanol solvent then total triglycerides was measured using the home made Nile red triglycerides assay. No significant changes were observed across the groups. Statistics was performed using Mann–Whitney U test. NC: Normal Chow, HFD: High Fat Diet, STZ: streptozotocin, Pio: Pioglitazone

## 4.5 Discussion

### 4.5.1 Measurement Sterol Responsive Element Binding Protein-1C mRNA

Data from the previous chapter highlighted the liver tissue as a primary target of the HFD. However, Taqman gene array, was unable to be used to measure the expression of the master regulator of lipogenesis SREBP-1C. As the assay for this specific isoform of SREBP1 is unavailable.

Fatty acid derivatives can inhibit hepatic fatty acid synthesis by indirectly suppressing SREBP-1C, which can be induced by insulin (Jump *et al.*, 2005). Insulin directly up-regulates the transcription and proteolytic maturation of SREBP-1C. However, this action is independent of IRS-1 which mediates insulin stimulated glucose uptake (Sajan *et al.*, 2004). There is evidence that supports the insulin mediated SREBP-1C action, particularly in the liver; rat hepatocytes (Foretz *et al.*, 1999) as well as in vivo rat liver treated with insulin (Shimomura *et al.*, 1999) express increased amounts of SREBP-1c mRNA. Lipogenic gene expression changes that are mediated by insulin can be blocked in hepatocytes that express a dominant-negative SREBP-1c (Foretz *et al.*, 1999). Fasting reduces adipose and liver SREBP-1C in normal animals (Kim *et al.*, 1998). The decreased liver levels of SREBP-1C mRNA expression observed here could be an indication of an insulin resistant state. Adipose tissue SREBP-1C was not altered, however, skeletal muscle had an elevated SREBP-1C mRNA levels in HFD animals. The decrease in SREBP1c levels in liver suggest that *de novo* lipogenesis is highly unlikely to contribute to the observed steatosis in the HFD animals.

#### 4.5.2 HFD and non-alcoholic fatty liver disease (NAFLD)

Obesity is said to be the primary cause of developing steatosis in NAFLD. Since obesity is normally a result, at least in part, of over feeding, particularly when combined with the consumption of high amounts of fat, one would think that steatosis is a manifestation of obesity. This has long been the hypothesis, however, this study demonstrated that HFD alone in the absence of increased adiposity leads to the development of steatosis. There are few studies that demonstrate similar observations, most of which are based on clinical data and non-invasive procedures. A clinical study that was based on hepatic ultrasound and patients histories reported that 18.77% individuals with NAFLD were found to be lean (Younossi *et al.*, 2012). Another study reported that 1 in 8 NAFLD patients attending tertiary liver centre had normal BMI, this again was based on ultrasound (Margariti *et al.*, 2012). Liver histological studies completed on subsets including automobile crash victims and liver donors have reported steatosis in approximately 15% of non-obese subjects (Verdelho Machado and Cortez-Pinto, 2012). The most interesting study was in India in 2010 where in a rural population with a low NAFLD prevalence, 75% of recruited patients had BMI less than 25 kg/m<sup>2</sup> and 54% were neither overweight nor had abdominal obesity, were presented with steatosis. This high percentage was referred to the possible fact that the Asian population have higher levels of fat deposition than Caucasians (Das *et al.*, 2010). However a recent study comparing South Asian and Caucasian men reported that overfeeding with a HFD resulted in an increased in liver fat content that is similar in both population (Wulan *et al.*, 2015).

NAFLD histological changes predominantly affect the liver parenchyma, they mainly occur in perivenular regions also called acinar zone 3. However, there is an increasing recognition that portal and periportal lesions can also be seen as part of the spectrum of fatty liver disease (Hübscher, 2006). In this study, the HFD and HFD/STZ livers presented with steatosis that was located in both zone 1 and 2. The HFD/STZ+pio had similar patterns with some animals extending zone 3. Features of steatohepatitis include hepatocellular injury that is characterised by inflammation and fibrosis (Hübscher, 2006), although there was no evidence of fibrosis in this study, HFD animals had some evidence of lobular inflammation. This could be indicative of the development of more serious injury beyond simple fatty change and an indication of a higher susceptibility to developing steatohepatitis.

#### **4.5.3 Molecular investigation of liver metabolic pathways**

High fat diets are associated with NAFLD in both humans and in animal models. The exact mechanisms underlying the development of NAFLD are under investigation. However, as mentioned previously, there are various possible pathways where alterations in lipid metabolism can result in the appearance of hepatic steatosis. Hepatic *de novo* lipogenesis genes are usually increased when NAFLD is reported (Berlanga *et al.*, 2014), these include PCK1 (Valenti *et al.*, 2008), ACC1 (Berlanga *et al.*, 2014) and SREBF2 (Caballero *et al.*, 2009). Moreover, knocking out FATP5 (Slc27a5) has been shown to reverse NAFLD in mice (Nassir and Ibdah, 2014, Doege *et al.*, 2008), SCD1 expression was positively correlated with liver fat percentage (Li *et al.*, 2009) and SCD1 null

mice on the methionine and choline deficient (MCD) diet showed decreased steatosis (Liu *et al.*, 2010). However, all of those genes were significantly lower in the HFD group livers as compared to NC. Similar results to those observed in this study in terms of gene expression have been described in relation to the stage of steatosis where FATP5, SREBP1c, ACC1 and SCD1 were reported to be significantly decreased in severe steatotic livers (Mitsuyoshi *et al.*, 2009, Fernández Gianotti *et al.*, 2013).

SREBP-1C activation upregulates lipogenic genes including SCD1 (Tabor *et al.*, 1999) and ACC1 (Magaña *et al.*, 1997) expression, and it is unsurprising that in HFD livers where SREBP1c mRNA levels are reduced, ACC1 and SCD1 mRNA is also lower than in NC. These data further suggest that *de novo* lipogenesis is not a factor in the development of steatosis in the HFD animals. Expression of genes involved in gluconeogenesis were also altered including ATF3, 4 (also considered an ER stress marker), FGF21 and EGR1. ATF4 deficiency is said to have a protective effect against diet induced hepatic steatosis (Li *et al.*, 2011, Xiao *et al.*, 2013) and an increase in ATF4 is indicative of ER stress. ATF3 is also considered as a transcriptional repressor induced by many stress signals (Ning *et al.*, 2011). These two genes in addition to Ddit (CHOP; an ER stress marker) are all indicative of increased liver ER stress. ATF3 and ATF4 tend to decrease transcriptional of certain genes including gluconeogenesis and Ddit3 regulates apoptosis; in liver Ddit3 has been shown to be induced in steatotic animals (Chikka *et al.*, 2013).

While FGF21 is known to regulate fatty acid metabolism preventing lipotoxicity (Fisher *et al.*, 2014) and has been shown to reverse hepatic steatosis (Xu *et al.*, 2009, Fisher *et al.*, 2014) increased levels were observed in the livers of HFD fed animals in this work. This increased expression could be an adaptive response to steatosis and an attempt to reduce liver fat accumulation. The EGR1 gene is downstream of FGF21 (Fisher *et al.*, 2010) and it is an essential factor for development of ethanol induced fatty liver (McMullen *et al.*, 2005). Another study reported similar findings but stated that EGR1 makes only a small contribution towards liver steatosis development (Donohue *et al.*, 2012). They showed that FGF21 and EGR1 are positively correlated ( $p=0.0002$ ,  $r=0.7198$ ). These actions of EGR1 are all in alcoholic fatty liver and its role in NAFLD is not yet reported. Most inflammatory genes were not altered by HFD however CCL2 was significantly increased, it's a monocyte chemoattractant protein that is released in response to tissue injury (Westerbacka *et al.*, 2007). In this study there was some evidence of lobular inflammation in the HFD group, but there was no evidence of increased monocyte recruitment. It is possible that this elevation of CCL2 combined with sporadic occurrence of lobular inflammation is evidence that the HFD animals are beginning to develop NASH-like symptoms.

One interesting finding was decreased expression of insulin receptor substrate 1. Hepatic insulin resistance is characterized by an impaired ability of insulin to suppress hepatic glucose production (Kotronen and Yki-Järvinen, 2008). Fat accumulation in the liver is associated with hepatic insulin resistance. In rats on a high fat diet, the activation of IRS1 and IRS2 in the liver is impaired,

leading to decreased glycogen synthase activity and increased gluconeogenesis (Samuel *et al.*, 2004). These observation along with the fact that its expression correlated with the averaged total fat intake ( $p=0.0007$ ,  $r=-0.6649$ ) are all indicative of insulin resistance in the HFD group.  $\beta$ -oxidation genes were not altered in the HFD animals which may suggest that the increased flux of fatty acids to the liver from the diet, in the absence of increased fatty acid breakdown, might be the cause of steatosis in this model. However an alternate explanation could be that export of lipid in terms of lipoprotein secretion is impaired in the HFD group. The lack of plasma for this set of animals made it impossible to measure circulating lipoprotein levels which would give potential insight into export of lipids from the liver.

The decreased expression in the insulin stimulated genes in the HFD/STZ group was expected; these include Fasn, Gck, PKI $\alpha$ , Apoc3 Adipor1 (Sibrowski *et al.*, 1982, Parks and Drake, 1982, Duivenvoorden *et al.*, 2005, Wang *et al.*, 2004), as there was no bioavailability of insulin. This applies to Acsl4, as its expression is reported to be increased in diabetic state (Westerbacka *et al.*, 2007).

#### **4.5.4 HFD and liver endoplasmic reticulum stress**

Since HFD feeding induced ER stress gene expression at the mRNA level further analysis was performed to measure protein levels by Western blot and immunocytochemistry Ddit3 (CHOP) was significantly elevated at the protein level and was found to be expressed in areas of the liver that appeared to exhibit signs of ischemia and lipid accumulation.

#### 4.5.5 Diet fat composition: does it reflect liver fats?

The fatty acids in the liver triglycerides are usually the saturated palmitic acid and stearic acid and the unsaturated oleic acid and linoleic acid (Wu *et al.*, 2011, Wang *et al.*, 2011). Both diets major components were unsaturated fatty acids and even though they had similar composition, the liver tissue free fatty acid content was significantly different. The NC liver had similar composition to that previously reported in mice liver with the major free fatty acid as palmitic acid (Wang *et al.*, 2011). However, fatty acid in the livers of the HFD group reflected that of the diet and had higher amount of oleic acid (Burdge and Wootton, 2003).

Previous studies had demonstrated that increased saturated fat leads to ER stress in rats who had diet induced steatosis (Wang *et al.*, 2006). Furthermore in hepatoma cell lines that were incubated with saturated fatty acid, a significant increase in ER response genes including CHOP has been reported.

This was followed by apoptosis and cell death. These findings were not observed when cells were treated with unsaturated FA (Wang *et al.*, 2006). Other *in vitro* studies demonstrate that saturated FA acids, palmitate in particular, caused a disturbance in the ER homeostasis and induce apoptosis however when oleate or linoleate were used they reduced or prevented palmitate-induced ER stress and apoptosis (Wei *et al.*, 2006, Wei *et al.*, 2007).

#### **4.5.6 Molecular investigation of skeletal muscle gene expression and total triglyceride content**

In muscle, increased intramyocellular fat accumulation has been associated with insulin resistance. An increase in muscle TG content results in a downregulation of insulin signalling pathways and reduced glucose uptake. HFD feeding did not have any effects on the muscle tissue gene expression which reflects the fact that there was no increase in total muscle TG content.

#### **4.5.7 Conclusion**

HFD feeding leads to the development of severe steatosis in the liver. A possible explanation would be that increased free fatty acid flow from the diet to the liver accumulate as they exceed the maximal rates of removal via lipoprotein secretion. The increase in lipid deposition, was associated with increased ER stress gene upregulation, and signs of inflammation around the lobules. The lipid accumulation resulted in the decreased expression of IRS1 and SREBP-1C both of which are downstream of insulin, this suggests the potential development of insulin resistance in the liver. While HFD caused severe changes in the liver it did not have any major effects on the skeletal muscle tissue. This identifies the liver as a key organ in terms of the response to a HFD in the absence of weight gain.

# **CHAPTER V:**

## **Effects of HFD on plasma lipoproteins.**

## 5.1 Introduction

The accumulation of triglycerides in the liver is the hallmark of NAFLD pathogenesis. In the fasting state, the majority of the fatty acids that flow to the liver are the plasma pools of NEFA. These provide the bulk of liver secreted fatty acid in the form of VLDL particles (Parks *et al.*, 1999). It has been shown that insulin resistance, in the fasting state, is associated with the dysregulation of the fatty acid flux that is derived from adipose tissue (Chen *et al.*, 1987, Kooner *et al.*, 1998). There is some existing evidence that, in patients with NAFLD, adipose tissue lipolysis is not suppressed by insulin to the same extent that as is in healthy individuals (Neuschwander-Tetri and Caldwell, 2003). In spite of this, there are many other fatty acid sources that contribute to fatty liver. It is important to take in account the fatty acid regulation in both the fed and fasted states for a better understanding of the mechanisms behind fatty liver. Apart from the peripheral adipose fat storage, fatty acids could be synthesised within the liver through *de novo* lipogenesis. Other sources include dietary fatty acids, these could enter the liver by two processes; either through the plasma NEFA spill over pool or the uptake of chylomicron remnants that are derived from the intestine (Donnelly *et al.*, 2005, Havel and Hamilton, 2004, Miles *et al.*, 2004).

There are various treatment strategies for NAFLD that focus on improving body weight status and glucose tolerance (Marchesini *et al.*, 2001, Caldwell *et al.*, 2001, Bajaj *et al.*, 2003). However, understanding the origins of

liver TG accumulation will strengthen current treatment regimens and could aid in the identification of new targets for therapy.

## **5.2 Aim**

Since the previous data in this study appeared to eliminate an increase in adipose tissue, increased free fatty acid flow to the liver and *de novo* liver lipogenesis pathways as the cause of the observed fatty liver, the aim of this chapter was to recreate a non-obese HFD model using the same HFD diet and check if it created similar fatty changes in the liver. One limitation of the previous study was the lack of plasma for triglycerides analysis, hence another aim was to collect plasma and assess triglyceride and free fatty acid composition and examine the effect of dietary fat upon these parameters

## 5.3 Materials and methods

### 5.3.1 Animal Model

Animals used in this study were handled by Annastazia Learoyd under the supervision of Dr Rebecca Trueman, School of Biomedical Sciences, QMC, University of Nottingham.

All experiments were carried out under Personal Home Office Licence 40/9559 and Project Home Office Licence 40/3124, in accordance with the UK Home Office Animals (Scientific Procedures) Act 1986 and International Associated of the study of Pain (IASP) guidelines. Eight Male Wistar Han rats (304.5±8.7g) were obtained from Charles River (Kent, U.K.) and individually housed for 6 weeks on NC (same as the previous study, NC<sup>Study1</sup>) and on standard light cycle (12/12hrs light-dark cycles).

At the start of the study the animals weighed an average of 412.8±17.17g, they were randomly allocated into two groups; normal chow (NC) fed (n=4) or high fat diet (HFD) fed (n=4). The HFD (D12492 from Research Diets, Inc. UK), as previously described, contained 60% calories as fat compared to 10% in the normal chow diet (D12450J from Research Diets, Inc. UK). Animals had free access to food and water at all times for a period of 9 weeks. Animal' weight was monitored weekly and plasma glucose was measured at the end of week 6 and 8.

**Table 5-1 | Diet composition in Kcal %**

<b>Ingredient</b>	<b>High Fat diet</b>	<b>Normal Chow</b>
Protein	20	20
Carbohydrate	20	70
Fat	60	10

### **5.3.2 Blood sampling and tissue collection**

At the end of the study animals were anesthetized then blood was obtained via cardiac puncture. Blood was collected in one millilitre lithium heparinized tubes. The tube was inverted couple of times and instantly centrifuged at 2000g for 10 min. Plasma was transferred to an Eppendorf tube and stored at 4°C ready for ultracentrifugation. The animals were then decapitated and fresh liver tissue was either removed, flash frozen in liquid nitrogen and stored in -80°C until further required, or placed in 4% PFA for overnight fixing and tissue processing.

### **5.3.3 Liver tissue analysis**

Fixed tissue was processed as previously described for H&E and PSR staining. A 300mg sample was processed for total triglyceride isolation and measurement. A total of 50mg was processed to RNA isolation for Taqman analysis.

### **5.3.4 Ultracentrifugation of plasma lipids**

Plasma lipoproteins were isolated by density gradient ultracentrifugation.

#### **5.3.4.1 Separation of chylomicrons**

One millilitre of plasma was added to a Beckman quick-seal ultracentrifuge tube using a syringe and needle. The ultracentrifuge tubes were topped up with 1.006 g/ml potassium bromide solution (KBr) and sealed with the tube topper. The tubes were then spun in a Beckman ultracentrifuge using

50.4 Ti rotor under vacuum at 12°C for 20min at 12,000 rpm with full acceleration and no break.

Following ultracentrifugation each tube was cut approximately 1.5 cm from the top using a tube slicer. The top chylomicron layer was transferred to an Eppendorf tube and stored at -20°C until required for GC analysis. The top of the tube slicer blade was dried with tissue paper then drawn back to expose the remaining lipoprotein fractions. The lower layer was transferred a new Beckman quick-seal ultracentrifuge tube using a syringe and needle to be prepared for VLDL separation.

#### **5.3.4.2 Separation of VLDL**

The ultracentrifuge tubes containing the remaining fraction from the chylomicron spin were topped up with 1.006 g/ml KBr solution and sealed with the tube topper. The tubes were spun at 39,000 rpm for 16hrs.

Following ultracentrifugation each tube was cut approximately 1.5 cm from the top using the tube slicer. The top VLDL layer was transferred to an Eppendorf tube and stored at -20°C until required for GC analysis. The top of the tube slicer blade was dried with tissue paper then drawn back to expose the remaining lipoprotein fractions. The lower layer was transferred to labelled LP4 tubes then stored at -20°C until required for further analysis.

#### **5.3.5 Lipid extraction from plasma lipoprotein Samples**

This method was adapted from Hara & Radin 1987. In a glass tube, one millilitre of plasma, was mixed with 6.8 ml of hexane:isopropanol solution (3:2

v/v). The mixture was then mixed by inversion followed by the addition of 4.5 ml sodium sulphate (1 g/15 ml water). The tube was left to stand until all layers have separated. The top layer was collected in a LP4 tube then evaporated using nitrogen gas. The extract was dissolved in 0.5ml of hexane and kept at -20°C until required for further analysis (Hara and Radin, 1978).

### **5.3.6 Analysis of Triglyceride content of chylomicron and VLDL fractions**

Total triglyceride was measured using the Nile Red Assay and 100µl was loaded on a TLC plate. The triglyceride band from the TLC plate was processed through FAME then analysed using GC.

### **5.3.7 Statistics**

GraphPad prism 6 statistical software was used to analyse the data. Analysis of body weight, plasma glucose and gas chromatography results was carried out using two-way analysis of variance (2-way-ANOVA) with bonferroni post-hoc test. Analysis of plasma fraction triglyceride content was by one-way-ANOVA with bonferroni post-hoc test. Total liver tissue triglycerides were analysed by student unpaired t-test. In all analyses a p value of less than 0.05 was considered statistically significant. Raw data is given in the appendix.

## 5.4 Results

### 5.4.1 Effects of HFD on body weight and plasma glucose levels

The HFD did not have any significant effect on the animal weights compared to the NC feeding, Figure 5-1. The HFD group plasma glucose concentration was  $8.15 \pm 0.7 \text{ mM}$  and it stayed stable until the end of the study ( $8.725 \pm 1.01 \text{ mM}$ ). HFD plasma glucose concentration was elevated significantly, averaged at  $8.15 \pm 0.7 \text{ mM}$  compared to  $6.73 \pm 0.66 \text{ mM}$  in the NC group by week 6 with a p value of 0.047, Figure 5-2.

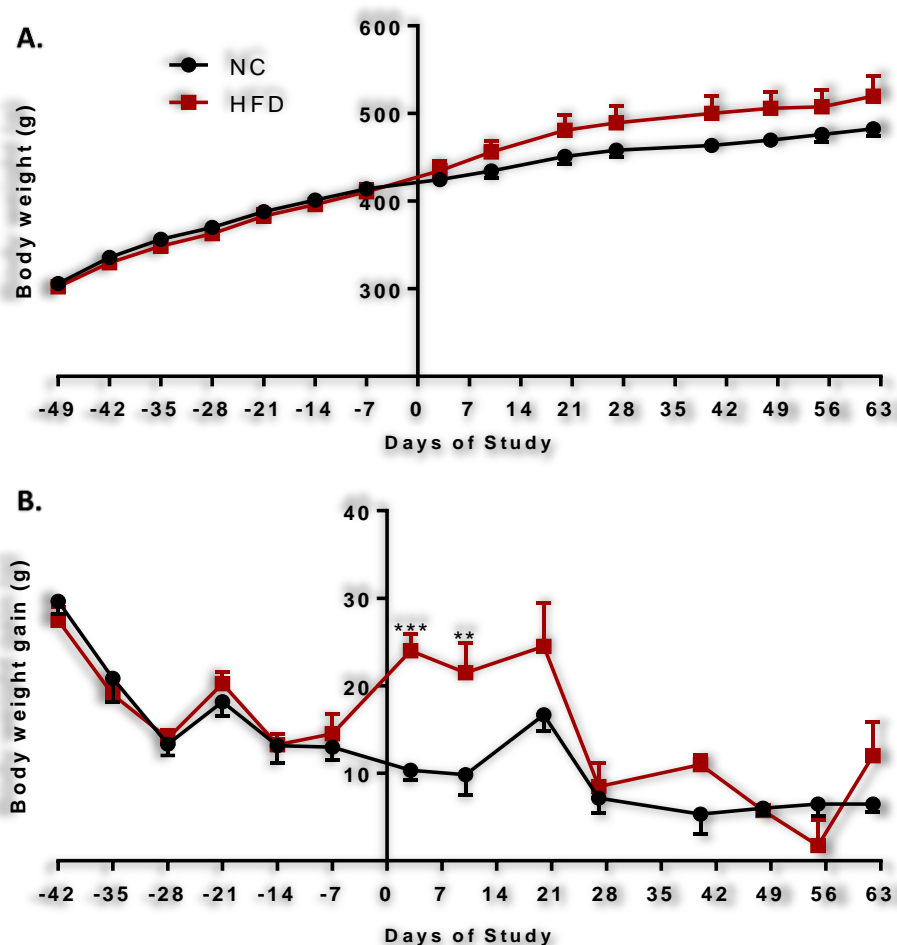


**Figure 5.1 | HFD effect on body weight.**

**A.** The animal weights were monitored and recorded weekly and **B.** average weekly weight gain was calculated their high fat diet (HFD) feeding did not lead to significant weight gain comparing to normal chow (NC) feeding. Data are presented as mean  $\pm$  SEM, analysis was by two-way-ANOVA with bonferroni post-hoc test,  $n=4$  for both groups.

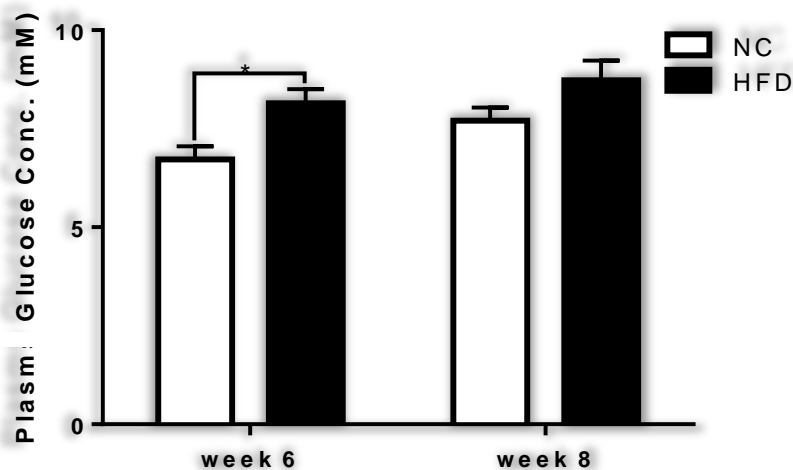


**Figure 5.2 | HFD effect on plasma glucose.**

Blood was collected from the lateral tail vein by week 6 and 8 of the study. Plasma was separated for the measurement of glucose. All data are presented as mean  $\pm$  SEM, analysis was by one-way-ANOVA with bonferroni post-hoc test, \* $p < 0.05$ ,  $n = 4$  for both groups. NC; Normal Chow, HFD; High Fat Diet.

#### 5.4.2 Liver tissue histology and triglyceride content

Liver tissue staining with H&E showed evidence of lipid droplets in the HFD group liver tissue, Figure 5-3. Meanwhile a PSR stain did not show any fibrosis in both groups.

Total triglyceride content was measured after isolating lipids from the liver tissue and showed that the HFD induced a 2 fold increase with a p value of 0.0014 when compared to the NC group, Figure 5-4.

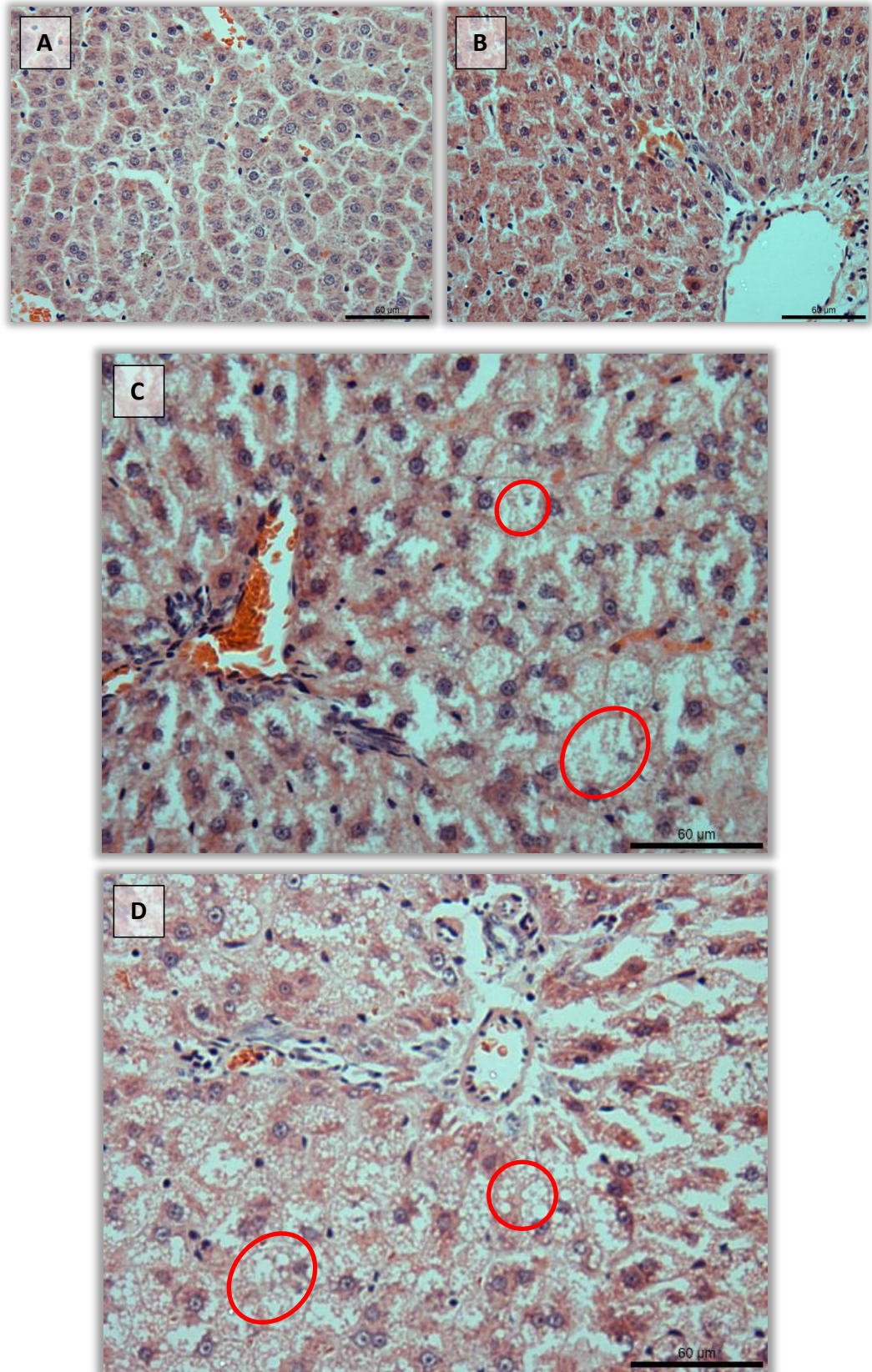


**Figure 5.3 | Liver histology.**

A representation of **A**, **B**, **C**, and **D**. HFD histological sections at x200 magnification, scale bar; 60µm. Five-µm paraformaldehyde fixed and paraffin embedded sections were stained with haematoxylin and eosin as describe in the methodology. The HFD group presented with evidence of steatosis (red circles).

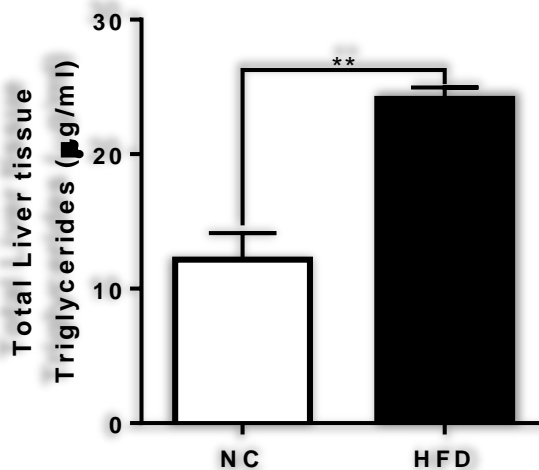


**Figure 5.4 | Liver tissue total triglyceride content.**

A 300mg of liver tissue was homogenized in sodium sulphate:hexane:isopropanol solvent mixture then total triglycerides was measured using the home made Nile red triglycerides assay. Data were analysed using student unpaired t-test and are presented as mean  $\pm$  SEM. \*\*P<0.001, NC: Normal Chow, HFD: High Fat Diet.

### 5.4.3 Plasma lipid triglycerides assessment

Total triglyceride content was measured after isolating lipids from the chylomicron and VLDL fractions and prior to processing to loading on the TLC plate. The NC group had higher triglycerides in the VLDL fraction with a p value of 0.01, otherwise groups had comparable amounts of TG in both fractions, Figure 5-5. The ratio of VLDL/chylomicron however was significantly higher in the NC group, 1.61 folds higher with a p value of 0.011, Figure 5-6.

The same extracts, along with diet extracts, were loaded to TLC plates, Figure 5-7. As previous, the loading front had phospholipids, then cholesterol, triglycerides has the largest fragment and the furthest migrated fragment was cholesterol ester.

For the GC data, any peaks that were detected and had a percentage of lower than one were eliminated from further analysis.

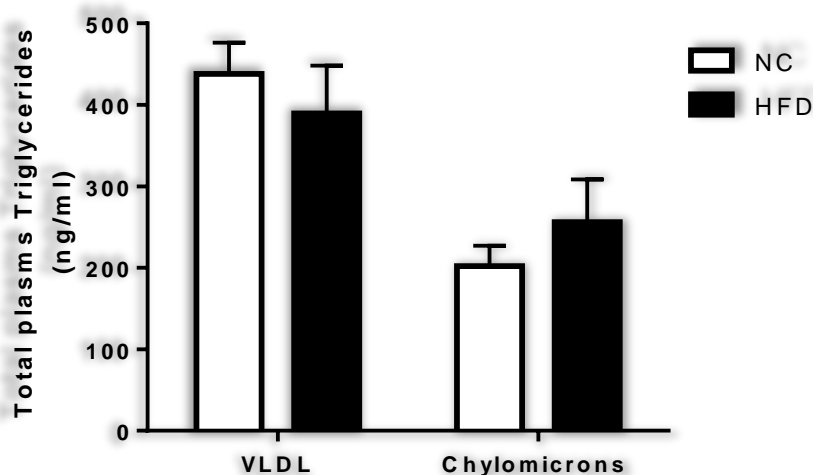


**Figure 5.5 | Plasma Lipoprotein Total Triglyceride Content.**

One millilitre of plasma was ultracentrifuged to separate chylomicrons and very low density lipoprotein (VLDL) fraction then total triglycerides were isolated as describe in the methodology. Total triglycerides was measured using the home made Nile red triglycerides assay. Data is presented as mean  $\pm$  SEM by One-way-ANOVA with bonferroni post-hoc test,  $n=4$  for both groups. NC; Normal Chow, HFD; High Fat Diet.

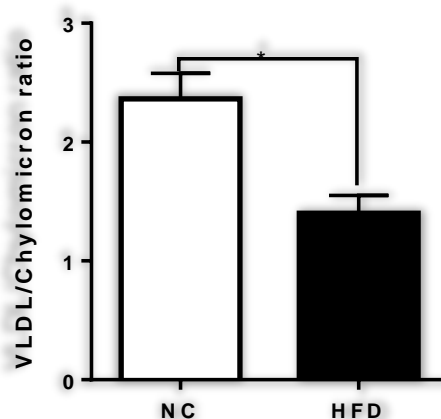


**Figure 5.6 | VLDL/Chylomicron Triglyceride Ratio.**

Total triglyceride measured by the triglyceride assay, Figure 5-5, was used to calculate the ratio of very low density lipoprotein (VLDL) to chylomicron. Data is presented as mean  $\pm$  SEM using unpaired t.testt,  $*p < 0.01$ ,  $n=4$  for both groups. NC; Normal Chow, HFD; High Fat Diet.

GC analysis showed that the NC and HFD had comparable triglyceride composition. In the HFD linoleic was the predominate triglyceride followed by linoleic, oleic, palmitic then stearic, linolenic acid at a percentage of  $\sim 34, 33, 19, 9$  and  $3$  respectively. The major difference between the diets is that NC did not show any linolenic acid in its composition and the major fatty acid was oleic; its

composition had ~43, 26, 19 and 12% of oleic, palmitic, linoleic and stearic acid respectively, Figure 5-8 and Appendix figure 7.

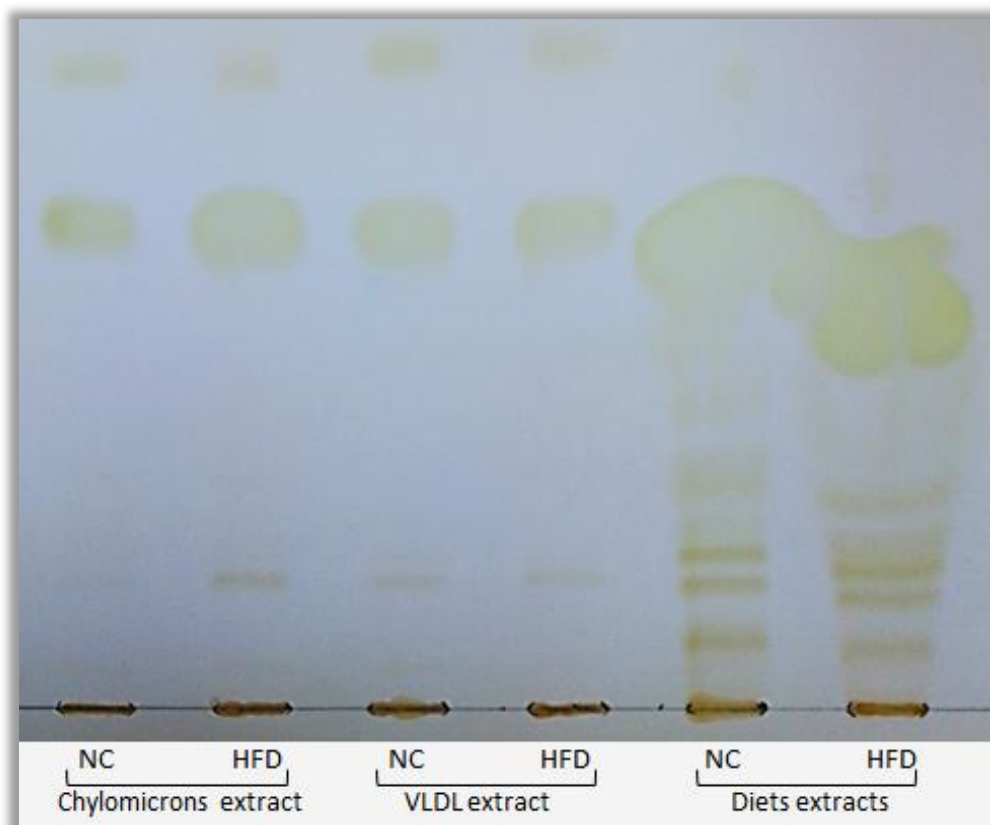


**Figure 5.7 | Thin layer chromatography of plasma fractions' total lipid extract.**

A representation of total lipids extracted from NC and HFD liver tissue. The extracts were loaded on a TLC plate then run using hexane:diethyl ether:glacial acetic acid single solvent system. The TLC plate was dried after the running front has reach about 1inch of the top of the plate then stained using iodine fumes. NC: Normal Chow, HFD: High Fat Diet.

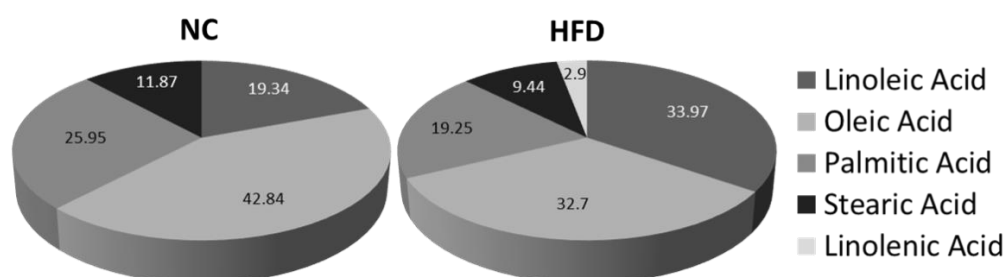


**Figure 5.8 | Diet fatty acid composition**

A total of 500mg of each of the normal chow (NC) and the high fat diet (HFD) was homogenized in a mixed sodium sulphate:hexane:isopropanol solvent, after running in a TLC plate TG band was cut out isolated, processed through FAME and subjected to gas chromatography (GC) analysis as described in the methodology. Data are presented as a percentage; both diets have similar composition with regards to the difference in percentage of distribution.

The chylomicron content of the NC diet group was composed of palmitic, oleic and stearic acids at a percentage of  $45.1 \pm 9.97$ ,  $26.99 \pm 5.41$  and  $15.19 \pm 3.52$  respectively. An average of  $5.4 \pm 0.39$  of palmitoleic was also observed.

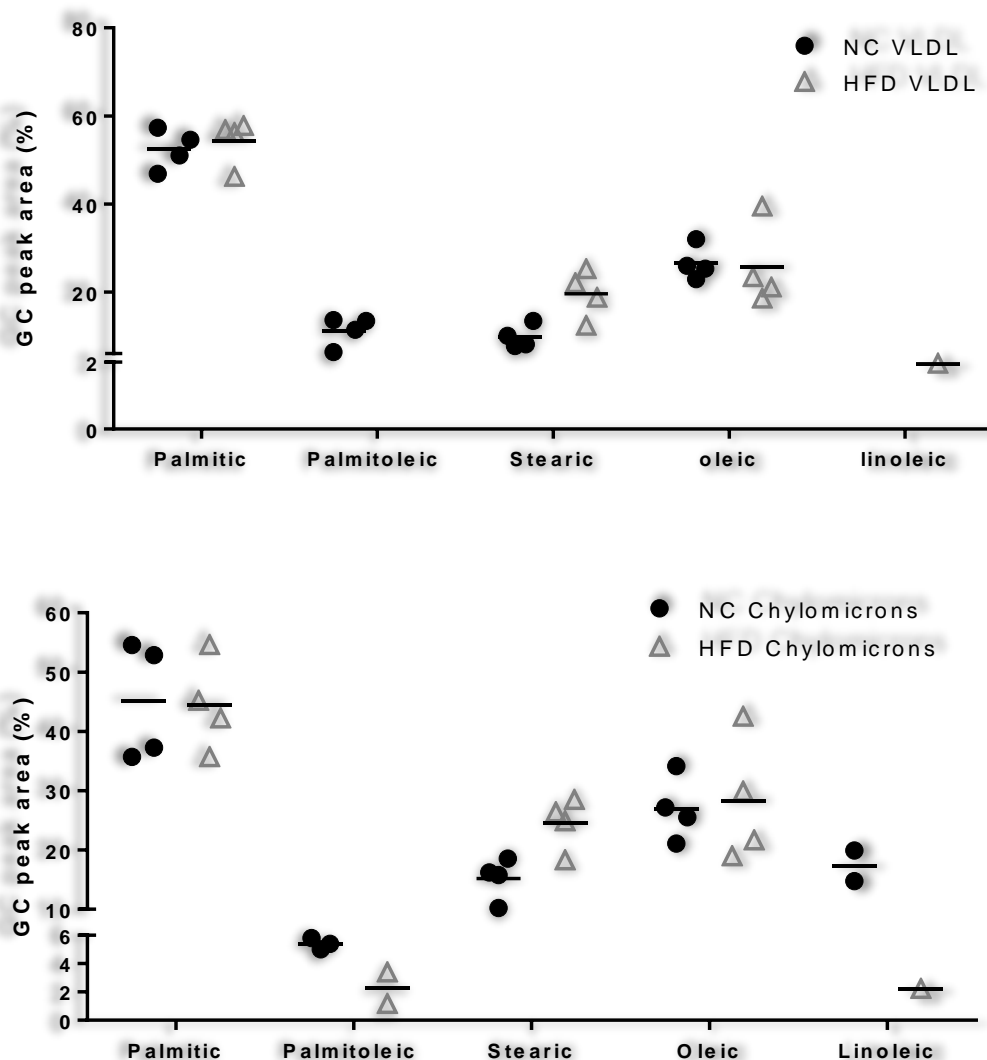


**Figure 5.9 | Plasma fractions triglycerides composition**

FAME processed triglyceride (TG) fragment isolated from the thin layer chromatography of plasma fractions. Total lipid extract was subject to gas chromatography. Peaks were identified in relation to a standard. Data are presented as mean  $\pm$  SEM by one-way-ANOVA test with bonferroni post-hoc test comparing pairs; NC and HFD for each TG, and TGs with in each group (n=4 for both NC and HFD). All data are presented as mean  $\pm$  SEM. Normal Chow, HFD; High Fat Diet.

Chylomicron triglyceride content of the NC and HFD groups were similar in terms of palmitic, oleic and stearic acids. Palmitoleic acid was observed at a significant level only in the NC samples. The VLDL triglyceride content of the NC

group was similar to the HFD group with no significant differences in fatty acid composition.

## 5.5 Discussion

Fat accumulation within hepatocytes, mainly in the form of triglyceride, is a prerequisite for the development of NAFLD. However, the metabolic abnormalities causing the lipid accretion is not fully understood (Donnelly *et al.*, 2005). It has been generally accepted that dietary manipulation can modify different tissue and cell lipid composition. For instance, the composition of membrane structural lipids is influenced by dietary fatty acid composition (Stubbs and Smith, 1984). Studies regarding plasma lipids date back to the 1960s. Since then, further research was performed to better understand the reasons behind the variabilities observed across subjects. One of the early papers by Dougherty (1987) demonstrated the effect of dietary intake on the lipid composition of several blood components including plasma, red blood cells and platelets. Their cross-national research involved subjects recruited from the USA, Italy and Finland. They demonstrated that the different races had their own fatty acid profile in various blood components that reflected the characteristics of their dietary fatty acid composition.

In here, the chylomicron fraction was separated as a reflection of the triglycerides derived from the diet which was then compared with both the diet and VLDL. The composition of chylomicron determined by GC analysis was reflective of the fatty acid composition of the diets. Similarly, the hepatic VLDL-triglyceride content was also comparable to that of the chylomicrons, the ratios between the chylomicrons- and VLDL-triglycerides were similar in both diets. This suggests that the triglycerides delivered to the liver are being repackaged

into VLDL particles and secreted again. However, there was one significant difference in the composition of the NC and the HFD VLDL-triglycerides: palmitoleic acid was present in the NC VLDL-triglyceride but not in the HFD VLDL. In humans, plasma VLDL-triglyceride palmitoleic acid was shown to increase in response to prolonged hyperalimentation (Volk *et al.*, 2014, Chong *et al.*, 2008, Aarsland and Wolfe, 1998). The increase in palmitoleic acid was associated with a parallel increase in *de novo* lipogenesis genes in the liver, but not in adipose tissue (Chong *et al.*, 2008). Similar to findings of the results of this study, increasing intake of dietary fat did not accumulate plasma lipid fractions (Volk *et al.*, 2014). That being said, and since human liver biopsies are particularly challenging to obtain from healthy individuals, the mentioned studies did not screen the status of the liver. The presence of a saturated fatty acid, a biomarker that is consistent with adverse health outcomes, in the circulation was then thought to be as more deteriorating.

In conclusion, high fat feeding did not change plasma triglyceride concentration, however it decreased the VLDL/Chylomicrons ratio and increased total liver triglyceride causing steatosis. This could indicate that the liver may be taking up increased levels of lipid as chylomicron remnant whilst secreting less as VLDL. On the other hand, high carbohydrate feeding leads to an increase in VLDL palmitoleic acid.

**CHAPTER VI:**

**General Discussion**

Dietary fat intake has often been claimed as being primarily responsible for increasing adiposity. Human studies have illustrated that HFD, with >30% of energy as fat, can easily lead to obesity (Hariri and Thibault, 2010). The main concern with obesity associated complications is the development of insulin resistance. However this study demonstrated that increasing dietary fat can have organ-specific effects before the development of overt obesity, causing steatosis in the liver. Feeding with a HFD for a period of 10 weeks in two separate studies induced steatosis that was accompanied by early signs of inflammatory change. The absence of obesity, along with a lack of changes in expression of genes involved in de-novo lipogenesis suggested the cause of this hepatic steatosis to be the increased dietary triglycerides accumulating in the liver. Recently sugar and high carbohydrate have been highlighted as the major cause for concern in the development of obesity, cardiovascular diseases and metabolic syndrome (Malhotra, 2013). High energy, high carbohydrate diets are considered to be the major risk factor for development of obesity. The results of this thesis however suggest the lipid content of diet may be a cause for concern even in the absence of weight gain. The reason behind marginalizing the effect of dietary fat on disease risk and highlighting dietary carbohydrate could be related to the increased in plasma VLDL saturated fatty acids that is associated with high carbohydrate feeding.

The HFD feeding-induced steatosis lead to the induction of liver ER stress that was evident by increased in CHOP expression levels and other ER stress related genes. The localization of the CHOP around lipid droplets and the portal vein, where ischemia was observed, indicates that HFD-induced liver

fatty changes may progress to liver injury and inflammation over time. Furthermore analysis of plasma lipoproteins showed that chylomicrons level was slightly higher in the HFD diet fed animals and the VLDL production was lower, the VLDL/chylomicron ratio was significantly higher in the NC fed group. This suggests that the liver may be taking up increased levels of lipid as chylomicron remnant whilst secreting less as VLDL.

While the liver showed ectopic fat deposition, adipose and skeletal muscle had very minor changes. Adipose tissue inflammatory status was not altered however early signs of what appeared to be remodelling macrophage infiltration was observed.

### **HFD effects on the streptozotocin diabetic model and pioglitazone intervention**

As mentioned previously the STZ-model is a well characterized and widely used as a robust model of type 1 diabetes (King, 2012). However, the combination of HFD and STZ in a model has emerged as an interesting alternative since the vast majority of diabetic patients are type 2 diabetics. In here, STZ injection induced a state of hyperglycemia and hypoinsulinemia and the effect on metabolic pathways observed were related to those changes. The drop in insulin secretion meant that peripheral tissue lacked insulin-induced effects.

Pioglitazone is an insulin sensitizer that works through activating PPAR $\gamma$  (Ding *et al.*, 2005, Waugh *et al.*, 2006). However in this study it did not have a major effect on whole body insulin and glucose levels.

## **Conclusion and further aspects**

In conclusion, the results of this thesis show that HFD feeding leads to liver steatosis. The lipid deposition in the liver causes ER stress. NAFLD has been shown to be associated with insulin resistance and recently it has been observed in patients with normal body mass index (Margariti *et al.*, 2012). Given that studies in human liver are limited, since liver biopsies cannot be routinely taken due to the risk of complications, this animal model provides a good model for HFD induced NAFLD.

A major complication of NAFLD is the development of NASH. The exact mechanism behind this progression is not yet fully elucidated. This model with the addition of an agent that disturbs the intestine and increases its permeability may produce a physiologically relevant model of NASH.

## References

- Aarsland, A. and Wolfe, R. R. (1998) 'Hepatic secretion of VLDL fatty acids during stimulated lipogenesis in men', *J Lipid Res*, 39(6), pp. 1280-6.
- Adams, L. A., Angulo, P. and Lindor, K. D. (2005) 'Nonalcoholic fatty liver disease', *CMAJ*, 172(7), pp. 899-905.
- Aizawa, Y., Seki, N., Nagano, T. and Abe, H. (2015) 'Chronic hepatitis C virus infection and lipoprotein metabolism', *World J Gastroenterol*, 21(36), pp. 10299-313.
- Alexander, C. A., Hamilton, R. L. and Havel, R. J. (1976) 'Subcellular localization of B apoprotein of plasma lipoproteins in rat liver', *J Cell Biol*, 69(2), pp. 241-63.
- Allard, J. P., Aghdassi, E., Mohammed, S., Raman, M., Avand, G., Arendt, B. M., Jalali, P., Kandasamy, T., Prayitno, N., Sherman, M., Guindi, M., Ma, D. W. and Heathcote, J. E. (2008) 'Nutritional assessment and hepatic fatty acid composition in non-alcoholic fatty liver disease (NAFLD): a cross-sectional study', *J Hepatol*, 48(2), pp. 300-7.
- Amir, M. and Czaja, M. J. (2011) 'Autophagy in nonalcoholic steatohepatitis', *Expert Rev Gastroenterol Hepatol*, 5(2), pp. 159-66.
- Andersen, C. L., Jensen, J. L. and Ørntoft, T. F. (2004) 'Normalization of real-time quantitative reverse transcription-PCR data: a model-based variance estimation approach to identify genes suited for normalization, applied to bladder and colon cancer data sets', *Cancer Res*, 64(15), pp. 5245-50.
- Anderson, N. and Borlak, J. (2008) 'Molecular mechanisms and therapeutic targets in steatosis and steatohepatitis', *Pharmacol Rev*, 60(3), pp. 311-57.
- Angulo, P. (2002) 'Nonalcoholic fatty liver disease', *N Engl J Med*, 346(16), pp. 1221-31.
- Araya, J., Rodrigo, R., Videla, L. A., Thielemann, L., Orellana, M., Pettinelli, P. and Poniachik, J. (2004) 'Increase in long-chain polyunsaturated fatty acid n - 6/n - 3 ratio in relation to hepatic steatosis in patients with non-alcoholic fatty liver disease', *Clin Sci (Lond)*, 106(6), pp. 635-43.
- Arkan, M. C., Hevener, A. L., Greten, F. R., Maeda, S., Li, Z. W., Long, J. M., Wynshaw-Boris, A., Poli, G., Olefsky, J. and Karin, M. (2005) 'IKK-beta links inflammation to obesity-induced insulin resistance', *Nat Med*, 11(2), pp. 191-8.
- Arvidsson, E., Viguerie, N., Andersson, I., Verdich, C., Langin, D. and Arner, P. (2004) 'Effects of different hypocaloric diets on protein secretion from adipose tissue of obese women', *Diabetes*, 53(8), pp. 1966-71.
- Baggio, L. L. and Drucker, D. J. (2006) 'Therapeutic approaches to preserve islet mass in type 2 diabetes', *Annu Rev Med*, 57, pp. 265-81.
- Bajaj, M., Suraamornkul, S., Pratipanawatr, T., Hardies, L. J., Pratipanawatr, W., Glass, L., Cersosimo, E., Miyazaki, Y. and DeFronzo, R. A. (2003) 'Pioglitazone reduces hepatic fat content and augments splanchnic glucose uptake in patients with type 2 diabetes', *Diabetes*, 52(6), pp. 1364-70.
- Bandsma, R. H., Wiegman, C. H., Herling, A. W., Burger, H. J., ter Harmsel, A., Meijer, A. J., Romijn, J. A., Reijngoud, D. J. and Kuipers, F. (2001) 'Acute inhibition of glucose-6-phosphate translocator activity leads to increased de novo

- lipogenesis and development of hepatic steatosis without affecting VLDL production in rats', *Diabetes*, 50(11), pp. 2591-7.
- Beaven, S. W., Matveyenko, A., Wroblewski, K., Chao, L., Wilpitz, D., Hsu, T. W., Lentz, J., Drew, B., Hevener, A. L. and Tontonoz, P. (2013) 'Reciprocal regulation of hepatic and adipose lipogenesis by liver X receptors in obesity and insulin resistance', *Cell Metab*, 18(1), pp. 106-17.
- Bechmann, L. P., Hannivoort, R. A., Gerken, G., Hotamisligil, G. S., Trauner, M. and Canbay, A. (2012) 'The interaction of hepatic lipid and glucose metabolism in liver diseases', *J Hepatol*, 56(4), pp. 952-64.
- Benatti, P., Peluso, G., Nicolai, R. and Calvani, M. (2004) 'Polyunsaturated fatty acids: biochemical, nutritional and epigenetic properties', *J Am Coll Nutr*, 23(4), pp. 281-302.
- Bennett, N. B., Ogston, C. M., McAndrew, G. M. and Ogston, D. (1966) 'Studies on the fibrinolytic enzyme system in obesity', *J Clin Pathol*, 19(3), pp. 241-3.
- Berger, J. P., Akiyama, T. E. and Meinke, P. T. (2005) 'PPARs: therapeutic targets for metabolic disease', *Trends Pharmacol Sci*, 26(5), pp. 244-51.
- Berk, P. D., Zhou, S. and Bradbury, M. W. (2005) 'Increased hepatocellular uptake of long chain fatty acids occurs by different mechanisms in fatty livers due to obesity or excess ethanol use, contributing to development of steatohepatitis in both settings', *Trans Am Clin Climatol Assoc*, 116, pp. 335-44; discussion 345.
- Berlanga, A., Guiu-Jurado, E., Porras, J. A. and Auguet, T. (2014) 'Molecular pathways in non-alcoholic fatty liver disease', *Clin Exp Gastroenterol*, 7, pp. 221-39.
- Bilan, P. J., Samokhvalov, V., Koshkina, A., Schertzer, J. D., Samaan, M. C. and Klip, A. (2009) 'Direct and macrophage-mediated actions of fatty acids causing insulin resistance in muscle cells', *Arch Physiol Biochem*, 115(4), pp. 176-90.
- Bjorkegren, J., Packard, C. J., Hamsten, A., Bedford, D., Caslake, M., Foster, L., Shepherd, J., Stewart, P. and Karpe, F. (1996) 'Accumulation of large very low density lipoprotein in plasma during intravenous infusion of a chylomicron-like triglyceride emulsion reflects competition for a common lipolytic pathway', *J Lipid Res*, 37(1), pp. 76-86.
- Boden, G., Chen, X., Ruiz, J., White, J. V. and Rossetti, L. (1994) 'Mechanisms of fatty acid-induced inhibition of glucose uptake', *J Clin Invest*, 93(6), pp. 2438-46.
- Bradbury, M. W. and Berk, P. D. (2004) 'Lipid metabolism in hepatic steatosis', *Clin Liver Dis*, 8(3), pp. 639-71, xi.
- Brake, D. K., Smith, E. O., Mersmann, H., Smith, C. W. and Robker, R. L. (2006) 'ICAM-1 expression in adipose tissue: effects of diet-induced obesity in mice', *Am J Physiol Cell Physiol*, 291(6), pp. C1232-9.
- Bruun, J. M., Helge, J. W., Richelsen, B. and Stallknecht, B. (2006) 'Diet and exercise reduce low-grade inflammation and macrophage infiltration in adipose tissue but not in skeletal muscle in severely obese subjects', *Am J Physiol Endocrinol Metab*, 290(5), pp. E961-7.
- Bruun, J. M., Verdich, C., Toubro, S., Astrup, A. and Richelsen, B. (2003) 'Association between measures of insulin sensitivity and circulating levels of interleukin-8, interleukin-6 and tumor necrosis factor-alpha. Effect of weight loss in obese men', *Eur J Endocrinol*, 148(5), pp. 535-42.

- Buque, X., Martinez, M. J., Cano, A., Miquilena-Colina, M. E., Garcia-Monzon, C., Aspichueta, P. and Ochoa, B. (2010) 'A subset of dysregulated metabolic and survival genes is associated with severity of hepatic steatosis in obese Zucker rats', *J Lipid Res*, 51(3), pp. 500-13.
- Burdge, G. C. and Wootton, S. A. (2003) 'Conversion of alpha-linolenic acid to palmitic, palmitoleic, stearic and oleic acids in men and women', *Prostaglandins Leukot Essent Fatty Acids*, 69(4), pp. 283-90.
- Caballero, F., Fernández, A., De Lacy, A. M., Fernández-Checa, J. C., Caballería, J. and García-Ruiz, C. (2009) 'Enhanced free cholesterol, SREBP-2 and StAR expression in human NASH', *J Hepatol*, 50(4), pp. 789-96.
- Cable, E. E., Finn, P. D., Stebbins, J. W., Hou, J., Ito, B. R., van Poelje, P. D., Linemeyer, D. L. and Erion, M. D. (2009) 'Reduction of hepatic steatosis in rats and mice after treatment with a liver-targeted thyroid hormone receptor agonist', *Hepatology*, 49(2), pp. 407-17.
- Caldwell, S. H., Hespeneheide, E. E., Redick, J. A., Iezzoni, J. C., Battle, E. H. and Sheppard, B. L. (2001) 'A pilot study of a thiazolidinedione, troglitazone, in nonalcoholic steatohepatitis', *Am J Gastroenterol*, 96(2), pp. 519-25.
- Chatzigeorgiou, A., Halapas, A., Kalafatakis, K. and Kamper, E. (2009) 'The use of animal models in the study of diabetes mellitus', *In Vivo*, 23(2), pp. 245-58.
- Chen, Y. D., Golay, A., Swislocki, A. L. and Reaven, G. M. (1987) 'Resistance to insulin suppression of plasma free fatty acid concentrations and insulin stimulation of glucose uptake in noninsulin-dependent diabetes mellitus', *J Clin Endocrinol Metab*, 64(1), pp. 17-21.
- Chida, D., Osaka, T., Hashimoto, O. and Iwakura, Y. (2006) 'Combined interleukin-6 and interleukin-1 deficiency causes obesity in young mice', *Diabetes*, 55(4), pp. 971-7.
- Chikka, M. R., McCabe, D. D., Tyra, H. M. and Rutkowski, D. T. (2013) 'C/EBP homologous protein (CHOP) contributes to suppression of metabolic genes during endoplasmic reticulum stress in the liver', *J Biol Chem*, 288(6), pp. 4405-15.
- Chong, M. F., Hodson, L., Bickerton, A. S., Roberts, R., Neville, M., Karpe, F., Frayn, K. N. and Fielding, B. A. (2008) 'Parallel activation of de novo lipogenesis and stearoyl-CoA desaturase activity after 3 d of high-carbohydrate feeding', *Am J Clin Nutr*, 87(4), pp. 817-23.
- Christiansen, T., Richelsen, B. and Bruun, J. M. (2005) 'Monocyte chemoattractant protein-1 is produced in isolated adipocytes, associated with adiposity and reduced after weight loss in morbid obese subjects', *Int J Obes (Lond)*, 29(1), pp. 146-50.
- Cinti, S., Mitchell, G., Barbatelli, G., Murano, I., Ceresi, E., Faloia, E., Wang, S., Fortier, M., Greenberg, A. S. and Obin, M. S. (2005) 'Adipocyte death defines macrophage localization and function in adipose tissue of obese mice and humans', *J Lipid Res*, 46(11), pp. 2347-55.
- Clark, J. M. (2006) 'The epidemiology of nonalcoholic fatty liver disease in adults', *J Clin Gastroenterol*, 40 Suppl 1, pp. S5-10.
- Cooper, A. D. (1997) 'Hepatic uptake of chylomicron remnants', *J Lipid Res*, 38(11), pp. 2173-92.

- Cortez-Pinto, H., Jesus, L., Barros, H., Lopes, C., Moura, M. C. and Camilo, M. E. (2006) 'How different is the dietary pattern in non-alcoholic steatohepatitis patients?', *Clin Nutr*, 25(5), pp. 816-23.
- Crawford, S. E. and Borensztajn, J. (1999) 'Plasma clearance and liver uptake of chylomicron remnants generated by hepatic lipase lipolysis: evidence for a lactoferrin-sensitive and apolipoprotein E-independent pathway', *J Lipid Res*, 40(5), pp. 797-805.
- Cui, W., Sun, Y., Wang, Z., Xu, C., Xu, L., Wang, F., Chen, Z., Peng, Y. and Li, R. (2011) 'Activation of liver X receptor decreases BACE1 expression and activity by reducing membrane cholesterol levels', *Neurochem Res*, 36(10), pp. 1910-21.
- Curat, C. A., Miranville, A., Sengenès, C., Diehl, M., Tonus, C., Busse, R. and Bouloumie, A. (2004) 'From blood monocytes to adipose tissue-resident macrophages: induction of diapedesis by human mature adipocytes', *Diabetes*, 53(5), pp. 1285-92.
- Cuzzocrea, S., Pisano, B., Dugo, L., Ianaro, A., Maffia, P., Patel, N. S., Di Paola, R., Ialenti, A., Genovese, T., Chatterjee, P. K., Di Rosa, M., Caputi, A. P. and Thiemermann, C. (2004) 'Rosiglitazone, a ligand of the peroxisome proliferator-activated receptor-gamma, reduces acute inflammation', *Eur J Pharmacol*, 483(1), pp. 79-93.
- Dallinga-Thie, G. M., Franssen, R., Mooij, H. L., Visser, M. E., Hassing, H. C., Peelman, F., Kastelein, J. J., Péterfy, M. and Nieuwdorp, M. (2010) 'The metabolism of triglyceride-rich lipoproteins revisited: new players, new insight', *Atherosclerosis*, 211(1), pp. 1-8.
- Das, K., Mukherjee, P. S., Ghosh, A., Ghosh, S., Mridha, A. R., Dhibar, T., Bhattacharya, B., Bhattacharya, D., Manna, B., Dhali, G. K., Santra, A. and Chowdhury, A. (2010) 'Nonobese population in a developing country has a high prevalence of nonalcoholic fatty liver and significant liver disease', *Hepatology*, 51(5), pp. 1593-602.
- David, S. and Kroner, A. (2011) 'Repertoire of microglial and macrophage responses after spinal cord injury', *Nat Rev Neurosci*, 12(7), pp. 388-99.
- Day, C. P. and James, O. F. (1998) 'Steatohepatitis: a tale of two "hits"?', *Gastroenterology*, 114(4), pp. 842-5.
- DeFronzo, R. A. and Ferrannini, E. (1991) 'Insulin resistance. A multifaceted syndrome responsible for NIDDM, obesity, hypertension, dyslipidemia, and atherosclerotic cardiovascular disease', *Diabetes Care*, 14(3), pp. 173-94.
- Del Gaudio, A., Boschi, L., Del Gaudio, G. A., Mastrangelo, L. and Munari, D. (2002) 'Liver damage in obese patients', *Obes Surg*, 12(6), pp. 802-4.
- Di Gregorio, G. B., Yao-Borengasser, A., Rasouli, N., Varma, V., Lu, T., Miles, L. M., Ranganathan, G., Peterson, C. A., McGehee, R. E. and Kern, P. A. (2005) 'Expression of CD68 and macrophage chemoattractant protein-1 genes in human adipose and muscle tissues: association with cytokine expression, insulin resistance, and reduction by pioglitazone', *Diabetes*, 54(8), pp. 2305-13.
- Ding, S. Y., Shen, Z. F., Chen, Y. T., Sun, S. J., Liu, Q. and Xie, M. Z. (2005) 'Pioglitazone can ameliorate insulin resistance in low-dose streptozotocin and high sucrose-fat diet induced obese rats', *Acta Pharmacol Sin*, 26(5), pp. 575-80.

- Doerge, H., Grimm, D., Falcon, A., Tsang, B., Storm, T. A., Xu, H., Ortegon, A. M., Kazantzis, M., Kay, M. A. and Stahl, A. (2008) 'Silencing of hepatic fatty acid transporter protein 5 in vivo reverses diet-induced non-alcoholic fatty liver disease and improves hyperglycemia', *J Biol Chem*, 283(32), pp. 22186-92.
- Donnelly, K. L., Smith, C. I., Schwarzenberg, S. J., Jessurun, J., Boldt, M. D. and Parks, E. J. (2005) 'Sources of fatty acids stored in liver and secreted via lipoproteins in patients with nonalcoholic fatty liver disease', *J Clin Invest*, 115(5), pp. 1343-51.
- Donohue, T. M., Osna, N. A., Trambly, C. S., Whitaker, N. P., Thomes, P. G., Todero, S. L. and Davis, J. S. (2012) 'Early growth response-1 contributes to steatosis development after acute ethanol administration', *Alcohol Clin Exp Res*, 36(5), pp. 759-67.
- Dowman, J. K., Tomlinson, J. W. and Newsome, P. N. (2010) 'Pathogenesis of non-alcoholic fatty liver disease', *Qjm*, 103(2), pp. 71-83.
- Dufour, J. F. and Clavien, P. A. (2009) *Signaling Pathways in Liver Diseases*. Springer-Verlag.
- Duivenvoorden, I., Teusink, B., Rensen, P. C., Romijn, J. A., Havekes, L. M. and Voshol, P. J. (2005) 'Apolipoprotein C3 deficiency results in diet-induced obesity and aggravated insulin resistance in mice', *Diabetes*, 54(3), pp. 664-71.
- Dyson, J. K., Anstee, Q. M. and McPherson, S. (2015) 'Republished: Non-alcoholic fatty liver disease: a practical approach to treatment', *Postgrad Med J*, 91(1072), pp. 92-101.
- Eaton, S., Bartlett, K. and Pourfarzam, M. (1996) 'Mammalian mitochondrial beta-oxidation', *Biochem J*, 320 ( Pt 2), pp. 345-57.
- Ekberg, K., Landau, B. R., Wajngot, A., Chandramouli, V., Efendic, S., Brunengraber, H. and Wahren, J. (1999) 'Contributions by kidney and liver to glucose production in the postabsorptive state and after 60 h of fasting', *Diabetes*, 48(2), pp. 292-8.
- Esposito, K., Pontillo, A., Giugliano, F., Giugliano, G., Marfella, R., Nicoletti, G. and Giugliano, D. (2003) 'Association of low interleukin-10 levels with the metabolic syndrome in obese women', *J Clin Endocrinol Metab*, 88(3), pp. 1055-8.
- Exton, J. H. and Park, C. R. (1967) 'Control of gluconeogenesis in liver. I. General features of gluconeogenesis in the perfused livers of rats', *J Biol Chem*, 242(11), pp. 2622-36.
- Fain, J. N., Madan, A. K., Hiler, M. L., Cheema, P. and Bahouth, S. W. (2004) 'Comparison of the release of adipokines by adipose tissue, adipose tissue matrix, and adipocytes from visceral and subcutaneous abdominal adipose tissues of obese humans', *Endocrinology*, 145(5), pp. 2273-82.
- Farrell, G. C., McCullough, A. J. and Day, C. P. (2013) *Non-Alcoholic Fatty Liver Disease: A Practical Guide*. Wiley.
- Fehrenbacher, J. C., Vasko, M. R. and Duarte, D. B. (2012) 'Models of inflammation: Carrageenan- or complete Freund's Adjuvant (CFA)-induced edema and hypersensitivity in the rat', *Curr Protoc Pharmacol*, Chapter 5, pp. Unit5.4.

- Ferhatovic, L., Banozic, A., Kostic, S., Kurir, T. T., Novak, A., Vrdoljak, L., Heffer, M., Sapunar, D. and Puljak, L. (2013) 'Expression of calcium/calmodulin-dependent protein kinase II and pain-related behavior in rat models of type 1 and type 2 diabetes', *Anesth Analg*, 116(3), pp. 712-21.
- Fernández Gianotti, T., Burgueño, A., Gonzales Mansilla, N., Pirola, C. J. and Sookoian, S. (2013) 'Fatty liver is associated with transcriptional downregulation of stearoyl-CoA desaturase and impaired protein dimerization', *PLoS One*, 8(9), pp. e76912.
- Ferré, P. and Foufelle, F. (2007) 'SREBP-1c transcription factor and lipid homeostasis: clinical perspective', *Horm Res*, 68(2), pp. 72-82.
- Fisher, E. A., Pan, M., Chen, X., Wu, X., Wang, H., Jamil, H., Sparks, J. D. and Williams, K. J. (2001) 'The triple threat to nascent apolipoprotein B. Evidence for multiple, distinct degradative pathways', *J Biol Chem*, 276(30), pp. 27855-63.
- Fisher, F. M., Chui, P. C., Antonellis, P. J., Bina, H. A., Kharitonkov, A., Flier, J. S. and Maratos-Flier, E. (2010) 'Obesity is a fibroblast growth factor 21 (FGF21)-resistant state', *Diabetes*, 59(11), pp. 2781-9.
- Fisher, F. M., Chui, P. C., Nasser, I. A., Popov, Y., Cunniff, J. C., Lundasen, T., Kharitonkov, A., Schuppan, D., Flier, J. S. and Maratos-Flier, E. (2014) 'Fibroblast growth factor 21 limits lipotoxicity by promoting hepatic fatty acid activation in mice on methionine and choline-deficient diets', *Gastroenterology*, 147(5), pp. 1073-83.e6.
- Foretz, M., Guichard, C., Ferré, P. and Foufelle, F. (1999) 'Sterol regulatory element binding protein-1c is a major mediator of insulin action on the hepatic expression of glucokinase and lipogenesis-related genes', *Proc Natl Acad Sci U S A*, 96(22), pp. 12737-42.
- Forman, B. M., Chen, J. and Evans, R. M. (1997) 'Hypolipidemic drugs, polyunsaturated fatty acids, and eicosanoids are ligands for peroxisome proliferator-activated receptors alpha and delta', *Proc Natl Acad Sci U S A*, 94(9), pp. 4312-7.
- Foster, J. D., Pederson, B. A. and Nordlie, R. C. (1997) 'Glucose-6-phosphatase structure, regulation, and function: an update', *Proc Soc Exp Biol Med*, 215(4), pp. 314-32.
- Franceschini, G., Maderna, P. and Sirtori, C. R. (1991) 'Reverse cholesterol transport: physiology and pharmacology', *Atherosclerosis*, 88(2-3), pp. 99-107.
- Frayn, K. N. (2003) *Metabolic regulation : a human perspective*. 2nd ed. edn. Oxford: Blackwell Science.
- Fukumoto, H., Kayano, T., Buse, J. B., Edwards, Y., Pilch, P. F., Bell, G. I. and Seino, S. (1989) 'Cloning and characterization of the major insulin-responsive glucose transporter expressed in human skeletal muscle and other insulin-responsive tissues', *J Biol Chem*, 264(14), pp. 7776-9.
- Ghanim, H., Aljada, A., Hofmeyer, D., Syed, T., Mohanty, P. and Dandona, P. (2004) 'Circulating mononuclear cells in the obese are in a proinflammatory state', *Circulation*, 110(12), pp. 1564-71.
- Ginsberg, H. N., Zhang, Y. L. and Hernandez-Ono, A. (2005) 'Regulation of plasma triglycerides in insulin resistance and diabetes', *Arch Med Res*, 36(3), pp. 232-40.

- Glatzle, J., Wang, Y., Adelson, D. W., Kalogeris, T. J., Zittel, T. T., Tso, P., Wei, J. Y. and Raybould, H. E. (2003) 'Chylomicron components activate duodenal vagal afferents via a cholecystinin A receptor-mediated pathway to inhibit gastric motor function in the rat', *J Physiol*, 550(Pt 2), pp. 657-64.
- Goldberg, I. J. (1996) 'Lipoprotein lipase and lipolysis: central roles in lipoprotein metabolism and atherogenesis', *J Lipid Res*, 37(4), pp. 693-707.
- Goldberg, I. J., Eckel, R. H. and Abumrad, N. A. (2009) 'Regulation of fatty acid uptake into tissues: lipoprotein lipase- and CD36-mediated pathways', *J Lipid Res*, 50 Suppl, pp. S86-90.
- Gonzalez-Periz, A., Horrillo, R., Ferre, N., Gronert, K., Dong, B., Moran-Salvador, E., Titos, E., Martinez-Clemente, M., Lopez-Parra, M., Arroyo, V. and Claria, J. (2009) 'Obesity-induced insulin resistance and hepatic steatosis are alleviated by omega-3 fatty acids: a role for resolvins and protectins', *Faseb j*, 23(6), pp. 1946-57.
- Goodman, M. N., Berger, M. and Ruderman, N. B. (1974) 'Glucose metabolism in rat skeletal muscle at rest. Effect of starvation, diabetes, ketone bodies and free fatty acids', *Diabetes*, 23(11), pp. 881-8.
- Goudriaan, J. R., den Boer, M. A., Rensen, P. C., Febbraio, M., Kuipers, F., Romijn, J. A., Havekes, L. M. and Voshol, P. J. (2005) 'CD36 deficiency in mice impairs lipoprotein lipase-mediated triglyceride clearance', *J Lipid Res*, 46(10), pp. 2175-81.
- Grace, C. S. and Goldrick, R. B. (1968) 'Fibrinolysis and body bulid. Interrelationships between blood fibrinolysis, body composition and parameters of lipid and carbohydrate metabolism', *J Atheroscler Res*, 8(4), pp. 705-19.
- Green, P. H. and Glickman, R. M. (1981) 'Intestinal lipoprotein metabolism', *J Lipid Res*, 22(8), pp. 1153-73.
- Gruen, M. L., Hao, M., Piston, D. W. and Hastay, A. H. (2007) 'Leptin requires canonical migratory signaling pathways for induction of monocyte and macrophage chemotaxis', *Am J Physiol Cell Physiol*, 293(5), pp. C1481-8.
- Guillen, N., Navarro, M. A., Arnal, C., Noone, E., Arbones-Mainar, J. M., Acin, S., Surra, J. C., Muniesa, P., Roche, H. M. and Osada, J. (2009) 'Microarray analysis of hepatic gene expression identifies new genes involved in steatotic liver', *Physiol Genomics*, 37(3), pp. 187-98.
- Haemmerle, G., Zimmermann, R., Strauss, J. G., Kratky, D., Riederer, M., Knipping, G. and Zechner, R. (2002) 'Hormone-sensitive lipase deficiency in mice changes the plasma lipid profile by affecting the tissue-specific expression pattern of lipoprotein lipase in adipose tissue and muscle', *J Biol Chem*, 277(15), pp. 12946-52.
- Hara, A. and Radin, N. S. (1978) 'Lipid extraction of tissues with a low-toxicity solvent', *Anal Biochem*, 90(1), pp. 420-6.
- Hariri, N. and Thibault, L. (2010) 'High-fat diet-induced obesity in animal models', *Nutr Res Rev*, 23(2), pp. 270-99.
- Harmon, R. C., Tiniakos, D. G. and Argo, C. K. (2011) 'Inflammation in nonalcoholic steatohepatitis', *Expert Rev Gastroenterol Hepatol*, 5(2), pp. 189-200.

- Havel, R. J. and Hamilton, R. L. (2004) 'Hepatic catabolism of remnant lipoproteins: where the action is', *Arterioscler Thromb Vasc Biol*, 24(2), pp. 213-5.
- Hedeskov, C. J., Capito, K., Islin, H., Hansen, S. E. and Thams, P. (1992) 'Long-term fat-feeding-induced insulin resistance in normal NMRI mice: postreceptor changes of liver, muscle and adipose tissue metabolism resembling those of type 2 diabetes', *Acta Diabetol*, 29(1), pp. 14-9.
- Heinrichsdorff, J. and Olefsky, J. M. (2012) 'Fetuin-A: the missing link in lipid-induced inflammation', *Nat Med: Vol. 8*. United States, pp. 1182-3.
- Hersberger, M. and von Eckardstein, A. (2003) 'Low high-density lipoprotein cholesterol: physiological background, clinical importance and drug treatment', *Drugs*, 63(18), pp. 1907-45.
- Holm, C. (2003) 'Molecular mechanisms regulating hormone-sensitive lipase and lipolysis', *Biochem Soc Trans*, 31(Pt 6), pp. 1120-4.
- Hosogai, N., Fukuhara, A., Oshima, K., Miyata, Y., Tanaka, S., Segawa, K., Furukawa, S., Tochino, Y., Komuro, R., Matsuda, M. and Shimomura, I. (2007) 'Adipose tissue hypoxia in obesity and its impact on adipocytokine dysregulation', *Diabetes*, 56(4), pp. 901-11.
- Hotamisligil, G. S. (2005) 'Role of endoplasmic reticulum stress and c-Jun NH2-terminal kinase pathways in inflammation and origin of obesity and diabetes', *Diabetes*, 54 Suppl 2, pp. S73-8.
- Hotamisligil, G. S. (2006) 'Inflammation and metabolic disorders', *Nature*, 444(7121), pp. 860-7.
- Hotamisligil, G. S., Murray, D. L., Choy, L. N. and Spiegelman, B. M. (1994) 'Tumor necrosis factor alpha inhibits signaling from the insulin receptor', *Proc Natl Acad Sci U S A*, 91(11), pp. 4854-8.
- Hotamisligil, G. S., Shargill, N. S. and Spiegelman, B. M. (1993) 'Adipose expression of tumor necrosis factor-alpha: direct role in obesity-linked insulin resistance', *Science*, 259(5091), pp. 87-91.
- Hu, E., Liang, P. and Spiegelman, B. M. (1996) 'AdipoQ is a novel adipose-specific gene dysregulated in obesity', *J Biol Chem*, 271(18), pp. 10697-703.
- Hughes, S and A, M. 2007. PCR, The Method Express Series. Bloxham, Oxfordshire: Scion Publishing: PCR-Methods Express.
- Hübscher, S. G. (2006) 'Histological assessment of non-alcoholic fatty liver disease', *Histopathology*, 49(5), pp. 450-65.
- Inoue, M., Ohtake, T., Motomura, W., Takahashi, N., Hosoki, Y., Miyoshi, S., Suzuki, Y., Saito, H., Kohgo, Y. and Okumura, T. (2005) 'Increased expression of PPARgamma in high fat diet-induced liver steatosis in mice', *Biochem Biophys Res Commun*, 336(1), pp. 215-22.
- Jump, D. B., Botolin, D., Wang, Y., Xu, J., Christian, B. and Demeure, O. (2005) 'Fatty acid regulation of hepatic gene transcription', *J Nutr*, 135(11), pp. 2503-6.
- Kahn, C. R., Chen, L. and Cohen, S. E. (2000) 'Unraveling the mechanism of action of thiazolidinediones', *J Clin Invest*, 106(11), pp. 1305-7.
- Kaiser, N., Nesher, R., Donath, M. Y., Fraenkel, M., Behar, V., Magnan, C., Ktorza, A., Cerasi, E. and Leibowitz, G. (2005) 'Psammomys obesus, a model for

- environment-gene interactions in type 2 diabetes', *Diabetes*, 54 Suppl 2, pp. S137-44.
- Kalupahana, N. S., Moustaid-Moussa, N. and Claycombe, K. J. (2012) 'Immunity as a link between obesity and insulin resistance', *Mol Aspects Med*, 33(1), pp. 26-34.
- Karpe, F., Steiner, G., Olivecrona, T., Carlson, L. A. and Hamsten, A. (1993) 'Metabolism of triglyceride-rich lipoproteins during alimentary lipemia', *J Clin Invest*, 91(3), pp. 748-58.
- Kawasaki, F., Matsuda, M., Kanda, Y., Inoue, H. and Kaku, K. (2005) 'Structural and functional analysis of pancreatic islets preserved by pioglitazone in db/db mice', *Am J Physiol Endocrinol Metab*, 288(3), pp. E510-8.
- Kechagias, S., Ernersson, A., Dahlqvist, O., Lundberg, P., Lindström, T., Nystrom, F. H. and Group, F. F. S. (2008) 'Fast-food-based hyper-alimentation can induce rapid and profound elevation of serum alanine aminotransferase in healthy subjects', *Gut*, 57(5), pp. 649-54.
- Kekwick, A. and Pawan, G. L. (1956) 'Calorie intake in relation to body-weight changes in the obese', *Lancet*, 271(6935), pp. 155-61.
- Kim, H., Mendez, R., Zheng, Z., Chang, L., Cai, J., Zhang, R. and Zhang, K. (2014) 'Liver-Enriched Transcription Factor CREBH Interacts With Peroxisome Proliferator-Activated Receptor alpha to Regulate Metabolic Hormone FGF21', *Endocrinology*, 155(3), pp. 769-82.
- Kim, H. S., Xiao, C., Wang, R. H., Lahusen, T., Xu, X., Vassilopoulos, A., Vazquez-Ortiz, G., Jeong, W. I., Park, O., Ki, S. H., Gao, B. and Deng, C. X. (2010) 'Hepatic-specific disruption of SIRT6 in mice results in fatty liver formation due to enhanced glycolysis and triglyceride synthesis', *Cell Metab*, 12(3), pp. 224-36.
- Kim, J. B., Sarraf, P., Wright, M., Yao, K. M., Mueller, E., Solanes, G., Lowell, B. B. and Spiegelman, B. M. (1998) 'Nutritional and insulin regulation of fatty acid synthetase and leptin gene expression through ADD1/SREBP1', *J Clin Invest*, 101(1), pp. 1-9.
- Kim, T. H., Choi, S. E., Ha, E. S., Jung, J. G., Han, S. J., Kim, H. J., Kim, D. J., Kang, Y. and Lee, K. W. (2011) 'IL-6 induction of TLR-4 gene expression via STAT3 has an effect on insulin resistance in human skeletal muscle', *Acta Diabetol*.
- King, A. J. (2012) 'The use of animal models in diabetes research', *Br J Pharmacol*, 166(3), pp. 877-94.
- Kneeman, J. M., Misdraji, J. and Corey, K. E. (2012) 'Secondary causes of nonalcoholic fatty liver disease', *Therap Adv Gastroenterol*, 5(3), pp. 199-207.
- Kooner, J. S., Baliga, R. R., Wilding, J., Crook, D., Packard, C. J., Banks, L. M., Peart, S., Aitman, T. J. and Scott, J. (1998) 'Abdominal obesity, impaired nonesterified fatty acid suppression, and insulin-mediated glucose disposal are early metabolic abnormalities in families with premature myocardial infarction', *Arterioscler Thromb Vasc Biol*, 18(7), pp. 1021-6.
- Kotronen, A. and Yki-Järvinen, H. (2008) 'Fatty liver: a novel component of the metabolic syndrome', *Arterioscler Thromb Vasc Biol*, 28(1), pp. 27-38.

- Kwiterovich, P. O. (2000) 'The metabolic pathways of high-density lipoprotein, low-density lipoprotein, and triglycerides: a current review', *Am J Cardiol*, 86(12A), pp. 5L-10L.
- Lee, C. H., Olson, P. and Evans, R. M. (2003) 'Minireview: lipid metabolism, metabolic diseases, and peroxisome proliferator-activated receptors', *Endocrinology*, 144(6), pp. 2201-7.
- Lee, J. Y., Sohn, K. H., Rhee, S. H. and Hwang, D. (2001) 'Saturated fatty acids, but not unsaturated fatty acids, induce the expression of cyclooxygenase-2 mediated through Toll-like receptor 4', *J Biol Chem*, 276(20), pp. 16683-9.
- Lenzen, S. (2008) 'The mechanisms of alloxan- and streptozotocin-induced diabetes', *Diabetologia*, 51(2), pp. 216-26.
- Lewis, G. F. and Steiner, G. (1996) 'Acute effects of insulin in the control of VLDL production in humans. Implications for the insulin-resistant state', *Diabetes Care*, 19(4), pp. 390-3.
- Li, H., Meng, Q., Xiao, F., Chen, S., Du, Y., Yu, J., Wang, C. and Guo, F. (2011) 'ATF4 deficiency protects mice from high-carbohydrate-diet-induced liver steatosis', *Biochem J*, 438(2), pp. 283-9.
- Li, Z. Z., Berk, M., McIntyre, T. M. and Feldstein, A. E. (2009) 'Hepatic lipid partitioning and liver damage in nonalcoholic fatty liver disease: role of stearyl-CoA desaturase', *J Biol Chem*, 284(9), pp. 5637-44.
- Liu, Q., Bengmark, S. and Qu, S. (2010) 'The role of hepatic fat accumulation in pathogenesis of non-alcoholic fatty liver disease (NAFLD)', *Lipids Health Dis*, 9, pp. 42.
- Loewen, C. J. and Levine, T. P. (2002) 'Cholesterol homeostasis: not until the SCAP lady INSIGs', *Curr Biol*, 12(22), pp. R779-81.
- Lumeng, C. N., Bodzin, J. L. and Saltiel, A. R. (2007a) 'Obesity induces a phenotypic switch in adipose tissue macrophage polarization', *J Clin Invest*, 117(1), pp. 175-84.
- Lumeng, C. N., DelProposto, J. B., Westcott, D. J. and Saltiel, A. R. (2008) 'Phenotypic switching of adipose tissue macrophages with obesity is generated by spatiotemporal differences in macrophage subtypes', *Diabetes*, 57(12), pp. 3239-46.
- Lumeng, C. N., Deyoung, S. M., Bodzin, J. L. and Saltiel, A. R. (2007b) 'Increased inflammatory properties of adipose tissue macrophages recruited during diet-induced obesity', *Diabetes*, 56(1), pp. 16-23.
- Luo, J., Quan, J., Tsai, J., Hobensack, C. K., Sullivan, C., Hector, R. and Reaven, G. M. (1998) 'Nongenetic mouse models of non-insulin-dependent diabetes mellitus', *Metabolism*, 47(6), pp. 663-8.
- Lutz, T. A. and Woods, S. C. (2012) 'Overview of animal models of obesity', *Curr Protoc Pharmacol*, Chapter 5, pp. Unit5.61.
- Magaña, M. M., Lin, S. S., Dooley, K. A. and Osborne, T. F. (1997) 'Sterol regulation of acetyl coenzyme A carboxylase promoter requires two interdependent binding sites for sterol regulatory element binding proteins', *J Lipid Res*, 38(8), pp. 1630-8.

- Mahley, R. W. and Ji, Z. S. (1999) 'Remnant lipoprotein metabolism: key pathways involving cell-surface heparan sulfate proteoglycans and apolipoprotein E', *J Lipid Res*, 40(1), pp. 1-16.
- Majithiya, J. B., Paramar, A. N. and Balaraman, R. (2005) 'Pioglitazone, a PPARgamma agonist, restores endothelial function in aorta of streptozotocin-induced diabetic rats', *Cardiovasc Res*, 66(1), pp. 150-61.
- Malhotra, A. (2013) 'Saturated fat is not the major issue', *Bmj*, 347, pp. f6340.
- Malmström, R., Packard, C. J., Caslake, M., Bedford, D., Stewart, P., Yki-Järvinen, H., Shepherd, J. and Taskinen, M. R. (1998) 'Effects of insulin and acipimox on VLDL1 and VLDL2 apolipoprotein B production in normal subjects', *Diabetes*, 47(5), pp. 779-87.
- Mann, J. and Truswell, A. S. (2007) *Essentials of human nutrition*. 3rd ed. edn. Oxford: Oxford University Press.
- Marchesini, G., Brizi, M., Bianchi, G., Tomassetti, S., Zoli, M. and Melchionda, N. (2001) 'Metformin in non-alcoholic steatohepatitis', *Lancet*, 358(9285), pp. 893-4.
- Margariti, E., Deutsch, M., Manolakopoulos, S. and Papatheodoridis, G. V. (2012) 'Non-alcoholic fatty liver disease may develop in individuals with normal body mass index', *Ann Gastroenterol*, 25(1), pp. 45-51.
- Maslova, E., Halldorsson, T. I., Astrup, A. and Olsen, S. F. (2015) 'Dietary protein-to-carbohydrate ratio and added sugar as determinants of excessive gestational weight gain: a prospective cohort study', *BMJ Open*, 5(2), pp. e005839.
- Matsuo, T., Iwashita, S., Komuro, M. and Suzuki, M. (1999) 'Effects of high-fat diet intake on glucose uptake in central and peripheral tissues of non-obese rats', *J Nutr Sci Vitaminol (Tokyo)*, 45(5), pp. 667-73.
- Matsuzaka, T. and Shimano, H. (2009) 'Elovl6: a new player in fatty acid metabolism and insulin sensitivity', *J Mol Med (Berl)*, 87(4), pp. 379-84.
- McMullen, M. R., Pritchard, M. T., Wang, Q., Millward, C. A., Croniger, C. M. and Nagy, L. E. (2005) 'Early growth response-1 transcription factor is essential for ethanol-induced fatty liver injury in mice', *Gastroenterology*, 128(7), pp. 2066-76.
- Meigs, J. B., Muller, D. C., Nathan, D. M., Blake, D. R., Andres, R. and Aging, B. L. S. o. (2003) 'The natural history of progression from normal glucose tolerance to type 2 diabetes in the Baltimore Longitudinal Study of Aging', *Diabetes*, 52(6), pp. 1475-84.
- Miles, J. M., Park, Y. S., Walewicz, D., Russell-Lopez, C., Windsor, S., Isley, W. L., Coppack, S. W. and Harris, W. S. (2004) 'Systemic and forearm triglyceride metabolism: fate of lipoprotein lipase-generated glycerol and free fatty acids', *Diabetes*, 53(3), pp. 521-7.
- Mitsuyoshi, H., Yasui, K., Harano, Y., Endo, M., Tsuji, K., Minami, M., Itoh, Y., Okanoue, T. and Yoshikawa, T. (2009) 'Analysis of hepatic genes involved in the metabolism of fatty acids and iron in nonalcoholic fatty liver disease', *Hepatol Res*, 39(4), pp. 366-73.
- Mobley, C., Marshall, T. A., Milgrom, P. and Coldwell, S. E. (2009) 'The contribution of dietary factors to dental caries and disparities in caries', *Acad Pediatr*, 9(6), pp. 410-4.

- Musso, G., Gambino, R., De Michieli, F., Cassader, M., Rizzetto, M., Durazzo, M., Fagà, E., Silli, B. and Pagano, G. (2003) 'Dietary habits and their relations to insulin resistance and postprandial lipemia in nonalcoholic steatohepatitis', *Hepatology*, 37(4), pp. 909-16.
- Nakamura, M. T., Yudell, B. E. and Loor, J. J. (2014) 'Regulation of energy metabolism by long-chain fatty acids', *Prog Lipid Res*, 53, pp. 124-44.
- Nassir, F. and Ibdah, J. A. (2014) 'Role of mitochondria in nonalcoholic fatty liver disease', *Int J Mol Sci*, 15(5), pp. 8713-42.
- Neuschwander-Tetri, B. A. and Caldwell, S. H. (2003) 'Nonalcoholic steatohepatitis: summary of an AASLD Single Topic Conference', *Hepatology*, 37(5), pp. 1202-19.
- Neve, B., Fernandez-Zapico, M. E., Ashkenazi-Katalan, V., Dina, C., Hamid, Y. H., Joly, E., Vaillant, E., Benmezroua, Y., Durand, E., Bakaher, N., Delannoy, V., Vaxillaire, M., Cook, T., Dallinga-Thie, G. M., Jansen, H., Charles, M. A., Clément, K., Galan, P., Hercberg, S., Helbecque, N., Charpentier, G., Prentki, M., Hansen, T., Pedersen, O., Urrutia, R., Melloul, D. and Froguel, P. (2005) 'Role of transcription factor KLF11 and its diabetes-associated gene variants in pancreatic beta cell function', *Proc Natl Acad Sci U S A*, 102(13), pp. 4807-12.
- Nguyen, M. T., Favellyukis, S., Nguyen, A. K., Reichart, D., Scott, P. A., Jenn, A., Liu-Bryan, R., Glass, C. K., Neels, J. G. and Olefsky, J. M. (2007) 'A subpopulation of macrophages infiltrates hypertrophic adipose tissue and is activated by free fatty acids via Toll-like receptors 2 and 4 and JNK-dependent pathways', *J Biol Chem*, 282(48), pp. 35279-92.
- Ning, J., Hong, T., Ward, A., Pi, J., Liu, Z., Liu, H. Y. and Cao, W. (2011) 'Constitutive role for IRE1alpha-XBP1 signaling pathway in the insulin-mediated hepatic lipogenic program', *Endocrinology*, 152(6), pp. 2247-55.
- Nordlie, R. C., Sukalski, K. A. and Johnson, W. T. (1993) 'Human microsomal glucose-6-phosphatase system', *Eur J Pediatr*, 152 Suppl 1, pp. S2-6.
- Novotny, D., Vaverkova, H., Karasek, D., Lukes, J., Slavik, L., Malina, P. and Orsag, J. (2014) 'Evaluation of total adiponectin, adipocyte fatty acid binding protein and fibroblast growth factor 21 levels in individuals with metabolic syndrome', *Physiol Res*.
- O'Fallon, J. V., Busboom, J. R., Nelson, M. L. and Gaskins, C. T. (2007) 'A direct method for fatty acid methyl ester synthesis: application to wet meat tissues, oils, and feedstuffs', *J Anim Sci*, 85(6), pp. 1511-21.
- Ochi, A., Mori, K., Emoto, M., Nakatani, S., Morioka, T., Motoyama, K., Fukumoto, S., Imanishi, Y., Koyama, H., Ishimura, E. and Inaba, M. (2014) 'Direct inhibitory effects of pioglitazone on hepatic fetuin-a expression', *PLoS One*, 9(2), pp. e88704.
- Olefsky, J. M. and Glass, C. K. (2010) 'Macrophages, inflammation, and insulin resistance', *Annu Rev Physiol*, 72, pp. 219-46.
- Orme, J. and Mohan, C. (2012) 'Macrophage subpopulations in systemic lupus erythematosus', *Discov Med*, 13(69), pp. 151-8.
- Oya, J., Nakagami, T., Sasaki, S., Jimba, S., Murakami, K., Kasahara, T., Wasada, T., Sekiguchi, H., Hasegawa, M., Endo, Y. and Iwamoto, Y. (2010) 'Intake of n-3 polyunsaturated fatty acids and non-alcoholic fatty liver disease: a cross-

- sectional study in Japanese men and women', *Eur J Clin Nutr*, 64(10), pp. 1179-85.
- Pachikian, B. D., Neyrinck, A. M., Cani, P. D., Portois, L., Deldicque, L., De Backer, F. C., Bindels, L. B., Sohet, F. M., Malaisse, W. J., Francaux, M., Carpentier, Y. A. and Delzenne, N. M. (2008) 'Hepatic steatosis in n-3 fatty acid depleted mice: focus on metabolic alterations related to tissue fatty acid composition', *BMC Physiol*, 8, pp. 21.
- Pang, C., Gao, Z., Yin, J., Zhang, J., Jia, W. and Ye, J. (2008) 'Macrophage infiltration into adipose tissue may promote angiogenesis for adipose tissue remodeling in obesity', *Am J Physiol Endocrinol Metab*, 295(2), pp. E313-22.
- Parks, E. J., Krauss, R. M., Christiansen, M. P., Neese, R. A. and Hellerstein, M. K. (1999) 'Effects of a low-fat, high-carbohydrate diet on VLDL-triglyceride assembly, production, and clearance', *J Clin Invest*, 104(8), pp. 1087-96.
- Parks, W. C. and Drake, R. L. (1982) 'Insulin mediates the stimulation of pyruvate kinase by a dual mechanism', *Biochem J*, 208(2), pp. 333-7.
- Patsouris, D., Li, P. P., Thapar, D., Chapman, J., Olefsky, J. M. and Neels, J. G. (2008) 'Ablation of CD11c-positive cells normalizes insulin sensitivity in obese insulin resistant animals', *Cell Metab*, 8(4), pp. 301-9.
- Pavlic, M., Xiao, C., Szeto, L., Patterson, B. W. and Lewis, G. F. (2010) 'Insulin acutely inhibits intestinal lipoprotein secretion in humans in part by suppressing plasma free fatty acids', *Diabetes*, 59(3), pp. 580-7.
- Pedersen, B. K. (2006) 'The anti-inflammatory effect of exercise: its role in diabetes and cardiovascular disease control', *Essays Biochem*, 42, pp. 105-17.
- Postic, C. and Girard, J. (2008) 'The role of the lipogenic pathway in the development of hepatic steatosis', *Diabetes Metab*, 34(6 Pt 2), pp. 643-8.
- Pot, G. K., Prynne, C. J., Roberts, C., Olson, A., Nicholson, S. K., Whitton, C., Teucher, B., Bates, B., Henderson, H., Pigott, S., Swan, G. and Stephen, A. M. (2012) 'National Diet and Nutrition Survey: fat and fatty acid intake from the first year of the rolling programme and comparison with previous surveys', *Br J Nutr*, 107(3), pp. 405-15.
- Pradhan, A. D., Manson, J. E., Rifai, N., Buring, J. E. and Ridker, P. M. (2001) 'C-reactive protein, interleukin 6, and risk of developing type 2 diabetes mellitus', *JAMA*, 286(3), pp. 327-34.
- Preiss-Landl, K., Zimmermann, R., Hämmerle, G. and Zechner, R. (2002) 'Lipoprotein lipase: the regulation of tissue specific expression and its role in lipid and energy metabolism', *Curr Opin Lipidol*, 13(5), pp. 471-81.
- Price, P. T., Nelson, C. M. and Clarke, S. D. (2000) 'Omega-3 polyunsaturated fatty acid regulation of gene expression', *Curr Opin Lipidol*, 11(1), pp. 3-7.
- Puri, P., Baillie, R. A., Wiest, M. M., Mirshahi, F., Choudhury, J., Cheung, O., Sargeant, C., Contos, M. J. and Sanyal, A. J. (2007) 'A lipidomic analysis of nonalcoholic fatty liver disease', *Hepatology*, 46(4), pp. 1081-90.
- Qin, W., Sundaram, M., Wang, Y., Zhou, H., Zhong, S., Chang, C. C., Manhas, S., Yao, E. F., Parks, R. J., McFie, P. J., Stone, S. J., Jiang, Z. G., Wang, C., Figeys, D., Jia, W. and Yao, Z. (2011) 'Missense mutation in APOC3 within the C-terminal lipid binding domain of human ApoC-III results in impaired assembly and secretion

- of triacylglycerol-rich very low density lipoproteins: evidence that ApoC-III plays a major role in the formation of lipid precursors within the microsomal lumen', *J Biol Chem*, 286(31), pp. 27769-80.
- Randle, P. J., Garland, P. B., Hales, C. N. and Newsholme, E. A. (1963) 'The glucose fatty-acid cycle. Its role in insulin sensitivity and the metabolic disturbances of diabetes mellitus', *Lancet*, 1(7285), pp. 785-9.
- Randle, P. J., Priestman, D. A., Mistry, S. C. and Halsall, A. (1994) 'Glucose fatty acid interactions and the regulation of glucose disposal', *J Cell Biochem*, 55 Suppl, pp. 1-11.
- Reaven, G. M., Chen, Y. D., Hollenbeck, C. B., Sheu, W. H., Ostrega, D. and Polonsky, K. S. (1993) 'Plasma insulin, C-peptide, and proinsulin concentrations in obese and nonobese individuals with varying degrees of glucose tolerance', *J Clin Endocrinol Metab*, 76(1), pp. 44-8.
- Reddy, J. K. and Rao, M. S. (2006) 'Lipid metabolism and liver inflammation. II. Fatty liver disease and fatty acid oxidation', *Am J Physiol Gastrointest Liver Physiol*, 290(5), pp. G852-8.
- Ricoult, S. J. and Manning, B. D. (2013) 'The multifaceted role of mTORC1 in the control of lipid metabolism', *EMBO Rep*, 14(3), pp. 242-51.
- Roheim, P. S. (1986) 'Atherosclerosis and lipoprotein metabolism: role of reverse cholesterol transport', *Am J Cardiol*, 57(5), pp. 3C-10C.
- Romijn, H. J., van Uum, J. F., Breedijk, I., Emmering, J., Radu, I. and Pool, C. W. (1999) 'Double immunolabeling of neuropeptides in the human hypothalamus as analyzed by confocal laser scanning fluorescence microscopy', *J Histochem Cytochem*, 47(2), pp. 229-36.
- Ryan, C. K., Johnson, L. A., Germin, B. I. and Marcos, A. (2002) 'One hundred consecutive hepatic biopsies in the workup of living donors for right lobe liver transplantation', *Liver Transpl*, 8(12), pp. 1114-22.
- Rydén, L., Standl, E., Bartnik, M., Van den Berghe, G., Betteridge, J., de Boer, M. J., Cosentino, F., Jönsson, B., Laakso, M., Malmberg, K., Priori, S., Ostergren, J., Tuomilehto, J., Thrainsdottir, I., Vanhorebeek, I., Stramba-Badiale, M., Lindgren, P., Qiao, Q., Priori, S. G., Blanc, J. J., Budaj, A., Camm, J., Dean, V., Deckers, J., Dickstein, K., Lekakis, J., McGregor, K., Metra, M., Morais, J., Osterspey, A., Tamargo, J., Zamorano, J. L., Deckers, J. W., Bertrand, M., Charbonnel, B., Erdmann, E., Ferrannini, E., Flyvbjerg, A., Gohlke, H., Juanatey, J. R., Graham, I., Monteiro, P. F., Parhofer, K., Pyörälä, K., Raz, I., Schernthaner, G., Volpe, M., Wood, D., (ESC), T. F. o. D. a. C. D. o. t. E. S. o. C. and (EASD), E. A. f. t. S. o. D. (2007) 'Guidelines on diabetes, pre-diabetes, and cardiovascular diseases: executive summary. The Task Force on Diabetes and Cardiovascular Diseases of the European Society of Cardiology (ESC) and of the European Association for the Study of Diabetes (EASD)', *Eur Heart J*, 28(1), pp. 88-136.
- Sachithanandan, N., Fam, B. C., Fynch, S., Dzamko, N., Watt, M. J., Wormald, S., Honeyman, J., Galic, S., Proietto, J., Andrikopoulos, S., Hevener, A. L., Kay, T. W. and Steinberg, G. R. (2010) 'Liver-specific suppressor of cytokine signaling-3 deletion in mice enhances hepatic insulin sensitivity and lipogenesis resulting in fatty liver and obesity', *Hepatology*, 52(5), pp. 1632-42.
- Saini, K. S., Thompson, C., Winterford, C. M., Walker, N. I. and Cameron, D. P. (1996) 'Streptozotocin at low doses induces apoptosis and at high doses causes

- necrosis in a murine pancreatic beta cell line, INS-1', *Biochem Mol Biol Int*, 39(6), pp. 1229-36.
- Sajan, M. P., Standaert, M. L., Miura, A., Kahn, C. R. and Farese, R. V. (2004) 'Tissue-specific differences in activation of atypical protein kinase C and protein kinase B in muscle, liver, and adipocytes of insulin receptor substrate-1 knockout mice', *Mol Endocrinol*, 18(10), pp. 2513-21.
- Saltiel, A. R. and Kahn, C. R. (2001) 'Insulin signalling and the regulation of glucose and lipid metabolism', *Nature*, 414(6865), pp. 799-806.
- Samuel, V. T., Liu, Z. X., Qu, X., Elder, B. D., Bilz, S., Befroy, D., Romanelli, A. J. and Shulman, G. I. (2004) 'Mechanism of hepatic insulin resistance in non-alcoholic fatty liver disease', *J Biol Chem*, 279(31), pp. 32345-53.
- Samuel, V. T., Liu, Z. X., Wang, A., Beddow, S. A., Geisler, J. G., Kahn, M., Zhang, X. M., Monia, B. P., Bhanot, S. and Shulman, G. I. (2007) 'Inhibition of protein kinase Cepsilon prevents hepatic insulin resistance in nonalcoholic fatty liver disease', *J Clin Invest*, 117(3), pp. 739-45.
- Schenk, S., Saberi, M. and Olefsky, J. M. (2008) 'Insulin sensitivity: modulation by nutrients and inflammation', *J Clin Invest*, 118(9), pp. 2992-3002.
- Schmittgen, T. D. and Livak, K. J. (2008) 'Analyzing real-time PCR data by the comparative CT method', *Nat. Protocols*, 3(6), pp. 1101-1108.
- Schnell, S. A., Staines, W. A. and Wessendorf, M. W. (1999) 'Reduction of lipofuscin-like autofluorescence in fluorescently labeled tissue', *J Histochem Cytochem*, 47(6), pp. 719-30.
- Schweiger, M., Schreiber, R., Haemmerle, G., Lass, A., Fledelius, C., Jacobsen, P., Tornqvist, H., Zechner, R. and Zimmermann, R. (2006) 'Adipose triglyceride lipase and hormone-sensitive lipase are the major enzymes in adipose tissue triacylglycerol catabolism', *J Biol Chem*, 281(52), pp. 40236-41.
- Schäffler, A., Schölmerich, J. and Büchler, C. (2005) 'Mechanisms of disease: adipocytokines and visceral adipose tissue--emerging role in nonalcoholic fatty liver disease', *Nat Clin Pract Gastroenterol Hepatol*, 2(6), pp. 273-80.
- Sebastian, S., Horton, J. D. and Wilson, J. E. (2000) 'Anabolic function of the type II isozyme of hexokinase in hepatic lipid synthesis', *Biochem Biophys Res Commun*, 270(3), pp. 886-91.
- Sheth, S. G., Gordon, F. D. and Chopra, S. (1997) 'Nonalcoholic steatohepatitis', *Ann Intern Med*, 126(2), pp. 137-45.
- Shimomura, I., Bashmakov, Y., Ikemoto, S., Horton, J. D., Brown, M. S. and Goldstein, J. L. (1999) 'Insulin selectively increases SREBP-1c mRNA in the livers of rats with streptozotocin-induced diabetes', *Proc Natl Acad Sci U S A*, 96(24), pp. 13656-61.
- Shoelson, S. E., Herrero, L. and Naaz, A. (2007) 'Obesity, inflammation, and insulin resistance', *Gastroenterology*, 132(6), pp. 2169-80.
- Sibrowski, W., Staegemann, U. and Seitz, H. J. (1982) 'Accelerated turnover of hepatic glucokinase in starved and streptozotocin-diabetic rat', *Eur J Biochem*, 127(3), pp. 571-4.
- Sips, F. L., Tiemann, C. A., Oosterveer, M. H., Groen, A. K., Hilbers, P. A. and van Riel, N. A. (2014) 'A computational model for the analysis of lipoprotein

- distributions in the mouse: translating FPLC profiles to lipoprotein metabolism', *PLoS Comput Biol*, 10(5), pp. e1003579.
- Song, R., Wang, X., Mao, Y., Li, H., Li, Z., Xu, W., Wang, R., Guo, T., Jin, L., Zhang, X., Zhang, Y., Zhou, N., Hu, R., Jia, J., Lei, Z., Irwin, D. M., Niu, G. and Tan, H. (2013) 'Resistin disrupts glycogen synthesis under high insulin and high glucose levels by down-regulating the hepatic levels of GSK3beta', *Gene*, 529(1), pp. 50-6.
- Soni, K. G., Lehner, R., Metalnikov, P., O'Donnell, P., Semache, M., Gao, W., Ashman, K., Pshezhetsky, A. V. and Mitchell, G. A. (2004) 'Carboxylesterase 3 (EC 3.1.1.1) is a major adipocyte lipase', *J Biol Chem*, 279(39), pp. 40683-9.
- Sparks, J. D. and Sparks, C. E. (1994) 'Insulin regulation of triacylglycerol-rich lipoprotein synthesis and secretion', *Biochim Biophys Acta*, 1215(1-2), pp. 9-32.
- Srinivasan, K., Viswanad, B., Asrat, L., Kaul, C. L. and Ramarao, P. (2005) 'Combination of high-fat diet-fed and low-dose streptozotocin-treated rat: a model for type 2 diabetes and pharmacological screening', *Pharmacol Res*, 52(4), pp. 313-20.
- Stanton, M. C., Chen, S. C., Jackson, J. V., Rojas-Triana, A., Kinsley, D., Cui, L., Fine, J. S., Greenfeder, S., Bober, L. A. and Jenh, C. H. (2011) 'Inflammatory Signals shift from adipose to liver during high fat feeding and influence the development of steatohepatitis in mice', *J Inflamm (Lond)*, 8, pp. 8.
- Strandberg, L., Lorentzon, M., Hellqvist, A., Nilsson, S., Wallenius, V., Ohlsson, C. and Jansson, J. O. (2006) 'Interleukin-1 system gene polymorphisms are associated with fat mass in young men', *J Clin Endocrinol Metab*, 91(7), pp. 2749-54.
- Stubbs, C. D. and Smith, A. D. (1984) 'The modification of mammalian membrane polyunsaturated fatty acid composition in relation to membrane fluidity and function', *Biochim Biophys Acta*, 779(1), pp. 89-137.
- Sullivan, S. (2010) 'Implications of diet on nonalcoholic fatty liver disease', *Curr Opin Gastroenterol*, 26(2), pp. 160-4.
- Sun, X., Han, R., Wang, Z. and Chen, Y. (2006) 'Regulation of adiponectin receptors in hepatocytes by the peroxisome proliferator-activated receptor-gamma agonist rosiglitazone', *Diabetologia*, 49(6), pp. 1303-10.
- Sun, Z., Gong, J., Wu, H., Xu, W., Wu, L., Xu, D., Gao, J., Wu, J. W., Yang, H., Yang, M. and Li, P. (2013) 'Perilipin1 promotes unilocular lipid droplet formation through the activation of Fsp27 in adipocytes', *Nat Commun*, 4, pp. 1594.
- Surmi, B. K. and Hasty, A. H. (2008) 'Macrophage infiltration into adipose tissue: initiation, propagation and remodeling', *Future Lipidol*, 3(5), pp. 545-556.
- Svegliati-Baroni, G., Candelaresi, C., Saccomanno, S., Ferretti, G., Bachetti, T., Marzioni, M., De Minicis, S., Nobili, L., Salzano, R., Omenetti, A., Pacetti, D., Sigmund, S., Benedetti, A. and Casini, A. (2006) 'A model of insulin resistance and nonalcoholic steatohepatitis in rats: role of peroxisome proliferator-activated receptor-alpha and n-3 polyunsaturated fatty acid treatment on liver injury', *Am J Pathol*, 169(3), pp. 846-60.
- Swan, G. (2004) 'Findings from the latest National Diet and Nutrition Survey', *Proc Nutr Soc*, 63(4), pp. 505-12.
- Szczepaniak, L. S., Nurenberg, P., Leonard, D., Browning, J. D., Reingold, J. S., Grundy, S., Hobbs, H. H. and Dobbins, R. L. (2005) 'Magnetic resonance spectroscopy

- to measure hepatic triglyceride content: prevalence of hepatic steatosis in the general population', *Am J Physiol Endocrinol Metab*, 288(2), pp. E462-8.
- Szkudelski, T. (2001) 'The mechanism of alloxan and streptozotocin action in B cells of the rat pancreas', *Physiol Res*, 50(6), pp. 537-46.
- Tabor, D. E., Kim, J. B., Spiegelman, B. M. and Edwards, P. A. (1999) 'Identification of conserved cis-elements and transcription factors required for sterol-regulated transcription of stearoyl-CoA desaturase 1 and 2', *J Biol Chem*, 274(29), pp. 20603-10.
- Tam, C. S., Sparks, L. M., Johannsen, D. L., Covington, J. D., Church, T. S. and Ravussin, E. (2012) 'Low Macrophage Accumulation in Skeletal Muscle of Obese Type 2 Diabetics and Elderly Subjects', *Obesity (Silver Spring)*.
- Taniguchi, A., Fukushima, M., Sakai, M., Miwa, K., Makita, T., Nagata, I., Nagasaka, S., Doi, K., Okumura, T., Fukuda, A., Kishimoto, H., Fukuda, T., Nakaishi, S., Tokuyama, K. and Nakai, Y. (2000) 'Remnant-like particle cholesterol, triglycerides, and insulin resistance in nonobese Japanese type 2 diabetic patients', *Diabetes Care*, 23(12), pp. 1766-9.
- Taniguchi, C. M., Ueki, K. and Kahn, R. (2005) 'Complementary roles of IRS-1 and IRS-2 in the hepatic regulation of metabolism', *J Clin Invest*, 115(3), pp. 718-27.
- Tilg, H. and Hotamisligil, G. S. (2006) 'Nonalcoholic fatty liver disease: Cytokine-adipokine interplay and regulation of insulin resistance', *Gastroenterology*, 131(3), pp. 934-45.
- Tirone, T. A. and Brunicaardi, F. C. (2001) 'Overview of glucose regulation', *World J Surg*, 25(4), pp. 461-7.
- Towle, H. C. (2001) 'Glucose and cAMP: adversaries in the regulation of hepatic gene expression', *Proc Natl Acad Sci U S A*, 98(24), pp. 13476-8.
- Trayhurn, P. and Wood, I. S. (2004) 'Adipokines: inflammation and the pleiotropic role of white adipose tissue', *Br J Nutr*, 92(3), pp. 347-55.
- Tsou, C. L., Peters, W., Si, Y., Slaymaker, S., Aslanian, A. M., Weisberg, S. P., Mack, M. and Charo, I. F. (2007) 'Critical roles for CCR2 and MCP-3 in monocyte mobilization from bone marrow and recruitment to inflammatory sites', *J Clin Invest*, 117(4), pp. 902-9.
- Tsukumo, D. M., Carvalho-Filho, M. A., Carvalheira, J. B., Prada, P. O., Hirabara, S. M., Schenka, A. A., Araujo, E. P., Vassallo, J., Curi, R., Velloso, L. A. and Saad, M. J. (2007) 'Loss-of-function mutation in Toll-like receptor 4 prevents diet-induced obesity and insulin resistance', *Diabetes*, 56(8), pp. 1986-98.
- Ueki, K. and Kadowaki, T. (2011) 'The other sweet face of XBP-1', *Nat Med: Vol. 3. United States*, pp. 246-8.
- Valenti, L., Rametta, R., Dongiovanni, P., Maggioni, M., Fracanzani, A. L., Zappa, M., Lattuada, E., Roviato, G. and Fargion, S. (2008) 'Increased expression and activity of the transcription factor FOXO1 in nonalcoholic steatohepatitis', *Diabetes*, 57(5), pp. 1355-62.
- van Greevenbroek, M. M. and de Bruin, T. W. (1998) 'Chylomicron synthesis by intestinal cells in vitro and in vivo', *Atherosclerosis*, 141 Suppl 1, pp. S9-16.
- Varma, V., Yao-Borengasser, A., Rasouli, N., Nolen, G. T., Phanavanh, B., Starks, T., Gurley, C., Simpson, P., McGehee, R. E., Jr., Kern, P. A. and Peterson, C. A.

- (2009) 'Muscle inflammatory response and insulin resistance: synergistic interaction between macrophages and fatty acids leads to impaired insulin action', *Am J Physiol Endocrinol Metab*, 296(6), pp. E1300-10.
- Verdelho Machado, M. and Cortez-Pinto, H. (2012) 'Fatty liver in lean patients: is it a different disease?', *Ann Gastroenterol*, 25(1), pp. 1-2.
- Volk, B. M., Kunces, L. J., Freidenreich, D. J., Kupchak, B. R., Saenz, C., Artistizabal, J. C., Fernandez, M. L., Bruno, R. S., Maresh, C. M., Kraemer, W. J., Phinney, S. D. and Volek, J. S. (2014) 'Effects of step-wise increases in dietary carbohydrate on circulating saturated Fatty acids and palmitoleic Acid in adults with metabolic syndrome', *PLoS One*, 9(11), pp. e113605.
- Wang, D., Wei, Y. and Pagliassotti, M. J. (2006) 'Saturated fatty acids promote endoplasmic reticulum stress and liver injury in rats with hepatic steatosis', *Endocrinology*, 147(2), pp. 943-51.
- Wang, H. and Eckel, R. H. (2009) 'Lipoprotein lipase: from gene to obesity', *Am J Physiol Endocrinol Metab*, 297(2), pp. E271-88.
- Wang, H., Zhang, H., Jia, Y., Zhang, Z., Craig, R., Wang, X. and Elbein, S. C. (2004) 'Adiponectin receptor 1 gene (ADIPOR1) as a candidate for type 2 diabetes and insulin resistance', *Diabetes*, 53(8), pp. 2132-6.
- Wang, X., Cao, Y., Fu, Y., Guo, G. and Zhang, X. (2011) 'Liver fatty acid composition in mice with or without nonalcoholic fatty liver disease', *Lipids Health Dis*, 10, pp. 234.
- Waugh, J., Keating, G. M., Plosker, G. L., Easthope, S. and Robinson, D. M. (2006) 'Pioglitazone: a review of its use in type 2 diabetes mellitus', *Drugs*, 66(1), pp. 85-109.
- Wei, Y., Wang, D. and Pagliassotti, M. J. (2007) 'Saturated fatty acid-mediated endoplasmic reticulum stress and apoptosis are augmented by trans-10, cis-12-conjugated linoleic acid in liver cells', *Mol Cell Biochem*, 303(1-2), pp. 105-13.
- Wei, Y., Wang, D., Topczewski, F. and Pagliassotti, M. J. (2006) 'Saturated fatty acids induce endoplasmic reticulum stress and apoptosis independently of ceramide in liver cells', *Am J Physiol Endocrinol Metab*, 291(2), pp. E275-81.
- Weisberg, S. P., McCann, D., Desai, M., Rosenbaum, M., Leibel, R. L. and Ferrante, A. W. (2003) 'Obesity is associated with macrophage accumulation in adipose tissue', *J Clin Invest*, 112(12), pp. 1796-808.
- Wentworth, J. M., Naselli, G., Brown, W. A., Doyle, L., Phipson, B., Smyth, G. K., Wabitsch, M., O'Brien, P. E. and Harrison, L. C. (2010) 'Pro-inflammatory CD11c+CD206+ adipose tissue macrophages are associated with insulin resistance in human obesity', *Diabetes*, 59(7), pp. 1648-56.
- Westerbacka, J., Kolak, M., Kiviluoto, T., Arkkila, P., Siren, J., Hamsten, A., Fisher, R. M. and Yki-Jarvinen, H. (2007) 'Genes involved in fatty acid partitioning and binding, lipolysis, monocyte/macrophage recruitment, and inflammation are overexpressed in the human fatty liver of insulin-resistant subjects', *Diabetes*, 56(11), pp. 2759-65.
- Westerbacka, J., Lammi, K., Häkkinen, A. M., Rissanen, A., Salminen, I., Aro, A. and Yki-Järvinen, H. (2005) 'Dietary fat content modifies liver fat in overweight nondiabetic subjects', *J Clin Endocrinol Metab*, 90(5), pp. 2804-9.

- Wolfe, R. R. (1998) 'Metabolic interactions between glucose and fatty acids in humans', *Am J Clin Nutr*, 67(3 Suppl), pp. 519S-526S.
- Wolfum, C., Asilmaz, E., Luca, E., Friedman, J. M. and Stoffel, M. (2004) 'Foxa2 regulates lipid metabolism and ketogenesis in the liver during fasting and in diabetes', *Nature*, 432(7020), pp. 1027-32.
- Wu, X., Tong, Y., Shankar, K., Baumgardner, J. N., Kang, J., Badeaux, J., Badger, T. M. and Ronis, M. J. (2011) 'Lipid fatty acid profile analyses in liver and serum in rats with nonalcoholic steatohepatitis using improved gas chromatography-mass spectrometry methodology', *J Agric Food Chem*, 59(2), pp. 747-54.
- Wulan, S., Schrauwen-Hinderling, V., Westerterp, K. and Plasqui, G. (2015) 'Liver fat accumulation in response to overfeeding with a high-fat diet: a comparison between South Asian and Caucasian men', *Nutrition & Metabolism*, 12(1), pp. 18.
- Xiao, G., Zhang, T., Yu, S., Lee, S., Calabuig-Navarro, V., Yamauchi, J., Ringquist, S. and Dong, H. H. (2013) 'ATF4 protein deficiency protects against high fructose-induced hypertriglyceridemia in mice', *J Biol Chem*, 288(35), pp. 25350-61.
- Xu, H., Barnes, G. T., Yang, Q., Tan, G., Yang, D., Chou, C. J., Sole, J., Nichols, A., Ross, J. S., Tartaglia, L. A. and Chen, H. (2003) 'Chronic inflammation in fat plays a crucial role in the development of obesity-related insulin resistance', *J Clin Invest*, 112(12), pp. 1821-30.
- Xu, H. E., Lambert, M. H., Montana, V. G., Parks, D. J., Blanchard, S. G., Brown, P. J., Sternbach, D. D., Lehmann, J. M., Wisely, G. B., Willson, T. M., Kliewer, S. A. and Milburn, M. V. (1999) 'Molecular recognition of fatty acids by peroxisome proliferator-activated receptors', *Mol Cell*, 3(3), pp. 397-403.
- Xu, J., Lloyd, D. J., Hale, C., Stanislaus, S., Chen, M., Sivits, G., Vonderfecht, S., Hecht, R., Li, Y. S., Lindberg, R. A., Chen, J. L., Jung, D. Y., Zhang, Z., Ko, H. J., Kim, J. K. and Véniant, M. M. (2009) 'Fibroblast growth factor 21 reverses hepatic steatosis, increases energy expenditure, and improves insulin sensitivity in diet-induced obese mice', *Diabetes*, 58(1), pp. 250-9.
- Yang, R. Z., Lee, M. J., Hu, H., Pollin, T. I., Ryan, A. S., Nicklas, B. J., Snitker, S., Horenstein, R. B., Hull, K., Goldberg, N. H., Goldberg, A. P., Shuldiner, A. R., Fried, S. K. and Gong, D. W. (2006) 'Acute-phase serum amyloid A: an inflammatory adipokine and potential link between obesity and its metabolic complications', *PLoS Med*, 3(6), pp. e287.
- Ye, J., Gao, Z., Yin, J. and He, Q. (2007) 'Hypoxia is a potential risk factor for chronic inflammation and adiponectin reduction in adipose tissue of ob/ob and dietary obese mice', *Am J Physiol Endocrinol Metab*, 293(4), pp. E1118-28.
- Younossi, Z. M., Gorreta, F., Ong, J. P., Schlauch, K., Del Giacco, L., Elariny, H., Van Meter, A., Younoszai, A., Goodman, Z., Baranova, A., Christensen, A., Grant, G. and Chandhoke, V. (2005) 'Hepatic gene expression in patients with obesity-related non-alcoholic steatohepatitis', *Liver Int*, 25(4), pp. 760-71.
- Younossi, Z. M., Stepanova, M., Negro, F., Hallaji, S., Younossi, Y., Lam, B. and Srishord, M. (2012) 'Nonalcoholic fatty liver disease in lean individuals in the United States', *Medicine (Baltimore)*, 91(6), pp. 319-27.
- Zhang, D., Christianson, J., Liu, Z. X., Tian, L., Choi, C. S., Neschen, S., Dong, J., Wood, P. A. and Shulman, G. I. (2010) 'Resistance to high-fat diet-induced obesity and

- insulin resistance in mice with very long-chain acyl-CoA dehydrogenase deficiency', *Cell Metab*, 11(5), pp. 402-11.
- Zhang, D., Liu, Z. X., Choi, C. S., Tian, L., Kibbey, R., Dong, J., Cline, G. W., Wood, P. A. and Shulman, G. I. (2007) 'Mitochondrial dysfunction due to long-chain Acyl-CoA dehydrogenase deficiency causes hepatic steatosis and hepatic insulin resistance', *Proc Natl Acad Sci U S A*, 104(43), pp. 17075-80.
- Zhang, H., Chen, Q., Yang, M., Zhu, B., Cui, Y., Xue, Y., Gong, N., Cui, A., Wang, M., Shen, L., Zhang, S., Fang, F. and Chang, Y. (2013) 'Mouse KLF11 regulates hepatic lipid metabolism', *J Hepatol*, 58(4), pp. 763-70.
- Zhang, M., Lv, X. Y., Li, J., Xu, Z. G. and Chen, L. (2008) 'The characterization of high-fat diet and multiple low-dose streptozotocin induced type 2 diabetes rat model', *Exp Diabetes Res*, 2008, pp. 704045.

# Appendix

The appendix includes a summary of the raw data that was presented in this thesis along with some additional figures as a supplementation to the results. The data is divided in to the chapters that it was presented in.

## List of Tables

<b>CHAPTER II</b>	
Table 1   animals' biometrics raw data	1
<b>CHAPTER III</b>	
Table 2   Adipocytes sizing	4
Table 3   Adipose immunohistochemistry raw data	4
Table 4   Adipose tissue inflammatory gene expression - normalized to GAPDH	5
Table 5   Muscle TaqMan Gene expression Raw Data.	6
Table 6   Liver Western Blots Normalized Densitometry Raw Data.	6
<b>CHAPTER IV</b>	
Table 7   SREBP-1C TaqMan Gene expression Raw Data	8
Table 8   Liver Tissue TaqMan Gene Array Data Summary	8
Table 9   CHOP Western Blot Normalized Raw Data	12
Table 10   Liver Triglyceride Content Raw Data	12
Table 11   Skeletal Muscle Tissue TaqMan Gene Array Data Summary	13
Table 12   Skeletal muscle Total Triglycerides content ( $\mu\text{g/ml}$ ) raw data	15
<b>CHAPTER V</b>	
Table 13   Chapter 6 Animals Biometric and Triglycerides Raw Data	16
Table 14   Chapter 6 Animals Plasma GC analysis	16

## List of Figures

<b>CHAPTER II</b>	
Figure 1   Proteins separated using SDS-PAGE then stained with coomassie blue.	3
Figure 2   Agilent analysis to assess total RNA purity and integrity	3
<b>CHAPTER III</b>	
Figure 3   Adipocytes sizing using Image J.	4
Figure 4   Skeletal Muscle Immunohistochemistry.	5
<b>CHAPTER IV</b>	
Figure 5   HFD, STZ and Pioglitazone effect on adipose, liver and skeletal muscle SREBP-1C mRNA expression level	8
Figure 6   Thin Layer Chromatography of Total Lipids Extracted from the Liver Samples.	12
<b>CHAPTER V</b>	
Figure 7   Thin Layer Chromatography of Total Lipids Extracted from Plasma lipoprotein Samples.	16

## 8.1 Chapter II

**Table 1 | animals' biometrics raw data**

Animal Group	Insulin(ng/ml)		Glucose(mM)			Weight (g)			Average Food Intake (kcal)		Average Food Intake (g)		
	Day18	Day49	Day18	Day 49	Day 21	Day0	Day21	Day49					
NC	A 5	1.32	3.53	6.23	5.49	221	424	486	527	88.20	± 11.74	28.74	± 3.79
	A 9	1.25	0.18	6.40	6.13	212	427	513	601	91.89	± 15.00	30.15	± 4.84
	A 13	1.49	2.58	7.10	6.51	243	455	533	609	101.52	± 11.00	33.48	± 3.55
	A 18	1.40	1.67	7.94	6.19	184	418	520	608	89.77	± 13.54	29.98	± 4.37
	A 22	1.88	1.71	7.24	5.95	180	424	562	638	96.47	± 14.71	32.36	± 4.75
HFD	B 8	2.84	2.75	7.15	7.90	231	454	569	664	102.58	± 14.53	20.12	± 2.77
	B 10	0.84	1.55	8.01	7.21	219	474	585	680	120.52	± 20.27	23.68	± 3.87
	B 16	2.03	2.02	7.39	7.45	214	400	480	548	89.31	± 17.41	18.12	± 3.32
	B 20	2.55	3.03	7.24	6.72	205	536	686	810	125.69	± 15.85	25.34	± 3.02
	B 26	3.13	4.45	7.55	7.80	175	375	471	568	89.38	± 10.17	18.81	± 1.94
HFD/STZ	D 4	0.31	0.22	20.33	19.96	207	432	464	487	104.01	± 12.45	20.12	± 2.37
	D 6	0.23	5.64	18.55	20.18	202	486	461	495	122.96	± 21.38	23.87	± 4.08
	D 17	0.62	0.33	21.66	21.73	242	458	434	453	101.47	± 14.27	20.51	± 2.72
	D 12	0.35	0.18	19.43	18.65	198	462	493	574	124.44	± 31.15	24.56	± 5.94
	D 19	0.73	0.40	20.40	20.15	183	459	508	587	120.30	± 28.77	24.24	± 5.49
	D 23	1.16	0.17	22.11	21.81	178	439	384	447	106.59	± 13.39	21.89	± 2.55
HFD/STZ + pio	C 3	0.35	0.33	27.07	21.30	215	405	443	480	106.80	± 12.47	19.88	± 3.02
	C 11	0.23		20.18		227	450	397	407	103.75	± 15.82	20.21	± 2.93
	C 15	0.69	0.33	21.91	19.16	221	488	415	412	102.32	± 15.34	21.47	± 4.90
	C 21	0.26	0.26	19.54	19.51	225	406	401	439	107.70	± 25.65	20.93	± 2.93
	C 25	0.43	0.79	20.62	21.89	205	464	491	532	102.60	± 15.38	23.11	± 3.25
	C 24	0.27	0.55	22.22	22.16	176	372	367	376	112.16	± 17.04	19.95	± 3.31

## 8.2 Chapter III

### 8.2.1 Materials and methods

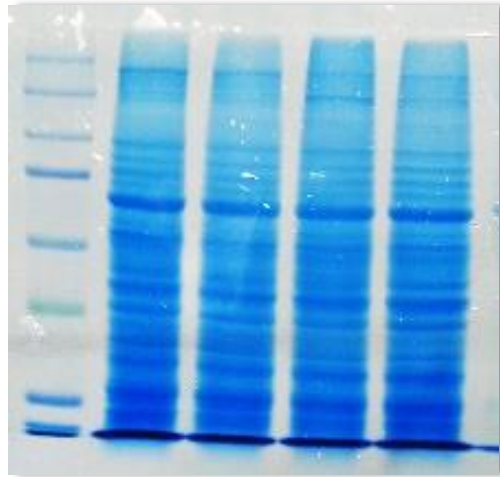


Figure 1 | Proteins separated using SDS-PAGE then stained with coomassie blue.

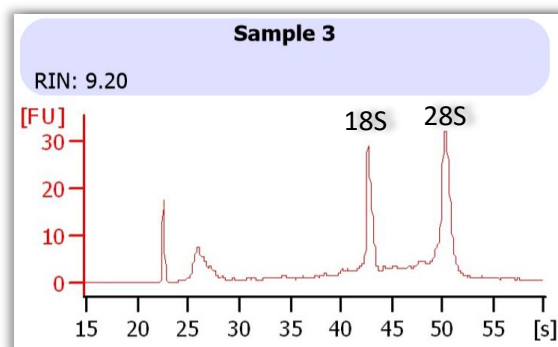
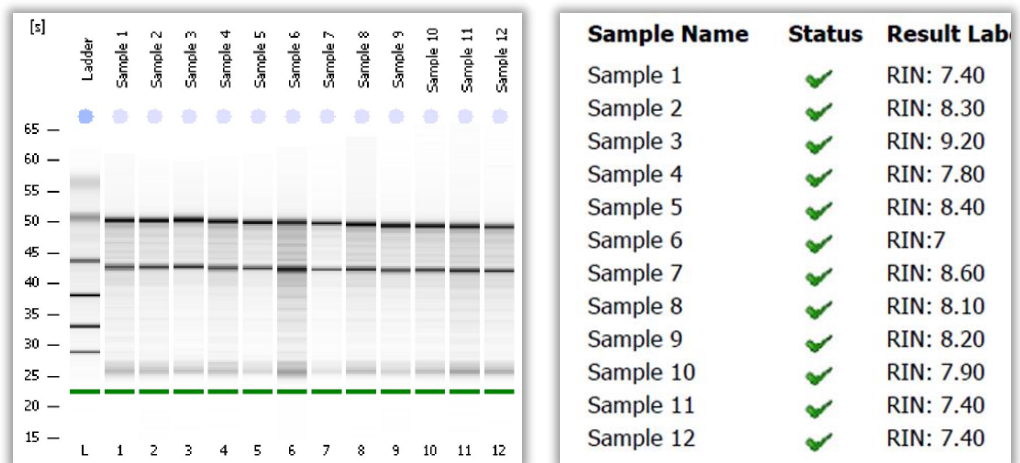


Figure 2 | Agilent analysis to assess total RNA purity and integrity

## 8.2.2 Adipose Tissue raw data

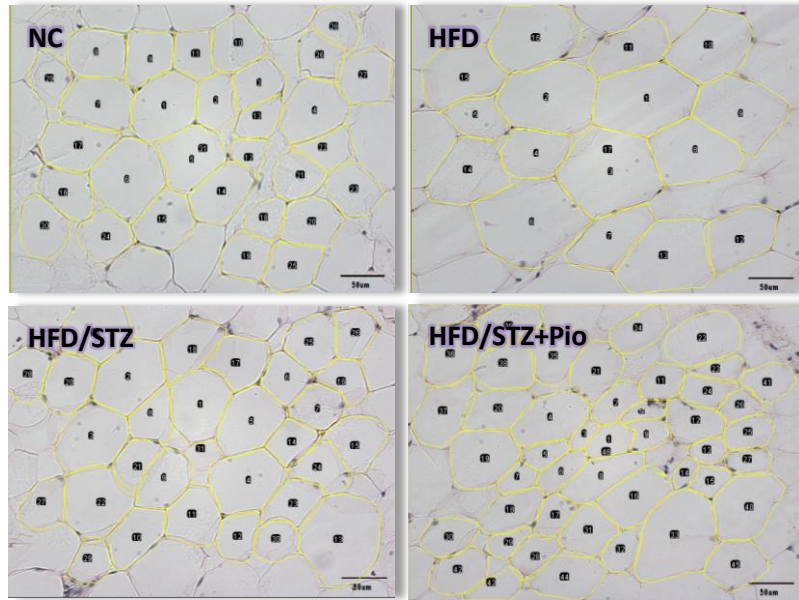


Figure 3 | Adipocytes sizing using Image J.

Table 2 | Adipocytes sizing

	NC	HFD	HFD/STZ	HFD/STZ+pio
Average	3.500734	4.249986	2.049902	2.920662
STD	1.363534	2.202629	0.985282	1.187701
Cell number	157	132	340	220
N number	5	5	6	6

Table 3 | Adipose immunohistochemistry raw data

		CD86	CD163	CD86/163	CD206
NC	A 5	39.6±16.61	33.02±12.92	17.23±11.11	17.00±7.07
	A 9	31.68±11.42	28.49±10.52	16.93±6.146	22.54±4.88
	A 13	26.93±8.499	25.28±9.72	11.51±6.369	29.83±9.44
	A 18	44.16±19.83	28.38±13.43	15.54±7.328	33.58±9.75
	A 22	34.22±13.32	27.84±14.9	14.54±8.52	30.58±11.94
HFD	B 8	44.08±10.03	33.42±10.32	19.44±9.89	14.68±5.90
	B 10	55.98±7.983	32.9±11.75	17.47±8.988	44.25±10.41
	B 16	34.82±10.4	25.57±9.778	13.69±6.48	32.17±10.67
	B 20	35.97±11.33	32.15±11.43	15.18±12.07	35.07±16.17
	B 26	45.32±15.59	27.11±11.57	16.88±9.625	32.95±11.87
HFD/STZ	D 4	43.03±15.8	32.69±15.23	17.37±10.51	23.85±9.12
	D 6	41.33±11.74	28.72±12.09	16.72±8.955	12.11±3.09
	D 17	50.3±10.27	29.36±8.016	13.15±6.564	25.78±9.11
	D 12	39.39±8.721	27.79±9.176	16.75±7.189	38.85±15.21
	D 19	48.45±14.46	42.06±15.02	26.76±14.45	26.01±7.16
D 23	50.47±14.05	36.68±16.82	24.21±12.16	23.34±6.78	
HFD/STZ + pio	C 3	49.25±12.53	36.2±9.773	15.44±8.513	16.18±9.47
	C 11	51.95±11.45	38.15±11.72	14.51±7.502	23.49±4.80
	C 15	44.13±12.28	35.64±15.5	22.14±13.92	28.46±10.81
	C 21	36.99±12.78	37.65±11.75	20.03±11.33	33.08±13.08
	C 25	40.92±12.8	33.42±13.77	14.5±5.576	27.77±9.80
	C 24	48.22±10.15	42.19±13.87	22.48±7.242	20.67±7.63

**Table 4 | Adipose tissue inflammatory gene expression - normalized to GAPDH**

GENE		GAPDAH	IL-6	TNF- $\alpha$	IL-1 $\beta$	IL 10
Slope		-3.5284	-3.3237	-3.4427	-3.7227	-3.6573
Intercept		31.3066	27.5822	30.5885	31.1109	34.5959
R2		-0.9909	-0.9966	-0.9912	-0.9849	-0.9670
NC	A 5	0.0868	0.6836	0.2403	1.7460	3.6141
	A 9	0.1771	0.2481	0.0395	0.9382	1.8589
	A 13	0.2098	0.4285	0.0928	1.2212	0.7407
	A 18	0.4479	0.0651	0.1018	1.7632	0.6146
	A 22	0.2614	0.1980	0.0692	1.4252	2.0707
HFD	B 8	0.2604	0.1652	0.1297	0.8329	1.4768
	B 10	0.3350	1.5977	0.0567	1.2363	0.6251
	B 16	0.1648	0.5131	0.2094	1.7749	2.0892
	B 20	0.2735	0.0856	0.0095	1.4106	1.0076
	B 26	0.3270	0.2880	0.0066	1.6041	1.1148
HFD/STZ +Pio	C 3	0.2720	1.7993	0.1555	1.6419	4.8236
	C 11	0.2252	1.7251	0.0037	0.9323	1.7576
	C 15	0.5115	1.1457	0.0012	0.9323	0.1953
	C 21	0.2149	2.1974	0.0427	1.0519	2.2338
	C 24	0.1776	0.3483	0.0356	1.5867	1.8126
	C 25	0.2376	2.4347	0.0901	2.1236	1.2730
HFD/STZ	D 4	0.1893	0.5843	0.1081	1.1962	1.2601
	D 6	0.2556	2.4729	0.0075	1.5599	2.8976
	D 12	0.3006	1.4258	0.0078	1.2925	2.9384
	D 17	0.2768	1.2782	0.0235	1.3300	1.4089
	D 19	0.1204	0.5575	0.0796	1.1018	2.0072
	D 23	0.3636	1.5893	0.0301	1.1778	0.6167

### 8.2.3 Skeletal Muscle Tissue immunohistochemistry and raw data

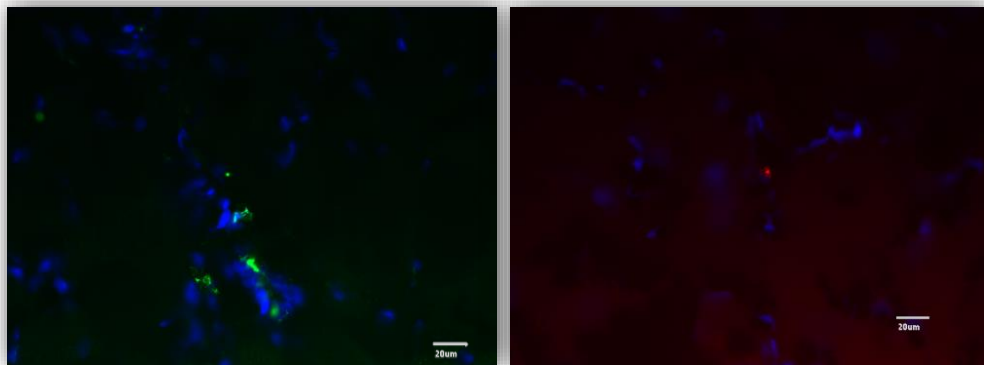


**Figure 4 | Skeletal Muscle Immunohistochemistry.**

Green representing anti CD206 and red as anti CD163. Blue is the nuclei stained with DAPI

**Table 5 | Muscle TaqMan Gene expression Raw Data.**Gene expression is normalized to  $\beta$ -actin

Group		$\beta$ -actin	SREBP-1C	TNF- $\alpha$	IL-6
Slope		-3.3237	-3.4427	-3.7227	-3.6573
Intercept		27.5822	30.5885	31.1109	34.6689
R2		-0.9876	-0.9918	-0.9854	-0.9760
NC	5 A	0.342	0.647	0.573	0.981
	9 A	0.196	0.327	2.056	0.174
	13 A	0.287	0.998	0.789	0.959
	18 A	0.218	0.647	0.865	0.061
	22 A	0.258	0.066	1.353	0.604
HFD	8 B	0.246	0.931	1.228	0.441
	10 B	0.281	1.211	0.349	0.055
	16 B	0.22	1.136	0.540	0.152
	20 B	0.22	1.236	0.731	0.556
	26 B	0.284	0.727	1.518	0.130
HFD/STZ + Pio	3 C	0.238	1.397	0.746	3.266
	11 C	0.276	0.836	0.943	1.028
	15 C	0.277	0.858	1.713	4.034
	21 C	0.233	1.353	1.923	1.201
	24 C	0.166	1.043	1.364	0.102
HFD/STZ	25 C	0.174	1.247	0.779	1.452
	4 D	0.339	2.275	0.414	1.416
	6 D	0.358	2.299	0.842	0.486
	12 D	0.256	2.433	2.122	1.618
	17 D	0.193	2.418	1.237	0.284
19 D	0.305	0.581	0.883	0.464	
23 D	0.134	0.789	1.772	5.345	

**8.2.4 Liver Tissue raw data****Table 6 | Liver Western Blots Normalized Densitometry Raw Data.**

		CD206	CD86	CD163
NC	A 5	0.471264368	0.152047	0.710983
	A 9	0.779735683	0.139394	0.294667
	A 13	0.372826087	0.262626	0.749107
	A 18	0.694063927	0.220388	0.919231
	A 22	0.505670103	0.184956	1.064286
HFD	B 8	0.634854772	0.146053	0.7072
	B 10	0.87012987	0.202899	0.427778
	B 16	0.767272727	0.197351	0.825
	B 20	1.113821138	0.184821	1.076923
	B 26	0.984555985	0.121094	0.29589

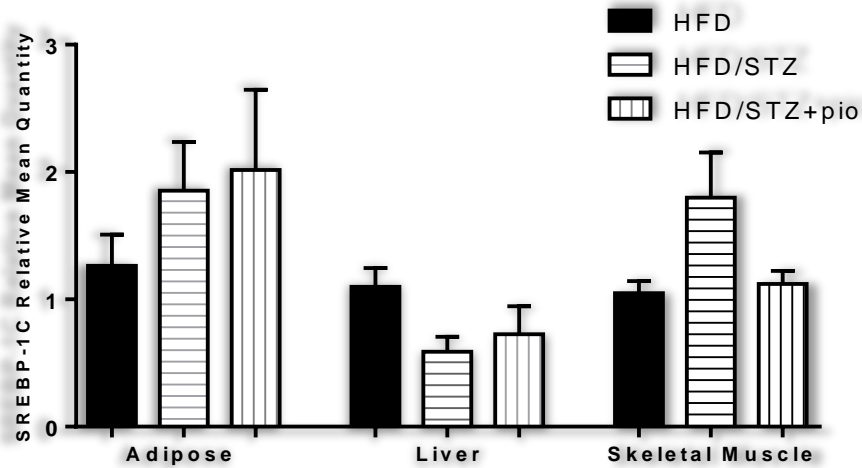


**Figure 5 | HFD, STZ and Pioglitazone effect on adipose, liver and skeletal muscle SREBP-1C mRNA expression level.** Liver mRNA was extracted using TRI-reagent then reversed transcribed to cDNA as described in the methods. Expression level was analysed using Taqman RT-PCR where quantity was measured relative to a standard curve. GAPDH was used as a reference control for normalization. HFD significantly decreased liver SREBP-1C while it increased it in skeletal muscles. All data are presented as mean  $\pm$  SEM with a one-way-ANOVA test with bonferroni post-hoc test comparing pairs; HFD and HFD/STZ, HFD/STZ and HFD/STZ+Pio: (n=5 for NC and HFD, n=6 for HFD/STZ and HFD/STZ+pio). \*P<0.05, NC; Normal Chow, HFD; High Fat Diet, STZ; streptozotocin, Pio; pioglitazone.

**Table 7 | SREBP-1C TaqMan Gene expression Raw Data**

	Adipose	Liver	Muscle
<b>Slope</b>	<b>-3.317</b>	<b>-3.415</b>	<b>-3.619</b>
<b>Intercept</b>	<b>28.203</b>	<b>30.384</b>	<b>30.093</b>
<b>R2</b>	<b>-0.998</b>	<b>-0.997</b>	<b>-0.995</b>
<b>NC</b>	5	3.614	1.574
	9	1.858	2.798
	13	0.740	3.467
	18	0.614	1.131
	22	2.071	2.035
<b>HFD</b>	8	1.474	1.37
	10	0.625	0.969
	16	2.089	1.41
	20	1.007	1.144
	26	1.114	0.601
<b>HFD/STZ</b>	4	1.260	0.434
	6	2.897	1.145
	12	2.938	0.379
	17	1.408	0.455
	19	2.009	0.664
<b>HFD/STZ+Pio</b>	23	0.616	0.452
	3	4.823	0.713
	11	1.757	0.355
	15	0.195	0.333
	21	2.233	0.208
	24	1.813	1.21
	25	1.273	1.54

**Table 8 | Liver Tissue TaqMan Gene Array Data Summary**

Gene Symbol	NC		HFD		HFD/STZ*		HFD/STZ+Pio <sup>#</sup>		P value and Fold change					
	Average	± STD	Average	± STD	Average	± STD	Average	± STD	HFD/NC	STZ*/HFD	Pio <sup>#</sup> /STZ*			
Acaca	3.631	± 0.557	2.341	± 1.176	1.168	± 0.720	1.019	± 0.501	<b>0.04830</b>	-1.55	0.07201	-2.00	0.68560	-1.15
Acacb	0.172	± 0.057	0.122	± 0.072	0.064	± 0.027	0.064	± 0.037	0.29581	-1.41	0.09686	-1.91	0.98980	-1.00
Acadl	8.111	± 2.193	10.832	± 3.096	10.596	± 1.746	10.993	± 1.606	0.14741	1.34	0.87672	-1.02	0.69037	1.04
Acadvl	5.081	± 0.979	5.676	± 1.281	5.523	± 0.454	5.162	± 0.416	0.43329	1.12	0.78965	-1.03	0.20633	-1.07
Acsl4	3.646	± 1.190	3.077	± 0.661	5.353	± 1.428	4.176	± 1.677	0.37704	-1.19	<b>0.04310</b>	1.74	0.24751	-1.28
Adipor1	3.606	± 0.535	3.666	± 0.138	2.093	± 0.471	2.577	± 0.728	0.83467	1.02	<b>0.00090</b>	-1.75	0.20161	1.23
Adipor2	1.115	± 0.304	0.983	± 0.336	0.666	± 0.090	0.804	± 0.164	0.53080	-1.14	0.05234	-1.47	0.41760	1.21
Ahsg	614.70	± 181.93	432.97	± 61.82	407.80	± 179.89	427.48	± 109.79	0.10072	-1.42	0.79771	-1.06	0.82374	1.05
Apoc3	171.63	± 39.04	143.25	± 50.08	84.30	± 25.63	92.22	± 14.24	0.34688	-1.20	<b>0.02930</b>	-1.70	0.52315	1.09
Atf3	0.263	± 0.103	0.936	± 0.555	0.525	± 0.156	0.542	± 0.193	<b>0.00630</b>	3.56	0.11364	-1.78	0.86450	1.03
Atf4	8.339	± 2.137	11.679	± 2.100	13.004	± 0.554	13.667	± 1.909	<b>0.02820</b>	1.40	0.20944	1.11	0.47588	1.05
Atg5	0.627	± 0.081	0.543	± 0.065	0.591	± 0.122	0.596	± 0.061	0.10936	-1.15	0.44986	1.09	0.93217	1.01
Atg7	0.441	± 0.130	0.344	± 0.093	0.301	± 0.048	0.285	± 0.048	0.21096	-1.28	0.35077	-1.14	0.57024	-1.06
Bace1	0.031	± 0.003	0.067	± 0.055	0.041	± 0.015	0.044	± 0.013	0.24147	2.15	0.29421	-1.63	0.71155	1.08
Casp3	1.162	± 0.297	1.121	± 0.395	0.922	± 0.302	0.963	± 0.220	0.85748	-1.04	0.36659	-1.22	0.79427	1.04
Cat	49.68	± 6.79	36.33	± 12.20	38.53	± 10.25	39.04	± 12.34	0.09303	-1.37	0.75174	1.06	0.94033	1.01
Ccl2	0.042	± 0.024	0.116	± 0.043	0.019	± 0.011	0.013	± 0.004	<b>0.00060</b>	2.76	<b>0.00006</b>	-6.10	0.28561	-1.45
Ccl3	0.066	± 0.044	0.187	± 0.172	0.057	± 0.039	0.040	± 0.021	0.16784	2.83	0.10373	-3.26	0.38465	-1.45
Cd163	1.056	± 0.249	0.702	± 0.172	0.962	± 0.300	0.575	± 0.061	0.06440	-1.50	0.12160	1.37	<b>0.03040</b>	-1.67
Cd36	0.020	± 0.004	0.028	± 0.013	0.024	± 0.017	0.018	± 0.006	0.20525	1.44	0.67394	-1.17	0.42043	-1.34
Cd68	0.516	± 0.120	0.368	± 0.092	0.370	± 0.064	0.322	± 0.049	<b>0.03460</b>	-1.40	0.95871	1.01	0.16930	-1.15
Cd86	0.088	± 0.051	0.084	± 0.048	0.039	± 0.027	0.041	± 0.028	0.90862	-1.04	0.52840	-2.17	0.87784	1.07
Cebpa	3.631	± 0.657	3.699	± 0.587	3.863	± 1.510	4.579	± 1.957	0.86692	1.02	0.82578	1.04	0.49438	1.19
Cidec	2.980	± 0.325	3.358	± 1.126	3.429	± 1.052	3.314	± 0.314	0.49150	1.13	0.91621	1.02	0.80241	-1.03

<b>Cpt1b</b>	0.150	±	0.026	0.179	±	0.031	0.199	±	0.037	0.162	±	0.042	0.14785	1.19	0.35374	1.11	0.13268	-1.23
<b>Creb1</b>	0.410	±	0.051	0.390	±	0.049	0.345	±	0.047	0.372	±	0.031	0.55503	-1.05	0.15481	-1.13	0.27734	1.08
<b>Creb3</b>	1.383	±	0.318	1.126	±	0.349	0.967	±	0.386	0.828	±	0.260	0.25922	-1.23	0.49425	-1.17	0.48178	-1.17
<b>Ddit3</b>	0.232	±	0.032	0.381	±	0.052	0.390	±	0.089	0.371	±	0.074	<b><u>0.00780</u></b>	1.64	0.83215	1.03	0.69436	-1.05
<b>Dgat2</b>	6.796	±	2.200	7.362	±	1.082	7.083	±	2.846	6.571	±	0.990	0.65489	1.08	0.85813	-1.04	0.71232	-1.08
<b>Edem2</b>	1.813	±	0.477	1.595	±	0.495	0.660	±	0.108	1.141	±	0.521	0.49973	-1.14	<b><u>0.00600</u></b>	-2.42	0.05109	1.73
<b>Egr1</b>	4.594	±	1.802	9.306	±	2.813	10.001	±	1.695	10.203	±	2.513	<b><u>0.01140</u></b>	2.03	0.62427	1.07	0.87351	1.02
<b>Elovl6</b>	0.088	±	0.067	0.044	±	0.034	0.025	±	0.015	0.024	±	0.019	0.23305	-1.98	0.27423	-1.78	0.92215	-1.04
<b>Ern1</b>	1.282	±	0.224	1.370	±	0.293	1.520	±	0.422	1.225	±	0.225	0.60890	1.07	0.51942	1.11	0.16152	-1.24
<b>Ero1l</b>	0.865	±	0.469	0.701	±	0.352	0.552	±	0.198	0.561	±	0.214	0.55068	-1.23	0.39731	-1.27	0.94440	1.02
<b>Fabp4</b>	0.317	±	0.111	0.444	±	0.114	0.501	±	0.192	0.388	±	0.156	0.11350	1.40	0.57259	1.13	0.31803	-1.29
<b>Fabp5</b>	4.168	±	2.325	3.150	±	2.086	0.634	±	0.083	1.316	±	0.750	0.48696	-1.32	0.06400	-4.97	0.75622	2.08
<b>Fasn</b>	6.292	±	1.666	4.141	±	3.161	0.440	±	0.194	0.729	±	0.385	0.21504	-1.52	<b><u>0.00620</u></b>	-9.41	0.13149	1.66
<b>Fgf21</b>	0.327	±	0.343	1.307	±	0.518	1.643	±	0.883	1.627	±	0.327	<b><u>0.04500</u></b>	4.00	0.47421	1.26	0.96735	-1.01
<b>Foxa2</b>	0.437	±	0.137	0.309	±	0.049	0.575	±	0.298	0.482	±	0.109	0.12221	-1.41	0.12018	1.86	0.52738	-1.19
<b>Foxo1</b>	0.882	±	0.064	0.950	±	0.084	1.021	±	0.407	1.009	±	0.248	0.24475	1.08	0.74670	1.07	0.95554	-1.01
<b>G6pc</b>	0.600	±	0.338	0.575	±	0.506	0.129	±	0.059	0.156	±	0.131	0.92919	-1.04	0.08634	-4.45	0.68457	1.21
<b>G6pd</b>	0.546	±	0.155	0.355	±	0.100	0.357	±	0.201	0.265	±	0.072	0.14470	-1.54	0.98469	1.01	0.31758	-1.35
<b>Gck</b>	0.209	±	0.035	0.277	±	0.183	0.006	±	0.003	0.019	±	0.010	0.48821	1.33	<b><u>0.00340</u></b>	-49.37	0.99880	3.37
<b>Gpd1</b>	4.393	±	1.954	5.517	±	2.160	5.349	±	1.811	3.703	±	1.096	0.41356	1.26	0.89139	-1.03	0.37380	-1.44
<b>Gsk3b</b>	0.969	±	0.152	0.963	±	0.111	0.736	±	0.119	0.864	±	0.216	0.94659	-1.01	0.08580	-1.31	0.23341	1.17
<b>Hk2</b>	0.025	±	0.007	0.017	±	0.007	0.015	±	0.007	0.013	±	0.007	0.10054	-1.49	0.71084	-1.11	0.65950	-1.14
<b>Hmgcs2</b>	18.064	±	8.161	23.170	±	9.534	35.466	±	5.812	28.516	±	10.705	0.38954	1.28	0.09570	1.53	0.19244	-1.24
<b>Hspa5</b>	38.016	±	7.750	29.413	±	9.442	15.877	±	5.681	22.935	±	4.045	0.18649	-1.29	<b><u>0.01270</u></b>	-1.85	0.26660	1.44
<b>Il10</b>	0.008	±	0.005	0.005	±	0.003	0.002	±	0.001	0.002	±	0.001	0.24251	-1.61	0.25240	-2.39	0.85578	1.05
<b>Il1b</b>	0.086	±	0.023	0.124	±	0.092	0.074	±	0.033	0.068	±	0.031	0.40446	1.43	0.24454	-1.68	0.74328	-1.09
<b>Irs1</b>	1.201	±	0.230	0.772	±	0.155	0.779	±	0.268	0.605	±	0.203	<b><u>0.01900</u></b>	-1.56	0.95743	1.01	0.23207	-1.29

<b>Klf11</b>	0.274	±	0.063	0.318	±	0.126	0.274	±	0.083	0.223	±	0.044	0.50234	1.16	0.52864	-1.16	0.26671	-1.22
<b>Ldha</b>	17.111	±	3.860	21.989	±	7.889	11.323	±	1.061	15.519	±	3.461	0.29851	1.29	<b><u>0.00770</u></b>	-1.94	0.48690	1.37
<b>Lpl</b>	0.268	±	0.030	0.271	±	0.079	0.304	±	0.095	0.283	±	0.061	0.93745	1.01	0.56588	1.12	0.67680	-1.07
<b>Me1</b>	0.428	±	0.146	0.609	±	0.337	0.725	±	0.336	0.468	±	0.152	0.30250	1.42	0.58379	1.19	0.11931	-1.55
<b>Mlxipl</b>	7.443	±	2.417	5.806	±	1.502	4.067	±	0.900	4.365	±	2.104	0.23448	-1.28	0.38630	-1.43	0.75633	1.07
<b>Mrc1</b>	1.196	±	0.350	1.385	±	0.526	1.365	±	0.319	0.968	±	0.279	0.52151	1.16	0.93998	-1.01	0.24250	-1.41
<b>Mtor</b>	0.530	±	0.156	0.391	±	0.140	0.393	±	0.155	0.462	±	0.142	0.17818	-1.35	0.98615	1.00	0.44021	1.18
<b>Nr1h2</b>	0.275	±	0.099	0.245	±	0.082	0.159	±	0.014	0.200	±	0.031	0.61575	-1.12	0.11710	-1.53	0.85310	1.25
<b>Nr1h3</b>	2.816	±	0.744	2.572	±	1.059	2.236	±	0.322	2.598	±	0.641	0.68436	-1.09	0.47487	-1.15	0.24416	1.16
<b>Nr1h4</b>	2.176	±	0.669	2.644	±	0.725	2.531	±	0.709	2.166	±	0.338	0.31960	1.22	0.79873	-1.05	0.28225	-1.17
<b>Pck1</b>	26.299	±	3.978	11.681	±	1.980	8.428	±	4.661	5.867	±	3.668	<b><u>0.00008</u></b>	-2.25	0.18219	-1.39	0.31503	-1.44
<b>Pdk2</b>	4.346	±	2.953	4.848	±	2.140	4.576	±	1.575	4.397	±	1.775	0.76646	1.12	0.81366	-1.06	0.85743	-1.04
<b>Pklr</b>	5.848	±	2.760	3.480	±	2.021	0.686	±	0.333	0.443	±	0.149	0.16023	-1.68	<b><u>0.04000</u></b>	-5.07	0.16833	-1.55
<b>Plin2</b>	0.640	±	0.284	1.248	±	0.620	0.872	±	0.445	0.358	±	0.157	0.08154	1.95	0.27142	-1.43	0.17270	-2.43
<b>Ppara</b>	0.740	±	0.147	1.057	±	0.500	1.290	±	0.633	1.133	±	0.449	0.21128	1.43	0.52134	1.22	0.63075	-1.14
<b>Ppard</b>	0.324	±	0.040	0.263	±	0.036	0.372	±	0.128	0.290	±	0.015	0.62560	-1.23	0.09955	1.41	0.19039	-1.28
<b>Ppargc1a</b>	0.159	±	0.058	0.123	±	0.077	0.128	±	0.118	0.074	±	0.032	0.42091	-1.30	0.93162	1.04	0.30205	-1.74
<b>Ppargc1b</b>	0.282	±	0.048	0.297	±	0.139	0.378	±	0.233	0.204	±	0.069	0.82793	1.05	0.51628	1.27	0.11144	-1.85
<b>Pparg</b>	0.148	±	0.034	0.142	±	0.033	0.121	±	0.042	0.134	±	0.015	0.79475	-1.04	0.37653	-1.18	0.49501	1.11
<b>Prkce</b>	0.960	±	0.080	0.946	±	0.403	0.642	±	0.063	0.804	±	0.384	0.94683	-1.02	0.13500	-1.47	0.38094	1.25
<b>Rxra</b>	8.057	±	1.991	6.550	±	2.788	7.348	±	2.812	5.675	±	0.769	0.35394	-1.23	0.64903	1.12	0.19019	-1.29
<b>Scd1</b>	28.465	±	9.872	8.885	±	6.456	0.063	±	0.062	0.027	±	0.014	<b><u>0.00010</u></b>	-3.20	0.06260	-142.01	0.24344	-2.31
<b>Serpine1</b>	0.470	±	0.174	0.697	±	0.472	0.506	±	0.417	0.376	±	0.181	0.34202	1.48	0.49185	-1.38	0.50059	-1.34
<b>Sirt3</b>	0.060	±	0.027	0.084	±	0.034	0.097	±	0.027	0.102	±	0.036	0.24131	1.41	0.50078	1.15	0.79635	1.05
<b>Sirt6</b>	0.274	±	0.040	0.242	±	0.028	0.283	±	0.078	0.283	±	0.032	0.17347	-1.13	0.29652	1.17	0.98296	1.00
<b>Slc27a2</b>	13.940	±	2.889	15.555	±	3.854	18.110	±	5.742	17.390	±	4.940	0.47476	1.12	0.41993	1.16	0.82055	-1.04
<b>Slc27a5</b>	5.264	±	1.323	2.644	±	0.391	3.904	±	0.938	3.928	±	1.429	<b><u>0.01110</u></b>	-1.99	0.36580	1.48	0.97566	1.01

<b>Slc2a2</b>	8.786	±	4.119	7.359	±	3.933	7.736	±	3.100	4.601	±	1.196	0.59070	-1.19	0.86255	1.05	0.32240	-1.68
<b>Socs3</b>	4.134	±	0.394	3.266	±	0.543	3.321	±	0.617	3.014	±	0.223	<b><u>0.03220</u></b>	-1.27	0.88075	1.02	0.32132	-1.10
<b>Srebf1</b>	1.041	±	0.358	0.852	±	0.267	0.558	±	0.129	0.708	±	0.298	0.37079	-1.22	0.27250	-1.53	0.28424	1.27
<b>Srebf2</b>	2.555	±	0.741	1.524	±	0.416	0.984	±	0.362	1.487	±	0.463	<b><u>0.04300</u></b>	-1.68	0.27250	-1.55	0.99910	1.51
<b>Tnf</b>	0.015	±	0.006	0.026	±	0.018	0.011	±	0.006	0.012	±	0.006	0.23935	1.74	0.09350	-2.31	0.84399	1.06
<b>Ucp2</b>	1.045	±	0.219	0.963	±	0.180	0.887	±	0.348	0.790	±	0.348	0.53713	-1.08	0.66896	-1.09	0.64035	-1.12
<b>Xbp1</b>	28.293	±	11.111	24.877	±	2.953	26.222	±	7.721	33.969	±	10.618	0.52512	-1.14	0.72339	1.05	0.17893	1.30

**Table 9 | CHOP Western Blot Normalized Raw Data**

		CHOP signal	Actin signal	Normalized signal
NC	5	17300	68200	0.253666
	9	17000	52500	0.32381
	13	15800	61600	0.256494
	18	16900	70700	0.239038
HFD	8	41200	74400	0.553763
	10	36400	79200	0.459596
	16	34200	55300	0.618445
	20	23800	60000	0.396667

**Table 10 | Liver Triglyceride Content Raw Data**

Animal group	Total TG (µg/ml)	Percentage				Calculated amount (µg/ml)				
		Palmitic	Stearic	Oleic	Linoleic	Palmitic	Stearic	Oleic	Linoleic	
NC	5	4.349	33.63	4.32	17.81	33.66	1.463	0.188	0.775	1.464
	9	8.114	32.94	5.14	37.84	24.08	2.673	0.417	3.070	1.954
	13	6.123	39.82	7.77	20.42	31.37	2.438	0.476	1.250	1.921
	18	4.732	37.86	9.84	24.4	27.9	1.792	0.466	1.155	1.320
	22	5.138	38.91	6.21	24.32	30.56	1.999	0.319	1.250	1.570
HFD	8	19.718	25.7	4.4	34.37	28.02	5.068	0.868	6.777	5.525
	10	11.108	28.42	4.61	40.36	24.43	3.157	0.512	4.483	2.714
	16	26.892	29.96	4.3	35.08	30.65	8.057	1.156	9.434	8.242
	20	16.601	27.31	4.52	36.23	23.63	4.534	0.750	6.015	3.923
	26	25.598	28.31	4.94	35.57	25.76	7.247	1.265	9.105	6.594

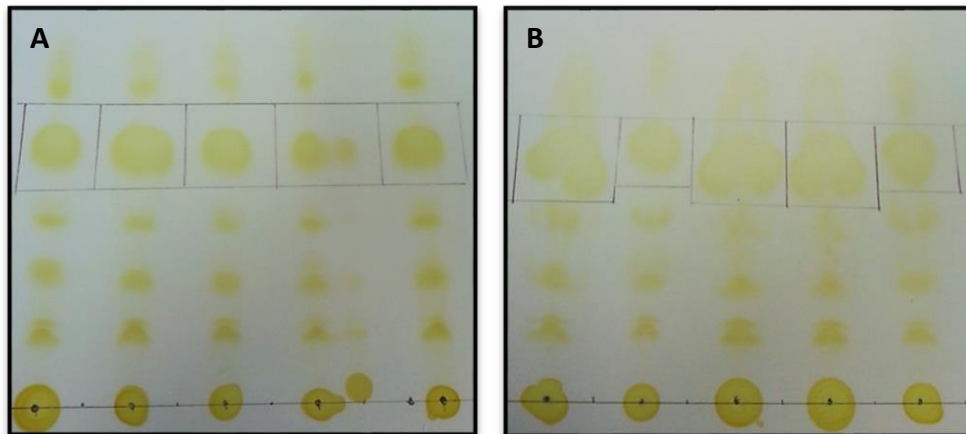


**Figure 6 | Thin Layer Chromatography of Total Lipids Extracted from the Liver Samples.** Plate A. includes the Normal Chow samples while B. includes the high fat diet samples. The boxed bands represents the triglycerides that was excised for further analysis with the gas chromatography.

**Table 11 | Skeletal Muscle Tissue TaqMan Gene Array Data Summary**

Gene Symbol	NC		HFD		HFD/STZ*		HFD/STZ+Pio <sup>#</sup>		P value and Fold change					
	Average	± STD	Average	± STD	Average	± STD	Average	± STD	HFD/NC	STZ/HFD	HFD/STZ+Pio			
Acaca	0.288	± 0.026	0.220	± 0.020	0.203	± 0.047	0.336	± 0.107	0.4058	-1.31	0.5344	-1.08	<b>0.0262</b>	1.66
Acacb	4.804	± 1.579	5.781	± 1.307	6.935	± 0.361	6.468	± 1.815	0.3546	1.20	0.1397	1.20	0.6318	-1.07
Acad	10.235	± 4.520	9.599	± 1.674	11.508	± 2.885	17.155	± 3.406	0.7755	-1.07	0.2510	1.20	0.0894	1.49
Acadvl	6.192	± 1.892	5.003	± 1.167	4.484	± 1.645	5.984	± 1.853	0.2657	-1.24	0.5959	-1.12	0.2714	1.33
Acsl4	0.986	± 0.718	1.441	± 0.249	2.127	± 0.672	2.189	± 0.976	0.2169	1.46	0.0701	1.48	0.9199	1.03
Adipor1	12.054	± 4.131	13.875	± 1.889	13.322	± 1.725	12.148	± 3.479	0.3964	1.15	0.6643	-1.04	0.5677	-1.10
Adipor2	3.062	± 0.692	3.301	± 0.699	3.516	± 0.458	3.349	± 0.149	0.6029	1.08	0.6141	1.07	0.5153	-1.05
Atf3	0.113	± 0.078	0.096	± 0.044	0.153	± 0.084	0.261	± 0.035	0.6914	-1.17	0.2302	1.58	0.0950	1.71
Atf4	14.719	± 1.781	14.058	± 2.000	16.705	± 2.013	17.254	± 2.609	0.5957	-1.05	0.0898	1.19	0.7501	1.03
Atg5	0.436	± 0.096	0.493	± 0.074	0.339	± 0.055	0.396	± 0.115	0.3246	1.13	0.0600	-1.45	0.4050	1.17
Atg7	0.358	± 0.068	0.373	± 0.088	0.182	± 0.039	0.167	± 0.051	0.7695	1.04	<b>0.0024</b>	-2.05	0.6668	-1.09
Bace1	0.021	± 0.010	0.027	± 0.010	0.025	± 0.010	0.023	± 0.001	0.4355	1.27	0.8726	-1.04	0.6972	-1.10
Casp3	0.046	± 0.023	0.044	± 0.010	0.055	± 0.020	0.051	± 0.015	0.8368	-1.05	0.3309	1.24	0.7937	-1.07
Cat	11.129	± 3.523	14.435	± 3.756	20.161	± 5.094	26.413	± 6.859	0.1891	1.30	0.0923	1.40	0.1937	1.31
Ccl2	0.054	± 0.013	0.050	± 0.046	0.060	± 0.027	0.137	± 0.085	0.8532	-1.09	0.6959	1.21	0.1388	2.27
Cd16	0.252	± 0.226	0.272	± 0.139	0.240	± 0.091	0.506	± 0.064	0.8667	1.08	0.7044	-1.13	0.0580	2.11
Cd36	0.228	± 0.163	0.227	± 0.194	0.249	± 0.015	1.215	± 0.530	0.9926	-1.00	0.8545	1.10	<b>0.0015</b>	4.87
Cd68	0.020	± 0.007	0.055	± 0.029	0.050	± 0.026	0.080	± 0.047	0.0519	2.77	0.7750	-1.11	0.3058	1.60
Cebpa	0.135	± 0.066	0.069	± 0.026	0.103	± 0.042	0.168	± 0.066	0.0721	-1.94	0.1770	1.49	0.1464	1.63
Cidec	0.068	± 0.050	0.041	± 0.031	0.012	± 0.008	0.025	± 0.012	0.3381	-1.66	0.1146	-3.46	0.1323	2.14
Cpt1b	8.014	± 4.190	7.410	± 1.539	9.359	± 2.106	11.758	± 2.407	0.7700	-1.08	0.1514	1.26	0.1842	1.26
Creb1	0.594	± 0.113	0.604	± 0.103	0.582	± 0.116	0.611	± 0.092	0.8876	1.02	0.7671	-1.04	0.7018	1.05
Creb3	0.711	± 0.123	0.849	± 0.163	0.595	± 0.175	0.687	± 0.115	0.1703	1.19	0.0591	-1.43	0.4135	1.15
Ddit3	0.371	± 0.180	0.271	± 0.046	0.368	± 0.164	0.420	± 0.105	0.3238	-1.37	0.3010	1.36	0.6168	1.14
Dgat2	42.791	± 38.414	18.317	± 1.774	9.733	± 8.707	35.097	± 23.752	0.2496	-2.34	0.1016	-1.88	0.0918	3.61
Edem2	0.168	± 0.119	0.216	± 0.078	0.088	± 0.053	0.048	± 0.007	0.4687	1.29	0.1133	-2.46	0.2539	-1.85
Egr1	0.645	± 0.357	1.028	± 0.105	0.851	± 0.068	2.062	± 1.302	0.0852	1.59	0.0538	-1.21	0.1769	2.42
Elovl6	0.016	± 0.006	0.017	± 0.011	0.016	± 0.006	0.101	± 0.050	0.9126	1.04	0.9318	-1.04	<b>0.0343</b>	6.28

Ern1	1.192	±	0.253	1.356	±	0.114	1.248	±	0.091	1.042	±	0.238	0.2736	1.14	0.2416	-1.09	0.2216	-1.20
Ero1l	0.135	±	0.090	0.097	±	0.021	0.097	±	0.033	0.110	±	0.057	0.3850	-1.39	0.9929	1.00	0.7066	1.13
Fabp	0.037	±	0.008	0.045	±	0.005	0.036	±	0.020	0.082	±	0.001	0.1206	1.20	0.3875	-1.24	<b>0.0003</b>	2.28
Fabp4	3.977	±	2.325	3.781	±	1.181	3.195	±	0.431	5.634	±	0.931	0.8708	-1.05	0.3817	-1.18	0.9031	1.76
Fasn	0.153	±	0.064	0.136	±	0.034	0.118	±	0.029	0.112	±	0.034	0.6154	-1.13	0.4207	-1.16	0.7939	-1.05
Foxo1	16.221	±	8.138	23.999	±	8.166	17.614	±	7.460	17.406	±	6.851	0.1698	1.48	0.2658	-1.36	0.9685	-1.01
G6pd	0.170	±	0.059	0.280	±	0.094	0.160	±	0.026	0.245	±	0.061	0.9807	1.65	0.9436	-1.75	0.9435	1.53
Gpd1	19.846	±	8.060	21.991	±	0.976	14.372	±	2.787	12.844	±	5.085	0.9711	1.11	0.1289	-1.53	0.9171	-1.12
Gsk3b	4.032	±	0.737	3.895	±	0.504	5.367	±	1.643	3.868	±	0.862	0.7416	-1.04	0.0959	1.38	0.1572	-1.39
Hk2	1.508	±	0.714	1.208	±	0.265	0.722	±	0.193	0.976	±	0.315	0.4040	-1.25	0.3705	-1.67	0.2190	1.35
Hmgcs2	0.058	±	0.056	0.059	±	0.020	0.190	±	0.078	1.116	±	0.567	0.9649	1.02	0.9082	3.20	<b>0.0013</b>	5.88
Hspa5	4.666	±	1.824	4.218	±	0.252	3.981	±	0.767	4.534	±	1.468	0.6019	-1.11	0.5304	-1.06	0.5289	1.14
Il6	0.064	±	0.035	0.051	±	0.042	0.132	±	0.037	0.231	±	0.130	0.5890	-1.27	0.2980	2.62	0.1936	1.75
Irs1	0.570	±	0.572	0.786	±	0.311	1.687	±	0.973	0.486	±	0.463	0.4787	1.38	0.0885	2.15	<b>0.0433</b>	-3.47
Klf11	0.294	±	0.111	0.362	±	0.120	0.600	±	0.131	0.566	±	0.133	0.3841	1.23	<b>0.0357</b>	1.66	0.7281	-1.06
Ldha	50.472	±	25.610	61.528	±	9.185	76.118	±	8.673	51.064	±	15.533	0.9012	1.22	0.6425	1.24	0.1571	-1.49
Lpl	10.187	±	9.935	4.023	±	1.085	4.676	±	2.647	10.143	±	4.261	0.2052	-2.53	0.6270	1.16	0.0721	2.17
Me1	4.845	±	2.904	5.741	±	0.900	5.076	±	0.592	4.385	±	0.928	0.5285	1.18	0.3046	-1.13	0.3148	-1.16
Mlxipl	18.844	±	2.039	26.598	±	8.236	13.061	±	1.606	22.041	±	6.736	0.0753	1.41	<b>0.0082</b>	-2.04	0.1149	1.69
Mrc1	0.302	±	0.240	0.445	±	0.262	0.461	±	0.111	0.819	±	0.209	0.4293	1.47	0.9092	1.04	0.9140	1.78
Mtor	0.815	±	0.211	0.755	±	0.205	0.913	±	0.300	0.740	±	0.172	0.6602	-1.08	0.3781	1.21	0.3572	-1.23
Nr1h2	0.208	±	0.053	0.260	±	0.049	0.204	±	0.005	0.195	±	0.027	0.1456	1.25	0.1039	-1.28	0.6268	-1.04
Nr1h3	0.534	±	0.156	0.553	±	0.185	0.476	±	0.130	0.350	±	0.064	0.8644	1.04	0.5075	-1.16	0.1310	-1.36
Pdk2	27.371	±	11.905	34.447	±	6.859	37.837	±	2.040	32.125	±	11.149	0.2828	1.26	0.3766	1.10	0.3524	-1.18
Plin1	0.489	±	0.437	0.410	±	0.399	0.325	±	0.230	0.090	±	0.078	0.7846	-1.19	0.7176	-1.26	0.1564	-3.62
Plin2	0.806	±	0.323	1.005	±	0.470	1.636	±	0.502	1.691	±	0.109	0.4593	1.25	0.0931	1.63	0.8364	1.03
Ppara	0.950	±	0.292	0.859	±	0.307	0.468	±	0.072	0.824	±	0.307	0.6449	-1.11	0.1441	-1.84	0.0645	1.76
Ppard	1.880	±	0.184	2.476	±	0.894	2.100	±	0.114	2.233	±	0.541	0.2374	1.32	0.4373	-1.18	0.6465	1.06
Pparg	0.040	±	0.017	0.064	±	0.032	0.046	±	0.021	0.059	±	0.022	0.1801	1.58	0.3600	-1.39	0.4130	1.29
Ppargc1a	1.223	±	0.683	1.520	±	0.384	2.404	±	1.481	1.934	±	0.658	0.4214	1.24	0.2345	1.58	0.5837	-1.24
Ppargc1b	1.066	±	0.640	0.724	±	0.193	0.217	±	0.074	0.389	±	0.178	0.4855	-1.47	0.1783	-3.33	0.1249	1.79

<b>Prkce</b>	2.561 ± 0.718	1.862 ± 0.387	2.304 ± 0.300	2.367 ± 0.467	0.0914	-1.38	0.1032	1.24	0.8280	1.03
<b>Rrad</b>	0.041 ± 0.030	0.058 ± 0.067	0.038 ± 0.033	0.143 ± 0.172	0.6344	1.39	0.6041	-1.53	0.2736	3.81
<b>Rxra</b>	5.320 ± 1.004	6.873 ± 0.579	7.406 ± 0.460	5.374 ± 1.592	0.0720	1.29	0.1777	1.08	<b>0.0341</b>	-1.38
<b>Scd1</b>	0.053 ± 0.021	0.089 ± 0.071	0.010 ± 0.005	0.068 ± 0.097	0.3687	1.68	0.0672	-8.73	0.2769	6.69
<b>Serpine1</b>	1.077 ± 0.380	1.139 ± 0.696	0.926 ± 0.442	3.395 ± 2.575	0.8785	1.06	0.6126	-1.23	0.1077	3.67
<b>Sirt3</b>	0.056 ± 0.016	0.045 ± 0.011	0.030 ± 0.012	0.037 ± 0.018	0.2423	-1.25	0.1004	-1.48	0.5730	1.22
<b>Sirt6</b>	0.353 ± 0.095	0.363 ± 0.064	0.373 ± 0.084	0.320 ± 0.074	0.8552	1.03	0.8514	1.03	0.3797	-1.17
<b>Socs3</b>	0.240 ± 0.213	0.131 ± 0.037	0.232 ± 0.178	0.625 ± 0.410	0.3506	-1.83	0.3101	1.77	0.1289	2.69
<b>Srebf1</b>	1.103 ± 0.638	1.675 ± 0.457	3.358 ± 0.934	1.765 ± 0.681	0.1418	1.52	<b>0.0071</b>	2.01	<b>0.0155</b>	-1.90
<b>Srebf2</b>	1.768 ± 0.578	1.763 ± 0.321	2.812 ± 0.477	2.266 ± 0.415	0.9852	-1.00	<b>0.0127</b>	1.60	0.1348	-1.24
<b>Ucp2</b>	0.580 ± 0.297	0.821 ± 0.316	0.571 ± 0.051	0.951 ± 0.355	0.2486	1.42	0.2356	-1.44	0.1320	1.67
<b>Xbp1</b>	1.446 ± 0.351	1.369 ± 0.168	1.248 ± 0.163	1.146 ± 0.157	0.6707	-1.06	0.3110	-1.10	0.4039	-1.09

**Table 12 | Skeletal muscle Total Triglycerides content (µg/ml ) raw data**

NC	HFD	HFD/STZ+pio	HFD/STZ
0.69452	0.401699	0.691765	0.421529
0.382276	0.441226	0.747041	0.301416
0.608301	0.596853	0.600887	0.421425
0.572101	0.91459	0.734759	0.343003
0.728479	2.692307	1.579727	0.656362
		0.91295	1.468837

### 8.3 Chapter V:

**Table 13 | Chapter 6 Animals Biometric and Triglycerides Raw Data**

Animal Group	Glucose(mM)		Weight (g)			Total Liver Triglyceride (µg/ml)				
	Week 6	Week 8	Day -49	Day 0	Day 59	Liver	VLDL	Chylomicrons	VLDL/Chy	
NC	17	6.4	7.8	304	425	487	5.86	0.4562	0.1588	2.8728
	18	6	8.6	305	438	488	3.11	0.3958	0.1583	2.5005
	19	7	7	299	404	459	3.03	0.4631	0.2503	1.8504
	20	7.5	7.4	302	398	465	4.21	0.5371	0.2409	2.2294
HFD	1	7.4	8.2	297	429	492	7.46	0.3856	0.2136	1.8052
	2	8.7	8.5	305	428	506	8.58	0.2920	0.2658	1.0985
	3	7.7	8	318	465	587	7.68	0.2247	0.1493	1.5050
	4	8.8	10.2	289	417	494	8.44	0.5556	0.3961	1.4028

**Table 14 | Chapter 6 Animals Plasma GC analysis**

Animal Group	Chylomicron					VLDL				
	C16:0	C16:1	C18:0	C18:1	C18:2	C16:0	C16:1	C18:0	C18:1	C18:2
NC	17	37.3	5.0	15.8	27.2	14.7	51.0	13.6	10.1	25.3
	18	54.6	5.8	18.5	21.1		57.3	6.4	13.4	22.9
	19	35.7		10.2	34.1	19.9	54.6	11.4	8.1	25.9
	20	52.9	5.4	16.2	25.5		46.8	13.4	7.8	32.0
HFD	1	54.6		26.4	19.0		56.9		22.1	21.1
	2	45.2		24.9	29.9		57.8		18.8	23.5
	3	42.3	3.4	28.5	21.7		56.2		25.3	18.6
	4	35.7	1.2	18.3	42.5	2.2	46.2		12.4	39.5

C16:0 Palmitic acid  
 C16:1 Palmitoleic acid  
 C18:0 stearic acid  
 C18:1 Oleic acid

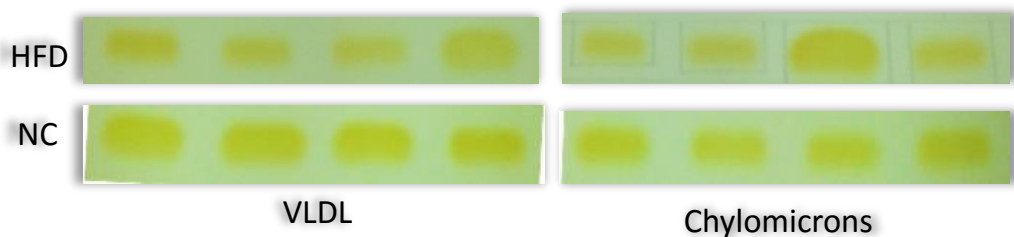


**Figure 7 | Thin Layer Chromatography of Total Lipids Extracted from Plasma lipoprotein Samples.** Figure represents the triglyceride bands that was excised for further analysis with the gas chromatography